ARGONAUTE10 inhibits INDEHISCENT to regulate shoot apical meristem and replum development in *Arabidopsis thaliana*

A thesis submitted for the degree of Doctor of Philosophy

Manoj Kumar Valluru
December 2017

Department of Molecular Biology and Biotechnology
University of Sheffield

Acknowledgments

गुरु ब्रम्हा गुरु विष्णू	*Guru Brahmaa Guru Vishnu*
गुरुः देवो महेश्वरा	*Gurur Devo Maheshwarah*
गुरु शाक्षात परब्रम्हा	*Guru Saakshaata Parabrahma*
तस्मै श्री गुरुवे नमः	*Tasmai Shri Guruve Namah*

This verse from Skanda Purana translates as: The true teacher is Brahma (God as Creator), The true teacher is Vishnu (God as Sustenance), The true teacher is Shiva (God as the destroyer of the ego or ignorance), My Salutation to such a teacher, who is verily united with God.

Abstract

ARGONAUTE10 (*AGO10*) regulates shoot apical meristem (SAM) and gynoecium development by controlling Class III *HOMEODOMAIN-LEUCINE ZIPPER* (*HD-ZIP III*) transcription factor expression. The *ago10^{zwl-3}* mutant failed to establish SAM, leaf adaxial identity, and carpel margin meristems (CMMs). However, the factors that act downstream of *AGO10* and *HD-ZIP III* genes to regulate development are not known. This work has identified that the INDEHISCENT (IND) bHLH transcription factor functions downstream of *AGO10* and *HD-ZIP III* genes to ensure proper SAM and replum development. IND overexpression causes SAM defects similar to *ago10^{zwl-3}* mutants, and the *ind* mutation partially rescues *ago10* mutant phenotypes. IND overexpression negatively regulates tissue bilateral symmetry by repressing polar auxin transport (PAT), *AGO10* and probably *CUC1* expression. However, HD-ZIP III transcription factors PHB and REV indirectly repress *IND* and promote *CUC1* expression. AGO10 and IND regulate each other antagonistically. AGO10 repression of *IND* is essential for SAM and replum development because overexpression of IND impairs tissue bilateral symmetry. This is the first study to demonstrate a role for IND in SAM development and that the main function of AGO10 is to maintain proper *IND* expression.

Table of Contents

List of tables and figures

Chapter 3

Chapter 4

List of abbreviations

AGO	ARGONAUTE
ARF	AUXIN RESPONSE FACTOR
AS	ASYMMETRIC LEAVES
AUX	Auxin
BAP	6-Benzylaminopurine
ChIP	Chromatin immunoprecipitation
CHY	Cycloheximide
CMM	Carpel margin meristem
CUC	CUP-SHAPED COTYLEDON
CUP	Cup-shaped or single leaf
CYT	Cytokinin
CZ	Central zone
DEX	Dexamethasone
DMSO	Dimethyl sulfoxide
EMS	Ethyl methanesulfonate
EtH	Ethanol
ETT	ETTIN
FC	Fold change
GEO	Gene Expression Omnibus
GR	Glucocorticoid receptor
GSEA	Gene Set Enrichment Analysis
GUS	β-Glucuronidase
HD-ZIP III	Class III HOMEODOMAIN-LEUCINE ZIPPER
HEC	HECATE
IAA	Indole-3-acetic acid
IND	INDEHISCENT
LM	Large meristem
NES	Normalized Enrichment Score
NM	No-meristem or flat apex
NPA	N-1-naphthylphthalamic acid

OC	Organizing centre
PAT	Polar auxin transport
PHB	PHABULOSA
PHV	PHAVOLUTA
PID	PINOID
PIN	Pin-shaped or filamentous-like
PIN1	PIN-FORMED 1
PL	Pointed leaves
PZ	Peripheral zone
REV	REVOLUTA
RPL	REPLUMLESS
RZ	Rib zone
SAM	Shoot apical meristem
SPT	SPATULA
TF	Transcription factor
VM	Valve margin
WT	Wild type

Chapter 1

General Introduction

CHAPTER 1. General Introduction

Aristotle considered the parts of plants as 'organs,' which can move upwards *qua* 'fiery' or downwards *qua* 'earthy,' depending on the organ's function (Johansen, 1997). Embryologist Caspar Friedrich Wolff studied the development of these organs and concluded that all the above-ground plant organs are shoot apex derivatives (Aulie, 1961). The shoot apex consists of an apical meristem and subjacent leaf primordia. The shoot apical meristem (SAM) maintains its basic structure from germination throughout the life of the plant, which in some tree species can be hundreds of years. The intermediate juvenile meristems undergo a transition from a vegetative phase to the formation of the inflorescence and to flowering. The gynoecium is derived from carpels that arise from the terminating floral meristem and fruit is formed from the gynoecium after flowering.

Wolff observed the commonality of development between foliage leaves and floral petals, and wrote: *"All parts of the plant – except the shoot and the root –can be attributed to the structure of the leaf; they are nothing but modifications of leaves" (From the Doctoral Thesis 'Theoria generationis' of Caspar Friedrich Wolff, submitted in 1759 to the University of Halle, Germany)* (Aulie, 1961). Interestingly, carpels are also considered to be evolved from leaves (Scutt et al., 2006). Girin *et al.* stated that "*Carpels are modified leaves, the gynoecium can thus be seen as two modified leaves (the presumptive valves) fused to two modified meristems (the presumptive repla)*." Many of the genes involved in fruit development also have a role in SAM and leaf development (Girin et al., 2009). Understanding how these genes function in the SAM and leaf primordia can provide insight into their function in fruit development. This introduction will provide an overview of the similar elements of postembryonic-SAM and fruit development and generate an integrated view of the topic.

1.1 Shoot apical meristem and leaf primordia

Arabidopsis thaliana is a good model system for understanding the mechanisms of the complex processes of SAM and leaf development. In *Arabidopsis,* the SAM develops during embryogenesis between the two embryonic leaves or cotyledons. The SAM is a domed triangle consisting of approximately 500 cells, and is divided into three distinct

cell layers (L1, L2, and L3) (Barton, 2010; Dodsworth, 2009) (Fig 1.2). The L1 and L2 (tunica layers) grow as two-dimensional sheets of cells by anticlinal cell divisions: L1 (protoderm) gives rise to epidermal cells and L2 gives rise to mesophyll cells. L3 (Corpus) cells can divide into all planes to form the central tissues of the leaf and stem. Cells from all three meristem layers participate in leaf primordium formation. The SAM can be divided into three functional zones: central zone (CZ), peripheral zone (PZ) and rib zone (RZ) (Fig 1.2). Approximately 35 stem cells reside in the CZ, which is maintained by a low cell division rate (Dodsworth, 2009). The CZ generates cells for both PZ and RZ. The PZ is responsible for the formation of lateral organ primordia (e.g., leaves), whereas the RZ maintains the majority of shoot (stem) growth. This process pushes the SAM upward and sustains the continuous acropetal growth of the shoot, and produces intermittently lateral appendages at precise phyllotactic locations. Maintenance of SAM and the initiation of new leaves are regulated by streams of signals such as phytohormones and transcription factors from different directions.

1.1.1 Hormonal regulation

Plant hormones or phytohormones are also termed plant growth regulators. Plant hormones are produced in multiple tissues and flow between organs via the vasculature. They also use special transporters and are involved in different developmental processes, as well as in responses to external signals (Santner et al., 2009; Wolters and Jurgens, 2009). There are seven classical plant hormones namely auxin, cytokinin, gibberellins, abscisic acid, ethylene, salicylic acid and jasmonic acid. Particularly auxin, cytokinin, and gibberellins are involved in lateral organ initiation and patterning of the SAM. Auxin, cytokinin and gibberellin signals can crosstalk and regulate different transcription factors that can be either synergistic or antagonistic. These transcription factors can regulate tissue polarity (e.g., leaf adaxial and abaxial polarity), stem cell maintenance in the SAM, and proper organ separation (e.g., boundary formation by separation of leaf primordia from SAM). Changes in auxin, cytokinin and gibberellin biosynthesis or distribution can affect development and tissue patterning. In the next subsections, the major plant hormones auxin and cytokinin are briefly described, and their roles in regulating SAM and leaf development are discussed.
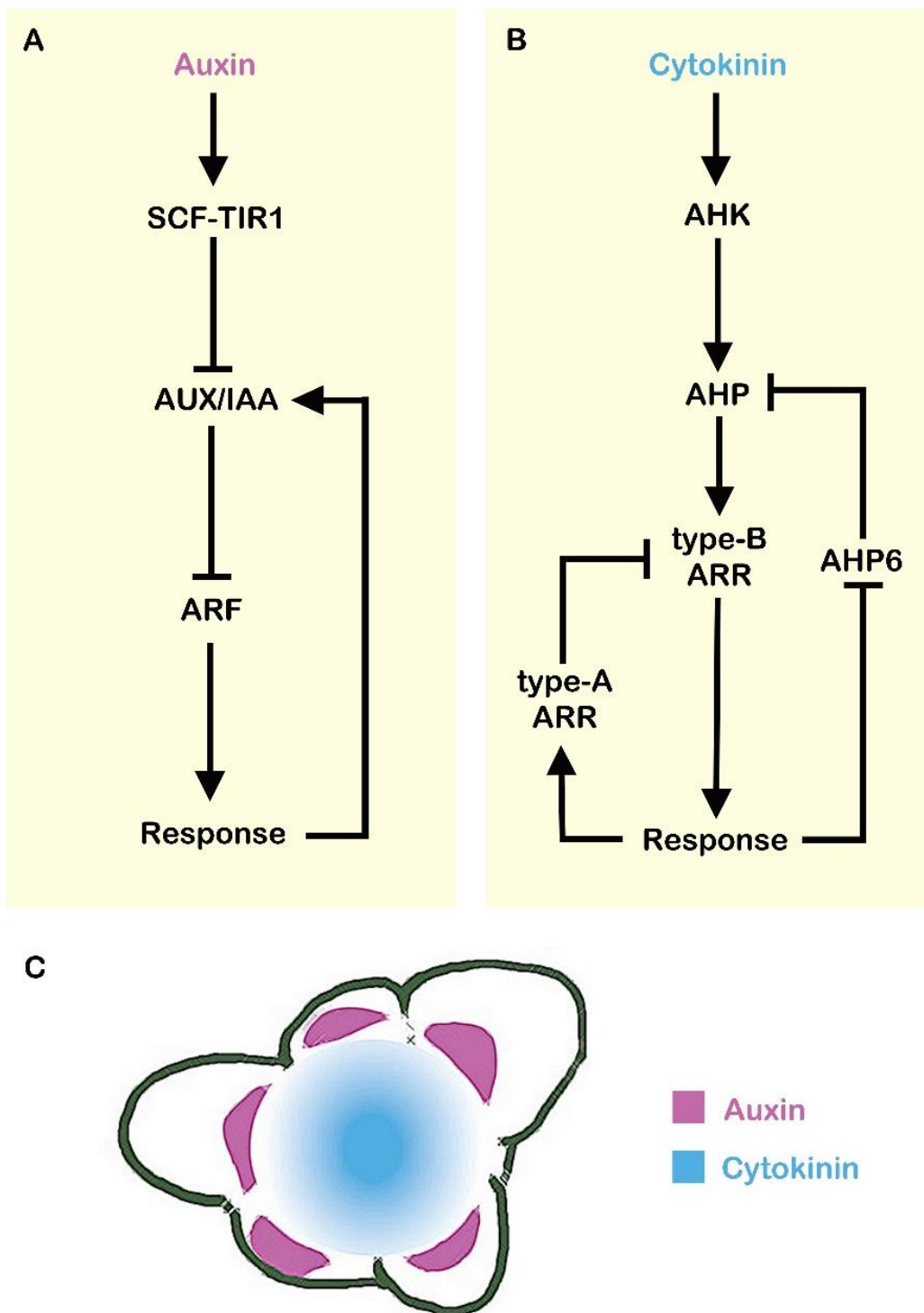
Figure 1.1 Key elements of auxin and cytokinin signal perception. Elements of the **(A)** auxin and **(B)** cytokinin signalling are outlined above as discussed in the text. **(C)** Auxin and cytokinin activity at the vegetative SAM showing auxin maxima at locations of primordia formation (purple) and cytokinin maximum at the OC (blue).

1.1.1.1 Auxins regulate SAM and leaf development

Auxin is a well-studied phytohormone. Indole-3-acetic acid (IAA) is the predominant auxin in plants. IAA biosynthesis occurs mostly through one tryptophan (Trp)-independent and four Trp-dependent pathways named after the main intermediates: the indole-3-acetamide (IAM), indole-3-acetaldoxime (IAOx), tryptamine (TAM), and indole-3-pyruvic acid (IPA) pathways. The TAM and IPA pathways are well studied in planta. The *TAA* gene family encode Tryptophan Aminotransferase of *Arabidopsis* 1 (TAA1), a long-predicted key enzyme in the IPA pathway, and its paralogue TRYPTOPHAN AMINOTRANSFERASE RELATED (TAR) catalyzes the transamination of tryptophan to form IPA. The IAA levels are reduced in *taa* mutants, and this shows that the TAA dependent IPA pathway contributes to IAA production (Sparks et al., 2013; Stepanova et al., 2008; Teale et al., 2006; Vanneste and Friml, 2009). However, TAA1 and YUCCA (YUC) proteins function in the same pathway for auxin biosynthesis (Stepanova et al., 2011). The flavin monooxygenase-like enzymes of the YUC family catalyze the conversion of the tryptophan to N-hydroxyl-tryptamine, a precursor of indole-3-acetaldoxime that can be subsequently used in the biosynthesis of IAA. In *Arabidopsis*, the YUC family has 11 members. Mutations in multiple *YUC* genes impair local auxin biosynthesis and accumulation, which results in severe developmental defects such as production of curled leaves and infertile radialised fruits (pin shaped) (Cheng et al., 2006). The auxin synthesized by YUC proteins is necessary for floral, leaf, root apex and shoot apex development (Cheng et al., 2006; Sparks et al., 2013; Teale et al., 2006; Vanneste and Friml, 2009).

In plants, high auxin concentrations are required for the initiation of a new organ (Fig 1.1C, 1.2). Auxin has two distinct major modes of transport: one is for rapid, long-distance source-to-sink transport through the vascular cambium and vascular parenchyma. The other, short-range transport occurs in a cell-to-cell manner by means of the polar distribution of particular influx and efflux carrier proteins. The AUXIN1/LIKE-AUX1 (AUX/LAX) family influx carrier proteins work to pump auxin into the cell, and the PIN-FORMED (PIN), ABC TRANSPORTER B (ABCB) and PIN-LIKES (PILS) efflux carrier proteins transport auxin from cells into the apoplast. The PINOID (PID) serine-threonine protein kinase facilitates trafficking of the PIN to the plasma membrane and directly controls PIN polarity via direct phosphorylation of the transporter (Friml et al., 2004;

Sparks et al., 2013; Teale et al., 2006; Vanneste and Friml, 2009). Auxin distribution is the key for auxin-mediated developmental processes (Larsson et al., 2014; Qi et al., 2014). Auxin accumulates locally within a single cell or a small group of cells generating auxin maxima, and as a result auxin gradients form within tissues. AUX1 and PIN1 are expressed in the SAM, and PIN transporters are required for the creation of auxin maxima (Fig 1.2) (Caggiano et al., 2017; Heisler et al., 2005). AUX1 is also required for the restriction of organ boundaries and *aux1* mutation results in the formation of fused organs and interferes with auxin uptake (Lincoln et al., 1990; Reinhardt et al., 2003). There are eight PIN proteins in *Arabidopsis*, and loss of PIN1 function leads to a characteristic pin or cup shaped leaf that is one of the hallmarks of defective auxin efflux (Aida et al., 2002; Friml et al., 2003; Furutani et al., 2004; Liu et al., 1993). Multiple *pin* mutants show defects in embryo development, organogenesis, and meristem patterning (Friml et al., 2003; Liu et al., 1993; Vieten et al., 2005). PIN1 regulates patterning at the meristem through the control of *CUP-SHAPED COTYLEDON* (*CUC*) gene expression (Aida et al., 2002; Furutani et al., 2004; Sparks et al., 2013; Teale et al., 2006; Vanneste and Friml, 2009; Vernoux et al., 2010). PID control organ separation and *pid* mutants also have pin-like inflorescences (Fig 1.2) (Christensen et al., 2000; Furutani et al., 2004; Vernoux et al., 2010).

Although much less is known about the ways the IAA is catabolized, different studies indicate that the oxidation of IAA into 2-oxindole-3-acetic acid (oxIAA) is most common mechanism to inactivate auxin (Stepanova and Alonso, 2016). In *Arabidopsis thaliana*, DIOXYGENASE OF AUXIN OXIDATION (DAO) enzymes catalyse the oxidative reaction (Zhang and Peer, 2017). Oxidation of IAA regulate several developmental processes, including root hair elongation, lateral root formation, rosette size, and fertility (Stepanova and Alonso, 2016; Zhang and Peer, 2017).

The complex auxin responses are perceived by two groups of genes and a four-protein receptor complex: *Aux/IAA* genes, *AUXIN RESPONSE FACTOR (ARF)* genes and the SCF[TIR1] complex (Sparks et al., 2013; Teale et al., 2006; Vanneste and Friml, 2009). The *Aux/IAA* gene family consists of 29 members in *Arabidopsis* (Rouse et al., 1998). *Aux/IAA* genes negatively regulate auxin signalling. Typically, *Aux/IAA* genes encode proteins with four highly conserved domains and have indeed been found in the nucleus. Domain I is

required for transcriptional repression, and Domain II (degron) is essential for auxin-stimulated Aux/IAA proteolysis. The other domains form homo- and heterodimers with ARFs. The ARFs (23 members in *Arabidopsis*) are a class of plant-specific transcription factors, which are grouped into three subsets and vary between 57 and 129 kDa in size. The amino acid sequence in a non-conserved central domain region determines whether a particular ARF can either activate or repress transcription (Ulmasov et al., 1999). The amino-terminal B3-like DNA-binding domain of ARFs bind to the auxin-responsive element (ARE; TGTCTC), a consensus sequence found in promoters of auxin-inducible genes, in an auxin-independent manner (Boer et al., 2014; Ulmasov et al., 1999; Ulmasov et al., 1995). The carboxy-terminal region of the Aux/IAA proteins interact with ARFs, and this interaction blocks ARE-mediated transcription (Sparks et al., 2013; Teale et al., 2006; Vanneste and Friml, 2009). The SCF^{TIR1} complex consists of the E3 ubiquitin-protein ligase RINGBOX PROTEIN 1 (RBX1), S PHASE KINASE ASSOCIATED PROTEIN 1 (SKP1), CULLIN 1 (CUL1) and F-box protein TIR1 (700 predicted F-box genes in *Arabidopsis*) (Dharmasiri et al., 2005; Gray et al., 2001; Kepinski and Leyser, 2005). The domain II (degron) of Aux/IAA interacts with TIR1, and auxin enhances interaction between Aux/IAA and TIR1. An increase in auxin levels recruits Aux/IAA-ARF inhibitors to the SCF^{TIR1} complex and directs Aux/IAA proteins for degradation by the 26S proteasome, releasing the ARFs so that they can act as transcription factors (Fig 1.1A) (Boer et al., 2014; Gray et al., 2001; Rouse et al., 1998). ARFs are highly involved in regulating organogenesis during plant development. Transcription factors ARF3 and ARF4 mediate the KANADI (KAN) pathway and establish leaf abaxial polarity, ARF7 and ARF19 regulate leaf expansion and lateral root development (Fahlgren et al., 2006; Hunter et al., 2006; Kelley et al., 2012; Nemhauser et al., 2000; Sessions et al., 1997; Sessions and Zambryski, 1995; Tsukaya, 2013; Vanneste and Friml, 2009). MONOPTEROS (MP) induces expression of LEAFY (LFY) and AINTEGUMENTA (ANT) to regulate organogenesis. MP is only expressed at the meristem periphery (Fig 1.2), and mutation in *MP* induces a *pin*-like phenotype (Aida et al., 2002; Bhatia et al., 2016; Vernoux et al., 2010). Auxin has emerged as a crucial hormone in the shoot meristem, and it is also associated with another essential hormone "cytokinin" in SAM development (Fig 1.1C) (Su et al., 2011).

1.1.1.2 Cytokinins regulate SAM and leaf development

The cytokinins are N6-substituted adenine-based molecules that affect many aspects of plant growth and development, including germination, root and shoot meristem function and leaf senescence (Kieber and Schaller, 2014; Santner et al., 2009; Wolters and Jurgens, 2009). The most abundant cytokinin in *Arabidopsis* is trans-zeatin (tZ). The enzyme ADENOSINE PHOSPHATE-ISOPENTENYLTRANSFERASE (IPT) converts AMP and dimethylallyl pyrophosphate (DMAPP) to the active cytokinin N6-(Δ2-isopentenyl)adenine (iP) riboside 5'-tri-, 5'-di- or 5'-monophosphate. The *Arabidopsis* genome encodes nine IPT enzymes, designated as AtIPT1 to 9. The cytokinins have isoprenoid side chains, and initial products are converted to tZ by hydroxylation of the isoprenoid side chain by a cytochrome P450 enzyme. Cytokinin ribotides are converted into active free-base cytokinins by the LONELY GUY (LOG) family of enzymes (LOG1-8 in *Arabidopsis*). LOG7 and LOG4 play a significant role in SAM growth, and disruption of *LOG* genes leads to severe retardation of shoot growth and defects in the maintenance of the apical meristem (Fig 1.2). The *Arabidopsis* genome encodes seven *CYTOKININ OXIDASE GENES* (*CKX*), and these enzymes break-down the N6-side chains from a subset of cytokinins (tZ and iP). *CKX* genes are induced rapidly upon cytokinin treatment, and overexpression of these genes leads to a reduced level of endogenous cytokinin. Long distance transport of cytokinins occurs in the xylem and phloem (Kieber and Schaller, 2014; Santner et al., 2009).

Cytokinins such as tZ and iP, as well as dihydrozeatin, benzyladenine and kinetin, directly bind to membrane-associated ARABIDOPSIS HISTIDINE KINASE RECEPTORS (AHK2, AHK3, and AHK4), and that binding occurs through the CHASE domain. AHK2 and AHK3 receptors are involved in the control of leaf cell formation and root branching (Hutchison et al., 2006; Riefler et al., 2006). AHKs transfer a phosphate to ARABIDOPSIS HISTIDINE-CONTAINING PHOSPHOTRANSFER (AHP) proteins (AHP1-5 in *Arabidopsis*) and these proteins are translocated into the nucleus where they phosphorylate ARABIDOPSIS RESPONSE REGULATOR (ARR) proteins (Hwang and Sheen, 2001; Kieber and Schaller, 2014; Santner et al., 2009; Sheen, 2002). The ARRs are transcription factors classified into two groups: negative (type-A ARRs) or positive (type-B ARRs) effectors of cytokinin signalling. There are ten type-A ARRs and eleven type-B ARRs in the *Arabidopsis* genome. The type-B ARRs (ARR14, ARR18, ARR19, ARR20, and ARR21) can alter or activate

cytokinin signalling. The type-B *arr* mutants exhibit reduced shoot development, aborted primary root growth, enlarged seed size and repression of cytokinin-regulated genes (Argyros et al., 2008; Mason et al., 2005). The type-A ARRs are transcriptionally induced in response to cytokinin, and these type-A ARRs (ARR3, ARR4, ARR5, ARR6, ARR7, ARR8, ARR9, and ARR15) function as negative regulators of cytokinin signalling (Fig 1.1B). Type-A *arr* mutants exhibited an increased sensitivity for the induction of cytokinin-regulated gene expression (Buechel et al., 2010; Jennifer et al., 2004; Kieber and Schaller, 2014).

The class I KNOTTED-LIKE (KNOX) homeobox transcription factors (SHOOT MERISTEMLESS (STM), BREVIPEDICELLUS (BP), KNOTTED-LIKE FROM ARABIDOPSIS THALIANA 2 (KNAT2), and KNOTTED1-LIKE HOMEOBOX GENE 6 (KNAT6) are required to establish and maintain the SAM (Fig 1.2). The KNOX transcription factors increase cytokinin levels in the SAM by inducing the expression of *IPT7*, and *KNOX* genes are up-regulated in response to induced elevation of cytokinin levels (Yanai et al., 2005). These studies show that there may be a positive feedback loop between cytokinin and KNOX signalling in the SAM. The low GA/high cytokinin environment in the SAM favours formation and maintenance of the SAM identity (Kieber and Schaller, 2014; Tsukaya, 2013; Vernoux et al., 2010). In the SAM, GA biosynthesis occurs in leaf primordia (Hu et al., 2008). *GA 20-oxidase* (*GA20ox*) and *GA 3β-hydroxylase* (*GA3ox*) genes regulate GA biosynthesis (Sun, 2008). In order to maintain SAM, STM and BP promotes cytokinin biosynthesis by inducing *IPT7* and suppress gibberellin biosynthesis in the SAM by downregulating GA-biosynthesis gene *GA20ox1* (Fig 1.2) (Hay et al., 2002; Jasinski et al., 2005). However, STM and BP do not regulate *GA3ox1* gene expression (Hay et al., 2002). Increased *GA3ox1-GUS* expression in the SAM and stem were previously reported and loss of *ga3ox1* affects both stem and leaf development, which suggests that *GA3ox1* function in SAM may be promoted by different pathway (Mitchum et al., 2006; Talon et al., 1990).

The transcription factor WUSCHEL (WUS) positively regulates cell proliferation in the SAM. In the SAM, cytokinin up-regulates WUS expression by CVL1/CLV3 and WUS represses *type-A ARR* gene expression to promote cell proliferation. WUS and the bHLH transcription factor HECATE 1 (HEC1) competitively regulate ARR7, and ARR7 is

repressed by WUS and activated by HEC1 (Fig 1.2) (Schuster et al., 2014). MP-mediated auxin signalling negatively regulates type-A ARRs (ARR7 and ARR15), which are negative regulators of cytokinin signalling (Fig 1.1, 1.2) (Schuster et al., 2014; Zhao et al., 2010). Auxin and cytokinin signalling maintain appropriate auxin and cytokinin concentrations during plant development. Auxin and cytokinin interactions are essential for organ formation and meristem function (Muller and Sheen, 2008; Su et al., 2011).

1.1.2 CLAVATA/WUSCHEL loop

The CZ harbours a small group of cells in the L3 layer underneath the stem cell region known as the organizing centre (OC) (Fig 1.2). Cells in the OC express the homeodomain protein WUS, and it is essential for the maintenance of the stem cell reservoir (Perales and Reddy, 2012; van der Graaff et al., 2009). In *wus* mutants, stem cells are not maintained and are consumed by developing organ primordia, resulting in premature termination of the SAM (Barton, 2010; Dodsworth, 2009; Miwa et al., 2009; Williams and Fletcher, 2005). The stem cells communicate with the OC via the CLAVATA (CLV) signalling pathway. The *CLV3* gene encodes a small secreted polypeptide that is produced by the stem cells in the CZ (L1 and L2). *clv3* mutants show enlarged SAMs accompanied by over-proliferation of cells in the CZ, and conversely, overexpression of *CLV3* results in reduced *WUS* expression and premature termination of the SAM. The *CLV1* gene encodes a leucine-rich repeat (LRR) receptor-like kinase, and the *CLV2* gene encodes an LRR receptor-like protein without a kinase domain; both are expressed in the L3 layer (OC) of the SAM. CLV3 interacts with the CLV1–CLV2 receptor complex in the L3 and overlaps with WUS expression in the L3 layer (Dodsworth, 2009; Miwa et al., 2009; Perales and Reddy, 2012). CLV signalling limits the size of the *WUS* expression domain by decreasing the number of *WUS*-expressing cells and inhibits cell division within the CZ, leading to a decrease in the number of *CLV3*-expressing cells. Decreased CLV3 production leads to an increase in the number of *WUS*-expressing cells, and this elegant negative feedback loop between CLV3 and WUS stabilizes the number of stem cells in the SAM (Fig 1.2) (Dodsworth, 2009).
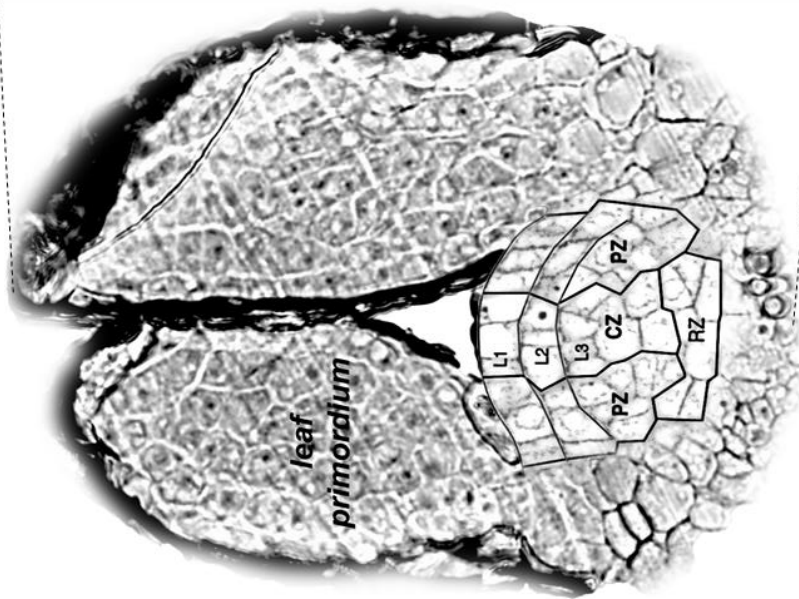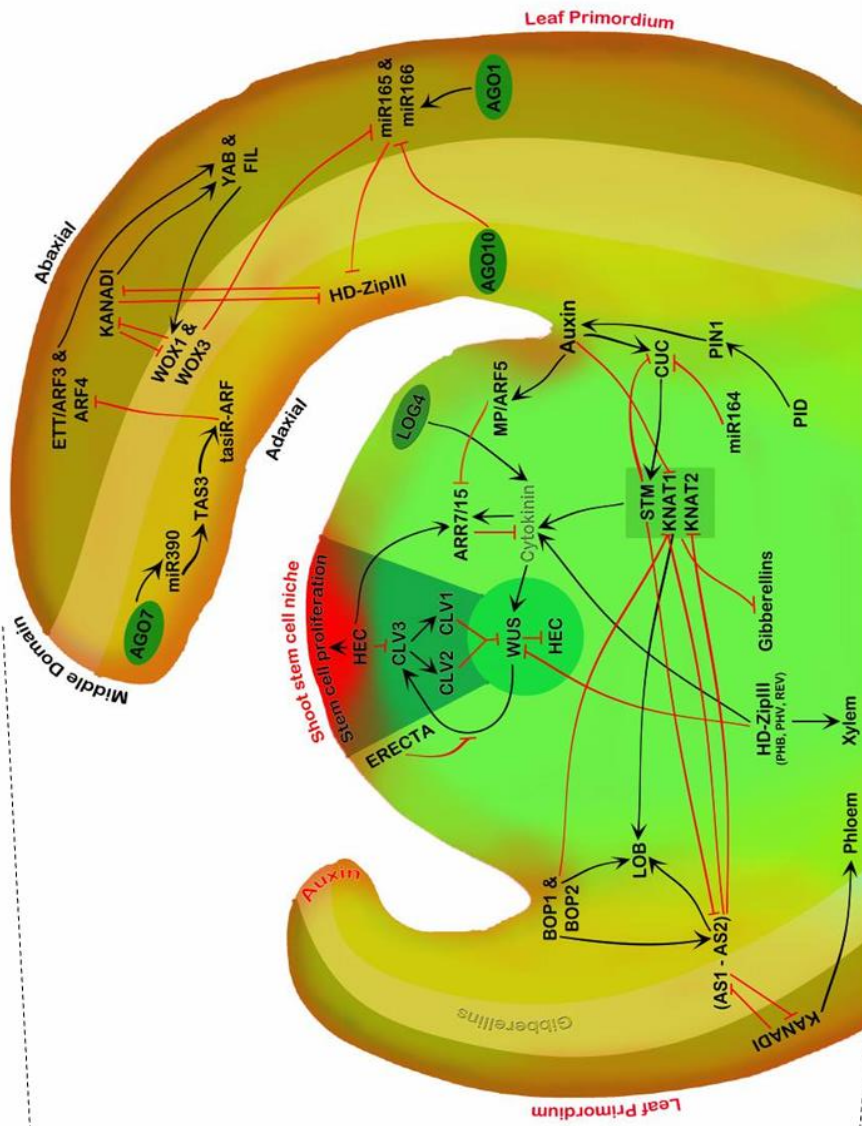
Figure 1.2 The shoot apical meristem of Arabidopsis thaliana and the integrated network of SAM regulation. A longitudinal section through the SAM (left) shows approximate outlines of the central zone (CZ), peripheral zone (PZ), rib zone (RZ) and cell layers (L1, L2 and L3). The population of stem cells at the apex of the meristem is maintained through HEC1, CLV and WUS signalling. The class III HD-ZIP proteins negatively regulate *WUS*, and WUS levels in turn are increased by cytokinins. Cytokinin biosynthesis is increased by *LOG4, HD-ZIP III* and *KNOX* genes (*STM, KNAT1* and *KNAT2*) that are expressed in the meristem. Cytokinins induce expression of *ARR7/15*, and auxin-induced MP inhibits ARR7/15 activity. The class III *HD-ZIP* transcripts are targets of miRNA 166/5. AGO10 positively regulates class III HD-ZIP proteins by preferentially loading miRNA 166/5. YABBYs, KAN, ARF3 and ARF4 are expressed in the abaxial domain; WOX1 and WOX3 are expressed in mid-domain; AS1, AS2, AGO7 and class III HD-ZIP proteins are expressed in adaxial domain of leaf primordia. In the leaf primordia: AGO7 inhibits *ARF3/4* expression to preserve the adaxial domain, KAN inhibits class III HD-ZIP proteins to preserve the abaxial domain and WOX1/3 inhibits KAN to preserve the mid-domain. KNOX proteins inhibit gibberellins in the SAM. KNOX interactions are as follows: AS1-AS2 inhibit *KNAT1*, *KNAT2* and *KNAT6* expression, STM inhibits *AS1-AS2* to prevent differentiation, CUC activates STM, and STM restricts *CUC* expression by inducing miR164. LOB is activated by AS1, A2, BOP1, BOP2 and KNAT1. Note in the diagram that the regions of high auxin activity in leaf primordia are demarcated in red and high cytokinin activity within the central meristem in green.

1.1.3 Adaxial, abaxial and boundary genes

During germination, the SAM becomes active and stem cells in the CZ divide into founder cells, and these are pushed outward into the peripheral zone to form leaf primordium (Barton, 2010; Tsukaya, 2013). At this stage, the leaf primordium establishes polarity along the adaxial (upper side) and abaxial (lower side) axis. The adaxial side of leaf primordium is closest to the SAM, and abaxial is away from the centre of the SAM (Fig 1.2). Class III HOMEO DOMAIN LEUCINE ZIPPER (HD-ZIP) transcription factors PHABULOSA (PHB), PHAVOLUTA (PHV), REVOLUTA (REV), CORONA (CNA) and INCURVATA promote adaxial leaf fate (upper side of the leaf) (Elhiti and Stasolla, 2009; Liu et al., 2009; Mallory et al., 2004; McConnell et al., 2001; Zhou et al., 2007). HD-ZIP III transcription factors also downregulate WUS transcription in wild-type plants, and this shows that HD-ZIP III repress stem cell fate in the SAM. Loss of *HD-ZIP III* results in embryo defects with an enlarged SAM and formation of radial and abaxialised leaves (Barkoulas et al., 2007; Fambrini and Pugliesi, 2013; Szakonyi et al., 2010; Tsukaya, 2013). *HD-ZIP III* genes positively regulate the transcription of *LITTLE ZIPPER* (*ZPR*) genes and ZPR proteins negatively regulate HD-ZIP III activity by forming heterodimers with HD-ZIP III proteins (Kim et al., 2008; Wenkel et al., 2007). In addition to *ZPRs*, *HD-ZIP III* transcripts are degraded by microRNAs (miRNAs) miR165/166 in *Arabidopsis* (Fig 1.2) (Zhu et al., 2011b).

Transcription factors YABBY (YAB), KANADI (KAN), ETTIN (ETT)/AUXIN RESPONSE TRANSCRIPTION FACTOR 3 (ARF3) and ARF4 promote abaxial leaf fate (lower side of the leaf) (Fig 1.2) (Tsukaya, 2013). *FILAMENTOUS FLOWER* (*YAB1/FIL*), *YAB2*, *YAB3,* and *YAB5* are members of the *YAB* gene family. *YAB* family genes encode HIGH-MOBILITY GROUP (HMG)-like proteins and interact in a complex with LEUNIG and LEUNIG-LIKE co-repressors as well as the co-regulator SUESS. Loss of *YAB1* and *YAB3* leads to partial loss of abaxial fate (Eshed et al., 2004; Kumaran et al., 2002; Sarojam et al., 2010; Siegfried et al., 1999). The combined loss of *ARF3* and *ARF4* genes results in adaxialised leaves. ARF3 and ARF4, are negatively regulated by trans-acting small interfering RNA (TAS3) via miR390 (Fahlgren et al., 2006; Garcia et al., 2006; Hunter et al., 2006).

KAN (*KAN1, KAN2, and KAN3*) genes are GARP-domain transcription factors and loss of *KAN* gene function results in adaxialisation of leaves. KAN promotes abaxial fate through

suppression of the adaxial *HD-ZIP III* transcription factors and LOB-domain transcription factor *ASYMMETRIC LEAVES2* (*AS2*). AS2 also suppresses *KAN* genes, class *I KNOX* genes, and *ARF3* (Emery et al., 2003; Kelley et al., 2012; Tsukaya, 2013). KAN and HD-ZIP III transcription factors suppress each other to promote abaxial and adaxial leaf fate (Emery et al., 2003). In addition to the two-domain theory (adaxial and abaxial), Nakata et al. (2012) reported a three-domain theory (adaxial, middle and abaxial). Nakata et al. (2012) found that *PRESSED FLOWER (PRS)/WUSCHEL-RELATED HOMEOBOX 3 (WOX3)* and *WOX1* genes promote middle domain leaf fate. In *prs wox1* double mutants, adaxial and abaxial-like cell types coexist in the region neighbouring the margin and this suggest *PRS* and *WOX1* are required for normal patterning of adaxial and abaxial side–specific tissues in the lateral region (Nakata et al., 2012; Nakata and Okada, 2012). A recent study reported that YAB1 is also expressed in the middle domain, and this suggests that the middle domain is a part of the abaxial domain. *KAN* family genes suppress the expression of both middle domain genes *WOX1* and *WOX3* (Fig 1.2) (Nakata et al., 2012; Nakata and Okada, 2012; Tsukaya, 2013).

As the leaf primordium grows away from the SAM, a clear physical boundary is formed between the developing leaf and the SAM. The *LATERAL ORGAN BOUNDARY* (*LOB*)*, CUC* and *BLADE ON PETIOLE* (*BOP*) gene families express at the boundary and regulate leaf development (Fig 1.2). JAGGED LATERAL ORGANS (JLO) and LOB are the members of the LOB family. Loss of *JLO* leads to inactivation of SAM and causes leaf lobing (Fambrini and Pugliesi, 2013; Szakonyi et al., 2010; Tsukaya, 2013). *JLO* upregulates *KNOX* expression, and *LOB* is activated by *BP/KNAT1* (*KNOX* gene), *AS1, AS2, BOP1* and *BOP2*. BOP 1 and 2 activate AS1-AS2 on the adaxial side of leaf primordium and suppress the expression of class *I KNOX* genes in leaf primordia (Ikezaki et al., 2010; Tsukaya, 2013). In the *bop* mutant, the adaxial and abaxial polarity is disturbed, and ectopic lamina is formed in the place of the petiole (Tsukaya, 2013). CUC genes (CUC1-3) encode NAC domain transcription factors, and they promote expression of class *I KNOX* genes (STM and KNAT6). Conversely STM represses *CUC1* and *CUC2* transcripts by activating miR164 (Fig 1.2). CUC transcription factors regulate development of leaf marginal structures, and *cuc* mutants lack SAM and form goblet-shaped cotyledons (Hasson et al., 2011; Laufs et al., 2004; Sieber et al., 2007; Spinelli et al., 2011; Taoka et al., 2004). Different miRNAs maintain the level of abaxial/ adaxial identity and boundary genes by cleaving the target

mRNA. These miRNAs are transcribed by RNA-dependent RNA polymerases and processed by DICER like, and ARGONAUTE (AGO) proteins, which are central to plant small-RNA biogenesis and function (Fig 1.3).

1.2 ARGONAUTE proteins

In plants, transcriptional gene silencing (TGS) maintains genome integrity and post-transcriptional gene silencing (PTGS) control the expression of mRNA transcripts to regulate defence against invading pathogens, developmental transition and responses to environmental stresses. RNA silencing pathways are directed by a specific class of small RNA (sRNA) such as short interfering RNAs (siRNAs) and microRNAs (miRNAs) or hairpin RNAs (hpRNAs) (Axtell, 2013; Voinnet, 2009). Small RNAs derived from single-stranded precursors with a hairpin structure are called hpRNAs or miRNAs and those derived from double-stranded precursors referred to as siRNAs. Regulatory small RNAs in plants are predominantly 18 to 21 nucleotides in length. Biochemical steps involved in the plant RNA silencing pathways are (1) double-stranded RNA (dsRNA) synthesis, (2) dsRNA processing into 18–21 nucleotide long sRNAs, (3) methylation of sRNA, and (4) sRNA incorporation into effector RNA-induced silencing complex (Fig 1.3) (Axtell, 2013; Brodersen and Voinnet, 2006; Rubio-Somoza and Weigel, 2011; Voinnet, 2009).

Generally, dsRNA is synthesized by one of six RNA-DEPENDENT RNA POLYMERASES (RDR1–6) using an RNA template. DAWDLE (DDL) stabilizes pri-miRNAs or dsRNA for their conversion in nuclear processing centre called D-body. The physical interaction of the C2H2-zinc finger protein SERRATE (SE) with the double-stranded RNA-binding protein HYPONASTIC LEAVES1 (HYL1), one of the DICER RNase III-like endonuclease family (DCL1-4) proteins and nuclear cap-binding complex (CBC) occurs in the D-body. These proteins interact in order to process dsRNA and result in the release of short double-stranded duplexes 18–21 nucleotides long. Upon dicing by DCL, sRNA duplexes are either retained in the nucleus for TGS or exported to the cytoplasm for PTGS. Mature miRNAs are exported to the cytoplasm through the action of the exportin 5 orthologue HASTY. Exported mature miRNAs are methylated by HUA ENHANCER 1 (HEN1), and this reaction protects miRNAs from being degraded by the SMALL RNA DEGRADING NUCLEASE (SDN) class of exonucleases (Axtell, 2013; Brodersen and Voinnet, 2006;

Rubio-Somoza and Weigel, 2011; Voinnet, 2009). The miRNA is loaded into a RNaseH-like ARGONAUTE (AGO) protein to form the catalytic core of an RNA-induced silencing complex (RISC) that scans the cell for complementary nucleic acids to execute their function. AGO proteins carry out the RNA silencing reaction by endonucleolytic cleavage or ''slicing'' at the centre of sRNA-target hybrids (Fig 1.3). This depends on the class of sRNA loaded by AGO and AGO protein family member loaded with the sRNA (Hock and Meister, 2008; Kim, 2011; Meister, 2013). AGOs are large proteins that typically have a molecular weight of 90-100 kDa and are composed of a single variable N-terminal domain and a conserved C-terminal domain, including the PAZ, MID and PIWI domains. The N-terminal domain regulates the separation of the sRNA-target hybrid duplex post cleavage. The PAZ and MID domains anchor the 3' and 5' ends of the bound sRNA to the target mRNA, and PIWI domain specifies the endonuclease or slicer activity (Fig 1.3). PIWI domains show extensive homology to RNase H and carry an Asp-Asp-His (DDH) motif in its active site. Mutation in the DDH motif abolishes the endonuclease activity of AGOs (Hock and Meister, 2008; Kim, 2011; Meister, 2013).

1.2.1 ARGONAUTE proteins control SAM and leaf development

AGO proteins are encoded by different species, and many organisms encode multiple members of the family. The *Arabidopsis* genome encodes ten AGO family members. Loss-of-function *ago* mutants display different plant developmental defects such as the establishment of leaf adaxial-abaxial polarity, shoot apical meristem and root development (Kim, 2011; Zhang and Zhang, 2012; Zhu et al., 2011b). AGO1 is the prominent member of the *Arabidopsis* AGO protein family because it is required for the function of most miRNAs including miR165/166. AGO1 represses the HD-ZIP III transcripts in the abaxial domain via miR165/166 (Fig 1.2). The closest homologue of the *AGO1* gene is *AGO10* and has 78% identity with *AGO1* in their PAZ/PIWI domains but less than 20% similarity in their N-terminal regions. Some of the *ago1* mutant phenotypes resemble those of *ago10* mutants, and double mutants result in embryonic lethality (Kim, 2011; Zhang and Zhang, 2012; Zhu et al., 2011b).

AGO1 and 10 compete for miR165/166, although AGO10 has a stronger binding affinity for miR166 than AGO1 (Lynn et al., 1999; Mallory et al., 2009). Zhu et al. (2011) found that in the *ago10* mutant miR166 has increased binding affinity to AGO1, which resulted

in the down-regulation of HD-ZIP III transcripts. AGO10 possesses the DDH motif and plants expressing AGO10, or *AGO10 DDH* mutants showed normal *HD-ZIP III* family gene expression. Zhu and colleagues also showed that AGO10 positively regulates *HD-ZIP III* family genes by acting as a specific decoy for miR166/165, and that AGO10 is not involved in the translational repression of *HD-ZIP III* genes (Fig 1.2) (Zhang and Zhang, 2012; Zhu et al., 2011b). This shows that AGO10 preserves adaxial identity by regulating HD-ZIP III, and it also behaves very differently from other AGOs.

Transacting short interfering RNA (siRNA) are derived from non-coding, single-stranded transcripts, the pri-tasiRNAs, are converted into dsRNA by DCL4, RDR6, DRB4, and SGS3. Similar to miRNAs, mature tasiRNAs guide cleavage and degrade cellular transcripts. In *Arabidopsis*, there are three ta-siRNA gene families (*TAS1, TAS2*, and *TAS3*) that are transcribed to produce tasiRNAs (Axtell, 2013; Fahlgren et al., 2006; Kim, 2011; Rubio-Somoza and Weigel, 2011; Voinnet, 2009). In TAS3 tasiRNA biogenesis, miR390 is explicitly loaded to AGO7 and triggers production of a TAS3 family of secondary siRNA. ARF3 (ETTIN) and ARF4 transcription factors specify leaf abaxial identity, and their transcripts are cleaved by AGO1 loaded with TAS3-derived trans-acting siRNA (Garcia et al., 2006; Iwasaki et al., 2013; Takahashi et al., 2013). TAS3 and AGO7 are expressed in the adaxial leaf domain, and their product tasiR-ARF regulates *ARF3/4* in this region. This shows that AGO7 preserves adaxial identity by suppressing abaxial domain genes *ARF3/4* (Fig 1.2) (Endo et al., 2013; Fahlgren et al., 2006; Hunter et al., 2006; Montgomery et al., 2008). The interplay between AGO10-loaded miR165/166 and AGO7- loaded miR390 sets the precise gradient boundaries between the abaxial and adaxial domains. These studies show that AGO1, AGO7 and AGO10 play an important role in SAM and leaf development (Fig 1.2).

ARGONAUTE

RNA Binding

Active Site
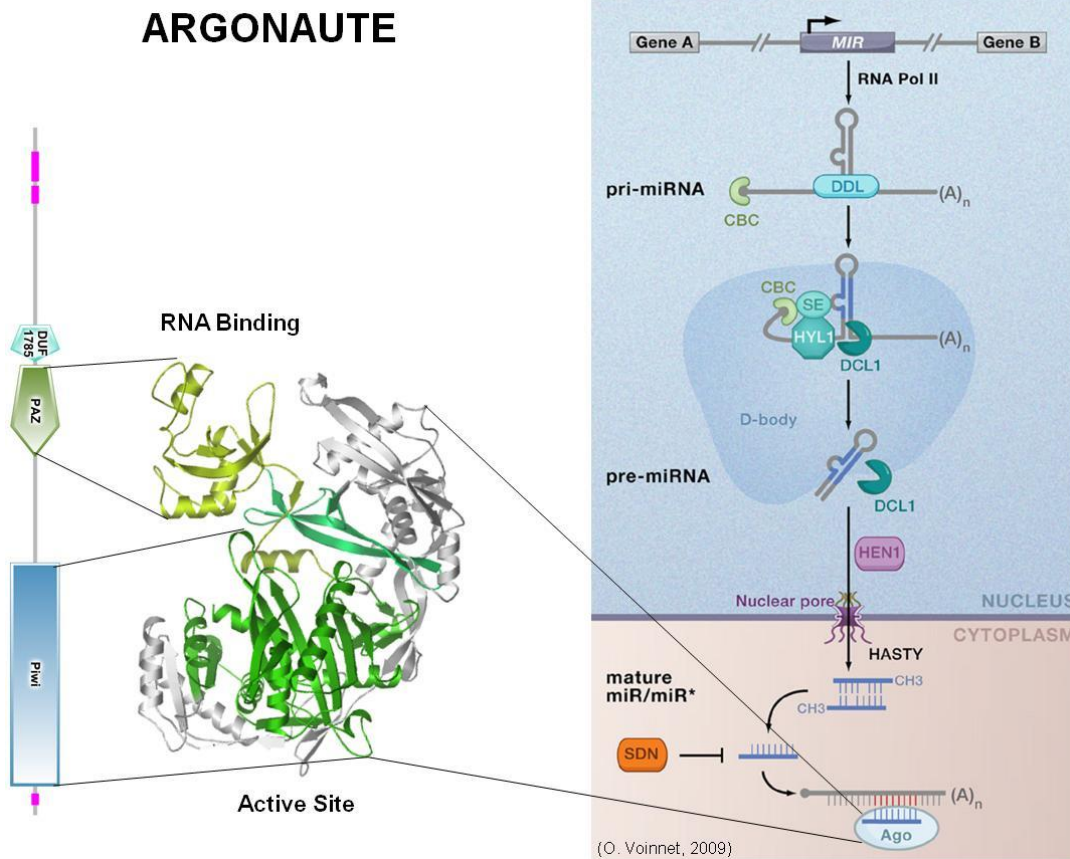
(O. Voinnet, 2009)

Figure 1.3 Biogenesis of Plant miRNAs and Structure of the Argonaute protein, modified image from (Voinnet, 2009). Plant pri-miRNAs are transcribed by RNA-dependent RNA polymerases (RNA Pol II), and protein DAWDLE (DDL) stabilises pri-miRNAs for their conversion in D-bodies (SE, HYL1, DCL1, and CBC) to stem-loop pre-miRNAs. The mature miRNAs produced by DCL1 are methylated by HEN1 and exported to the cytoplasm through HASTY. The non-methylated miRNA* is degraded by the SDN class of exonucleases. The miRNA strand is then incorporated into AGO proteins to carry out the RNA silencing reaction by slicing. Argonaute proteins consist of a variable N-terminal domain and three conserved C-terminal domains, the PAZ, MID and PIWI domains. PAZ and MID domain are required for small RNA binding, and the PIWI domain specifies the endonuclease activity.

1.3 Similar genes regulate SAM and floral to fruit transition

The juvenile SAM undergoes a complex transition to form a mature fruit. The juvenile SAM generates leaves and shoots during the vegetative phase, and in the reproductive phase, it becomes an inflorescence meristem and flowers are produced. After fertilisation, the female parts of the flower develop into a fruit. The transition from juvenile shoots to more mature vegetative shoots and the subsequent transition from the vegetative phase to the formation of inflorescence varies considerably among angiosperms. In recent years, studies on the mechanisms of differentiation of the floral meristem and their lateral outgrowths focused on *Arabidopsis* and tomato. In *Arabidopsis*, *LEAFY* (*LFY*) and *APETALA1* (*AP1*) genes promote initial floral meristem identity (Fletcher, 2002; Vijayraghavan et al., 2005). AGAMOUS (AG) is necessary for stem cell termination because the termination of stem cell activities in the floral meristem is required for normal flower development (Fletcher, 2002). Similar to the SAM, WUS also regulates stem cells in the floral meristem. AG terminates stem cells in the floral meristem by repressing the expression of the stem cell regulator WUS (Fig 1.4) (Fletcher, 2002). In the SAM, AGO1, AGO10 and HD-ZIP III transcription factors regulate stem cells and leaf development (Fig 1.2). Indeterminate flower, AGO10 is expressed in the floral meristem and the adaxial side of carpels. AGO1, AGO10, miR172-mediated regulation of *AP2* gene and miR165/166-mediated regulation of *HD-ZIP III* genes are necessary for floral stem cell termination. AGO10 regulates floral stem cell termination by repressing the expression of the WUS (Fig 1.4) (Ji et al., 2011; Landau et al., 2015). Loss of *AGO10* and reduced expression of the *HD-ZIP III* genes result in opposite effects on stem cell regulation between the SAM and the floral meristems (Ji et al., 2011; Landau et al., 2015; Tucker et al., 2013; Zhou et al., 2015; Zhu et al., 2011b). The reason for opposite effects in the two types of meristems is currently unknown, and this missing link should be investigated.

SAMs form leaves and associated meristems, whereas the floral meristem generates sepals, petals, stamens, and carpels (Fig 1.4). The *Arabidopsis* gynoecium is derived from the fusion of two carpels. It is a highly complex assembly comprised of different tissues that work together to support fertilisation and fruit development. These processes are regulated by different proteins and particularly the basic helix-loop-helix

(bHLH) transcription factors. In *Arabidopsis*, bHLH proteins are also involved in SAM developmental signalling, stomatal patterning, trichome, and root hair differentiation and axillary meristem formation (Li et al., 2006; Toledo-Ortiz et al., 2003; Zhao et al., 2012). The bHLH transcription factor superfamily is one of the largest transcription factor families in *Arabidopsis*. There are 147 *bHLH* genes in *Arabidopsis*, and based on structural analysis they are divided into 12 subfamilies (Li et al., 2006; Toledo-Ortiz et al., 2003). The bHLH is defined by the signature domain, which consists of 60 amino acids with two functionally distinct regions (N-terminal end and C-terminal end). The N-terminal end of the domain comprises 15 amino acids, this domain is involved in DNA binding (E-box binding (5'-CANNTG-3') and non-E-box binding) and the C-terminal end is essential for dimerization.

The patterning of gynoecia occurs along three axes: apical-basal, mediolateral, and abaxial-adaxial (Fig 1.4). The bHLH transcription factors SPATULA (SPT), HECATE1 (HEC1), HEC2 and HEC3 are involved in apical-basal patterning of the gynoecium by carpel fusion as well as transmitting tract formation (Fig 1.4) (Gremski et al., 2007; Ostergaard, 2009). Mutations in the *SPT* gene lead to defects in the development of the stigma, style, septum and transmitting tract. Similar defects were observed in *hec* double and triple mutants. The HEC proteins physically interact with SPT in yeast two-hybrid assays, which suggests that these factors may jointly activate or repress downstream target genes (Gremski et al., 2007; Ostergaard, 2009; Seymour et al., 2013). However, HEC1 is also involved in SAM stem cell maintenance by balancing proliferation versus differentiation (Fig 1.2) (Schuster et al., 2014). HEC1 function is critically dependent on SPT for stem cell proliferation (Schuster et al., 2014). In the SAM, HEC1 regulates cytokinin signalling by activating ARR7 (Fig 1.2).

HEC1 and SPT buffer auxin and cytokinin signals during gynoecium development (Fig 1.4). SPATULA enables cytokinin signalling by activating *ARR1* expression in gynoecia, and SPT is necessary for positive cytokinin signalling output in the young gynoecium (Reyes-Olalde et al., 2017). HEC1 and SPT stimulate auxin biosynthesis and activate the expression of PIN3 and regulate auxin distribution during early stages of gynoecium development. Auxin also activates ETT and restricts apical tissue proliferation by negatively regulating HEC1 and SPT (Nemhauser et al., 2000; Schuster et al., 2015).

INDEHISCENT (IND) belongs to the same clade of the *Arabidopsis* bHLH family as the HEC1/2/3 and IND is a paralogue of HEC3 that is only present in the *Brassicaceae* (Kay et al., 2013b). Interestingly, *hec spt* phenocopies *ind spt* unfused carpel phenotype and *35S::HEC1* inflorescence also looks similar to *35S::IND* inflorescence (Girin et al., 2011; Schuster et al., 2015; Sorefan et al., 2009a). However, IND do not interact with HEC1/2/3 or regulate their gene expression, which suggest they may function independently (Gremski, 2006). Similar to HEC1/2/3, IND also interact with SPT and regulates a common set of target genes (Girin et al., 2011; Gremski et al., 2007). Interestingly, IND directly regulates *SPT* gene expression (Girin et al., 2011; Groszmann et al., 2010; Ichihashi et al., 2010b). SPT and IND control radiality at the gynoecium apex by controlling polar auxin transport (PAT) (Moubayidin and Ostergaard, 2014), which is essential for medial versus lateral tissue specification in gynoecia (Larsson et al., 2014). SPT and IND control PAT by repressing *PINOID* (*PID*) expression, and this promotes apolar PIN localisation and subsequent formation of the radial auxin ring at the gynoecium apex (Moubayidin and Ostergaard, 2014). These studies show the close relationship between HECs, SPT and IND in fruit development signalling (Fig 1.4) (Girin et al., 2011; Liljegren et al., 2004a; Ostergaard, 2009; Seymour et al., 2013).

CUC genes regulate SAM formation and separation of organs from the meristem. They are expressed in the boundaries between organs (Wang et al., 2016). Overexpression of *CUC1* and *CUC2* prevents carpel fusion in the apical region. Interestingly *CUC1* and *CUC2* expression is negatively regulated in the apical region of the gynoecial primordium by *SPT,* and this repression is essential for carpel fusion (Nahar et al., 2012). These studies show that SPT, HEC1 and CUC1 play key roles in SAM development as well as carpel fusion (Fig 1.2, 1.4). Similar to SPT-HEC1 in SAM, we do not know if SPT-IND has a role in SAM development and this should be investigated.
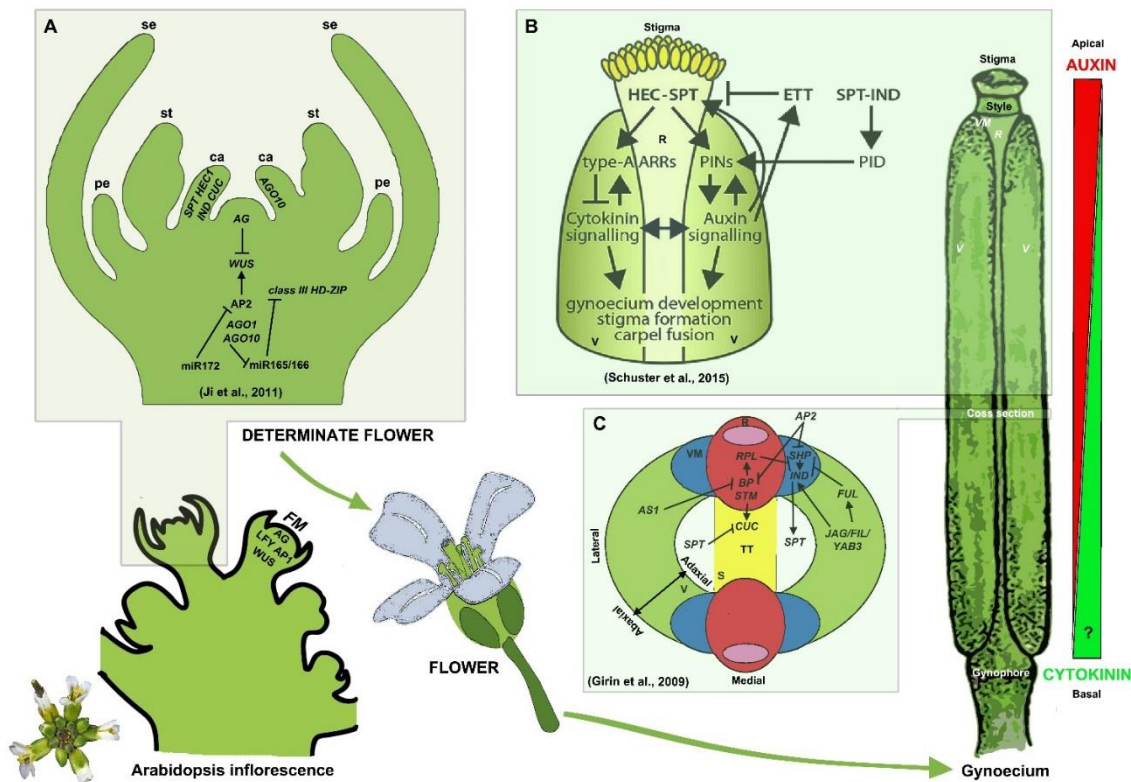
Figure 1.4 Key elements of Arabidopsis floral to gynoecium development pathway (1.4B modified image from (Schuster et al., 2015)). *Arabidopsis* inflorescence is showing floral meristem (FM) and determinate flower. (A) FM produce sepals (se), petals (pe), stamens (st) and carpels (ca). The stigma, style, valve (V), replum (R), septum (S), transmitting tract (TT), valve margin (VM) and gynophore are the different regions of the gynoecium. Distribution of auxin (red) and hypothetical distribution of cytokinin (green) across the apical-basal axis of the gynoecium. **(A)** AG, AGO1, AGO10 and class III HD-ZIPs regulate FM differentiation by controlling WUS. SPT heterodimerise with HEC and IND to regulate carpel development. The gynoecium is derived from the fusion of two carpels. **(B)** HEC1, SPT and IND buffer auxin and cytokinin signals to regulate stigma formation and gynoecium development. **(C)** Schematic cross-section of gynoecium showing different tissue regions across mediolateral axes with genetic interactions outlined above as discussed in the text.

The fruit develops from the gynoecium after fertilisation. The stigma, style, ovary, and gynophore are the four different regions of the gynoecium and the fruit. The ovary houses the developing seeds and comprises several distinct tissues: two valves (seedpod walls), replum (middle ridge), septum, and valve margins. The replum has meristematic properties because early repla are essential for the development of all the marginal tissues of the fruit (septum, repla, style, and stigma) (Girin et al., 2009; Roeder and Yanofsky, 2006). Replum development is promoted by the BEL1-like homeodomain transcription factor REPLUMLESS (RPL). RPL also regulates stem cell fate in the SAM by interacting with *KNOX I* meristem gene *BP/KNAT1* (Bhatt et al., 2004; Cole et al., 2006). Interestingly, KNOX I meristem genes *BP* and *STM* is also expressed in the replum and are involved in replum development (Ragni et al., 2008). ASYMMETRIC LEAVES (AS1) and AS2 are involved in leaf primordia formation by silencing *class I KNOX* meristem identity genes (Iwasaki et al., 2013; Xu et al., 2003). Similar to leaf primordia, AS1 is involved in medio-lateral patterning of the fruit, particularly regulating valve and replum development (Alonso-Cantabrana et al., 2007). AS1 possibly does this by negatively regulating *class I KNOX* meristem identity genes. CUC transcription factors activate *KNOX I* meristem gene *STM* expression in the SAM and STM restricts *CUC* expression by inducing miR164 (Laufs et al., 2004; Spinelli et al., 2011). In gynoecia, *CUC1* and *CUC2* are expressed in the inner edge and the middle of the septum (Kamiuchi et al., 2014; Nahar et al., 2012). CUC1 and CUC2 are required for septum and replum formation. These studies demonstrate that *RPL*, *AS1*, *KNOX I* and *CUC* genes regulate both SAM development and formation of medial tissues in gynoecium (Fig 1.2, 1.4).

The valve margins are the zones where the fruit opens. Each valve margin consists of two layers: a separation layer and a lignified layer. These layers allow the valve to separate from the replum. The SHATTERPROOF 1 (SHP1) and SHP2 MADS-box genes specify valve margin identity (Fig 1.4) (Liljegren et al., 2000). SHP positively regulates bHLH transcription factors *IND* and *ALCATRAZ* (*ALC*) (Liljegren et al., 2004a). IND and ALC heterodimerize to specify the separation layer, and IND is primarily responsible for the development of the lignified layer of the valve margin. A local auxin minimum is necessary for specification of the valve margin (Sorefan et al., 2009a). IND creates auxin minima in the valve margin cells by inhibiting PID and related kinases to direct the localisation of PIN auxin efflux carriers (Sorefan et al., 2009a). RPL negatively regulates

SHP, restricting its expression to the valve margin (Roeder et al., 2003). The MADS-box gene *FRUITFULL* (*FUL*) indirectly regulates valve cell development. In the *ful* mutant, *SHP*, *IND*, and *ALC* are all ectopically expressed throughout the valves, indicating that FUL negatively regulates *SHP*, *IND*, and *ALC* to prevent valve cell lignification (Fig 1.4) (Roeder et al., 2003). In the fruit, JAGGED (JAG)/ FILAMENTOUS FLOWER (FIL) activity promotes valve and valve margin formation. JAG/FIL positively regulates the valve-promoting gene *FUL* and the valve margin identity genes *SHP1, SHP2, IND* and *ALC* (Fig 1.4) (Gonzalez-Reig et al., 2012). In the SAM, JAG/FIL activity promotes leaf formation and abaxial leaf specification (Fig 1.2) (Kumaran et al., 2002; Siegfried et al., 1999). Interestingly, induced overexpression of *IND* produces several phenotypes, such as pin and cup shaped leaves (Fig 1.5) (Moubayidin and Ostergaard, 2014). *IND* overexpression phenocopies *ago10, hd-zip iii*, *cuc* mutants and *35S::miR166a* transgenic seedlings (Fig 1.5). IND-SPT regulates PAT in gynoecia. PAT also regulates leaf patterning in SAM (Reinhardt et al., 2003). This suggests that IND could regulate PAT and meristem genes to control SAM or leaf development, but this should be investigated further.

1.4 Hypothesis and Objectives

The studies discussed in section 1.3 demonstrate that genes involved in SAM development also regulate gynoecium and fruit development (Fig 1.5). IND regulates PAT and patterning in gynoecium and fruit. An important question to address is what roles does IND play to regulate SAM. We hypothesised that IND is associated with PAT and the AGO10-HD-ZIP III pathway to control SAM and leaf development in *Arabidopsis*. The first results section of my thesis will examine the link between IND and AGO10-HD-ZIP III pathway. The second results chapter will detail how other SAM-associated proteins are involved in the IND-AGO10-HD-ZIP III pathway. The third results chapter will detail how auxin and cytokinin regulate the IND gene-regulatory network. My three result chapters integrate experimental data and pathway construction and develop novel insights into how AGO10-IND function in SAM and gynoecium.
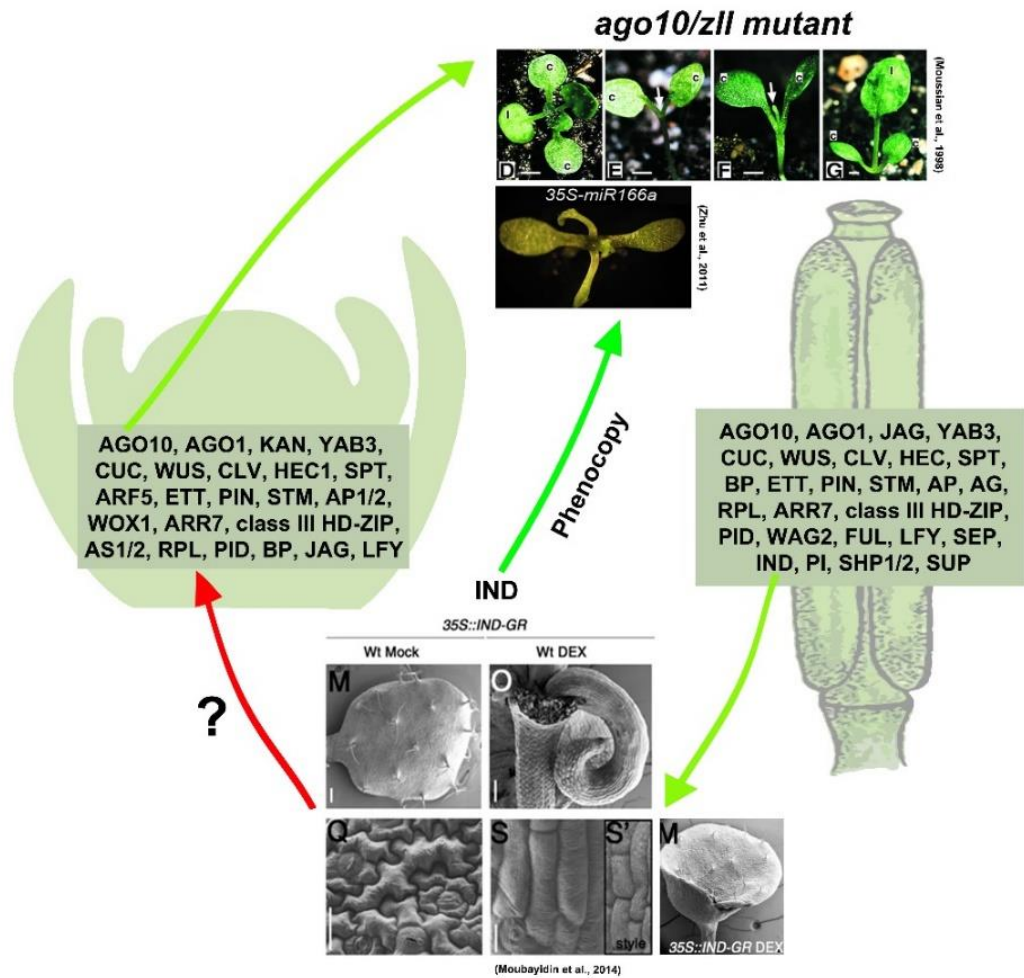
Figure 1.5 Similar genes regulate SAM (left) and fruit (right) development. Induced overexpression of *IND* produces several phenotypes (*35S::IND:GR*+DEX: pin and cup shaped) similar to *ago10* mutant and *35S::miR166a* transgenic seedlings (*ago10* E-G: no-meristem, pin and cup shaped). Phenotypes suggest that IND may have a regulatory role in the SAM, but the elements of this regulatory pathway are unknown.

Chapter 2
Materials and Methods

CHAPTER 2. Materials and Methods

2.1 Materials

2.1.1 General laboratory materials

General laboratory consumables such as Eppendorf tubes, polymerase chain reaction (PCR) plates and tissue culture plates were purchased from Star Labs. Levington® Advance Seed and Modular F2+S compost plus horticultural grade sand mixture (pH 5.3-6.0) was purchased from ICL, Ipswich, UK. General laboratory chemicals of analytical grade were purchased from Sigma-Aldrich, Fisher, Duchefa Biochemie, Alfa Aesar, and TAAB. Enzymes and reagents were ordered from Abcam, GE, BIO-RAD, Invitrogen, Gen script, and Roche, and gel extraction and miniprep kits were from Qiagen or Sigma. Water used for preparing growth media, buffers and solutions were either reverse osmosis filtered or deionised ultra-high-purity water; nuclease-free water for molecular works involving DNA and RNA was purchased from Fisher. Custom oligonucleotides and probes were synthesised by Sigma and Genscript.

2.1.2 Plant materials

All plant lines were of the Columbia (Col) and Landsberg erecta (L*er*) ecotypes. Details of the mutant and transgenic lines used in this study are presented in Table 2.1. Plant lines were originally bought from NASC seed stock centre (Nottingham, UK). See Acknowledgements for stock donors.

Table 2.1 Plant lines relating to multiple chapters.

Line	Allele	Gene name	Gene ID	Mutation	Reference
ind (Col)	*ind-2*	*INDEHISCENT*	AT4G00120	EMS	(Liljegren et al., 2004b)
ind (L*er*)	*ind-6*			Ds gene trap insertion	(Wu et al., 2006)
35S::IND-GR (Col)	*35S::IND:GR*			Transgene	(Sorefan et al., 2009b)
pIND:: GUS (Col)	*IND::GUS* L0266			Transgene	(Sorefan et al., 2009b)
ago10 (Col)	*ago10-4* SALK_138011	*ARGONAUTE10*	AT5G43810	T-DNA insertion	(Zhu et al., 2011a)
ago10 (L*er*)	*zwl-3*			EMS	(Endrizzi et al., 1996)
phb er (Col)	*phb-12 er-2* SALK_023802	*PHABULOSA*	AT2G34710	T-DNA insertion	(Prigge et al., 2005)

phv er (Col)	*phv-11 er-2* SALK JP91	*PHAVOLUTA*	AT1G30490	T-DNA insertion	(Prigge et al., 2005)
rev er (Col)	*rev-6 er-2* CS6961	*REVOLUTA*	AT5G60690	EMS	(Otsuga et al., 2001)
35S:LhGR>>PHB (Col)	35S:LhGR>>PHB	*PHABULOSA*	AT2G34710	Transgene	(Dello Ioio et al., 2012)
35S::REV-GR (L*er*)	35S::REV:GR	*REVOLUTA*	AT5G60690	Transgene	(Wenkel et al., 2007)
pIND::IND-YFP (Col)	*pIND::IND:YFP*	*INDEHISCENT*	AT4G00120	Transgene	(Simonini et al., 2016)
ago10 ind (L*er*)	*zwl-3 ind-6*	*ARGONAUTE10* and *INDEHISCENT*	AT5G43810 and AT4G00120	EMS and Ds gene trap insertion	Lab stock (Dr. Karim Sorefan)
ago10 ind (Col)	*ind-2 ago10-4*			T-DNA insertion and EMS	Lab stock (Peter Venn)
35S::IND-GR, pPIN1::PIN1-GFP (Col)	*35S::IND:GR pPIN1::PIN1:GFP*	*INDEHISCENT* and *PIN-FORMED1*	AT4G00120 and AT1G73590	Transgene	(Sorefan et al., 2009b)
35S::IND-GR, DR5::GFP (Col)	*35S::IND:GR DR5rev::GFP*	*INDEHISCENT* and DR5 AuxREs	AT4G00120	Transgene	(Sorefan et al., 2009b)

2.2 Plant methods

2.2.1 Plant growth conditions

Seeds were sown on Levington® compost and stratified at 4°C for three days. Plants were illuminated for 16 hours with light delivered at 120 µmol m^{-2} sec^{-1} at a constant temperature of 23°C in a Versatile Environmental Test Chamber MLR 350-HT (Sanyo, Japan). Distilled water was used for watering seeds in order to control the nutrient supplementation. For growth on agar, seeds were surface-sterilized in 70 % ethanol for 10 minutes then treated with 10 % bleach, 0.1 % (v/v) Triton X-100 for 5 minutes, and finally washed three times with autoclaved water. After stratification at 4°C for three days, the sterile seeds were sown on 0.8 % agar supplemented with ½ Murashige and Skoog salts (Murashige and Skoog, 1962) plus vitamins (MS; Duchefa Biochemie, M0222) and 0.5 % (w/v) glucose (D-(+)-Glucose, Sigma Aldrich, G7021) in sterile plates. Plates were sealed with micropore tape to maintain sterility while allowing gas exchange. For growth in liquid culture, sterile seeds were sown in 10mL 0.5 % MS medium in a 50mL Falcon tube. Tubes were constantly illuminated in light delivered at 120 µmol m^{-2} sec^{-1} at a constant temperature of 23°C, and aerated by shaking upright at 60 rotations per minute (rpm).

2.2.2 Hormone and chemical treatments

Hormones and chemicals were ordered and stored according to Table 2.2. Seedlings were grown in plant agar medium or liquid culture medium containing hormones and chemicals: 6-Benzylaminopurine (BAP), Indole-3-acetic acid (IAA), N-1-naphthylphthalamic acid (NPA), Abscisic acid (ABA), 1-Aminocyclopropane carboxylic acid (ACC), Jasmonic acid (JA), Cycloheximide (CHY), Dexamethasone (DEX) and mock solutions (Table 2.2). Final concentrations of 100 nM BAP, 10 μM IAA, 10 μM NPA, 10 μM ABA, 10 μM ACC, 10 μM JA, 10 μM DEX and 10 μM CHY were used for treatment. The mock solution contained DMSO (Fisher, BP231), dH2O (Fisher, W/0100/21) and EtOH (Fisher, E/0650DF/17). All treated plants with their respective controls were grown simultaneously under the same conditions.

Table 2.2 Hormones and chemicals.

Name	Company name and product code	Solvent	Stock concentration	Storage temperature (°C)
ABA	SLS #A1049	EtOH 70 % (v/v)	10 mM	-20
ACC	Sigma Aldrich #A3903	dH$_2$O	10 mM	-20
BAP	Duchefa #B0904	DMSO	100 mM	-20
IAA	Duchefa #I0901	DMSO	100 mM	-20
JA	Sigma Aldrich #J2500	EtOH 1.6 % (v/v)	10 mM	4
NPA	Duchefa #N0926	DMSO	100 mM	-20
CHY	Acros Organics #357420010	DMSO	10 mM	-20
DEX	Alfa Aesar #A17590	DMSO	10 mM	-20

2.2.3 Shoot apical meristem phenotype analysis

Analysis of SAM phenotypes was done on 3 and 7 day old seedlings. Seedlings were transferred to a Petri dish filled with sterile water. Forceps were used to hold one cotyledon while pulling the second cotyledon downwards to peel the seedling into two. This peeled cotyledon was transferred to a microscope slide and aligned on top of 1 % agarose gel. Two cotyledons of a seedling were observed under a light microscope to analyse the phenotype of shoot apical meristem (Fig 2.1).

Figure 2.1 Light microscope image of the 3-day-old shoot apical meristem.

2.3 Nucleic acid techniques

2.3.1 Plant genomic DNA extraction

Genomic DNA was extracted using Edward's extraction buffer (200 mM Tris (pH 7.5), 250 mM NaCl, 25 mM EDTA, 0.5% SDS). Individual *Arabidopsis* leaves, or seedlings were placed in 1.5 mL microcentrifuge tubes, flash frozen with liquid nitrogen and then ground with plastic pestles. 400 µL of Edward's extraction buffer was added and mixed by inversion. After centrifugation at 16000 rpm for 5 minutes, 300 µL of DNA-containing supernatant was transferred to fresh tubes containing 300 µL isopropanol and 1 µl GlycoBlue^{TM} (Ambion®, Thermo Fisher Scientific, U.S.), mixed by inversion and further centrifuged for 10 minutes. The supernatants were discarded, and the pellets were washed with 70 % EtOH before being air dried for 15 minutes at room temperature, and finally resuspended in 100 µL of Tris-EDTA (TE) buffer (10 mM Tris-HCl (pH 7.5), 1 mM EDTA) or 100 µL of dH$_2$O.

2.3.2 Plant total RNA extraction

Plant tissue was collected into 2 mL tubes containing a 4 mm steel ball bearing. Seedlings with metal balls are snap-frozen in liquid nitrogen and vortexed until they form a pale green powder. Once all samples are prepared, total nucleic acid (TNA) was extracted using a phenol-chloroform extraction procedure adapted from (White and Kaper, 1989). Tubes were transferred to ice, and 600 µL of freshly made extraction buffer (100 mM Glycine, 10 mM EDTA, 100 mM NaCl, 2 % SDS, pH9.5) was added to each sample. The homogenized material was transferred to a chilled microcentrifuge tube containing 600

µL phenol (pH4) and mixed immediately by vortexing for 10 seconds. Tubes were then centrifuged for 10 minutes at 16,000 × g at 4°C to separate plant debris from the supernatant. The upper phase was transferred to a fresh tube on ice, containing 600 µL of 25:24:1 phenol:chloroform:isoamyl alcohol and centrifuged for 10 minutes at 16,000 × g at 4°C. The upper phase containing RNA was transferred to a fresh tube containing 500µL chloroform:isoamyl alcohol, on ice. Tubes were vortexed for 10 seconds and centrifuged for 5 min 16,000 × g at 4°C. The upper phase was transferred to a sterile tube, and the TNA fraction was precipitated by the addition of 40 µL 4 M sodium acetate pH5.2, 800 µL absolute ethanol, and 1 µL GlycoBlue^{TM}. This was mixed by inversion and incubated for 15 minutes on ice or stored overnight at -20°C. The TNA was recovered from solution by centrifugation for 15 minutes at 16,000 × g at 4°C. The supernatant was removed by aspiration. To remove residual salts, the pellet was rinsed with 80 % ethanol and immediately centrifuged for 5 minutes at 16,000 × g at 4°C. The ethanol was removed by aspiration, and the pellet was allowed to dry at room temperature for 10 minutes. The TNA pellet was resuspended in the 30-50 µL RNase-free water on ice. The TNA extract was stored at -80°C.

Total RNA yield was quantified using NanoDrop (Thermofisher). A 260/280 ratio of 2.0 is generally accepted as 'pure' for RNA. RNA quality was checked on a 1% TBE agarose gel. The gel was loaded with approximately 1 µg TNA extract denatured for 5 minutes at 65°C with an equal volume of 2× gel-loading solution containing 10 ml deionized formamide, 200 µl 0.5 M EDTA, pH 8.0, 1mg xylene cyanol FF and 1 mg bromophenol blue. To remove contaminating genomic DNA, TNA was treated with DNase using the Ambion DNA-free™ kit or SIGMA Dnase I Kit (AMPD1). 1-2 µg TNA was incubated at 37°C for 30 minutes with 2U rDNaseI in DNase I Buffer. The DNase was inactivated using a 1:5 volume of DNase Inactivation Reagent and incubated for 2 minutes at room temperature, mixing 2-3 times. To remove the DNase enzyme, the tubes were centrifuged at 10,000 × g for 90 seconds. The supernatant containing the RNA was transferred to a fresh tube and stored at -80°C.

2.3.3 cDNA synthesis

Complementary DNA (cDNA) from 1–2 µg of DNase I treated TNA was synthesised using a High Capacity cDNA Reverse Transcription Kit (Invitrogen, #4374966). A 2X RT master

mix was prepared on ice containing 10X RT buffer, 10X RT random primers, 25X dNTP mix, reverse transcriptase, RNase inhibitor and nuclease-free dH2O. 10 µL of 2X RT master mix and 10 µL of RNA were mixed in a fresh PCR tube. Tubes were centrifuged to eliminate any air bubbles. Thermal cycler conditions listed below were used for the run. After the run, diluted (1:4) cDNA was stored at −20°C until use.

	Step 1	Step 2	Step 3	Step 4
Temperature (°C)	25	37	85	4
Time	10 minutes	120 minutes	5 minutes	∞

2.3.4 Primer design

Arabidopsis genomic DNA or mRNA sequences were acquired using Ensembl-Plant (http://plants.ensembl.org/) and TAIR (https://www.arabidopsis.org/). For qRT-PCR, to avoid amplification of contaminated genomic DNA, primers were designed to hybridize to the 3' end of one exon and an exon-exon junction, or the other half to the 5' end of the adjacent exon. Chromatin immunoprecipitation (ChIP) qRT-PCR primers were designed either side of the previously characterised or predicted transcription factor binding sites. Genotyping primers were designed either side of the predicted mutation site or reporter sequence. Primers for qRT-PCR assays and sequencing were designed using NCBI Primer-BLAST. A list of the primers used is provided in Table 2.3.

Table 2.3 List of primers used for qRT-PCR, genotyping, sequencing and ChIP qPCR.

qRT-PCR		
Name	Forward primer (5'-3')	Reverse primer (5'-3')
ACTIN2	TCAGATGCCCAGAAGTGTGTT	CCGTACAGATCCTTCCTGATA
AGO10	CCTTTGTAGCCATGCGGGTATTCA	TGCACCGCGCATAGGTATAACAG
AGO7	GGCCGGTCAAGTTTAAGCTTTGGTG	CGTGTCTGCAAATCAGTAGGGCAAG
ARF3	CCATATCGACCCATAGCGTTTTCAG	CCCAATGCAAAAGGGATAGTCAACA
ARF4	GCCATGGGCAGGTTTACTGGATAC	TAACATCAAACCCCTGTGAGGGTGA
ARR7	CTCAATGCCAGGACTTTCAGG	TCCTCTGCTCCTTCTTTGAGAC
AS1	TGAAGAAGGATGGTGAGATGGG	TCTCTCGGACCGAACTGTCT
AS2	CCAACTACACGCTTTTTGTATGC	TCCCTCTCCCTGCGAGTAAAT
CLV3	AAGGACTTTCCAACCGCAAG	AGTTGTTGAACTGGACCGGA
CUC1	GAGCCTTGGGAGCTTCCTGA	TGTTCGTTCTCAGTCCCGTT
CUC2	CAAGTGTGAGCCTTGGCAACT	TAGTTCTCAGTCCCGTCGGAT
CUC3	CTACAAAGGTAGGGCTCCACG	TGCAAATCACCCATTCCTCCTT
HEC1	GATCTTCCGTATCGCCGTGA	CTTCTATGCCTAGCCGCCAC
IND	GAACCGCCGTAACGTAAGGA	AAGCTGTGTCCATCTTCGCA
KAN	GCGGCCATGAAAGAGCAACT	CAGCAGGCTTGTTAGTGGTC
KNAT1	GGAGCTCCACCTGATGTGGTT	CAACATGTCACAGTATGCTTCCA

MP	AGGACTCAAACGTCAGCTCC	CGCGGAATCAGGAACACGTA
PHB	CATGCTGGAAACGACTCTTGTAGCC	CGTTGCCTGCTCGTAAGATACCATC
PHV	GGCTCCCAATACGGTAGCTCATTTC	CATCGACACCATAGTCTGCCCATTC
PID	TCCCTCTCTTCCGCCAGATT	AGCATAATGTGACCGTCGGA
PIN1	CAGGGGAATAGTAACGACAACC	ACCTTAGCCTGCGTCGTTTT
REV	GCTTCGACCCCTTTATGAGTCATCC	CAGGCTGCCTTCCTAATCCATACAC
RPL	CGACGAGGTTTACAAGAGGT	TAAGTTAGCGTACGGAGCAG
SPT	GGGAAGGTGGGTTAACTCATCCAAG	ACATAGAGATCCCGAAGTTGGGACA
STM	TTGTCAGAAGGTTGGAGCAC	TCAAGCCCTGGATCTTCACC
WOX1	CGACACGCAACCAGAGAAAC	CAACTGCATCATCTGCCACG
WUS	TCCCAGCTTCAATAACGGGA	CCTCCACCTACGTTGTTGTAAT
YAB1	CGTAACTGTCCGATGTGGTTG	AAGTAAGAGTGAGGACCGAGC
YAB2	TTGTGACGGTGAGATGTGGC	CCAGAGAGGTTGTGTGCTGT
YAB3	GGAGGAAATGCGAAGCGGAG	CCACTGATCTTCCGTTGCGA
YUC1	CCGGAACACCGTTCATGTGT	CGGTCGGTATTTCCAAACGA
ZPR1	TCAGACACACCCACGAGATTAG	CATCTTTTTCTCTTCCCGCCAC
Genotyping and Sequencing		
Name	Forward primer (5'-3')	Reverse primer (5'-3')
AGO10-1	TCTCTAGCGTCACTCTTCTTCT	TTAGCTCTCTTGTTGGTTGAGT
AGO10-2	AGCTGCATTCATCGAGCCT	CATACCGCCACTAACAGTACC
AGO10-3	AGAGAATCTGTGAAACCGAGC	AGCTTGAGGAACCGACGTAA
AGO10-1 (2)	CGCTGATTTGCCTACCAAGGA	
AGO10-2 (2)	AGTATCACGAGAACGGGAAAG	
AGO10-3 (2)	GCTTGTGCATCGCTTGAACC	
CYP79B2 1	CCATGCAGAGACAACAGAAACC	TCGGCTAAGAAGGACTTGACT
CYP79B2 2	AGAACACTGCACCTGACGG	GGCGTCGTCTCATCTCACTT
EGFP/YFP	CTACGGCAAGCTGACCCTGA	CCTTGAAGAAGATGGTGCGCT
GR	AGCATTACCACAGCTCACCC	GATCTCCAACCCAGGGCAAA
ChIP qPCR		
Name	Forward primer (5'-3')	Reverse primer (5'-3')
CUC1	CTGTCAAATATCACATCAGTTGCT	AACCCTAGAGTTCCCAAATGTT
AGO10	CCTCTTTACACGTGATTTTTAAAAGAGA	CACTCACCGACCAATGAAGAA
PID	TTCGTTTATTCTAGCCATTTCACA	CCTCTCGCTAATTTTTGTTTTGTT

2.3.5 Polymerase chain reaction (PCR)

PCR reactions were performed with 1X Q5 Reaction Buffer, 200 μM dNTPs, 0.5 μM of each primer, 0.02U/μl Q5® Hot Start High-Fidelity DNA Polymerase (NEB, M0493), 1X Q5 High GC Enhancer and 1-2 μg template in a total volume of 25 or 50 μL on T100™ Thermal Cycler (Bio-Rad). PCR conditions were one cycle at 98°C for 30 seconds and 35 cycles of 98°C for 10 seconds, 56 °C for 30 seconds followed by 72°C for 1 minute and one cycle at 72°C for 2 minutes. PCR products were checked by agarose gel electrophoresis. Samples were subsequently submitted for sequencing at the Core

Genomics Facility, University of Sheffield. Samples were sequenced using the Applied Biosystems' 3730 DNA Analyser, and sequencing results were analysed using SnapGene and BioEditor software.

2.3.6 Quantitative reverse transcriptase PCR (qRT-PCR)

qRT-PCR is a quick and dependable technique for monitoring the gene expression profile. The qRT-PCR has become the gold standard method of choice for the quantification of specific mRNAs and miRNAs. This method is fast, extremely sensitive, and accurate. It requires only very small amounts of input total RNA and is relatively simple to perform. Three biological and three technical repeats were performed for all the experiments. qRT-PCR was performed with SYBR Green Jump-start Taq Ready-mix (Sigma, S4438) on the Mx3005P qPCR System (Agilent Technologies Genomics). The SYBR Green I dye chemistry uses the SYBR Green I dye to detect PCR products by binding to double-stranded DNA formed during PCR. Because the SYBR Green I dye binds to all double-stranded DNA, the result is an increase in fluorescence intensity proportional to the amount of double-stranded PCR product produced. Reactions were prepared using 2X JumpStart Taq Ready Mix, 1X ROX Reference Dye, 300 nM forward primer, 300 nM reverse primer, 500 ng template DNA and nuclease-free water and 15 µl of each reaction was transferred to an optical 96 well plate (Star Labs). The plate was covered with an optical adhesive film (Bio-Rad, #MSB-1001), and the plate was centrifuged briefly to eliminate air bubbles from the solutions. PCR conditions listed below were used for the run. After the run, PCR products were checked by agarose gel electrophoresis and the melting curve analysis. The threshold cycle (CT) was automatically determined by the Mx3005P qPCR System, and comparative CT method (also known as the 2 −ΔΔCT method) was used to analyse the qRT-PCR data (Schmittgen and Livak, 2008). Housekeeping genes such as *UBIQUITIN C*, *BETA-ACTIN*, *GAPDH*, *18S RIBOSOMAL RNA* (*18S rRNA*), *5S RIBOSOMAL RNA* (*5S rRNA*) were used as these are common endogenous references in qRT-PCR. *ACTIN2* was used as a normalisation control.

Step	PCR					
	Initial denaturation	CYCLE (40 Cycles)		Dissociation/melt		
		Denature	Anneal/ Extend			
Time	2 minutes	15 seconds	1 minute	2 minute	1 minute	2 minutes
Temp	94 °C	94 °C	60 °C	94 °C	60 °C	94 °C

The below equation was used to compare the gene expression in two different samples (e.g. sample 1 and sample 2); each sample was related to an internal control gene. Sample 1 may be the treated sample and sample 2, the untreated control or Calibrator.

$$\Delta CT = (CT \text{ gene of interest} - CT \text{ normalisation control})$$
$$-\Delta\Delta CT = - [(\Delta CT) \text{ sample 1} - (\Delta CT) \text{ sample 2}]$$
$$\text{Fold change} = 2 -\Delta\Delta CT$$

2.3.7 Agarose gel electrophoresis

PCR products were mixed with 6x loading buffer (0.2 % w/v bromophenol blue, 50 % v/v glycerol) before routinely electrophoresed together with 5 μL of 100 bp or 1 kb DNA ladder (NEB) on 1 % w/v 10-well 100 mL agarose gels prepared using TAE (Tris/Acetate/EDTA) buffer containing ethidium bromide (3 μl of 10 mg/ml ethidium bromide). Gels were run at 150 V for 1 hour and then imaged using a gel imaging system (UVP gel doc).

2.3.8 DNA gel extraction

DNA was recovered from agarose gel using the QIAquick Gel Extraction Kit (Qiagen, #28704). Each DNA fragment of interest was excised from the agarose gel using a clean scalpel blade over a UVP gel doc UV-transilluminator and transferred to a pre-weighed 2 ml microcentrifuge tube. Buffer QG was added in a 3:1 ratio to the gel (v/w) and incubated at 50°C for 10 minutes with regular vortexing until all the material was dissolved. Isopropanol was added at a 1:1 ratio to the dissolved solution. The dissolved solution was then transferred to the QIAquick spin column, centrifuged at 14000 rpm for 1 minute at room temperature. The flow-through was discarded, the filter was washed with 500 μL Buffer GC and the tube centrifuged for 1 minute. Again the flow-through was discarded, the filter was washed with 750 μL Buffer PE and the tube was centrifuged for 1 minute at room temperature. Centrifugation was repeated after discarding the flowthrough in order to remove any remnant drops of wash buffer and dry the DNA-containing filter. The column was then transferred to a fresh microcentrifuge tube, 30 μL of Buffer EB was added to elute the DNA, left to stand for 5

minutes, and then the eluate collected after centrifugation at top speed for 1 minute at room temperature.

2.4 Chromatin immunoprecipitation (ChIP) methods

2.4.1 Chromatin immunoprecipitation

ChIP is a powerful method for studying transcription factor (TF)–DNA interactions *in vivo*. The immunoprecipitation (IP) of cross-linked chromatin with antibodies specific for TFs was followed by PCR, to detect a potential enrichment or depletion of a DNA sequence of interest within IP fractions, and is already routinely used in many labs. In contrast to animal cells, however, plant cells have a rigid cell wall which poses limitations to the simple utilization of protocols established for animals. The laboratory protocol has been optimised successfully in order to identify direct target genes of the IND TF in *Arabidopsis* (Girin et al., 2011). *35S::IND:GR* seeds were grown for 7 days in 50 ml of liquid culture medium with constant shaking. After 7 days of growth under constant light, seedlings were treated with a final concentration of 10 µM DEX (treatment) and DMSO (control) for 6 hours. DMSO is a vehicle control.

Seedlings were washed in distilled water and immersed in cross-link buffer consisting of 0.4 M sucrose, 10 mM Tris–HCl (pH 8.0), 1 mM EDTA, 1 mM PMSF and 1 % Formaldehyde. Glycine was added to 0.1 M and incubated for a further 10 minutes. The seedlings were washed in distilled water and frozen in liquid nitrogen. The tissue was resuspended in chromatin extraction buffer 1 (0.4 M sucrose, 10 mM Tris–HCl (pH 8.0), 5 mM β-mercaptoethanol, 1 mM phenylmethylsulfonyl fluoride (PMSF) and Protease Inhibitor Cocktail) and filtered through two layers of miracloth into a new ice-cold 50 ml tube. The solution was centrifuged for 10 minutes at 10,000 rpm at 4°C. The supernatant was discarded and the pellet resuspended in 1.5 ml of EB2 buffer (0.25 M sucrose, 10 mM Tris–HCl (pH 8.0), 5 mM b-mercaptoethanol, 10 mM $MgCl_2$, 1% Triton X-100, 1 mM PMSF, and Protease Inhibitor cocktail), before transferring the solution to a 1.5 ml microcentrifuge tube. The tube was centrifuged at 14,000 rpm for 10 minutes at 4°C, and the supernatant was discarded. The pellet was resuspended in 500 µl of EB3 buffer (1.7 M sucrose, 10 mM Tris–HCl (pH 8.0), 5 mM β-mercaptoethanol, 2 mM $MgCl_2$, 0.15 % Triton X-100, 1 mM PMSF, and Protease Inhibitor Cocktail). The solution was layered

onto another 500 µl of EB3 in a new 1.5 ml microcentrifuge tube and centrifuged at 14,000 rpm for 1 hour at 4°C. The supernatant was discarded, and nuclear lysis buffer (50 mM Tris-HCl (pH 8.0), 10 mM EDTA, 1 % SDS, 2 mM PMSF, and Protease inhibitor cocktail) was added to the final pellet. Sonication was performed on ice for 10 minutes at 13 microns for 20 seconds "ON cycle", 40 seconds "OFF cycle".

Sonication sheared the DNA to approximately 300- to 1,000-bp fragments with the main peak of 500 bp. After pre-clearing with 30 µl of Dynabeads-protein A (Invitrogen Ltd, 100-02D), immunoprecipitations were performed overnight at 4°C anti-GR antibody (Abcam, AB3580). No antibody control was included during immunoprecipitation step. After incubation, beads were washed once with 1 ml of high-salt wash buffer, once with 1 ml of low-salt wash buffer, once with 1 ml of LiCl buffer (one wash), and 1 ml of TE buffer. The washed beads and input fraction were resuspended in elution buffer (1 % SDS and 0.1 M NaHCO$_3$) and incubated overnight at 65°C. After cross-link reversal of the immunoprecipitated and Input DNA, the DNA was purified using the phenol-chloroform extraction. Each pellet was resuspended in 15 µl of TE buffer. The DNA concentration was determined using NanoDrop and was stored at -20°C until use.

2.4.2 ChIP qPCR and ChIP-Seq analysis

Before moving on to microarray hybridization or sequencing, the ChIP DNA was analysed by qPCR to confirm enrichment of known target genes relative to non-target control genes. Alternatively, if no known target was available as a positive control, the amounts of immunoprecipitated DNA were compared to that of the negative control, which was an immunoprecipitation that uses no antibody, or a sample without antigen. qPCR was performed using *35S::IND:GR* samples (DEX treated, DMSO treated and no antibody control). The values correspond to the fold enrichment between DEX treated input with the GR antibody and DMSO treated input with the GR antibody. Primers used for ChIP qPCR are listed in Table 2.3. Processed ChIP-Seq files were visualised using Integrative Genomics Viewer (IGV, Broad Institute, USA). Public datasets used for ChIP-Seq analysis are listed in Table 2.4.

2.5 Microarray methods

2.5.1 Microarray

The microarray is used to measure the expression levels of large numbers of genes simultaneously. For microarray, *35S::IND:GR* seeds were germinated in 10 ml of liquid culture medium with constant shaking. After 7 days growth under constant light, seedlings were treated with a final concentration of 10 µM DEX, 1 µM BAP and 10 µM IAA diluted in DMSO for 6 hours. The no-treatment controls were treated with the equivalent volume of DMSO (Fisher, #BP231). Treatments were done in biological triplicates. Tissue was collected before and after treatment and snap frozen in liquid nitrogen for TNA extraction. Dr Paul Heath performed the microarray (*Arabidopsis* Gene 1.0 ST Array, Thermofisher, #901915) at the University of Sheffield core facility for microarray and next generation sequencing. An Agilent 2100 bioanalyser was used to examine RNA integrity and concentration. Hybridization and scanning procedures were conducted according to the manufacturer (Affymetrix) using Affymetrix Gene Chip hybridisation system.

2.5.2 Microarray analysis

Arabidopsis Gene 1.0 ST Array CEL files were processed and normalised (RMA algorithm) using Affymetrix® Expression Console™ software. CHP files were generated after normalisation. *Arabidopsis* Gene 1.0 ST Array CHP files were analysed using Affymetrix® Transcriptome Analysis Console (TAC) software. *Arabidopsis* Gene 1.0 ST library files are modified to add TAIR ID and protein family details. These files are transferred to Affymetrix® TAC software. Statistical analysis was performed using Affymetrix® TAC software to obtain a list of differentially expressed genes following treatment. Fold change (FC) was calculated for Condition1 vs. Condition2 using 2^[Condition1 Bi-weight Avg Signal (log2) - Condition2 Bi-weight Avg Signal (log2)]. Condition Bi-weight Avg Signal (log2) is the Tukey's Bi-weight average of exon intensity of all the samples in a condition. Genes above 1.5 FC and below -1.5 FC were filtered based on significance (p-value ≤ 0.05) One-Way Between-Subject ANOVA p-value (Condition1 vs. Condition2). Filtered data were transferred to Excel for further analysis (Avg: Average).

Hierarchical clustering and data visualisation were done using EXPANDER (EXpression Analyzer and DisplayER) (http://acgt.cs.tau.ac.il/expander/) (Shamir et al., 2005). Similarity matrix analysis and heat maps were generated using Morpheus (https://software.broadinstitute.org/morpheus/). Pearson and Spearman rank correlations were selected for similarity matrix analysis. Pathway analysis was performed using MapMan (http://mapman.gabipd.org/) and STRING (https://string-db.org/) software. VENNY 2.0 was used for creating Venn diagrams. Gene ontology (GO) analysis was performed using Gene Set Enrichment Analysis (GSEA) software (http://software.broadinstitute.org/gsea/) (Subramanian et al., 2007) and PANTHER (http://pantherdb.org/). Public data sets used for the analysis are listed in Table 2.4.

Table 2.4 Data sets used for analysis.

Description	Method	ArrayExpress/GEO ID	Reference
AtGenExpress: Hormone treatment	Microarray	GSE39384	(Goda et al., 2008)
PlantCistromeDB	DAP-Seq	GSM1925338	(O'Malley et al., 2016)
REVOLUTA ChIP	ChIP-seq	GSE26722	(Brandt et al., 2012)
AGO1 and AGO10 CLIP	CLIP-Seq	GSE39885	(Zhu et al., 2011b)
SPATULA inducible expression	Microarray	GSE12913	(Reymond et al., 2012)
spatula mutant	Microarray	NASCARRAYS-505	(Josse et al., 2011)
HECATE inducible expression & *hec* mutant	Microarray	E-MTAB-2193	(Schuster et al., 2014)
CUC1 over expression	Microarray	GSE27482	(Takeda et al., 2011)
cuc1 mutant	Microarray	GSE20705	(Koyama et al., 2010)
Shoot meristem stem cell niche	Microarray	GSE28109	(Yadav et al., 2014)
IND inducible expression for 24 hours	Microarray	E-GEOD-28898	(Voinnet et al., 2011)
IND inducible expression with IAA and BAP	Microarray	E-MTAB-3812	This work
L*er* and mutants *ago10, ind, ago10 ind*	mRNA-Seq	-	Dr Karim Sorefan
L*er* and mutants *ago10, ind, ago10 ind*	sRNA-Seq	-	Dr Karim Sorefan

2.6 Bioinformatics

2.6.1 Sequence alignments

CLC Sequence Viewer (Qiagen) was used for sequence alignment (DNA, RNA, or protein), construction and visualisation of phylogenetic trees. NCBI basic local alignment search tool (BLAST) was also used for alignment. Multiple sequence alignments were done using multiple sequence comparison by log-expectation tool (MUSCLE) (http://www.ebi.ac.uk/Tools/msa/muscle/).

2.6.2 GSEA analysis

GSEA is a software developed by the Broad Institute. It was used to perform GO and MOTIF. Microarray dataset (*.gct format), GSEA library (*.gmt format), and phenotype label (*.cls format) files were used for GSEA analysis. One thousand sample permutations were selected for any analysis. GSEA computes four key statistics for the report: Enrichment Score (ES), Normalized Enrichment Score (NES), False Discovery Rate (FDR), and Nominal P-Value. ES reflects the degree to which a gene set is overrepresented at the top or bottom of a ranked list of genes (Fig 2.2). NES (actual ES/ mean (ESs against all permutations of the dataset)) can be used to compare analysis results across gene sets. After analysis, GSEA report was viewed in a web browser (HTML Report) and transferred to Excel. An enrichment map was created and visualised using Cytoscape (http://apps.cytoscape.org/apps/enrichmentmap). The parameters used for enrichment map generation were a p-value of 0.05 or below, a Q-value cut-off of 0.05 and an overlap coefficient cut-off of 0.5.
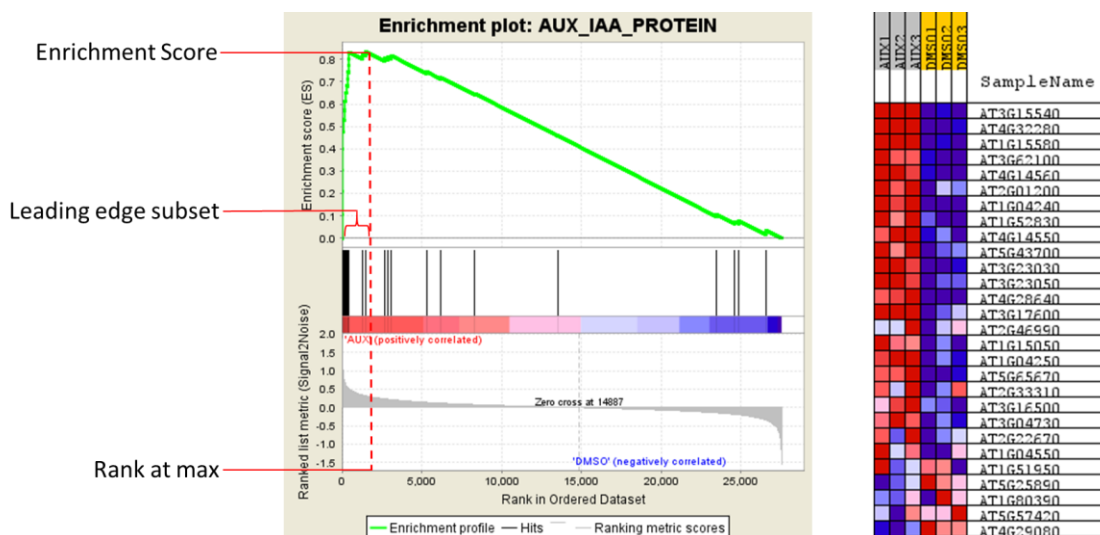
Figure 2.2 Profile of the running ES score and positions of geneset members on the rank ordered list. Blue-Pink O' Gram in the space of the analysed geneset.

2.6.3 Library files for GSEA

Gene set files for gene function, and protein families (Group of genes) were created using previously published *A. thaliana* TAIR GO (http://www.geneontology.org) and *Arabidopsis* Gene 1.0 ST Array library files (Thermofisher, 901915).

2.6.4 MOTIF and DAP-Seq analysis

PlantCistromeDB (http://neomorph.salk.edu/dap_web/pages/index.php) was created by O'Malley et al., using DNA affinity purification sequencing (DAP-seq) (O'Malley et al., 2016). PlantCistromeDB is the collection of motifs and peaks of 529 *Arabidopsis* transcription factors. Motif logos, peaks (FRiP ≥5%) and Target genes (FRiP ≥5%) were downloaded from PlantCistromeDB. The fraction of reads in peaks (FRiP) is the fraction of all mapped reads that fall into the called peak regions, calculated by dividing the usable reads in significantly enriched peaks by the total number of all usable reads. Downloaded Target genes (FRiP ≥5%) were analysed in Microsoft Excel 2013.

Arabidopsis Motif Scanner (AMS) and TAIR Patmatch were used to identify the positions of cis-regulatory elements in the 2000bp upstream promoter region in *Arabidopsis* genome. Motifs collected from PlantCistromeDB and *Arabidopsis* protein-binding microarray database were used to search in AMS and TAIR Patmatch. A GSEA Motif library file was created using the AMS output (Motifs and associated gene groups). This file was used for Motif GSEA analysis. Motif enrichment analysis using the GSEA tool is better when compared to the MEME Motif enrichment tool (http://meme-suite.org/tools/centrimo) because better statistics are generated using GSEA, such as a higher permutation.

2.6.5 Protein structure modelling

Available protein structures were downloaded from Protein Data Bank (PDB). Unavailable structures were created using protein structure prediction tools. One method is *ab initio* modelling, which involves predicting protein 3D structures from the amino acid sequence, but the prediction accuracy is low. Tools used for studying *in silico* protein interactions and pathways were outlined in Figure 2.3. Phyre2 (Kelley et al., 2015) was used to predict and analyse protein structure. Phyre2 uses advanced remote homology detection methods to build 3D models. *Arabidopsis* protein sequences were extracted from UniProt and submitted to Phyre2 for modelling. Predicted structures were downloaded in pdb format and used for further analysis. Self-assembly of identical protein subunits was predicted using Rosetta Symmetric Docking (http://rosie.rosettacommons.org/).
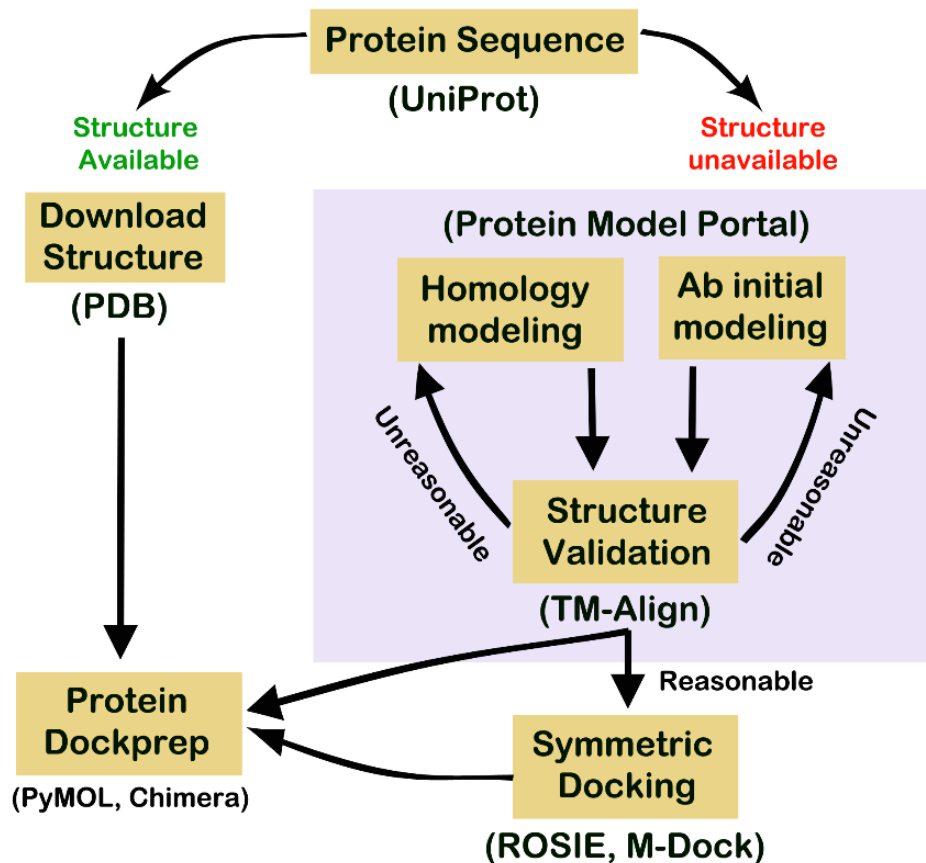
Figure 2.3 Tools and pathway for protein structure modelling.

2.7 Imaging techniques

2.7.1 β-Glucuronidase (GUS) assay

The promoter-driven GUS assay is the most commonly used technique for tissue-specific expression patterns in *Arabidopsis*. In this procedure, the GUS enzyme converts 5-bromo-4-chloro-3-indolyl glucuronide (X-Gluc) to a blue product. The staining is very sensitive. Processed samples were examined under a dissecting microscope for bright blue colour over a transparent background. GUS assay was performed on *pIND::GUS* seedlings and leaves at different developmental stages. Samples were vacuum infiltrated and incubated in the GUS assay buffer (0.1 M phosphate buffer [pH 7], 10 mM EDTA, 0.1 % Triton X-100, 1 mg/mL X-Glue A, 2 mM potassium ferricyanide) overnight at 37°C, and cleared in 50 % ethanol. GUS staining was observed under a light microscope and photographs were taken with a CCD camera.

2.7.2 Sample fixation, clearing, and preparation

Plastic embedding gives better cellular definition compared to paraffin embedding. Histology samples were embedded using 1 % Technovit 7100 resin solution (TAAB, #T218). Technovit 7100 penetrates and polymerizes all tissue specimens evenly for light-microscope examination. For this reason, this method is an ideal tool for visualizing plant cellular morphology and phenotype. Samples were fixed in fixing buffer consisting of a 7:1 ratio of 100 % Ethanol and acetic acid by vacuum infiltration for 20 minutes. Decolourised samples were incubated with 2x 100 % ethanol for 30 minutes. After incubation, samples were infiltrated in a sufficient amount of TECHNOVIT 1 solution for 1-48 hours, depending on specimen thickness and type of tissue. After incubation, 1 ml of the solution was poured into a Histoform S mould (TAAB, #T393), followed by the infiltrated specimens, which were positioned as required. At room temperature (23℃) the specimens set within approximately 2-4 hours. Histobloc (TAAB, #T395) was then placed in the recess of the embedding mould Histoform S. Technovit 3040 (TAAB, #T224) was poured into the recess at the back of the Histobloc to a level of about 2 mm above the base of the Histobloc. After about 10 minutes the Histobloc together with the fixed specimen was removed from the Histoform S mould. The samples were sectioned at 8-10 μm thick with a Histoknife (TAAB, #T553) on a microtome (Leica RM2145) and dried on glass slides. Staining or enzymatic reactions were carried out without removing the resin.

2.7.3 Embryo dissection and light microscopy

For late-stage embryo imaging, seeds were dissected using a light stereo microscope. A few seeds were transferred onto the slide with wet Whatman paper, and the embryos were dissected out of the seed coat under a light stereomicroscope using fine forceps and needles. The seed was held with fine forceps by the micropylar end, and an incision was made on the other end of the seed coat with a needle or another pair of fine forceps. Gentle pressure was applied on the micropylar side of the seed using the forceps slanted to one side, causing the embryos to pop out of the seed coat. These were immediately transferred into a vial containing a few millilitres of cold water. Isolated embryos were used for staining and imaging. Seedlings were also dissected using a light stereo microscope. Peeled cotyledons with SAM were imaged at different focus distances using a Leica light microscope. Photographs were taken with a CCD camera. Captured images

were visualised in WinJoe software and transferred to Helicon 3D viewer for focus stacking. Focus stacking combines multiple images taken at different focus distances to generate an image with a greater depth of field (Fig 2.4).
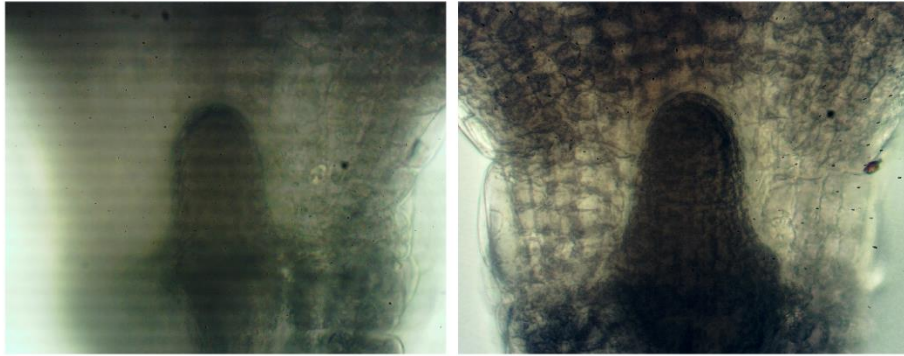
Figure 2.4 Single image (Left) and combined multiple images (right).

2.7.4 Confocal Microscopy

The small size of the *Arabidopsis* SAM makes it difficult to access, rendering analysis challenging. Analysis of *Arabidopsis* embryonic SAMs using confocal laser scanning microscopy permits the ready imaging of mature embryonic meristem organization, cells and cell layers from whole mount samples. For imaging and visual analysis of the 3 to 10 day old seedling phenotype, a stereomicroscope was used to dissect and analyse the plant material. SAMs were analysed by staining with 5 μg/mL of propidium iodide (PI) solution for 6 hours. The stained samples were mounted on microscope slides and imaged on a confocal microscope. Propidium iodide can be excited by a 514 nm argon laser beam and emits between 580-610 nm. Transgenic embryos or seedlings (*pPIN1::PIN1:GFP*, *DR5::GFP* and *pIND::IND:YFP*) were mounted on microscope slides with a slab of 1% plant agar and imaged using an Olympus FV1000 confocal microscope. YFP can be excited by a 514 nm argon laser beam and emits between 520-530 nm. GFP can be excited by a 488 nm argon laser beam and emits between 495-515 nm. Olympus FV1000 excitation lasers were listed in Table 2.5. Laser setting was selected and changed using software FV10-ASW. Captured images were processed using FV10-ASW viewer or Image J.

Table 2.5 Excitation Lasers.

Laser source	Excitation wavelength	Dyes & Fluorophores	Emission colour
405 Diode	405 nm	DAPI, Hoechst	Violet
Multi-line Argon	457 nm	CFP	Cyan
	488 nm	Alexa 488, Oregon Green, FITC, GFP, EGFP, DiO, Cy2	Green
	514 nm	YFP, EYFP	Yellow
Green HeNe	543 nm	Cy3, TRITC, mCherry, Alexa 543, Alexa 594	Orange-red
Red HeNe	633 nm	Alexa 633, Alexa 647, Cy5, TO-PRO3,	Far red

2.7.5 Scanning Electron Microscopy (SEM)

Samples were fixed in 3 % Glutaraldehyde/0.1 M sodium cacodylate buffer, washed in 0.1 M sodium cacodylate buffer to remove unbound fixative and secondarily fixed in 2 % aqueous osmium tetroxide for 1 hour. Specimens were dehydrated through a sequentially graded series of ethanol, 50 %-100 %, for 30 minutes per step, finally into 100 % ethanol before being dried over anhydrous copper sulphate. Specimens were critically point dried using CO_2 as the transitional fluid. After drying, the specimens were mounted on 12.5 mm diameter stubs, attached with sticky tabs and coated in an Edwards S150B sputter coater with approximately 25 - 30 nm of gold. Dr Chris Hill (Electron Microscopy Officer) processed samples before imaging. Specimens were viewed using a Philips SEM XL-20 Scanning Electron Microscope at an accelerating voltage of 20 kV in Biomedical Science Electron Microscopy Unit, University of Sheffield.

2.8 Statistical analysis

Phenotype and qRT-PCR data were analysed using tools within the GraphPad Prism 7 software. Student's t-test was performed using Microsoft Excel 2013, and one-way analysis of variance (ANOVA) with Tukey's multiple comparisons test was performed in GraphPad Prism 7. Unless otherwise stated, data are presented as mean +/- standard error of the mean (SEM). Significance was determined at a p-value at or below 0.05. False Discovery Rate (FDR) q-values were also generated from bioinformatics analysis (Microarray and GSEA). Q-values are the name given to the adjusted p-values.

Chapter 3

AGO10 and HD-ZIP III transcription factors regulate *IND*

CHAPTER 3. AGO10 and HD-ZIP III transcription factors regulate *IND*

3.1 Introduction

In *Arabidopsis*, leaf primordium development is dependent on establishing polarity along the adaxial (upper side) and abaxial (lower side) axes. The adaxial leaf face is promoted by the HD-ZIP III transcription factors PHABULOSA (PHB), PHAVOLUTA (PHV) and REVOLUTA (REV) (Elhiti and Stasolla, 2009; Liu et al., 2009; Mallory et al., 2004; McConnell et al., 2001; Zhou et al., 2007). Consequently, loss-of-function mutations in *HD-ZIP III* genes result in the formation of abaxialised and radialised leaves or terminated meristem with no leaves. Conversely, gain-of-function mutations in *HD ZIP III* genes cause adaxialised and radialised leaves (Barkoulas et al., 2007; Fambrini and Pugliesi, 2013; Prigge et al., 2005; Szakonyi et al., 2010; Tsukaya, 2013). Therefore, HD-ZIP III expression must be tightly controlled and this involves an elegant mechanism requiring miRNAs 165/166, AGO1 and AGO10.

HD-ZIP III expression is targeted and subsequently downregulated by the AGO1-miR165/166 in the shoot apical meristem (SAM) and leaf primordia (Liu et al., 2009; Miyashima et al., 2013; Tucker et al., 2013; Zhou et al., 2007; Zhou et al., 2015; Zhu et al., 2011b). However, AGO1 and AGO10 compete for miR165/166 binding. Although AGO10 has a stronger binding affinity for miR166 than AGO1, and AGO10 positively regulates *HD-ZIP III* family genes by acting as a specific decoy for miR166/165 (Lynn et al., 1999; Mallory et al., 2009), AGO10 is not involved in the post-translational repression of *HD-ZIP III* genes (Zhang and Zhang, 2012; Zhu et al., 2011b). Also, loss of function *ago10* mutants and *35S::miR166a* transgenic lines appear similar to *hd-zip iii* mutant seedlings (Endrizzi et al., 1996; Moussian et al., 2003; Moussian et al., 1998; Prigge et al., 2005; Zhu et al., 2011b). Together these studies suggest AGO10 promotes the adaxial leaf fate by positively regulating HD-ZIP III transcription factors.

In the reproductive phase, termination of stem cell activities in the floral meristem is essential for normal flower development. *AGO10* and *HD-ZIP III* genes regulate floral stem cell termination and promote normal flower development (Ji et al., 2011; Landau et al., 2015). Loss of *AGO10* results in prolonged stem cell activity in floral meristem and

ago10 mutants produce abnormal, bulged gynoecia (Ji et al., 2011). This shows that *AGO10* and *HD-ZIP III* genes play an important role in leaf development and floral differentiation. It is not known how AGO10 and HD-ZIP III transcription factors regulate other factors that control gynoecium patterning and this should be investigated.

The bHLH transcription factors IND and SPT regulate gynoecium patterning and their interaction is crucial for the fusion of carpels (Girin et al., 2011; Groszmann et al., 2010; Groszmann et al., 2008). The unfused apical carpel phenotype in the *spt* mutant were strongly enhanced in the *ind spt* double mutant (Girin et al., 2011). This shows that IND may regulate gynoecium development through the formation of a heterodimer with SPT. Moubayidin showed that overexpression of IND using *35S::IND:GR* seedlings produced radialised leaves (rod or pin-like and cup-like structures) and this leaf radialisation is lost in the *spt* mutant background (Moubayidin and Ostergaard, 2014). Therefore, both IND and SPT are necessary for mediating organ radialisation, similar to gynoecium development.

Since IND overexpression, *ago10* and *hd-zip iii* caused similar phenotypes, we hypothesised that IND is associated with the AGO10-HD-ZIP III pathway to control SAM or leaf development in *Arabidopsis*. In this chapter, we show that SAM development is regulated AGO10 by regulating *IND* expression. This chapter aims to study the connection between IND and AGO10-HD-ZIP III.

3.2 Results
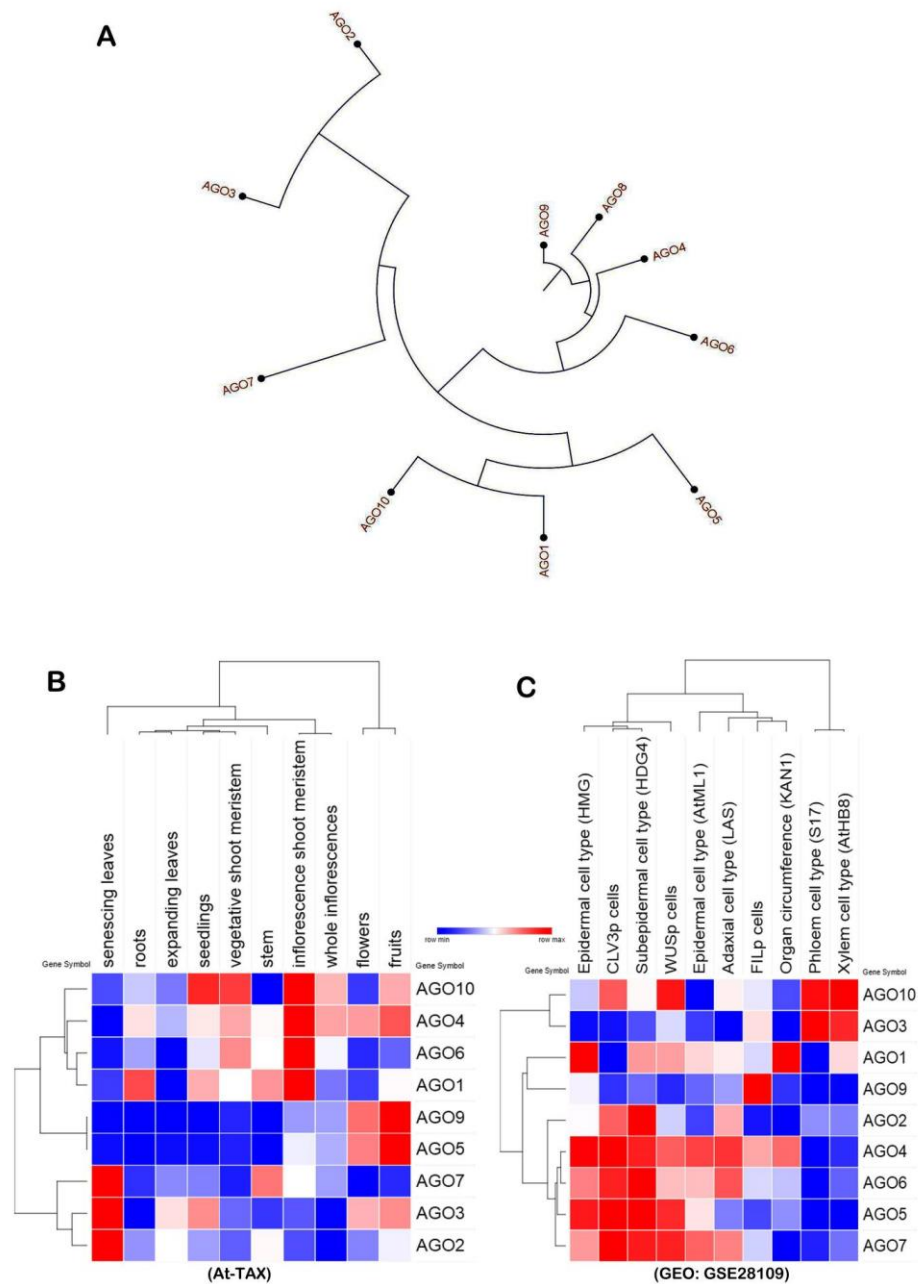
Figure 3.1 Argonaute protein family and their gene expression in *A. thaliana*. (A) Circular phylogram showing *Arabidopsis* AGO family amino acid sequence alignment classified into three different clades, namely the AGO1/AGO5/AGO10, AGO2/AGO3/AGO7, and AGO4/AGO6/AGO8/AGO9 clades. **(B)** Heat map with hierarchical clustering of samples and genes (one minus Pearson correlation): At-TAX developmental gene expression analysis of AGO family members (Z-score), **(C)** *AGO* family gene expression in *Arabidopsis* SAM protoplast cells (Z-score) (GEO:GSE28109). (Blue: low gene expression, Red: high gene expression).

3.2.1 Characterisation of *AGO* family gene expression in SAM and other tissues

The *Arabidopsis* genome encodes ten AGO family members. AGO amino acid sequences were aligned using CLC bio software. Based on their amino acid sequence homology AGO proteins were classified into three different clades: AGO1/AGO5/AGO10, AGO2/AGO3/AGO7 and AGO4/AGO6/AGO8/AGO9 clades (Fig 3.1A). The *Arabidopsis* AGO protein family can be divided into three functional groups: RNA slicers (AGO1/5/10), RNA binders (AGO2/3/7 (AGO7 also cuts)) and chromatin modifiers (AGO4/6/8/9) (Kim, 2011). *AGO1* and *AGO10* are expressed in SAM and leaf primordia, but their gene expression in other tissues is not known (Liu et al., 2009; Tucker et al., 2008). Also, gene expression of other *AGOs* has not been well characterised in SAM and other tissues. We investigated whether other AGOs may be important for SAM development. To characterise *AGO1* to *10* gene expression during *Arabidopsis* development, gene expression data from the *Arabidopsis thaliana* Tiling Array Express (At-TAX) database (Laubinger et al., 2008) was analysed using cluster analysis (Fig 3.1B). Hierarchical clustering (one minus Pearson correlation) was performed using Morpheus (Broad Institute, USA). Compared to other *AGOs*, higher *AGO2, AGO3,* and *AGO7* expression was observed in senescing leaves (Fig 3.1B). Higher *AGO4* and *AGO6* expression was observed in the vegetative shoot meristem and inflorescence shoot meristem (Fig 3.1B). Higher *AGO3, AGO4, AGO5* and *AGO9* expression was observed in stage 15 flowers and fruits (Fig 3.1B). *AGO10* was highly expressed in seedlings, the vegetative shoot meristem, inflorescence shoot meristem and stage 15 fruit (Fig 3.1B). *AGO1* was highly expressed in roots, seedlings, stem and the inflorescence shoot meristem (Fig 3.1B).

To investigate *AGO* expression in the different tissues of the SAM, we mined the SAM stem cell niche transcriptomic data sets (Yadav et al., 2009; Yadav et al., 2014). Yadav *et al.* (2009; 2014) used different promoters with fluorescent reporters to mark cells of SAM and protoplasted cells were FACS sorted (L1 epidermal cell type- *HIGH MOBILITY GROUP* (*HMG*), L1 differentiating cells- *MERISTEM LAYER 1* (*AtML1*), L2 subepidermal cell type- *HOMEODOMAIN GLABROUS 4* (*PHDG4*), OC *WUS*-expressing cells, CZ *CLV3*-expressing cells, PZ organ circumference-*KAN1*, Organ primordia-*FIL*, *LATERAL*

SUPPRESSOR (*LAS*)-expressing cells, Phloem- *S17* and Xylem-*AtHB8*). FACS sorted cells were processed for Affymetrix GeneChip ATH1 microarray (Yadav et al., 2014). To characterise *AGO1* to *10* gene expression in the SAM, gene expression data from processed microarray files (GEO: GSE28109) was analysed and hierarchical clustering was performed (one minus Pearson correlation) (Fig 3.1C). Higher *AGO2* and *AGO4-7* expression was observed in adaxial cells-*LAS* (Fig 3.1C). Higher *AGO9* expression was observed in organ primordia-*FIL* (Fig 3.1C). Higher *AGO3* expression was observed in Phloem-*S17* and Xylem-*AtHB8* (Fig 3.1C). *AGO4* to *AGO7* was highly expressed in epidermal (*HMG*, *AtML1*, and *HDG4*), *CLV3* and *WUS* cells (Fig 3.1C). *AGO1* was highly expressed in organ circumference-*KAN1*, epidermal (*HMG*, *AtML1*, and *HDG4*) and *WUSCHEL* cells (Fig 3.1C). *AGO10* was highly expressed in Phloem-*S17*, Xylem-*AtHB8*, *CLV3* and *WUS* cells (Fig 3.1C).

In summary, *AGO4* and *AGO6* expression in shoot meristem, *CLV3* cells, and *WUS* cells suggest they may have a role in the function of the SAM. *AGO1* and *AGO10* expression in the SAM match with previously published work (Liu et al., 2009; Tucker et al., 2008). *AGO10* expression in fruit, phloem cells, and xylem cells suggest a possible role of AGO10 in fruit and vascular development.
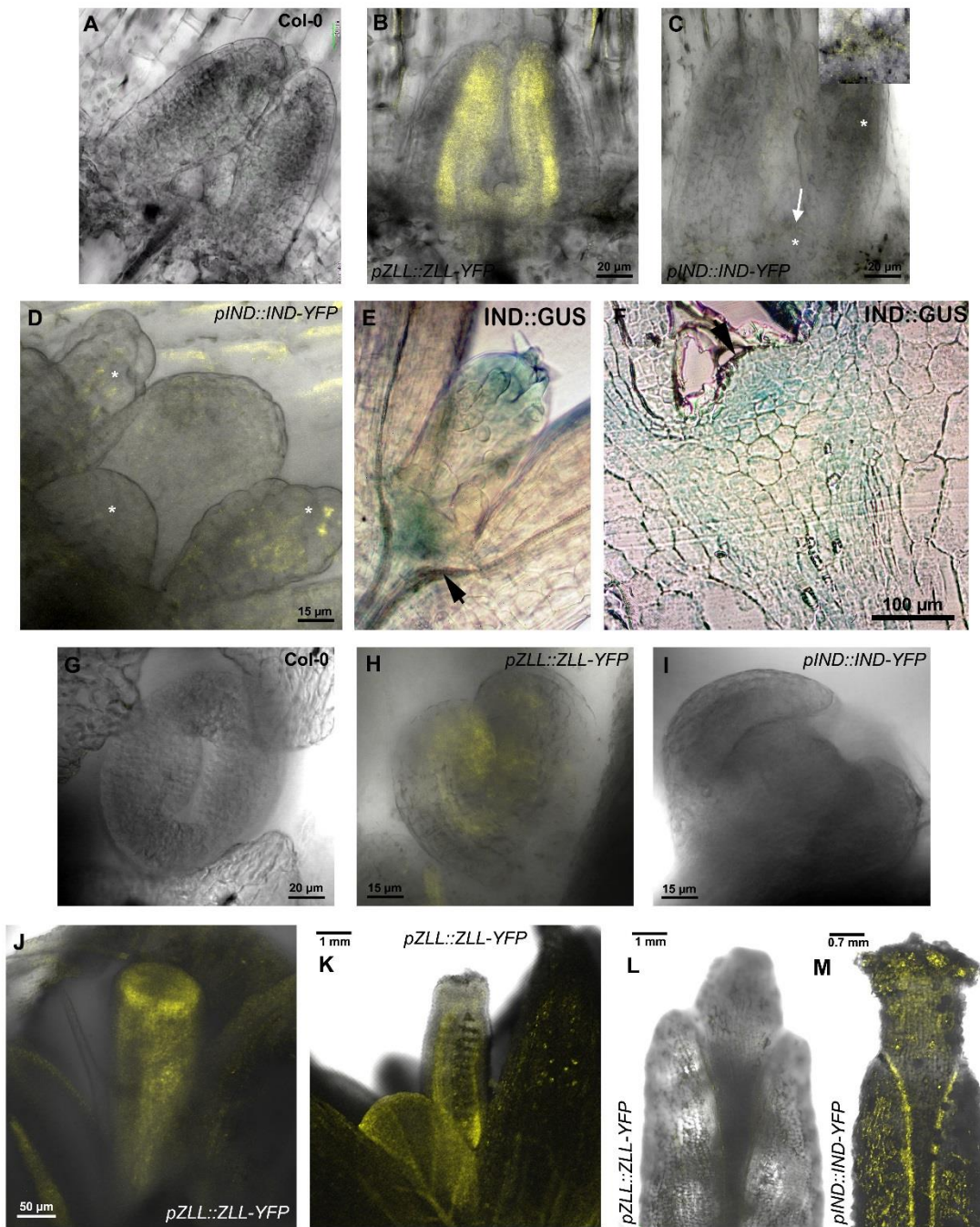
Figure 3.2 AGO10-YFP and IND-YFP expression in *Arabidopsis*. No YFP expression observed in Col-0 controls: 3 days old SAM **(A)** and stage 8 gynoecium **(G)**. AGO10-YFP expression observed in the SAM and adaxial side of leaf primordia (3DAG) **(B).** AGO10-YFP expression observed in the floral meristem **(H)**, style and non-distinct valves of stage 9 gynoecium **(J)**, valves of stage 12 gynoecium and petal vasculature **(K).** No AGO10-YFP expression observed in stage 17 fruit **(L).** Very weak (∗) IND-YFP expression observed in primordia and SAM (3DAG and 7DAG) **(C and D)**. Image show GUS expression in primordia and the SAM of *pIND::GUS* (7DAG) **(E).** The histological section shows GUS expression in the SAM of *pIND::GUS* (7DAG) **(F).** No IND-YFP expression observed in floral meristem **(I).** IND-YFP expression observed in stigma, style and valve margins of stage 14 fruit **(M).**

3.2.2 Characterisation of AGO10

3.2.2.1 AGO10 expression

To test whether *AGO10* gene expression pattern from the previous section matches with AGO10 protein expression, we used a *pZLL::ZLL-YFP* (*AGO10/ZLL/ZWILLE/PINHEAD*) transgenic line to characterise AGO10-YFP expression in seedlings, gynoecium, and fruit using confocal microscopy. Col-0 was used as a negative control. Confocal imaging was done to detect YFP expression using an argon laser at an excitation wavelength of 514 nm (Chapter 2, Section 2.7.4). Fluorescence corresponding to YFP expression was not observed in the Col-0 SAM with primordia (3DAG, Fig 3.2A) and stage 8 gynoecia (Fig 3.2G). AGO10-YFP expression was observed on the adaxial side of primordia and SAM (Fig 3.2B) of *pZLL::ZLL-YFP* (3DAG)*.* Flower and fruit development is divided into 20 stages (Smyth et al., 1990). YFP expression was observed in floral meristem (Fig 3.2H), style and presumptive valves of stage 9 gynoecia (Fig 3.2J), valves of stage 12 gynoecia and petal vasculature (Fig 3.2K) of *pZLL::ZLL-YFP.* AGO10-YFP expression was not observed in stage 17 fruit of *pZLL::ZLL-YFP* (Fig 3.2L)*.* The AGO10-YFP expression in leaf primordia and floral meristem is consistent with previously published work (Ji et al., 2011; Tucker et al., 2008). AGO10-YFP expression in SAM, leaf and reproductive tissues matched with *AGO10* gene expression. The AGO10-YFP expression in gynoecia suggests a novel role in early gynoecium development.

3.2.2.2 Genotyping *ago10* mutant *zwl-3*

Identification of the mutation in different *ago10* alleles can help determine the function of different domains and is also important for genotyping. The *ago10* alleles *zll* (*1 to 16*) and *pinhead* (*pnh 1 to 11*) have been commonly used in various studies (Poulsen et al., 2013). *zll-3* is the most commonly used *ago10* allele (Endrizzi et al., 1996; Mcconnell and Barton, 1995; Moussian et al., 1998), however, the mutation has not been characterised (Poulsen et al., 2013). Therefore, the *ago10* locus in *zll-3* plants was sequenced. The terms *zwillie-3* (*zwl-3*) or *ago10^{zwl-3}* were used in this thesis instead of *zll-3*, although *zwl-3/ago10^{zwl-3}* and *zll-3* are one of the same. To study the mutation, *AGO10* cDNA was PCR amplified using *zwl-3* and *Ler* (wild-type) cDNA samples, and PCR products were Sanger sequenced at the University of Sheffield (UOS) sequencing facility (Chapter 2, Section 2.3). Sequences were aligned using Bioedit software (Ibis Therapeutics, Canada) and analysed using NCBI tools (NCBI, USA). Unusually for an EMS mutant, we found that the

zwl-3 mutation was complex and had mutations that disrupted two domains of AGO10. Sequence analysis showed that *zwl-3* possess a missense mutation (G to A) at position 2399 bp downstream of the ATG. This mutation was predicted to cause an amino acid substitution (G to D) at position 707 aa of the AGO10 Piwi domain (Fig 3.3B, Fig 8.1 and 8.2), which can change the amino acid sequence and its functional activity (Endrizzi et al., 1996). The *zwl-3* missense mutation is identical to *zll-2* (Moussian et al., 1998; Poulsen et al., 2013). *zwl-3* also harbours a partial *CYP79B2* gene insertion in the *AGO10* exon2 region (Fig 3.3B, Fig 8.1 and 8.2). There is a possibility of duplication or deletion of *CYP79B2* gene in *zwl-3.* To examine mutations and changes in *CYP79B2*, sequencing was done on PCR amplified *zwl-3* and L*er CYP79B2* cDNA. Sequence analysis showed no mutation or deletion in *zwl-3 CYP79B2* in comparison to *Ler CYP79B2* (Fig 3.3B). This suggests possibly part of *CYP79B2* (Chr4) gene was copied to the *AGO10* exon2 region (Chr5). The *AGO10* exon2 region codes for the N-terminal domain, this domain is variable across different AGOs. Gregory *et al.* showed mutation within the N-terminus of AGO1 results in weak developmental defects in *ago1-38* (Gregory et al., 2008). Similar to *ago1-38,* the partial *CYP79B2* insertion in the *AGO10* exon2 region may enhance the loss of *ago10* activity in *zwl-3.*

3.2.2.3 *zwl-3* developmental phenotypes

To analyse SAM phenotypes, *zwl-3* and L*er* were grown on 0.5 % MS plant agar plates. 3-day old seedlings were dissected to image the SAM, and 14-day old seedlings were imaged without dissection. Imaging was performed using a light microscope. After imaging and analysis, *zwl-3* seedlings were classified into wild-type looking (WT), cup-shaped or single leaf (CUP), pin-shaped or filamentous-like (PIN) and no-meristem or flat apex (NM) phenotypes (Fig 3.4). The 3DAG *zwl-3* WT image shows two primordia, small emerging primordia and SAM (Fig 3.4) and 14DAG *zwl-3* WT image shows cotyledons and normal leaves similar to L*er* (Fig 3.4). The 3DAG *zwl-3* CUP image shows a bulged SAM with no primordia (Fig 3.4) and the 14DAG *zwl-3* CUP image shows cotyledons and cup-shaped single leaf (Fig 3.4). The 3DAG *zwl-3* PIN image shows pointed SAM with no primordia (Fig 3.4) and 14DAG *zwl-3* PIN image show cotyledons and pin-shaped SAM (Fig 3.4). The 3DAG *zwl-3* NM image shows dissected cotyledon with no SAM (Fig 3.4) and 14DAG *zwl-3* NM image show only cotyledons (Fig 3.4). All *zwl-3* seedlings produced

two cotyledons, which suggests that CUP, PIN, and NM were late stage embryo or post-embryonic meristem termination phenotypes.

The 14-day old *zwl-3* seedlings were quantified to examine the frequency of different phenotypes. The bar chart shows 29% WT, 11% CUP, 49% PIN and 11% NM *zwl-3* seedlings (3 biological replicates, n=50, Fig 3.5D). The WT *zwl-3* seedlings continued development and produced flowers and fruits allowing investigation into the role of *AGO10* in fruit development. The L*er* and *zwl-3* stage 17 fruits were imaged for phenotype analysis (Fig 3.5A). The image shows wild-type L*er* stage 17 fruit and small bulged stage 17 *zwl-3* fruit (Fig 3.5A). When compared to stage 17 L*er* fruit, a smaller replum was observed in stage 17 *zwl-3* fruit (Fig 3.5C). From phenotype analysis, we can draw that many of the *zwl-3* seedlings undergo meristem termination and few of the *zwl-3* seedlings undergo development and produce small bulged fruits with smaller repla.

3.2.2.4 Summary

In summary, the *zwl-3 AGO10* gene possesses two mutations, a missense mutation causing an amino acid substitution (G707D) in the Piwi domain, and insertion of a partial *CYP79B2* gene in the exon2 region. The meristem termination by the loss of *AGO10* in *ago10^{zwl-3}*, and expression of AGO10$^{pZLL::ZLL-YFP}$ in SAM and leaf primordia demonstrates that AGO10 is required for proper SAM development, in agreement with previously published work (Moussian et al., 1998; Tucker et al., 2008; Tucker et al., 2013). The bulged small fruit phenotype of *ago10^{zwl-3}* and expression of AGO10$^{pZLL::ZLL-YFP}$ in gynoecia suggests that AGO10 may also regulate fruit development.
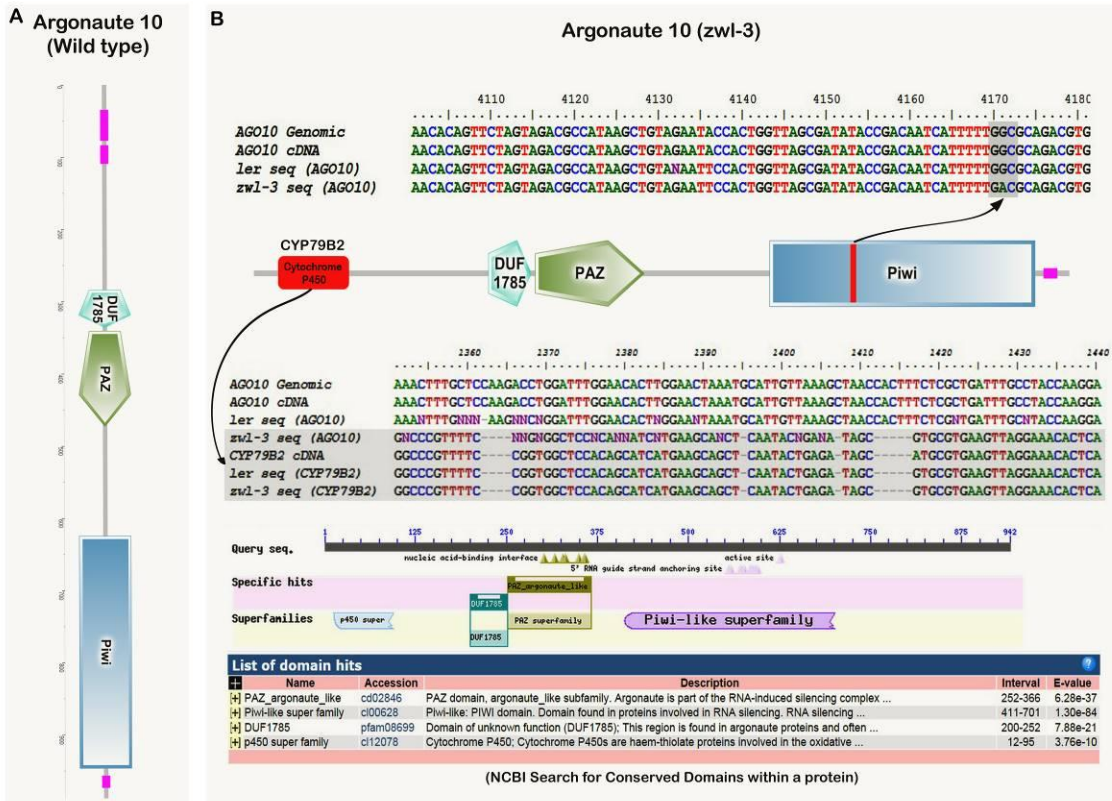
Figure 3.3 Mutations in *zwl-3* change the amino acid sequence in Piwi functional domain of AGO10. AGOs consist of a single variable N-terminal domain and three conserved C-terminal domains (PAZ, MID, and Piwi). The PAZ domain recognises, and anchors sRNA to its target mRNA, and the Piwi domain regulates catalytic activity (slice, bind or lock). When compared to wild-type AGO10 **(A),** *zwl-3* possesses a missense mutation (GGC to GAC) in the Piwi domain and also harbours an insertion (cytochrome P450: CYP79B2) in the exon2 region **(B)**. A missense mutation (GGC to GAC) at AGO10 Piwi domain can change the amino acid sequence (G to D).
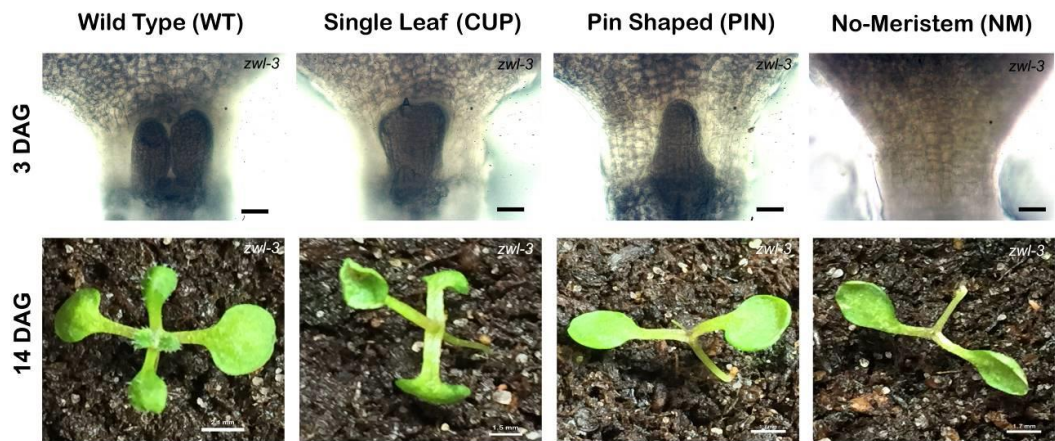
Figure 3.4 SAM phenotypes of *zwl-3* seedlings. *zwl-3* seedlings grown for 3 and 14 days either display cup-shaped or single leaf (CUP), pin-shaped or filamentous-like (PIN) and no-meristem or flat apex (NM) instead of a wild-type (WT). Scale bar for 3 DAG = 50 μm. Seedlings were imaged using a light microscope.
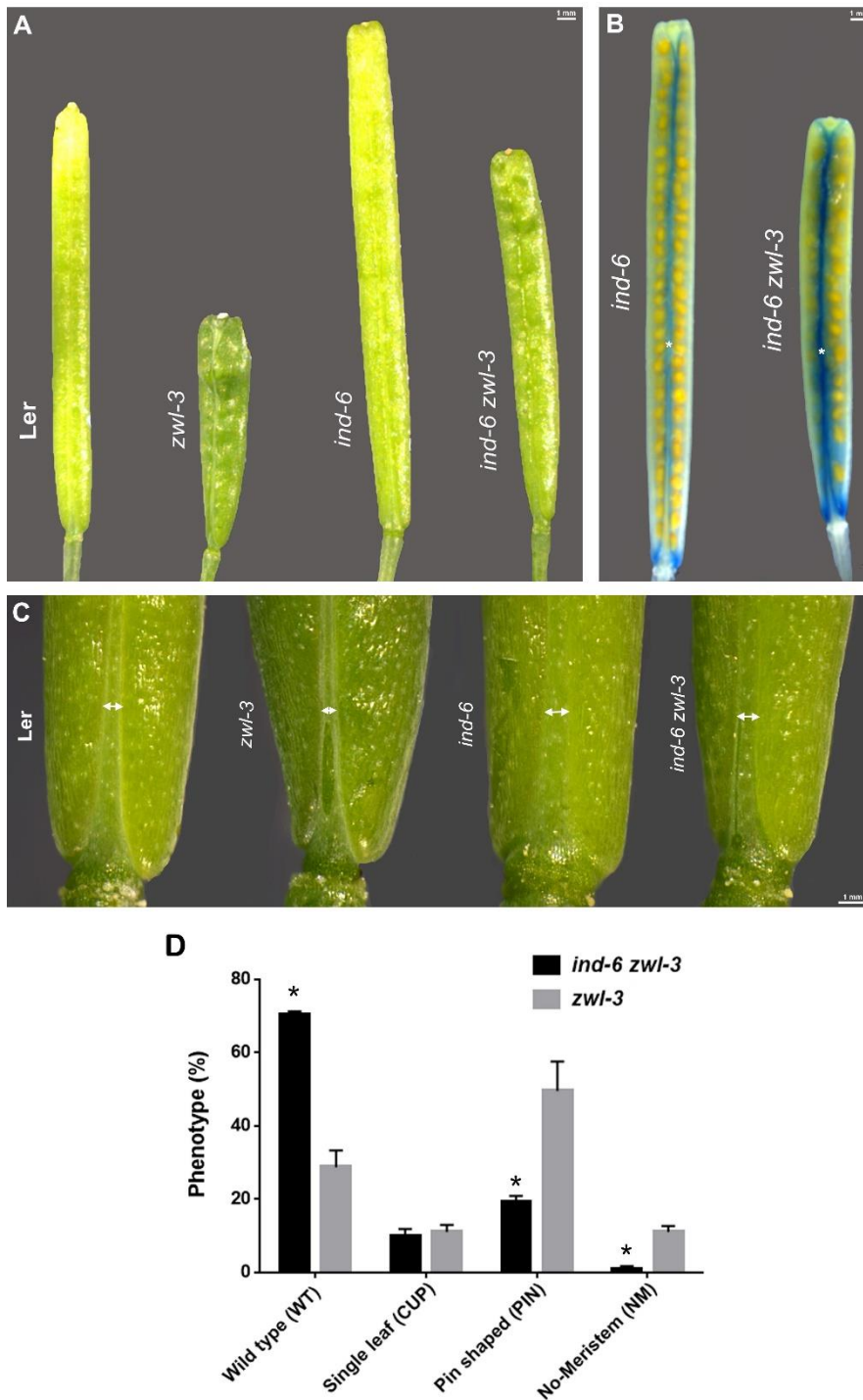
Figure 3.5 *ind* loss-of-function mutation rescues fruit and seedling phenotypes of *ago10^zwl-3*.

(A) Stage 17 fruit phenotypes of L*er, ind-6, zwl-3* and *ind-6 zwl-3* plants. **(B)** GUS staining in stage 17 fruit shows high expression in valve margins and repla of *ind-6 zwl-3* when compared to *ind-6*. **(C)** *AGO10* and *IND* regulate replum width. White line with double arrows indicates repla of L*er, ind-6, zwl-3* and *ind-6 zwl-3* stage 17 fruits**. (D)** Seedlings (14 DAG) shows a higher percentage of PIN and NM phenotypes in *zwl-3* and the WT phenotype in *ind-6 zwl-3* (n=3 biological replicates). Values are means ± SE. Tukey's multiple comparisons test (*ind-6 zwl-3* vs. *zwl-3*), *p<0.001.

58

3.2.3 Characterisation of IND

3.2.3.1 IND expression

Arabidopsis thaliana - Tiling Array Express data analysis showed *IND* gene expression in seedlings and the vegetative meristem (Laubinger et al., 2008). Therefore, the localisation of IND expression in the SAM and leaf primordia was investigated. In this study *pIND::GUS* and *pIND::IND-YFP* transgenic lines were used to characterise IND expression in SAM, leaf primordia and reproductive tissues. These transgenic lines were also previously used in different studies (Liljegren et al., 2004a; Simonini et al., 2016). Interestingly, IND-YFP expression was not observed in floral meristems of *pIND::IND-YFP* (Fig 3.2I). However, IND-YFP expression was observed in stigma, style and valve margins of stage 14 fruit (Fig 3.2M) of *pIND::IND-YFP* lines. The IND-YFP expression in fruit was consistent with previously published work (Simonini et al., 2016). Very weak IND-YFP expression was observed in primordia and SAM (Fig 3.2C and D) of *pIND::IND-YFP* (3DAG and 7DAG). In *pIND::GUS* (7DAG) lines, GUS activity was observed in SAM and leaf primordia and (Fig 3.2E). The histological resin sections of *pIND::GUS* seedlings (7DAG) showed GUS accumulation in the SAM (Fig 3.2F). The *IND* promoter-driven GUS and IND-YFP expression in the SAM and leaf primordia suggest that IND may have a role in SAM development.

3.2.3.2 Loss of *ind* developmental phenotypes

IND is required for valve margin development, but we do not know if the loss of *IND* can affect SAM development. Therefore, *ind* SAM and fruit developmental phenotypes were analysed using the *ind* allele *ind-6*. *ind-6* is an enhancer trap line that carries a Ds insertion after 183 nucleotides of *IND*, carrying a GUS reporter gene (Wu et al., 2006). To analyse the SAM phenotypes, *ind-6* and L*er* were grown on 0.5 % MS plant agar plates. The 3-day old seedlings were stained using propidium iodide (PI) and dissected to image the SAM. Imaging was done using confocal microscopy (Fig 3.8A). After imaging, the width of the SAM was measured for quantification (n=10 seedlings). The mean width of the *ind-6* SAM was 45 µm whereas the L*er* SAM was significantly larger or wider at 50 µm (p<0.05) (Fig 3.8B). Regardless of the small SAM, *ind-6* seedlings continued development and produced flowers and fruits. The L*er* and *ind-6* stage 17 fruits were imaged for phenotype analysis (Fig 3.5A). The image shows wild type L*er* stage 17 fruit and *ind-6* stage 17 fruit (Fig 3.5A). When compared to stage 17 L*er* fruit,

large repla (indicated by the white line with double arrows) and no valve margins were observed in stage 17 *ind-6* fruit (Fig 3.5C). The *ind-6* fruit phenotype data match with previously published work (Liljegren et al., 2004a; Wu et al., 2006). The *ind-6* small SAM phenotype suggests that IND regulate SAM size.

3.2.3.3 Overexpression of IND developmental phenotypes

The balance of abaxial and adaxial polarity is vital for normal leaf development (Szakonyi et al., 2010). Loss of abaxial polarity produces adaxialised leaves, and loss of adaxial polarity produces abaxialised leaves (Emery et al., 2003; Iwasaki et al., 2013; Kumaran et al., 2002; McConnell et al., 2001; Xu et al., 2003). Moubayidin and Ostergaard reported that overexpression of IND could produce radialised leaves, such as rod or pin-like and cup-like structures, but the polarity of these structures was not examined in detail (Moubayidin and Ostergaard, 2014).

To examine these phenotypes in detail, *35S::IND:GR* transgenic seeds were grown on half MS plant agar plates supplemented with 10 µM dexamethasone (DEX) or DMSO. DEX was used to induce IND activity. After 21 days, samples were imaged using light microscopy and processed for SEM imaging. Processed samples were imaged at the University of Sheffield Biomedical Science electron microscopy facility. The 21 DAG *35S::IND:GR*+DMSO images show normal leaves and a floral meristem (Fig 3.6K and L). After imaging and analysis, 21 DAG *35S::IND:GR*+DEX were classified into different phenotypes: pointed leaves (PL), cup-shaped or single leaf (CUP), pin-shaped or filamentous-like (PIN) and large meristem (LM) phenotypes (Fig 3.6A-J). The PL images (Fig 3.6E and F) show two leaves with trichomes on the adaxial surface and two pointed leaves with elongated epidermal cells. The CUP images (Fig 3.6A and B) show cotyledons, and a single CUP shaped leaf with trichomes on the inner epidermis, and the outer epidermis without trichomes. The PIN images (Fig 3.6C and D) show cotyledons and pin-shaped SAM with elongated epidermal cells. The LM images (Fig 3.6G-J) show a large SAM with pin-shaped primordia.

In *Arabidopsis*, leaves produced at an early stage of development lack trichomes on their abaxial surface (Telfer et al., 1997). Therefore, abaxialised and adaxialised leaves can be defined based on the distribution of trichomes on the leaf surface. The trichome

distribution in *35S::IND:GR*+DEX CUP, PIN and LM suggest that overexpression of IND promotes abaxialised leaves (Fig 3.6).

3.2.3.4 IND regulates leaf polarity genes

We hypothesised that overexpression of IND can regulate leaf polarity gene expression. Using qRT-PCR, leaf polarity gene expression was examined in 10 μM DEX, 10 μM cycloheximide (CHY) and DMSO-treated *35S::IND:GR* seedlings treated for 6 hours in liquid media. CHY is an effective protein synthesis inhibitor which was used in combination with DEX to examine IND-only regulated gene expression. A heat map of gene expression fold change (DEX vs. DMSO and DEX+CHY vs. CHY) in *35S::IND:GR* seedlings was generated using Morpheus. Gene expression fold change (DEX vs. DMSO and DEX+CHY vs. CHY) was also presented as a bar chart. Previous studies reported IND downregulates *PINOID* (*PID*) expression, so *PID* was used as a control to validate the *35S::IND:GR* qRT-PCR experiment. In this experiment, *PID* expression was decreased in the presence of DEX and significantly decreased in the presence of DEX+CHY ($p<0.05$, Fig 3.7B). The *PID* expression pattern is consistent with other published studies (Moubayidin and Ostergaard, 2014; Sorefan et al., 2009a).

The abaxial and adaxial leaf polarity is regulated by different genes (Garcia et al., 2006; Szakonyi et al., 2010). In *Arabidopsis*, *AGO10, PHB, PHV, REV, ZPR1, AGO7* and *AS1* regulate adaxial leaf polarity. These adaxial genes were screened in this experiment. *AGO10* expression was decreased in the presence of DEX with a twelve-fold decrease in expression in the presence of DEX+CHY ($p<0.05$, Fig 3.7B). *PHB* expression was increased two-fold in the presence of DEX ($p<0.05$) and DEX+CHY (Fig 3.7A). *PHV* expression was significantly decreased in the presence of DEX+CHY ($p<0.05$) whereas no change was observed in the presence of DEX (Fig 3.7A). No significant change of *REV* expression was observed in the presence of DEX and DEX+CHY (Fig 3.7A). *ZPR1* expression was significantly increased in the presence of DEX ($p<0.05$) and increased four-fold in the presence of DEX+CHY ($p<0.05$, Fig 3.7A). *AGO7* expression was increased three-fold in the presence of DEX ($p<0.05$) and increased in the presence of DEX+CHY ($p<0.05$, Fig 3.7A). *AS1* expression was increased in the presence of DEX ($p<0.05$) whereas no change was observed in the presence of DEX+CHY (Fig 3.7A). This data suggests   of *IND* may inhibit adaxial leaf polarity by downregulating *AGO10* and upregulating *ZPR1.* AGO10

positively regulates *PHB, PHV,* and *REV,* and ZPR1 negatively regulates PHB, PHV, and REV by forming non-functional heterodimers (Kim et al., 2008; Wenkel et al., 2007; Zhu et al., 2011b). Loss of *PHB, PHV* and *REV* function promotes abaxialised leaf growth (Emery et al., 2003; McConnell et al., 2001; Otsuga et al., 2001).

In *Arabidopsis*, *KAN, YAB1, ARF4,* and *WOX1* regulate abaxial leaf polarity. These abaxial genes were screened in this experiment. There was a five-fold increase in *WOX1* expression in the presence of DEX ($p<0.05$) but no change in expression was observed in the presence of DEX+CHY (Fig 3.7A). *KAN* and *YAB1* expression were increased in the presence of both DEX ($p<0.05$) and DEX+CHY (Fig 3.7A). *ARF4* expression was increased in the presence of DEX and DEX+CHY ($p<0.05$, Fig 3.7A). AGO7 negatively regulates *ARF4* expression (Garcia et al., 2006; Hunter et al., 2006; Montgomery et al., 2008), interestingly *AGO7* was increased ($p<0.05$) compared to *ARF4* in the presence of DEX (Fig 3.7A). This suggests that IND may not regulate abaxial leaf polarity via *ARF4.* However, overexpression of IND may promote abaxial leaf polarity by upregulating *KAN, YAB1,* and *WOX1.* In *Arabidopsis*, *KNAT1, WUS,* and *CLV3* regulate SAM development. *KNAT1, WUS* and *CLV3* genes were also screened in this experiment. *WUS* expression was variable (data not shown) and *CLV3* expression was not significantly regulated in the presence of DEX and DEX+CHY (Fig 3.7B). However *KNAT1* expression was increased in the presence of DEX ($p<0.05$) and also DEX+CHY (Fig 3.7A), suggesting IND upregulates *KNAT1* expression. Overexpression of KNAT1 negatively regulates leaf development by producing lobed leaves with ectopic meristems (Chuck et al., 1996). However, these phenotypes were not observed in *35S::IND:GR*+DEX seedlings and this suggests the phenotypes observed in *IND:GR* lines may not be caused by *KNAT1* overexpression.

3.2.3.5 Summary

In summary, IND-YFP expression and loss of *ind* phenotype studies demonstrate that IND may regulate SAM size. Phenotype analysis following IND overexpression and induction, and qRT-PCR suggests that IND may promote leaf abaxialisation and meristem termination.

Panel labels within figure:

A — Abaxial — + DEX — 1 mm — 100 µm

B — Adaxial — + DEX — 500 µm — 100 µm

C — + DEX — 1 mm

D — + DEX — 200 µm

K — + DMSO — 2 mm

E — + DEX — 1 mm

F — + DEX — 200 µm

L — + DMSO — 500 µm

G — + DEX — 1 mm

H — + DEX — 100 µm

I — + DEX — 1 mm

J — + DEX — 100 µm

M — DEX — DEX+CHY — -5 0 5

WOX1
AGO7
YAB1
ZPR1
KNAT1
CLV3
AS1
PHB
KAN
ARF4
PHV
REV
AGO10
PID
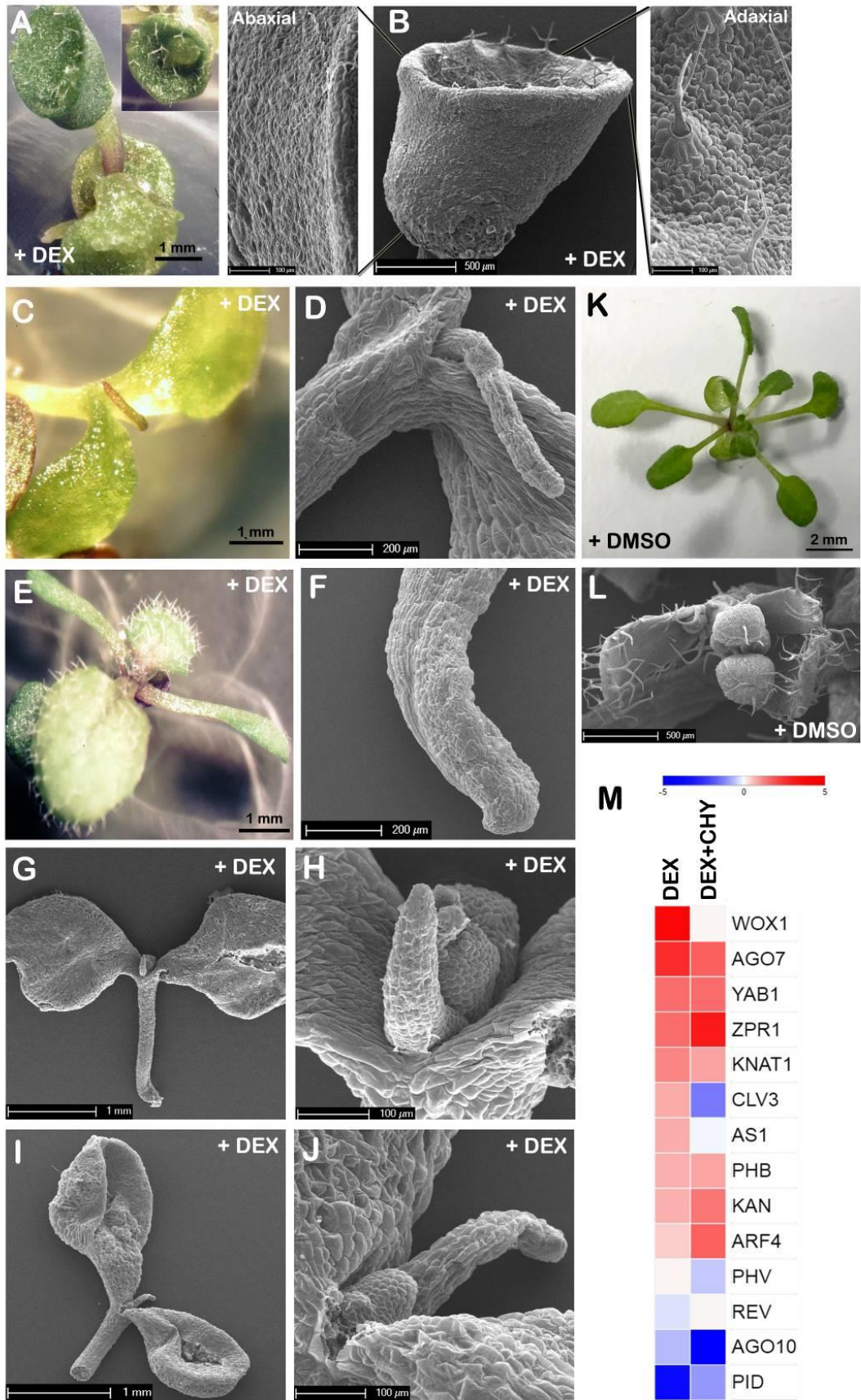
Figure 3.6 Phenotypic and molecular characterisation of an inducible IND line. *35S::IND:GR* seedlings treated with 10 µM dexamethasone and DMSO (21 DAG) either produce **(A and B)** cup-shaped or single leaf, **(C and D)** pin-shaped or filamentous-like, **(G-J)** large meristem and **(E and F)** pointed leaves instead of a **(K and L)** normal meristem. **(M)** Heat map of the meristem and leaf polarity identity genes that were differently expressed in *35S::IND:GR* seedlings treated for 6 hours with 10 µM dexamethasone (DEX vs. DMSO) and 10 µM dexamethasone plus 10 µM cycloheximide (DEX+CHY vs. CHY) (Fold change from qRT–PCR data, n=3 biological replicates). (Blue: low gene expression, Red: high gene expression).
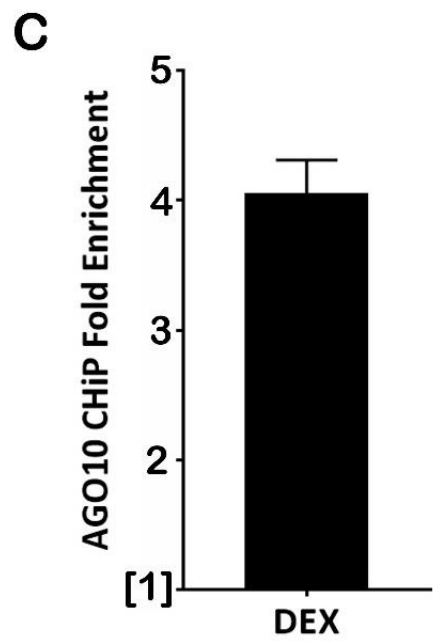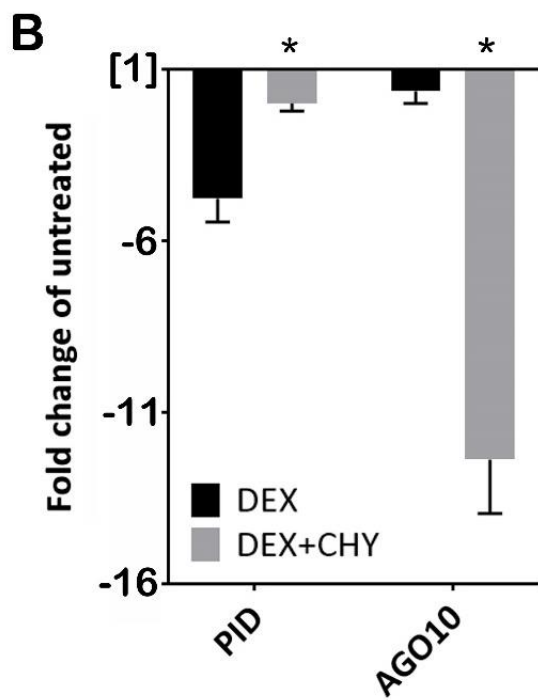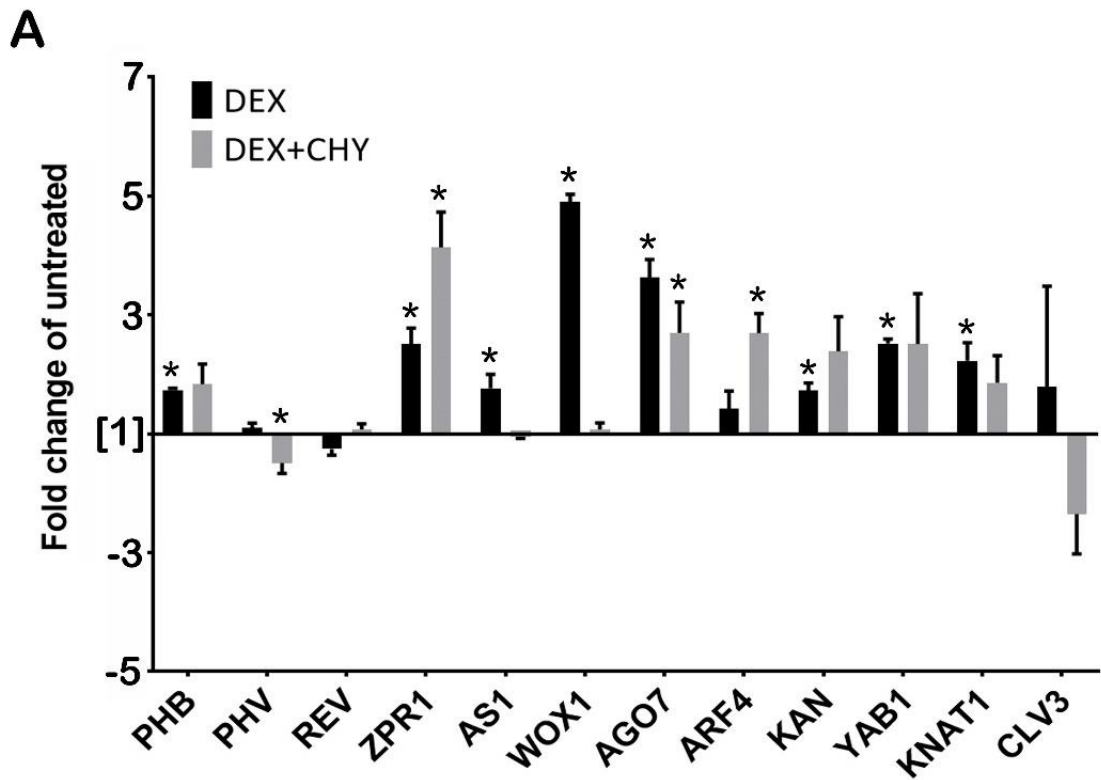
Figure 3.7 IND regulate leaf polarity genes. (A) The bar chart version of heat map from Fig 2.6M show differentially expressed meristem and leaf polarity identity genes in *35S::IND:GR* (Fold change from qRT-PCR data, DEX vs. DMSO and DEX+CHY vs. CHY, n=3). The bar chart shows *PHV* expression was decreased in the presence of DEX+CHY. *ARF4* expression was significantly increased in the presence of DEX+CHY. *AS1* and *WOX1* expression were significantly increased in the presence of DEX. *ZPR1* and *AGO7* expression were significantly increased in the presence of DEX and DEX+CHY. *KAN, YAB1, KNAT1* and *PHB* expression was significantly increased in the presence of DEX and also increased in the presence of DEX+CHY. No significant change of *REV* and *CLV3* expression was observed in the presence of DEX and DEX+CHY. **(B)** The bar chart shows *PID* and *AGO10* expression was decreased in the presence of DEX and decreased in the presence of DEX+CHY. **(C)** IND-*AGO10* promoter interaction was tested by ChIP-qRT-PCR using *35S::IND:GR* line, the bar chart shows four-fold enrichment for *AGO10* (upstream 926-1175 bp) in the presence of DEX (n=3). Values are means ± SE. Unpaired t-test (DEX vs. DMSO and DEX+CHY vs. CHY), *p<0.05.
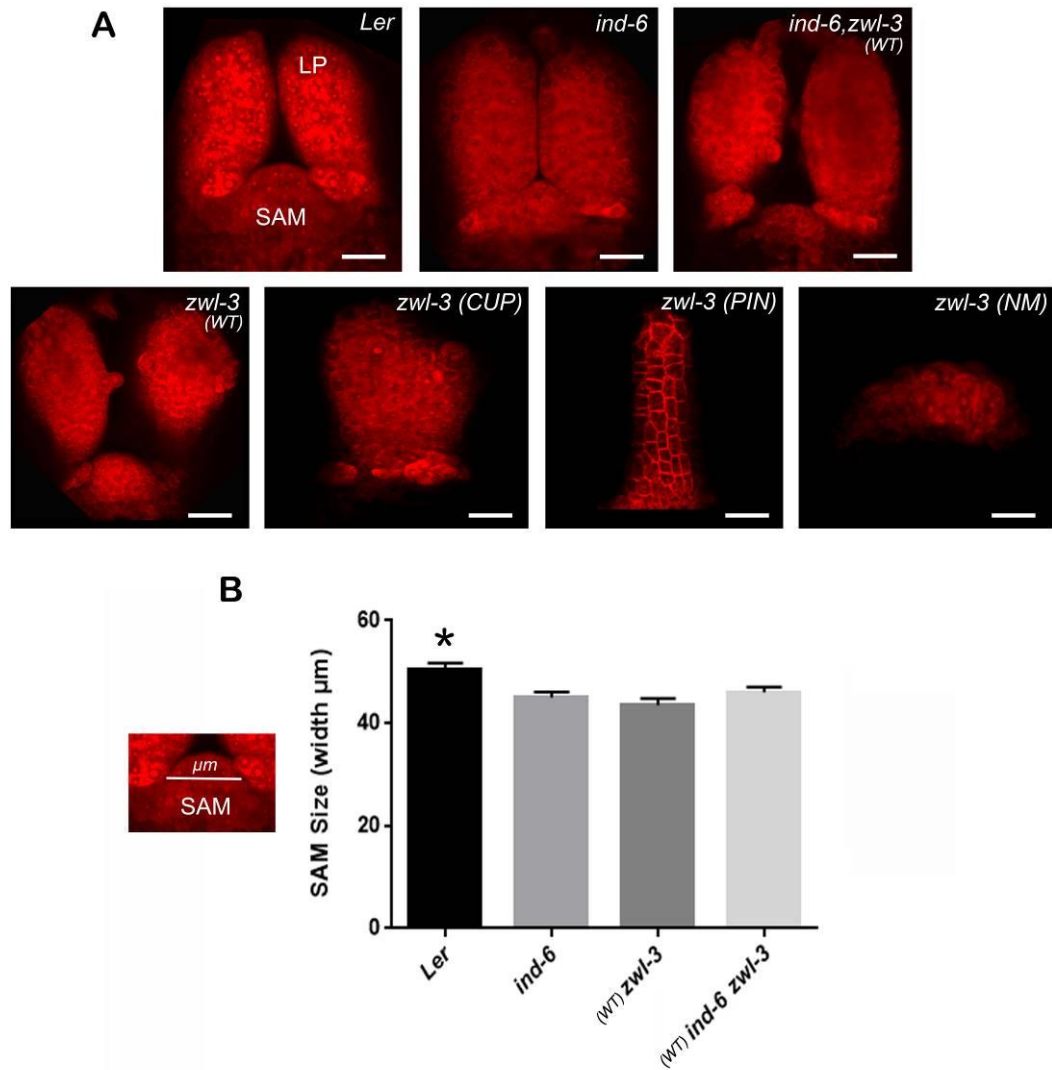
Figure 3.8 SAM phenotype of L*er* and mutants (*ind-6, zwl-3,* and *ind-6 zwl-3*). (A) Three-day-old seedlings stained with propidium iodide showing SAM with leaf primordia (LP) and abnormal phenotypes *zwl-3* CUP, *zwl-3* PIN and *zwl-3* NM (Scale bar = 50 μm). SAM size (width) was measured. **(B)** L*er* SAM was large compared to *ind-6, zwl-3* and *ind-6 zwl-3* (n=10). Values are means ± SE. Tukey's multiple comparisons test, *p<0.05 (L*er* vs. mutants).

3.2.4 *IND* and *AGO10* pathway

3.2.4.1 *IND* and *AGO10* negatively regulate each other

The data from section 3.2.3 shows that overexpression and DEX-induction of IND:GR can downregulate *AGO10*. We tested whether IND can possibly downregulate *AGO10* by binding to the *AGO10* promoter by ChIP. *35S::IND:GR* seeds were grown in liquid media and on day seven seedlings were treated with 10 μM DEX and DMSO for 6 hours. Treated samples were processed for ChIP (Chapter 2, Section 2.4). From previous yeast one-hybrid interaction study we know that IND can bind to G-box element CACGTG (Girin et al., 2011). A G-box element CACGTG was located 1162-1167 upstream of *AGO10*. *pAGO10* (primers designed to amplify upstream 926-1175 bp) was tested by qRT-PCR (Chapter 2, Section 2.3) and fold enrichment (DEX vs. DMSO) was determined. There was a four-fold enrichment for *pAGO10* (upstream 926-1175 bp) in the presence of DEX (Fig 3.7C). This data suggests IND binds to the *AGO10* promoter and downregulates *AGO10.*

AGO10 possibly downregulates *IND* to control the antagonistic function of IND in SAM development. To examine this, cDNA was prepared from 14 day old L*er,* and *zwl-3* (WT, CUP*,* PIN, and NM) seedlings and gene expression were quantified using qRT-PCR. Gene expression fold change (*zwl-3* vs. L*er*) shows that *IND* was upregulated in all *zwl-3* seedlings regardless of phenotype, and there was an eight-fold increase of *IND* expression in *zwl-3* PIN when compared to wild-type L*er* (p<0.05) (Fig 3.9). Upregulation of *IND* in *zwl-3* suggests that AGO10 negatively regulates *IND.*

IND interacts with SPT to regulate organ patterning, and SPT also interacts with HEC1 to regulate SAM development (Girin et al., 2011; Schuster et al., 2015; Schuster et al., 2014; Sparks and Benfey, 2014). *SPT* and *HEC1* gene expression was also screened in this experiment. *HEC1* expression was decreased in all *zwl-3* phenotypes, and there was a nine-fold decrease of *HEC1* expression in *zwl-3* NM compared to wild-type L*er* (p<0.05) (Fig 3.9). *SPT* expression was weakly decreased in all *zwl-3* phenotypes (Fig 3.9). This data suggests AGO10 positively regulates *HEC1* and may not regulate *SPT* expression*.* This shows that loss of *AGO10* in *ago10^{zwl-3}* possibly promotes IND and SPT interaction.

3.2.4.2 *IND* and *AGO10* double mutant *ind-6 zwl-3* developmental phenotypes

The data from sections 3.2.2 and 3.2.3 suggests that overexpression of IND phenocopies *ago10^{zwl-3}*. If IND overexpression is associated with *zwl-3* phenotypes, then the loss of *ind* in *zwl-3* should rescue the wild-type phenotype. L*er*, *zwl-3,* and *ind-6 zwl-3* were grown on half MS plant agar plates, and the SAM phenotype was analysed. The 3-day old seedlings were stained using propidium iodide (PI) and dissected to image the SAM, and 14-day old seedlings were imaged without dissection using light microscopy. PI-stained seedlings were imaged using confocal microscopy (Fig 3.8A). After imaging, the width of the SAM (L*er*, *zwl-3* WT*,* and *ind-6 zwl-3* WT) was measured for quantification (n=10 seedlings). After imaging and analysis, 3 and 14 day old *ind-6 zwl-3* seedlings were classified into WT, CUP, PIN and NM phenotypes and these phenotypes are similar to *zwl-3* (3.2.3, Fig 3.8A). The 3 day old *zwl-3* CUP tissue appeared as a packed cluster of small cells when compared to elongated cells in *zwl-3* PIN (Fig 3.8A)*.* The PI stained *zwl-3 WT* SAM and *ind-6 zwl-3 WT* SAM appeared small when compared to L*er* SAM (Fig 3.8A). The bar chart show 43.5 µm *zwl-3* WT SAM, 46 µm *ind-6 zwl-3* WT SAM and significantly large 50 µm L*er* SAM (L*er* vs. mutants, p<0.05) (Fig 3.8B). No significant difference was observed between *zwl-3* WT SAMs and *ind-6 zwl-3* WT SAMs. The 14 day old *zwl-3* and *ind-6 zwl-3* seedlings were quantified to examine the frequency of different phenotypes. The *ind-6 zwl-3* WT phenotype was present in 75% of samples when compared to *zwl-3* WT (p<0.05) (Fig 3.5D). No significant difference was observed between *ind-6 zwl-3* CUP and *zwl-3* CUP (Fig 3.5D)*.* The *ind-6 zwl-3* PIN phenotypes were significantly decreased (p<0.05) when compared to *zwl-3* PIN (Fig 3.5D). The proportion of *ind-6 zwl-3* NM seedlings was significantly decreased when compared to *zwl-3* NM (p<0.05) (Fig 3.5D). These data suggest that loss of *IND* in the *ind-6 zwl-3* double mutant rescues the WT phenotype.

The *ind-6 zwl-3* WT seedlings undergo development and produce flowers and fruits. The L*er*, *zwl-3* and *ind-6 zwl-3* stage 17 fruits were imaged for phenotype analysis (Fig 3.5A). The image shows small bulged stage 17 *zwl-3* fruit and big bulged stage 17 *ind-6 zwl-3* fruit (Fig 3.5A). The stage 17 *ind-6 zwl-3* fruit was small when compared to stage 17 L*er* fruit (Fig 3.5A). The stage 17 *zwl-3* fruit was very small (Fig 3.5A). When compared to stage 17 *ind-6 zwl-3* fruit, small repla were observed in stage 17 *zwl-3* fruit (Fig 3.5C). The stage 17 *ind-6 zwl-3* fruit replum looks similar to stage 17 L*er* fruit replum (Fig 3.5C).

Fruit phenotype analysis suggests that loss of *IND* in the *ind-6 zwl-3* double mutant also rescues fruit size and size of replum.

The *ind-6* mutant is an enhancer trap line that carries a Ds insertion and a GUS reporter gene (Wu et al., 2006). Wu *et al.* reported that the expression pattern of the GUS gene in an *ind-6* silique likely represents that of *IND* in WT (Wu et al., 2006). They also stated that the GUS signal was absent in other parts of the plants. This shows *ind-6 zwl-3* can be used to test if the loss of *AGO10* in *ago10^{zwl-3}* can upregulate *ind*-GUS expression in *ind-6 zwl-3*. To study this further, the GUS assay was used to examine stage 17 *ind-6* and *ind-6 zwl-3* fruits, and the resulting fruits were imaged using light microscopy. The image shows GUS activity accumulation in valve margins of stage 17 *ind-6* and *ind-6 zwl-3* fruits (Fig 3.5B). When compared to stage 17 *ind-6* fruit, high GUS activity accumulation was observed in valve margins and the replum of stage 17 *ind-6 zwl-3* fruit (Fig 3.5B). This data shows that loss of *AGO10* upregulates *ind*-GUS expression in the valve margins and replum. This suggests that AGO10 may negatively regulate *IND* expression in valve margins and replum.

3.2.4.3 Summary

In summary, IND binds to the *AGO10* promoter and downregulates *AGO10.* The phenotype analysis and qRT-PCR studies suggest that AGO10 may negatively regulate *IND* in seedlings to prevent meristem termination and in fruit to preserve the replum. This demonstrates that IND and AGO10 negatively regulate each other.
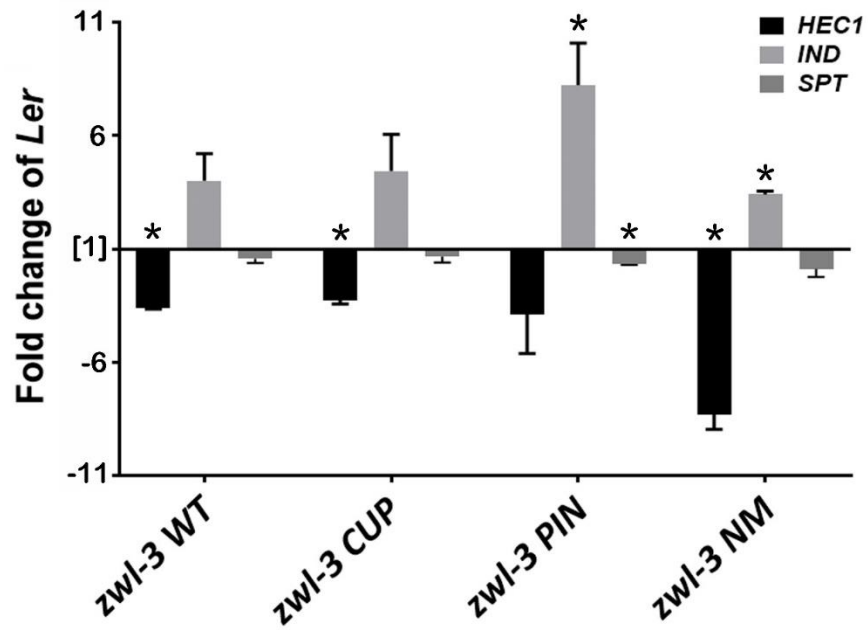
Figure 3.9 AGO10 regulates *IND* and *HEC1* gene expression. *IND*, *HEC1* and *SPT* gene expression was quantified in *zwl-3* and L*er* seedlings using qRT-PCR (n=3 biological replicates). The bar chart shows that *IND* gene expression was upregulated in *zwl-3* relative to L*er* and significantly upregulated in *zwl-3* PIN and NM. *HEC1* gene expression was downregulated in *zwl-3* relative to L*er* and significantly downregulated in *zwl-3* WT, CUP and NM. Values are means ± SE. Tukey's multiple comparisons test (L*er* vs. *zwl-3*), *p<0.05.

3.2.5 PHB and REV regulate *IND*, *SPT* and *HEC1* gene expression

The data from section 3.2.4 shows AGO10 negatively regulates *IND,* yet the regulatory mechanism is unknown. We do not know if AGO10 can downregulate *IND* via miRNA. The *Arabidopsis* small RNA project data was used to examine if *IND* is targeted by small RNAs (http://asrp.danforthcenter.org/). *Arabidopsis thaliana* small RNA project data is a collection of different studies from the Carrington laboratory. The data include identified *Arabidopsis* small RNAs sequences (GSE6682) and ARGONAUTE-small RNA interactions (GSE12037). These data tracks were loaded in a genome browser (JBrowse) and analysed for *PHB* (Control) and *IND* miRNA target sites. The miRNA166 and 165 target sites were observed in *PHB* (Fig 3.12A). No miRNA target sites were observed in *IND* (Fig 3.12B), but a transposable element (AT4TE00200) was located at the end of 3'-untranslated region (3'-UTR) region of *IND.* Small RNAs can prevent the expression of transposable elements (Dr Karim Sorefan also identified a possible miRNA target site in the transposable element region of *IND* and observed none in the coding region) (Hollister et al., 2011; Sorefan et al., 2012). The 5'-UTR and 3'-UTR do not code for protein, so this suggests that small RNAs do not inhibit *IND* expression. In addition, *Arabidopsis thaliana* - Tiling Array Express small RNA data also suggest that small RNAs do not inhibit *IND* expression (Fig 8.3). This shows that AGO10 inhibits *IND* via other proteins. Since AGO10 positively regulates *HD-ZIP III* transcription factors (*PHB*, *PHV*, and *REV*), they may regulate *IND* gene expression. To test this hypothesis, cDNA was prepared from 14 day old Col-0, *ago10-4, phb-12 er-2, phv-11 er-2* and *rev-6 er-2* seedlings and gene expression was quantified using qRT-PCR. Gene expression fold change (mutants vs. Col-0) was determined. There was a three-fold increase in *IND* expression in *ago10-4* (Fig 3.10A). There was a three-fold increase in *IND expression* in *phb-12 er-2, phv-11 er-2* and six-fold increase in *rev-6 er-2* (Fig 3.10A). Upregulation of *IND* in *hd-zip III* mutants (*phb-12 er-2, phv-11 er-2,* and *rev-6 er-2)* suggests that PHB, PHV, and REV negatively regulate *IND.*

PHB, PHV and REV transcription factors may directly regulate *IND, HEC1,* and *SPT.* We failed to construct a *35S::PHV:GR* plasmid. Therefore only *35S:LhGR>>PHB* and *35S::REV:GR* transgenic lines were used in this study to examine whether inducible activity of overexpressed HD-ZIP III transcription factors can regulate *IND, SPT,* and *HEC1* gene expression. Gene expression was examined following treatment with 10 μM DEX,

10 μM cycloheximide (CHY) and DMSO-treated seedlings (*35S:LhGR>>PHB* and *35S::REV:GR*) using qRT-PCR (treated for 6 hours in liquid media). Gene expression fold change (DEX vs. DMSO and DEX+CHY vs. CHY) was determined. *IND* expression was decreased two-fold in the presence of DEX (*35S:LhGR>>PHB* and *35S::REV:GR*) ($p < 0.05$), but no significant difference was observed in the presence of DEX+CHY (*35S:LhGR>>PHB* and *35S::REV:GR*) (Fig 3.10B). This suggests that PHB and REV downregulate *IND. HEC1* expression was decreased 1.5 fold in the presence of DEX (*35S:LhGR>>PHB*) ($p < 0.05$) and no significant difference was observed in the presence of DEX+CHY (*35S:LhGR>>PHB*) (Fig 3.10B). *HEC1* expression was increased two-fold in the presence of DEX+CHY (*35S::REV:GR*) ($p < 0.05$) and no significant difference was observed in the presence of DEX (*35S::REV:GR*) (Fig 3.10B). This suggests that REV upregulates *HEC1* and this result was consistent with previously published work (Reinhart et al., 2013)*. SPT* expression was significantly increased two-fold in the presence of DEX (*35S:LhGR>>PHB*) ($p < 0.05$) and also increased in the presence of DEX+CHY (*35S:LhGR>>PHB*) ($p < 0.05$) (Fig 3.10B). *SPT* expression was increased three-fold in the presence of DEX+CHY (*35S::REV:GR*) ($p < 0.05$) but no significant difference observed in the presence of DEX (*35S::REV:GR*) (Fig 3.10B). This suggests that PHB and REV directly upregulate *SPT.*

PHB, PHV and REV transcription factors may bind to the promoter region of *IND, SPT,* and *HEC1*. PHV DAP-seq (GEO:GSM1925338) (O'Malley et al., 2016) and REV ChIP-seq (GEO:GSE26722) (Brandt et al., 2012) datasets were analysed to study whether PHV and REV transcription factors bind to the promoter region of *IND, SPT,* and *HEC1* (no PHB datasets were found in GEO or ArrayExpress). DNA affinity purification sequencing (DAP-seq) is a high-throughput transcription factor binding site discovery method. O'Malley *et al.* used DAP-seq to examine *Arabidopsis* genomic DNA interaction with *in-vitro*-expressed transcription factors. PHV DAP-seq (GEO:GSM1925338) data were compared with a list of *bHLH* genes curated from the TAIR database, and a Venn diagram was generated using VENNY 2.1. The Venn diagram shows 7310 PHV target genes labelled in the blue intersecting circle, 96 *bHLH* genes labelled in the yellow intersecting circle and the overlapping region shows that PHV binds to *65* bHLHs (Fig 3.11A). *SPT* and *HEC1* were on the list of 65 *bHLHs*, but not *IND*. This suggests PHV binds to *SPT* and *HEC1. REV* ChIP-seq (GEO:GSE26722) data were compared with a list of *bHLH* genes, and a Venn diagram was generated using VENNY 2.1. Venn diagram shows 10744 REV target genes

labelled in the blue intersecting circle, 57 *bHLH* genes labelled in the yellow intersecting circle and the overlapping region shows that REV binds to 104 *bHLHs* (Fig 3.11A). *SPT* and *HEC1* were on the list of 104 *bHLHs*, but not *IND*. This suggests REV binds to *SPT* and *HEC1.*

In summary, these studies demonstrate that PHB and REV may negatively regulate *IND* by indirectly downregulating *IND* gene expression. The ChIP-seq and qRT-PCR experiments suggest that REV binds to *SPT* and *HEC1* and upregulates *SPT* and *HEC1* gene expression. The DAP-seq and qRT-PCR experiments suggest that PHV binds to *SPT* and *HEC1,* and PHB directly upregulates *SPT* gene expression. This shows that PHB and REV may promote *SPT* and *HEC1* and inhibit *IND*.
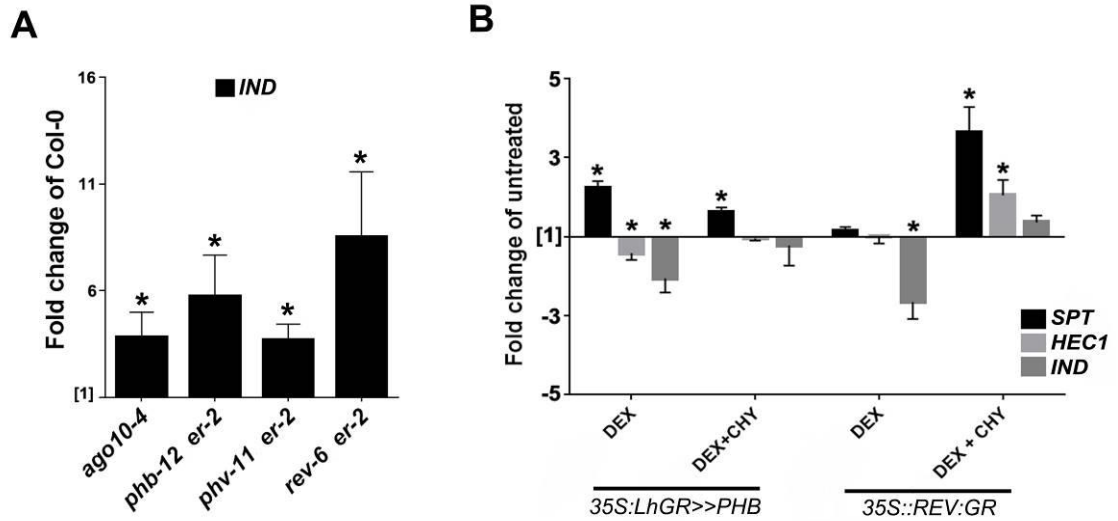
Figure 3.10 PHB and REV transcription factors regulate *IND, SPT,* and *HEC1*. (A) The bar chart shows *IND* was upregulated in 7-day-old *ago10-4, phb-12 er-2, phv-11 er-2* and *rev-6 er-2* seedlings (fold change of wild-type Col-0 vs. mutants) (n=3 biological replicates). **(B)** qRT-PCR was performed on DMSO, 10µM dexamethasone and 10µM cycloheximide-treated *35S:LhGR>>PHB* and *35S::REV:GR* seedlings (6 hours). The bar chart shows PHB and REV downregulate *IND* (DEX vs. DMSO), PHB directly upregulates *SPT,* and REV directly upregulates *SPT* and *HEC1* expression (DEX+CHY vs. CHY). Values are means ± SE. Unpaired t-test (Col-0 vs. mutants, DEX vs. DMSO and DEX+CHY vs. CHY), *$p<0.05$
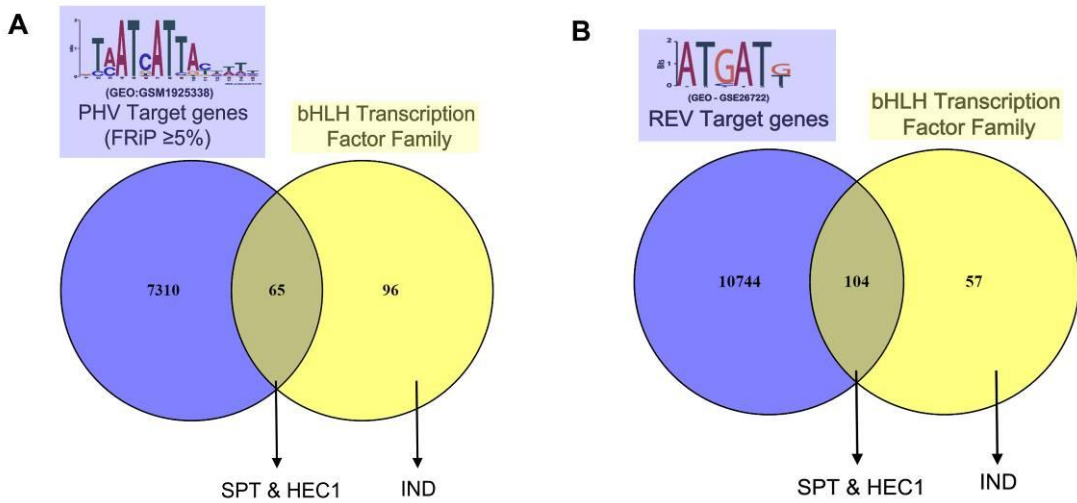
Figure 3.11 PHV and REV directly bind to *SPT* and *HEC1* genes. (A) PHV DAP-seq (blue, GEO:GSM1925338) and **(B)** REV ChIP-seq (blue, GEO:GSE26722) data were analysed to identify PHV and REV binding *bHLH* transcription factor family genes (yellow). **(A)** Venn diagram was showing that PHV can directly bind to *SPT* and *HEC1* but not to *IND*. **(B)** Venn diagram was showing that REV can directly bind to *SPT* and *HEC1* but not to *IND*.
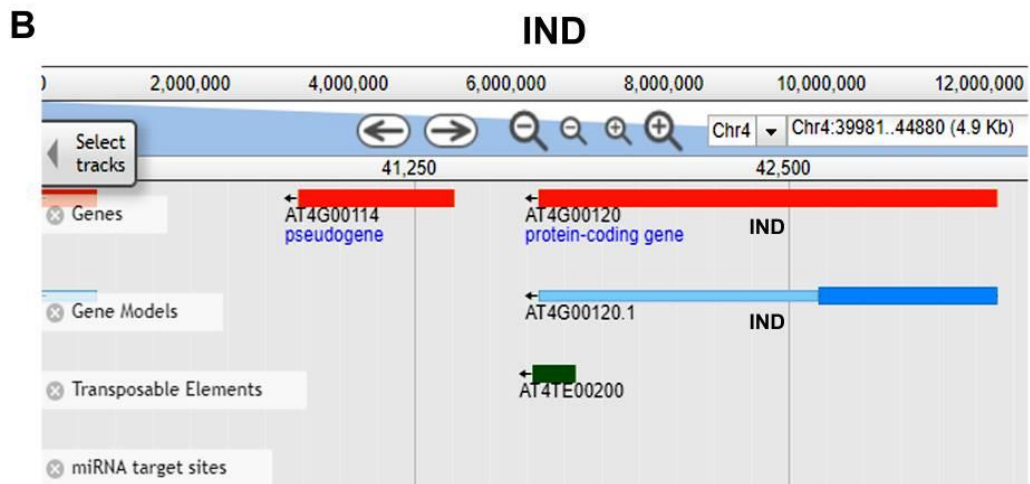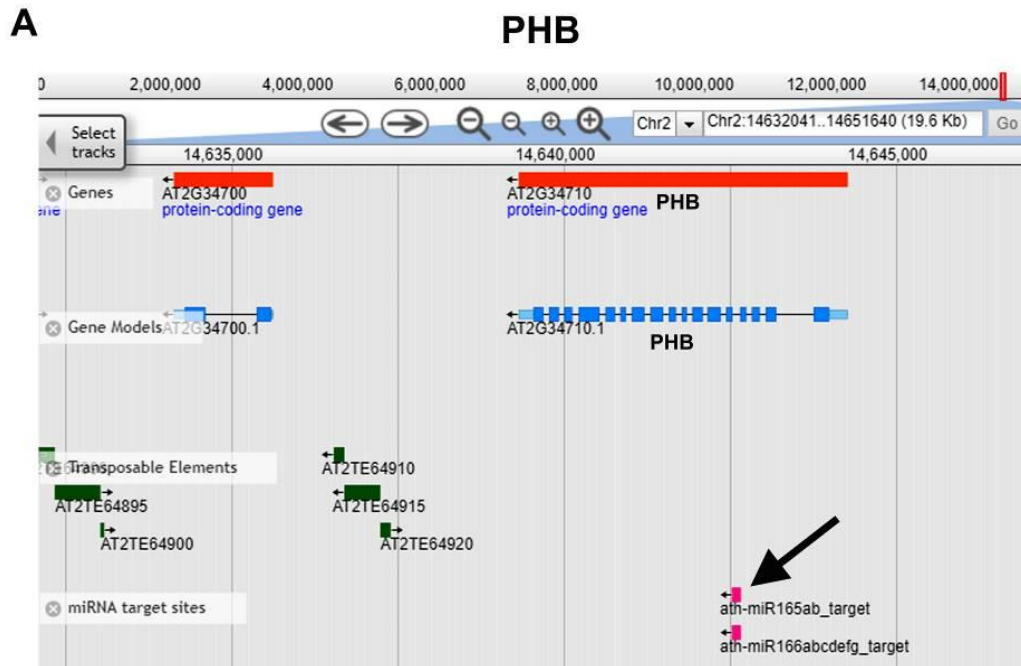
Figure 3.12 PHB and IND miRNA target sites. Image of small RNA project JBrowse-*Arabidopsis* shows the *PHB* and *IND* genes and miRNA target site tracks. **(A)** PHB is targeted by miRNA165 and miRNA166. **(B)** No miRNA target sites found for IND**.**

3.3 Discussion

3.3.1 IND may regulate SAM size and promote leaf abaxial fate

Wu *et al.* reported that IND could regulate cytokinesis (by unequal cell division) in the seven-layer zone of fruit at stage 17 (Wu et al., 2006). Cell size and cell proliferation in plants are organ-specific. In the meristem, cell divisions are often unequal, and cells actively control their size (Serrano-Mislata et al., 2015). This chapter show that *IND* is weakly expressed in the SAM and primordia, and that *ind* seedlings produced a small SAM but did not affect leaf polarity (Fig 3.2 and 3.8). If IND is regulating cytokinesis in the SAM, cell division orientation alone is not sufficient to regulate morphogenesis in the meristem. An altered cell division pattern in the meristem can lead to an altered pattern of expression of genes implicated in leaf development (Wyrzykowska and Fleming, 2003). Interestingly, overexpression of IND produced a large meristem (failed to produce leaves), with pin and cup shaped abaxialised leaves (Fig 3.6). In addition, induction of IND also upregulated leaf abaxial polarity genes *KAN, YAB1,* and *WOX1* (Fig 3.7). It has been demonstrated that YAB1 (FIL) acts redundantly to promote the expression of SHP/IND in valve margins (Dinneny et al., 2005). This indicates that IND and YAB1 may regulate each other in fruit as well as in leaves. Interestingly, induction of IND directly downregulated leaf adaxial polarity gene *AGO10*. Although, overexpression of IND seedling phenotypes were also similar to *ago10^{zwl-3}* phenotypes. These data, in agreement with our results, suggest that IND may regulate SAM size by regulating cytokinesis and promote leaf abaxial polarity by inhibiting *AGO10*. However, the pattern of cytokinesis in *ind* should be investigated.

3.3.2 AGO10-IND regulate SAM development

Argonaute proteins play a significant role in all sRNA guided gene-silencing processes (Kim, 2011; Meister, 2013). In *Arabidopsis*, AGO10 is involved in maintaining SAM and leaf polarity by preserving *HD-ZIP III* gene expression. AGO10 is expressed in seedlings, and particularly in the SAM and adaxial domain of the leaf (Liu et al., 2009; Tucker et al., 2008; Zhang and Zhang, 2012; Zhu et al., 2011b). Loss of *AGO10* in *ago10^{zwl-3}* inhibits SAM and leaf development. This chapter shows that *IND* is upregulated in *ago10^{zwl-3}* and loss of *IND* partially rescues *ago10^{zwl-3}* phenotypes (Fig 3.5 and 3.9). This demonstrates that AGO10 negatively regulate *IND* and thus promotes SAM development.

AGO10 does not splice *IND* via the miRNA pathway (Fig 4.12B). However, AGO10 may regulate *IND* via HD-ZIP III TFs. Interestingly, the PIN phenotype produced by overexpression of IND and *ago10*$^{zwl-3}$ resembles the *phb rev* mutant (Prigge et al., 2005). This chapter shows that PHB and REV indirectly downregulate *IND* gene expression (Fig 3.10). This suggests that AGO10 indirectly inhibits *IND* via HD-ZIP III transcription factors. IND belongs to the same clade of bHLH transcription factors as HEC proteins; IND regulates *SPT* gene expression and also directly interacts with SPT (Girin et al., 2011). Moubayidin demonstrated that IND and SPT are necessary for mediating leaf radialization (PIN and CUP) because the radialisation was lost in the *spt* mutant background (Moubayidin and Ostergaard, 2014). Interestingly this study has found that PHB and REV can upregulate *SPT*, and REV can also upregulate *HEC1* (Fig 3.11). In addition, *HEC1* expression was downregulated in *ago10*$^{zwl-3}$ (Fig 3.9). Interestingly, SPT and HEC1 interaction can regulate the SAM development (Schuster et al., 2014; Sparks and Benfey, 2014). Together these studies suggest that AGO10-PHB-REV may promote SAM development by repressing *IND* and promoting *SPT* and *HEC1* expression and possibly SPT-HEC1 dimer signalling (Fig 3.13).

3.3.3 AGO10-IND regulate gynoecium development

As well as in the vegetative SAM, AGO10 is also expressed in the floral meristem and regulates floral meristem differentiation (Ji et al., 2011). Since AGO10 is also expressed in the adaxial domain of carpels (Ji et al., 2011), AGO10 may possibly have a role in regulating adaxial polarity of fruit valves. AGO10 possibly regulates adaxial polarity of fruit valves via *HD-ZIP III* (Nole-Wilson et al., 2010). This chapter shows AGO10 expression in the floral meristem, gynoecium and up to stage 15 fruit, and that loss of *AGO10* in *ago10*$^{zwl-3}$ impairs replum and fruit growth (Fig 3.2 and 3.5). The homeodomain protein RPL regulates the development of fruit repla (Roeder et al., 2003). *rpl-1* and *zwl-3* stage 17 fruits produce small repla, and these fruits look alike (Roeder et al., 2003). Similar to RPL, AGO10 may regulate replum development.

In *Arabidopsis* fruit, SHP positively regulates *IND* to promote valve margin development (Liljegren et al., 2000; Liljegren et al., 2004a). Loss of *SHP* or *IND* produces indehiscent fruits without valve margins (Liljegren et al., 2000; Liljegren et al., 2004a). It has been

demonstrated that *SHP* and *IND* expression are inhibited in the replum by RPL (Roeder et al., 2003). Roeder *et al.* reported the ectopic expression of *SHP* and *IND* (*GT140*) in the replum of *rpl-1* stage 17 fruit and replum development is restored in *rpl-1 shp1 shp2*. This shows that SHP and IND inhibit replum development. Similar to *rpl-1* stage 17 fruits, ectopic *ind*-GUS expression was observed in the replum of *ind-6 zwl-3* fruit at stage 17, and replum development was restored in *ind-6 zwl-3* (Fig 3.5). Similar to RPL, AGO10 also inhibits *IND* to promote replum development. During fruit development, AGO10 expression was observed from stage 1 to stage 15 and IND/SHP expression was observed from stage 8 to stage 17 (Fig 3.2) (Ji et al., 2011; Liljegren et al., 2000; Liljegren et al., 2004a; Savidge et al., 1995). This suggests that AGO10 may inhibit *IND* at an early stage of fruit development and that IND may inhibit AGO10 at a late stage of fruit development. From this, we can draw that AGO10 and IND may inhibit each other (Fig 3.13).

3.3.4 Conclusion

This chapter demonstrates that IND regulates the size of the SAM and may promote leaf abaxial polarity by inhibiting *AGO10.* We found that AGO10 inhibits *IND* via PHB and REV in SAM to promote *SPT* and *HEC1* (Fig 3.13). Similar to the SAM, AGO10 may represses *IND* to promote replum development.
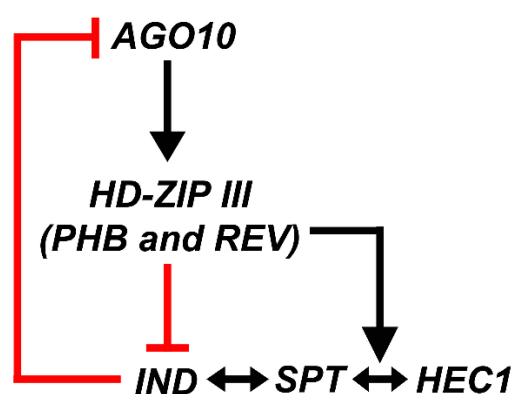
Figure 3.13 Schematic representation of the AGO10-PHB-REV-IND signalling cascade

Chapter 4

IND and HD-ZIP III transcription factors regulate *CUC1*

CHAPTER 4. IND and HD-ZIP III transcription factors regulate *CUC1*

4.1 Introduction

Leaf polarity in *Arabidopsis* is regulated by various signalling elements such as hormones, transcription factors and miRNAs. Importantly, gradients of these elements are crucial for establishing leaf adaxial and abaxial fate. In tomato, Kim *et al.* showed that movement of mRNA across cells could cause changes in leaf morphology (Kim et al., 2001).

The cell-to-cell movement of proteins and nucleic acids is regulated by plasmodesmata (Wu et al., 2002), and the auxin hormone gradient is regulated by PIN proteins (Friml et al., 2003). Change in gradients of these elements can affect leaf adaxial or abaxial fate and produce cup and pin-shaped leaves. These leaf phenotypes are also observed in *as1, ago10, hd-zip iii,* and *pin1 cuc1 cuc2* mutant lines as well as seedlings treated with polar auxin transport inhibitors (Aida et al., 2002; Moussian et al., 1998; Prigge et al., 2005; Xu et al., 2003; Zhao et al., 2010). AS1 is one of the key regulators of leaf adaxial fate. In tomato and *Arabidopsis*, loss of *as1* results in cup and needle or pin-shaped abaxialised leaves (Kim et al., 2003b; Xu et al., 2003; Zoulias et al., 2012).

In *Arabidopsis*, AGO10 inhibits miRNA165/166 and positively regulates *HD-Zip III* to establish the leaf adaxial domain (Liu et al., 2009). In a recent study, histological analysis revealed that *ago10^{zll-1}* mutants were able to initiate the cotyledons (Leaf 1 and 2) and embryonic meristem but failed to maintain the leaf polarity and the meristem in a proportion of seedlings after late stages of embryogenesis (Lee and Clark, 2015; Tucker et al., 2008; Tucker et al., 2013). This suggests *ago10^{zwl-3}* cup and pin phenotypes are embryonic or post-embryonic. The *hd-zip iii* mutant seedlings produce cup- and pin-shaped structures. In contrast, the *hd-zip iii* mutants produced cup and pin-shaped cotyledons Leaf 1 and 2), which suggests *HD-Zip III* genes are involved in patterning at an early stage of embryogenesis (Lee and Clark, 2015; Prigge et al., 2005).

During the early stage of embryogenesis, the apical cell differentiates and establishes peripheral and central domains, and at this stage each domain consists of four cells (Fig

4.1 B and C). These cells further divide to establish medial (SAM) and lateral (cotyledon-forming) domains at a late stage of embryogenesis (Fig 4.1 D). PIN proteins maintain high auxin levels in the apical cell; loss of *pin1* leads to frequent failure to form an embryo proper (Friml et al., 2003) (Fig 4.1 A and B). Prigge *et al.* discussed that *HD-Zip III* genes may be involved in differentiating between central and peripheral cells during wild-type embryogenesis (Fig 4.1 B and C). Loss of *hd-zip iii* promotes peripheral identity and generates single, radially symmetric cotyledons (Prigge et al., 2005). PIN1 and PID regulate the formation of auxin gradient maxima at the tips of the lateral domains and promote cotyledon outgrowth by preventing *CUC* gene expression from expanding to the lateral domain (Furutani et al., 2004). A single cup-shaped cotyledon is formed when the medial domain is not distinguished from the lateral (cotyledon-forming) domains (Fig 4.1 C and D). Aida *et al.* demonstrated that *cuc1 cuc2* double mutant seedlings completely lack an embryonic SAM, and two cotyledons are fused along both edges to form one cup-shaped structure (Aida et al., 1997). CUC1 and CUC2 genes are required for preventing cotyledons and floral organs from fusing with each other (Aida et al., 1997; Takada et al., 2001). This shows that *PIN1, PID* and *CUC* genes are crucial for establishing the boundary between the SAM and primordia, and for cotyledon outgrowth.

The pin and cup-shaped leaves in *ago10* mutants may have formed because of changes in *PIN1, PID* and *CUC* gene expression triggered during embryogenesis (e.g. modified cotyledons) and post embryogenesis (e.g. modified leaves). In Chapter 3, phenotype analysis showed that *ago10^{zll-3}* seedlings produced pin shaped meristems and the *ind^{ind-6}* mutation partially rescued the *ago10^{zll-3}* pin phenotype (Chapter 3, Fig 4.1E). We hypothesised that *ind^{ind-6}* may rescue the *ago10^{zll-3}* phenotype by regulating *PIN1, PID* or *CUC* gene expression (Fig 4.1E). A few of the pin phenotypes may have switched to cup phenotypes by rescuing *PIN1* and *PID* but not *CUC* in *ind^{ind-6} ago10^{zll-3}* (Fig 4.1E). Loss of *ago10-hd-zip iii* and overexpression of IND may promote cup and pin phenotypes by regulating PIN1, PID and CUC. We hypothesised that IND may promote pin and cup by negatively regulating *PIN1, PID* and *CUC in ago10^{zll-3}*. In this chapter, the link between the AGO10-PHB-REV-IND pathway (Chapter 3) and *PIN1-PID-CUC* is examined.

(Prigge et.al., 2005)

A B C D

Apical
Basal

Central
Peripheral

Medial
Lateral

polar auxin
transport
defective

rev phb phv
rev phb cna

cuc- or polar auxin
transport defective

Wild Type

E *zwl-3*   *ind-6 zwl-3*

PIN   CUP   WT

IND   PIN PID CUC ?

cuc or polar auxin transport defective?

84
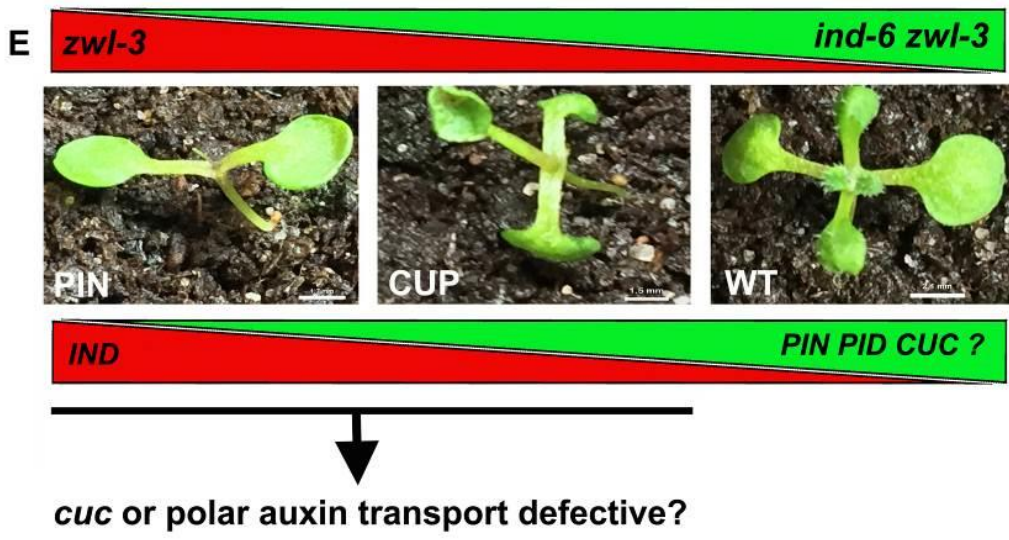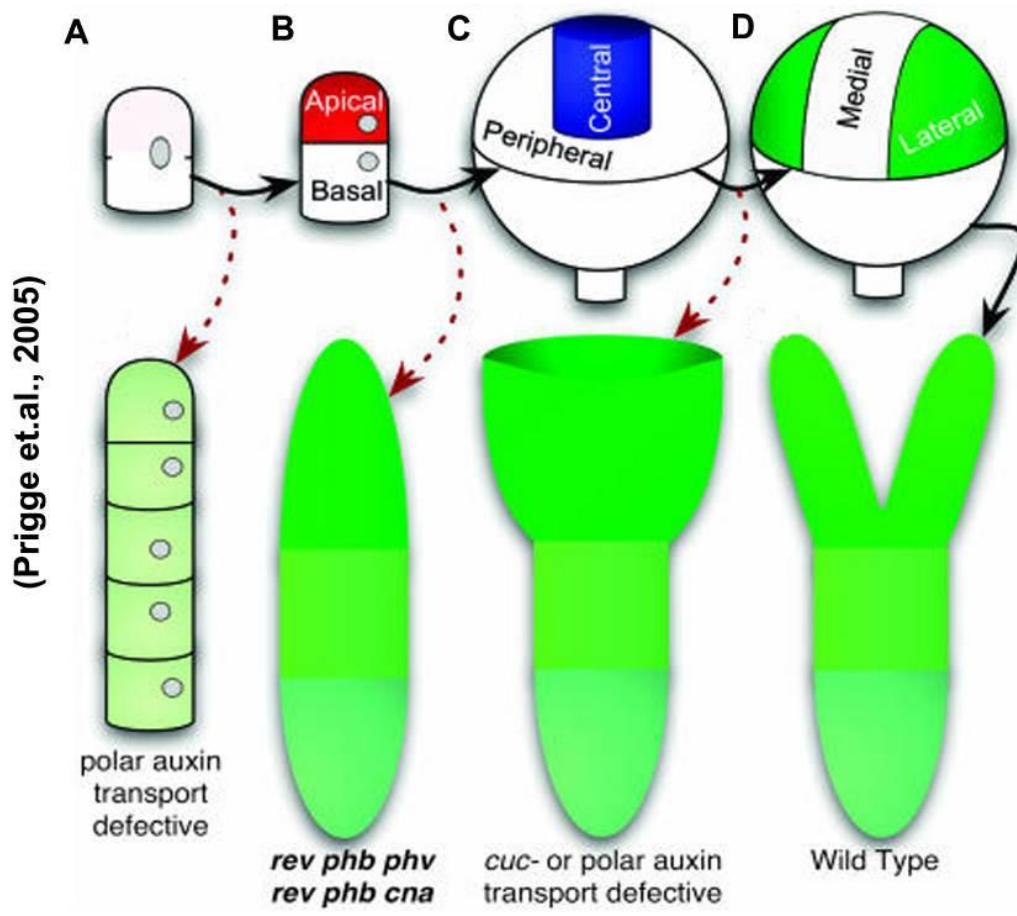
Figure 4.1 Illustration depicting mutants defective in certain patterning steps in embryogenesis. Image modified from (Prigge et al., 2005). The first zygotic **(A)** division is asymmetric and produces an apical and basal cell **(B)**. Apical-basal polarity is established after the first zygotic division. Apical-basal polarity is lost in multiple *pin* and *hd-zip iii* mutants and these mutants produce a defective embryo. Apical cells differentiate to establish central and peripheral domains **(C).** Medial and lateral (cotyledon-forming) domains are established at a late stage of embryogenesis **(D)**. Cotyledons are fused in *pin cuc* mutants because the medial domain is not distinguished from the lateral domains (red dashed arrow indicate the phenotypic change). **(E)** Schematic diagram describing a hypothesis to explain the various phenotypes of *ago10* mutants. Image shows a high frequency of WT phenotype in *ind-6 zwl-3* (top green) and high frequency of PIN phenotype in *zwl-3* (top red). Severe *ago10* pin phenotypes are caused by high *IND* gene expression (lower red) and possibly low expression of *PIN1, PID* and *CUC* (lower green) or polar auxin transport defective. The *ind^{ind-6}* mutation reduces the severity of *ago10^{zwl-3}* phenotypes by reducing *IND* expression and restoring *PIN1, PID* and *CUC* expression and auxin transport.

4.2 Results

4.2.1 *PIN1, PID, CUC* and SAM-associated gene expression in mutants

We hypothesised that the *ind^{ind-6}* mutation rescues the *ago10^{zwl-3}* phenotype by rescuing *PIN1, PID, CUC,* and perhaps the expression of other genes associated with SAM development (these genes were discussed in Chapter 1). We tested this hypothesis by measuring gene expression using qRT-PCR. *PIN1, PID* and *CUC* gene expression was examined along with other genes involved in SAM and leaf polarity in 7-day old L*er, ind-6, zwl-3* (WT, CUP, PIN and NM) and *ind-6 zwl-3* double mutant (WT, CUP and PIN) seedlings. A heat map depicting levels of gene expression in mutant seedlings was generated using Morpheus (Fig 4.2). The gene expression values ($2^{-\Delta CT}$) used for heat map is provided in the Table 8.1. We also measured the expression of genes that regulate leaf polarity such as *AS1, AS2, AGO10, PHB, PHV and REV* that regulate adaxial fate (Emery et al., 2003; Iwasaki et al., 2013; Zhu et al., 2011b), and *YABBYs, KAN, ARF3* and *ARF4* that regulate abaxial leaf fate (Eshed et al., 2004; Fahlgren et al., 2006; Garcia et al., 2006; Kelley et al., 2012; Siegfried et al., 1999).

When compared to L*er,* gene expression of *AS2, PHB, PHV* and *REV* was decreased in all mutant phenotypes of *zwl-3* and *ind-6 zwl-3* double mutant but not as strongly in *zwl-3* WT phenotypes (Fig 4.2). In addition, the severity of *ago10^{zwl-3}* phenotypes positively correlated with *PHB, PHV* and *REV*. Interestingly, *AS1* gene expression was increased in *zwl-3* (WT, CUP and PIN) and decreased in *ind-6 zwl-3* double mutant (CUP and PIN) (Fig 4.2). Increase in *AS1* expression alone may not be sufficient to rescue adaxial fate in *zwl-3.*

Consistent with the abaxialisation of *ago10^{zwl-3}* mutant meristem phenotypes, *KAN, ARF3* and *ARF4* expression was increased in *zwl-3* (PIN and CUP) (Fig 4.2). *ARF4* expression was also increased in *zwl-3* WT seedlings (Fig 4.2). When compared to L*er,* gene expression of *KAN, ARF3* and *ARF4* was decreased in *ind-6, zwl-3* (NM) and *ind-6 zwl-3* double mutant seedlings (CUP and PIN) (Fig 4.2). *YAB3* gene expression was decreased in *zwl-3* (CUP, PIN and NM) and *ind-6 zwl-3* (WT, CUP and PIN) (Fig 4.2). This shows that abaxial fate-determining genes were promoted in *zwl-3* compared to the *ind-6 zwl-3* double mutant*.* This suggests that IND may regulate leaf abaxial fate by

upregulating *KAN, ARF3* and *ARF4* gene expression in *zwl-3.* However, several lines of evidence suggest that overexpression of *ARF3* and *ARF4* in *ago10*[zwl-3] mutants is not sufficient to cause the meristem phenotypes (Fahlgren et al., 2006; Hunter et al., 2006).

The class I KNOX transcription factors (STM and BP) positively regulate cytokinin biosynthesis (Yanai et al., 2005). *BP* and *STM* gene expression was examined in mutants. *BP* gene expression was increased in *zwl-3* (WT, CUP and PIN) and *ind-6 zwl-3* double mutant (WT and CUP) (Fig 4.2). *STM* gene expression was decreased in *ind-6, zwl-3* (WT, CUP, PIN and NM) and *ind-6 zwl-3* double mutant (CUP and PIN) (Fig 4.2). This shows that *BP* may be positively regulating cytokinin biosynthesis in *zwl-3* and *ind-6 zwl-3.* Cytokinins induce the expression of *ARR7* and ARR7 negatively regulates cytokinin signalling in the SAM. Interestingly, *ARR7* gene expression was increased in *zwl-3* (CUP, PIN and NM) and *ind-6 zwl-3* (CUP and PIN) (Fig 4.2). Auxin signalling inhibits *ARR7* expression in the SAM. YUC1 regulates auxin biosynthesis, while PIN1 and PID regulate auxin transport. *YUC1* gene expression was decreased in *zwl-3* (CUP, PIN and NM) and *ind-6 zwl-3* (CUP and PIN) (Fig 4.2). Gene expression fold change of *PIN1* and *PID* (L*er* Vs. mutants) is presented in Figure 4.3B. *PIN1* gene expression was decreased in *zwl-3* (PIN) and *ind-6 zwl-3* (CUP and PIN) (p<0.05) (Fig 4.2 and Fig 4.3B). *PID* gene expression was decreased in *ind-6, zwl-3* (NM) and *ind-6 zwl-3* (CUP and PIN) (p<0.05) (Fig 4.2 and Fig 4.3B). This shows that *zwl-3* (CUP and PIN) and *ind-6 zwl-3* (CUP and PIN) are defective in auxin signalling. Loss of auxin signalling may have promoted *ARR7* expression in CUP and PIN because auxin signalling inhibits *ARR7* in normal SAMs via MP (ARF5) (Zhao et al., 2010).

However, PIN1 is also necessary for the proper spatial expression of *CUC1* (Aida et al., 2002). Loss of *cuc* mutants generates cup-shaped or fused cotyledon phenotypes which are similar to cup-shaped leaf in *zwl-3* and *ind-6 zwl-*3 mutants. *CUC1, CUC2* and *CUC3* gene expression were examined in mutants. Gene expression fold change of *CUC1, CUC2* and *CUC3* (L*er* Vs. mutants) was presented in Figure 4.3A. *CUC1* gene expression was decreased in *zwl-3* (WT, CUP, PIN and NM) (p<0.05) (Fig 4.2 and Fig 4.3A). Interestingly, *CUC1* gene expression in *ind-6 zwl-3* was similar to L*er* (Fig 4.2). *CUC2* and *CUC3* gene expression was decreased in *zwl-3* (CUP, PIN and NM) and *ind-6 zwl-3* (CUP and PIN) (Fig 4.2 and Fig 4.3B). *CUC1* and *CUC2* are required for *STM* expression, and STM can directly

activate *CUC1* gene expression. Interestingly, *CUC1* and *CUC2* gene expression was similar to L*er* (Fig 4.2)*.* This shows that loss of *ind^{ind-6}* in *ago10^{zll-3}* rescues *CUC1* gene expression, suggesting that IND may negatively regulate *CUC1* in *zwl-3.*

In summary, these results demonstrate that IND may downregulate the boundary specification gene *CUC1* and upregulate abaxial fate genes (*KAN, ARF3* and *ARF4*) in *ago10^{zll-3}*. *zwl-3* (CUP and PIN) and *ind-6 zwl-3* (CUP and PIN) phenotypes may be defective in auxin signalling. The increase in *ARR7* expression suggests that cytokinin signalling was negatively regulated in *zwl-3* (CUP and PIN) and *ind-6 zwl-3* (CUP and PIN) phenotypes.
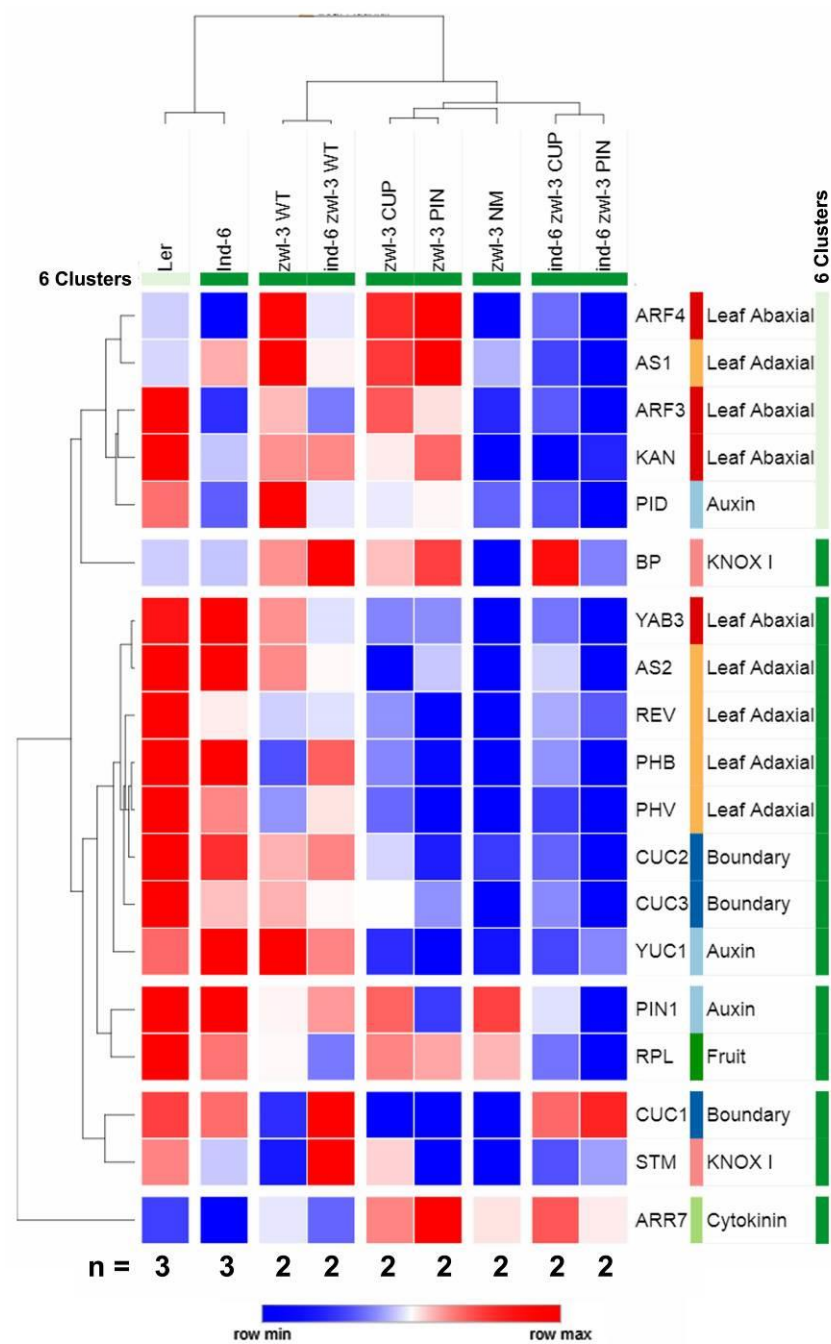
Figure 4.2 Gene expression in L*er* and mutant phenotypes (*ind-6, zwl-3,* and *ind-6 zwl-3*). The heat map shows hierarchical clustering of samples and genes (one minus Pearson correlation): *PIN1, PID, CUC* and other SAM and leaf polarity gene expression in 7 day old L*er, ind-6, zwl-3* (WT, CUP, PIN and NM) and *ind-6 zwl-3* (WT, CUP and PIN) seedlings (Z-score of $2^{-\Delta CT}$ values from qRT-PCR). Top, sample tree; left, gene tree. (Blue: decreased gene expression, Red: increased gene expression)
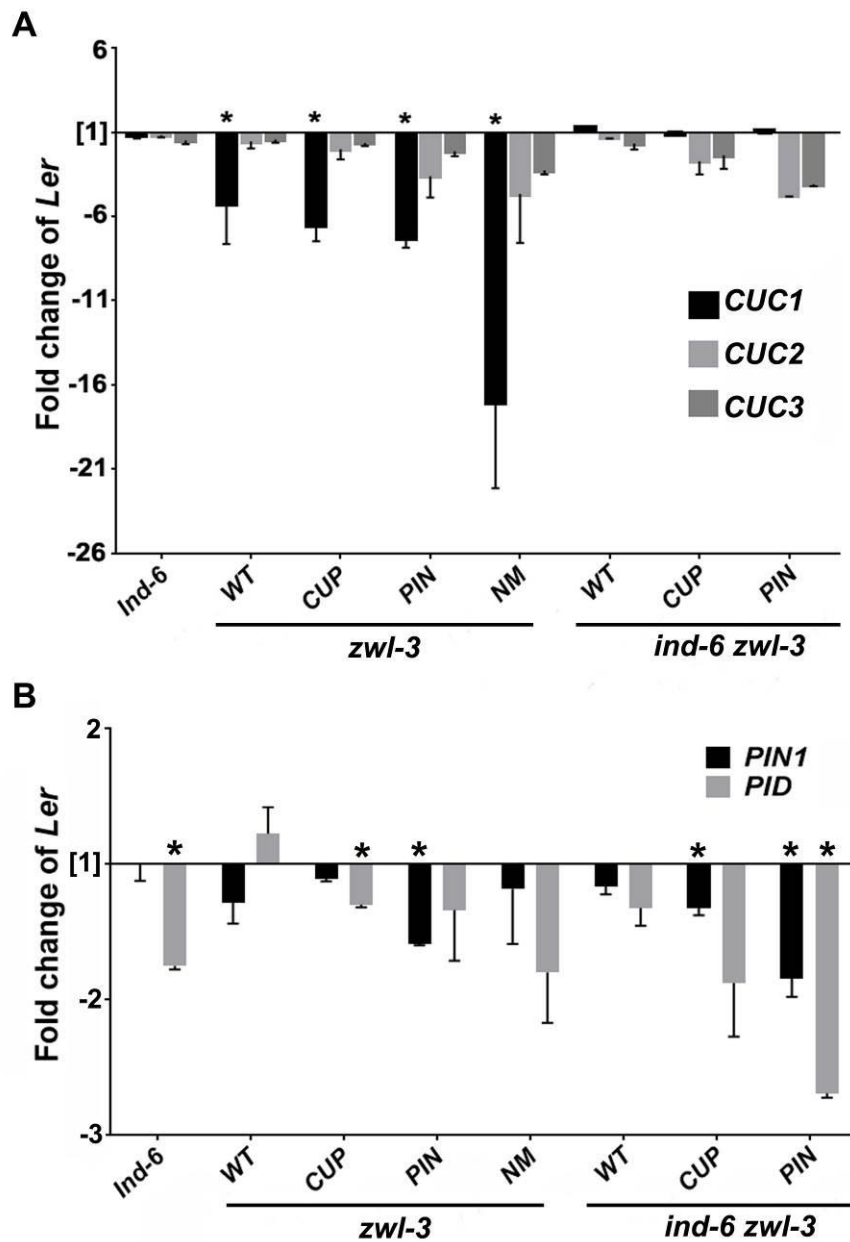
Figure 4.3 *PIN1, PID* and *CUC* family gene expression in L*er* and mutant phenotypes (*ind-6, zwl-3,* and *ind-6 zwl-3*). Using qRT-PCR, **(A)** the bar chart shows decreased *CUC1* expression in all *zwl-3* mutant phenotypes (WT, CUP, PIN and NM) but no significant change of *CUC1* expression in *ind-6 zwl-3* double mutants. *CUC2* and *CUC3* expression was decreased in *zwl-3* (CUP, PIN, and NM) and *ind-6 zwl-3* (CUP and PIN) seedlings. **(B)** The bar chart shows decreased *PID* expression in *ind-6, zwl-3* (NM) and *ind-6 zwl-3* (CUP and PIN), and decreased *PIN1* expression in *zwl-3* (PIN) and *ind-6 zwl-3* (CUP and PIN). (Fold change of wild-type L*er* Vs. mutants). Values are means ± SE. Tukey's multiple comparisons test (L*er* Vs. mutants), *p<0.05.
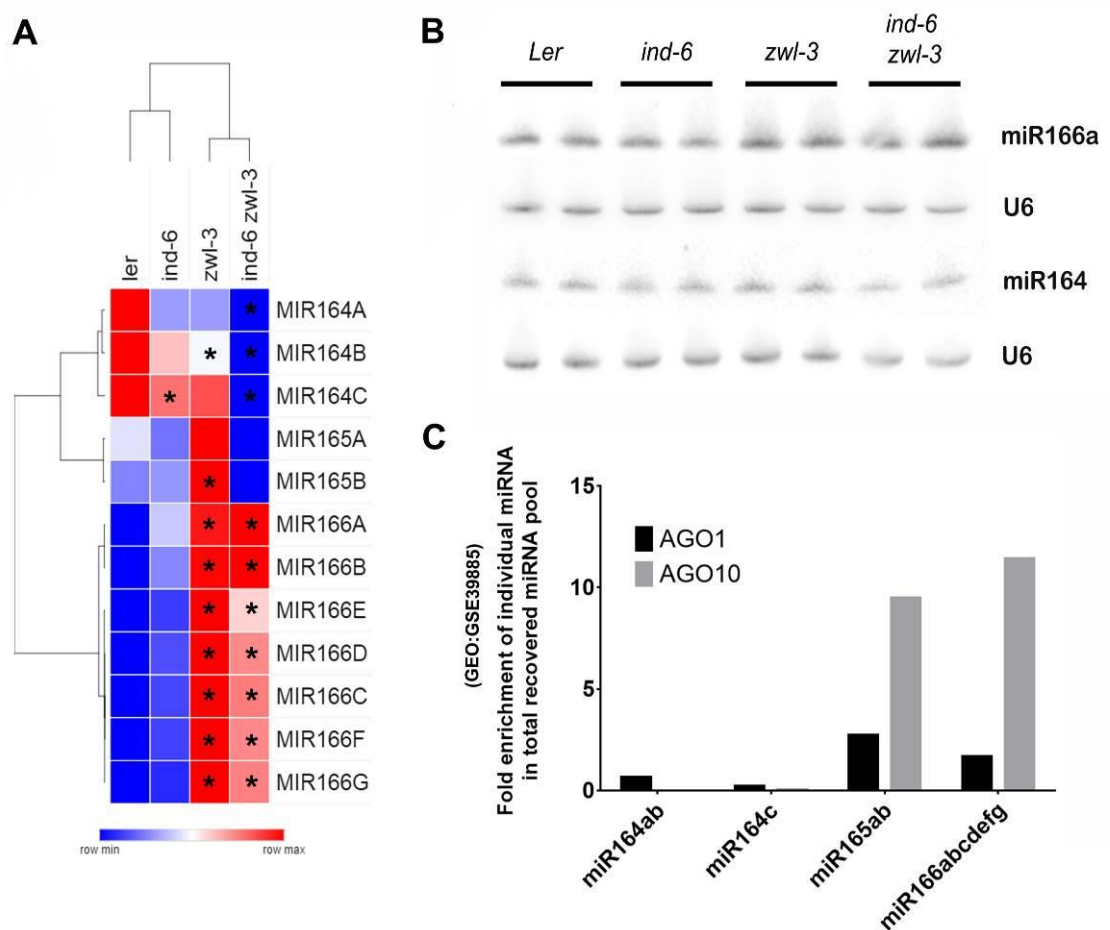
Figure 4.4 miRNA164, miRNA165 and miRNA166 expression in L*er* and mutants (*ind-6, zwl-3,* and *ind-6 zwl-3*). (A) Heat map with hierarchical clustering of samples and miRNA (one minus Pearson correlation): miR166A-G expression was increased in *zwl-3* and *ind-6 zwl-3,* and miR164A-C expression was decreased in *ind-6 zwl-3* (Z-score of sRNA-seq data, n=2 biological replicates). **(B)** The northern blot image show increased miR166a expression in *zwl-3* and *ind-6 zwl-3,* and decreased miR164 expression in *ind-6 zwl-3* (n=2 biological replicates). **(C)** AGO1 and AGO10 associated CLIP-Seq (RNA isolated by crosslinking immunoprecipitation) data (GEO:GSE39885) was analysed and fold enrichment of miRNA164a-c, miRNA165ab, and miRNA166a-g in the total recovered miRNA pool was determined. When compared to AGO1, miRNA165ab, and miRNA166a-g was highly enriched in AGO10. When compared to AGO10, miRNA164a-c was slightly more enriched in AGO1. Tukey's multiple comparisons test (L*er* Vs. mutants), *p<0.05 (Blue: decreased expression, Red: increased expression).

4.2.2 miRNA164, miRNA165 and miRNA166 expression in mutants

Previous studies show that miR164 can degrade *CUC1* and *CUC2* transcripts in *Arabidopsis* (Laufs et al., 2004; Sieber et al., 2007). The decrease of *CUC1* in *ago10^{zll-3}* suggests that AGO1 or AGO10 can possibly regulate *CUC1* via miR164. *CUC1* expression was rescued in *ind^{ind-6} ago10^{zll-3}*, which suggests IND could regulate *CUC1* via miR164. Small RNA-Seq was performed on L*er*, *ind-6, zwl-3* and *ind-6 zwl-3* seedlings (performed by Dr Karim Sorefan). In addition, AGO1 and AGO10 CLIP-Seq (RNA isolated by crosslinking immunoprecipitation) data (GEO: GSE39885) (Zhu et al., 2011b) was analysed to examine the link between AGO1-AGO10-IND and miR164. Northern blots were performed to examine miR166a, miR164 and U6 (control) expression in L*er*, *ind-6, zwl-3* and *ind-6 zwl-3* seedlings (Fig 4.4B) (experiment performed by Dr Karim Sorefan). MiR165ab and miR166a-g were used as positive controls because they target HD-ZIP III transcripts and it is known that AGO10 preferentially loads miR165ab and miR166a-g. A heat map of miRNA expression in L*er*, *ind-6, zwl-3* and *ind-6 zwl-3* seedlings was generated using Morpheus (Fig 4.4A). In *zwl-3* and *ind-6 zwl-3* seedlings, the levels of miR166a-g are significantly increased when compared to wild-type L*er* ($p<0.05$, Fig 4.4A). This was previously observed in multiple *ago10* loss-of-function mutants (Yu et al., 2017; Zhou et al., 2015). Data from northern blotting also shows an increase of miR166a expression in *zwl-3* and *ind-6 zwl-3,* which is consistent with RNA-Seq data (Fig 4.4B). It is not known how AGO10 can upregulate the levels of miR165ab and miR166a-g. MiR164a-c expression was decreased in *ind-6, zwl-3* and *ind-6 zwl-3* seedlings when compared to L*er* (Fig 4.4A). Data from northern blotting also shows a decrease of miR164 expression in *ind-6 zwl-3* and this matches with RNA-Seq data (Fig 4.4B). It is not known how the loss of *ind* can significantly downregulate the levels of miR164a-g in *ind-6 zwl-3* seedlings. AGO1 and AGO10 CLIP-Seq data was presented in Figure 4.4C. miR165ab and miR166a-g are highly enriched in AGO10 when compared to AGO1 (Fig 4.4C). MiR164a-c are slightly more enriched in AGO1 when compared to AGO10 (Fig 4.4C). This suggests miR164a-c are preferentially loaded into AGO1 to target *CUC1* and *CUC2* transcripts. If AGO1-miR164a-c is degrading *CUC1,* loss of *CUC1* expression should be observed in *zwl-3* and *ind-6 zwl-3* seedlings. If AGO10-miR164a-c is degrading *CUC1,* an increase in *CUC1* expression should be observed in *zwl-3* and *ind-6 zwl-3* seedlings. Interestingly, *CUC1* expression was decreased in *zwl-3* and restored in *ind-6 zwl-3.* These

results suggest a decrease in expression of *CUC1* in *zwl-3* seedlings is not associated with AGO10-miR164a-c or AGO1-miR164a-c.

4.2.3 PHB and REV upregulate *CUC1* gene expression

Prigge *et al.* demonstrated *phb rev* mutants could produce two cotyledons without a meristem, a fused single cotyledon and pin-shaped radially symmetric organ (Prigge et al., 2005). The *cuc* mutants also produce fused cotyledons. This suggests that there is a possible link between PHB-REV and CUC1. PHB and REV transcription factors may regulate *CUC1* gene expression. Therefore, *35S:LhGR>>PHB* and *35S::REV:GR* transgenic lines were used in this study to examine whether induction of PHB and REV can regulate *CUC1* gene expression. Gene expression was examined following treatment with 10 µM DEX and DMSO-treated seedlings (*35S:LhGR>>PHB* and *35S::REV:GR*) using qRT-PCR (treated 7-day old seedling for 6 hours in liquid media and also grown for 7 days on 10 µM DEX and DMSO treated half MS plant agar plates). Gene expression fold change (DEX vs. DMSO) was determined. No significant change of *CUC1* expression was observed in seedlings (*35S:LhGR>>PHB* and *35S::REV:GR*) treated with DEX for 6 hours (Fig 4.5D). *CUC1* expression was increased in seedlings (*35S:LhGR>>PHB* and *35S::REV:GR*) grown on DEX for 7 days (Fig 4.5D). This shows that PHB and REV transcription factors upregulate *CUC1* gene expression. Since this is not a rapid response, PHB and REV may be forming a complex with other transcription factors or regulating other proteins to upregulate *CUC1* gene expression. Therefore, we tested whether REV regulates *CUC1* directly.

If REV is directly upregulating *CUC1,* it may bind to the promoter region of *CUC1*. REV (*35S::FLAG-GR-REVd*) ChIP-seq dataset from the study published by Brandt *et al.* (GEO:GSE26722) (Brandt et al., 2012) was analysed to examine if the REV transcription factor can bind to the promoter region of *CUC1*. DEX-induced REV and control tracks were loaded into genome browser and aligned with the *Arabidopsis* TAIR 10 genome. The total read counts (*CUC1* promoter) from both DEX-induced REV and control samples were logged and analysed for statistical significance.
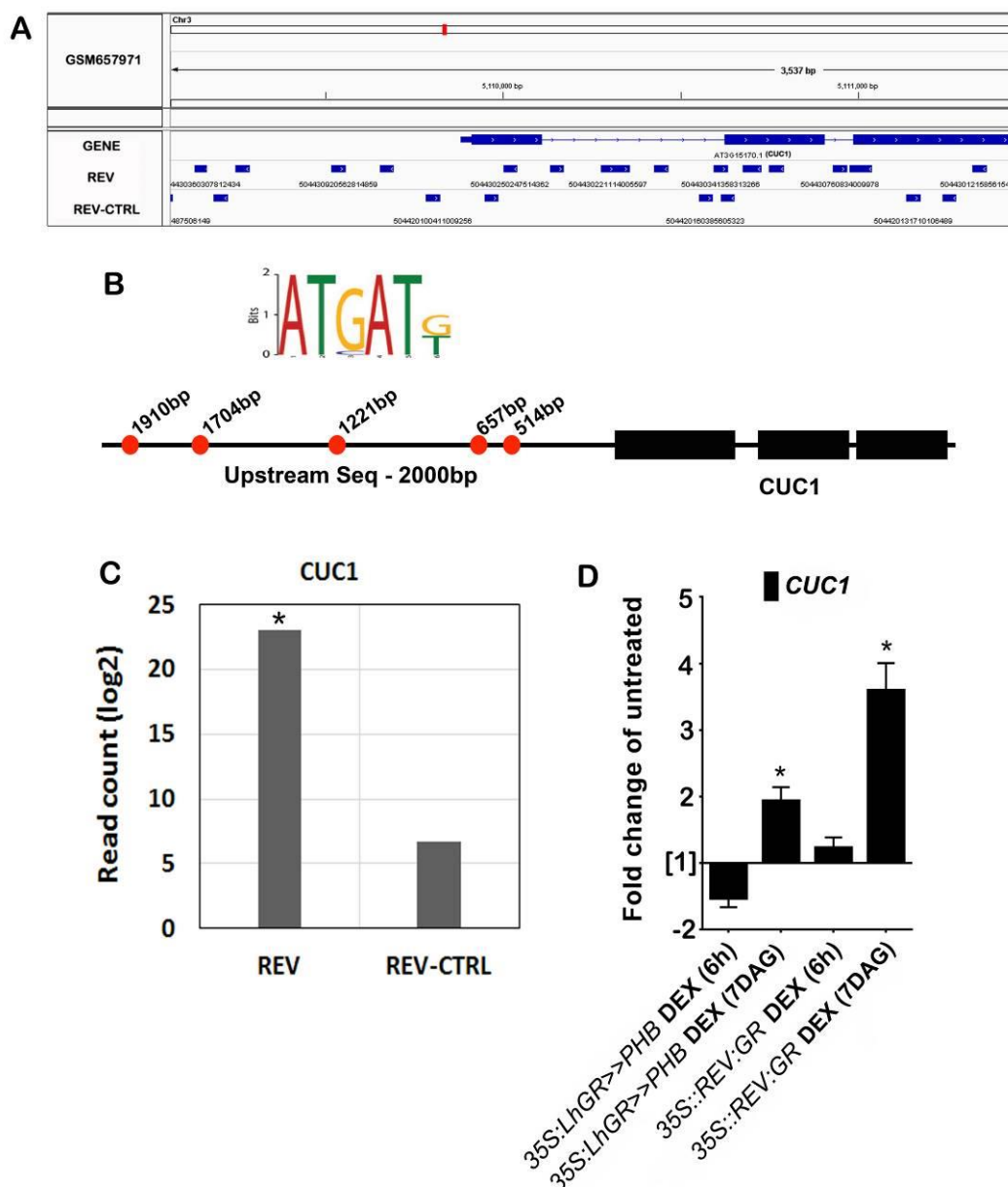
Figure 4.5 REV ChIP-Seq and *CUC1* gene expression. (A) Image exported from the IGV genome browser showing *CUC1* gene, REV (*35S::FLAG-GR-REVd* induced using DEX, ChIP-seq from GEO:GSE26722) and control peaks. **(B)** Image shows REV binding sites (514bp, 657bp, 1221bp, 1704bp and 1910bp) located in the upstream region of *CUC1* gene and REV binding sequence AT[G/C]AT. **(C)** The bar chart shows high *CUC1* sequence read counts in REV and low *CUC1* sequence read counts in control. **(D)** *CUC1* gene expression in *35S:LhGR>>PHB* and *35S::REV:GR* (fold change from qRT-PCR data, 6 hours DEX versus 6 hours DMSO and 7DAG DEX vs. 7DAG DMSO, n=3). The bar chart shows increased *CUC1* expression in *35S:LhGR>>PHB* and *35S::REV:GR* seedlings were grown in the presence of DEX for 7 days. Values are means ± SE. Unpaired t-test (6 hours DEX vs. 6 hours DMSO and 7DAG DEX vs. 7DAG DMSO), *p<0.05.

When compared to control, *CUC1* sequence read counts were significantly high in REV (p<0.05, Fig 4.5C). A previous study identified AT[G/C]AT as the *in vitro* binding sequence for HD-ZIP III proteins and this sequence was identified in the top 50 putative REV-target genes (Brandt et al., 2012; Sessa et al., 1998). Sequence motif AT[G/C]AT was found in the promoter region (514bp, 657bp, 1221bp, 1704bp and 1910bp) of the *CUC1* gene (Fig 4.5B). When compared to control, several REV peaks were observed in the upstream promoter region of the *CUC1* gene (Fig 4.5A). This shows that REV can bind to the promoter region of *CUC1* gene*.

In summary, these results demonstrate that PHB upregulates *CUC1* gene expression and REV may directly bind to the *CUC1* promoter and upregulate *CUC1* gene expression.

4.2.4 IND downregulates *CUC1* gene expression

The data from Chapter 3 shows increased expression of *IND* in *ago10^{zll-3},* and data in Section 4.2.1 shows decreased expression of *CUC1* in *ago10^{zll-3}*. Compared to *ago10^{zll-3}* mutants, *CUC1* gene expression was rescued in *ind^{ind-6} ago10^{zll-3}*. We hypothesised that IND overexpression in *ago10^{zll-3}* mutants may cause downregulation of *CUC1* expression. This was studied using qRT-PCR. The expression of *CUC1, CUC2* and *CUC3* transcripts was examined in 10 µM DEX, 10 µM cycloheximide (CHY) and DMSO-treated *35S::IND:GR* seedlings treated for 6 hours in liquid media. CHY is an effective protein synthesis inhibitor which was used in combination with DEX to examine whether IND induction immediately regulated gene expression. Gene expression fold change (DEX vs. DMSO and DEX+CHY vs. CHY) is presented in Figure 4.6A. *CUC1* gene expression was decreased in the presence of DEX (p<0.05) and DEX+CHY (p<0.05, Fig 4.6A). *CUC2* gene expression was increased in the presence of DEX+CHY (Fig 4.6A). *CUC3* gene expression was increased in the presence of DEX and decreased in the presence of DEX+CHY (Fig 4.6A). This shows that translation is not required for ectopic induction of IND to regulate *CUC1* expression. Therefore IND immediately downregulates *CUC1* gene expression.
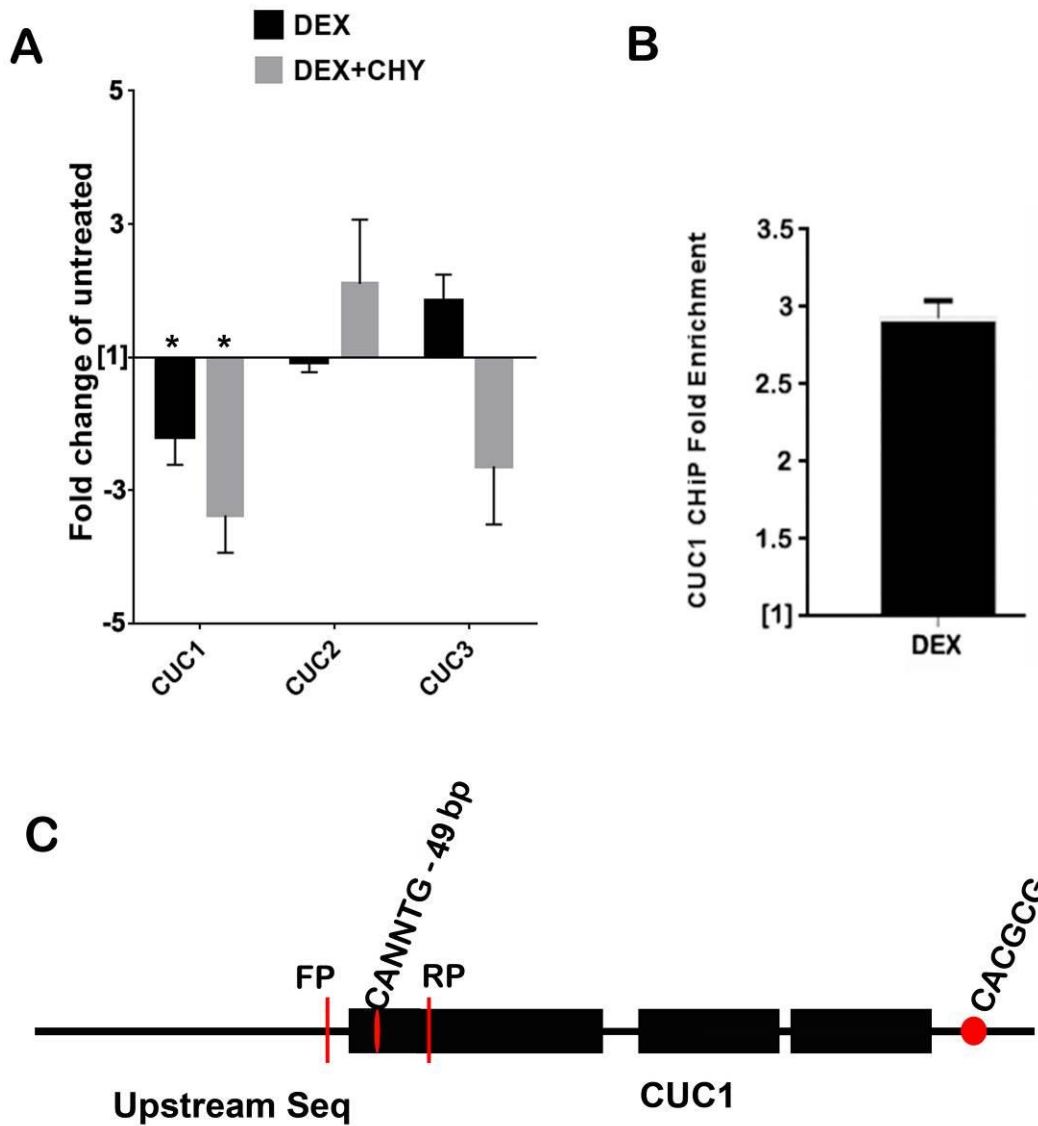
Figure 4.6 IND ChIP-qRT-PCR and *CUC* gene expression. (A) *CUC1, CUC2* and *CUC3* gene expression in *35S::IND:GR* (Fold change from qRT-PCR data, DEX vs. DMSO and DEX+CHY vs. CHY, n=3). The bar chart show decreased *CUC1* expression in the presence of DEX and DEX+CHY, increased *CUC2* expression in the presence of DEX+CHY and increased *CUC3* expression in the presence of DEX and decreased in the presence of DEX+CHY. **(B)** IND-*CUC1* promoter interaction was tested by ChIP-qRT-PCR using the *35S::IND:GR* line, the bar chart shows three-fold enrichment for *CUC1* (upstream 29 bp-34 bp 5'-UTR) in the presence of DEX (n=3). **(C)** Illustration of the *CUC1* gene showing E-box element CANNTG, E-box variant CACGCG, and ChIP-qRT-PCR forward and reverse primer sites. Values are means ± SE. Unpaired t-test (DEX vs. DMSO and DEX+CHY vs. CHY), *p<0.05.

IND can possibly downregulate *CUC1* by directly binding to the *CUC1* promoter. IND-*CUC1* promoter interaction was tested by ChIP. *35S::IND:GR* seeds were grown in liquid media and on day seven, seedlings were treated with 10 μM DEX and DMSO for 6 hours. Treated samples were processed for ChIP (Chapter 2, Section 2.4). From a previous yeast one-hybrid interaction study we know that IND can bind to the G-box element CACGTG and E-box variant CACGCG (Girin et al., 2011). An E-box element CANNTG was located 49 bp of 5'-UTR *CUC1* (Fig 4.6C)*. CUC1* expression was tested by qRT-PCR using primers designed to amplify upstream 29bp-34bp 5'-UTR (Chapter 2, Section 2.3) and fold enrichment (DEX Vs. DMSO) was determined. There was a three-fold enrichment for *CUC1* (upstream 29bp-34bp 5'-UTR) in the presence of DEX (Fig 4.6B). This data demonstrates that IND binds to the *CUC1* promoter*.*

In summary, these results demonstrated that IND may directly bound to the *CUC1* promoter and downregulated *CUC1* gene expression.

4.2.5 SPT and HEC1 do not directly regulate *CUC1* gene expression

4.2.5.1 *35S:SPT-VP16-GR* and *spt-12* microarray data analysis

In *Arabidopsis*, SPT promotes the growth of carpel marginal tissues, including the septum and transmitting tract. Girin *et al.* demonstrated that *spt* single mutants are defective in the development of septum, transmitting tract, stigma, and style (unfused style) (Fig 4.7D) (Girin et al., 2011). Stigma and style defects in the *spt* mutant gynoecium were strongly enhanced in the *ind spt* double mutant (Fig 4.7B and D) (Girin et al., 2011). A study by Girin *et al.* showed that IND and SPT interaction is crucial for the fusion of carpels (Girin et al., 2011). Interestingly, Nahar *et al.* reported that *CUC1* was accumulated ectopically in *spt* unfused carpels, and the split phenotype of carpels was suppressed in the *spt cuc1* double mutant (Fig 4.7D and E) (Nahar et al., 2012). This shows that SPT can positively regulate carpel fusion in the apical gynoecium through the negative regulation of *CUC1* expression. Results from section 4.2.4 suggest that IND can directly downregulate *CUC1* expression. It is not known if SPT downregulation of *CUC1* is IND-dependent or if SPT alone can directly downregulate *CUC1* gene expression. To test this, gene expression was analysed in the *spt* mutant (*spt-12,* ATH1 Genome Array, n=2, NASCARRAYS-505) and DEX+CHY-mediated induction of SPT (*35S::SPT-VP16-GR*, URGV *Arabidopsis thaliana* 25K CATMA_v2.2, n=3, GSE12913) microarray datasets

(Josse et al., 2011; Reymond et al., 2012). *PHB, PHV* and *REV* were also included in the analysis because Chapter 3 shows that they regulate *SPT.*

A list of differentially expressed genes was summarised in a table (Table 8.2). A total of 114 genes were differentially expressed in *35S::SPT-VP16-GR* seedlings (DEX+CHY vs. CHY) (FC >1 or <-1, p<0.05): 94 genes were upregulated and 20 genes were downregulated. A total of 1524 genes were differentially expressed in *spt-12* seedlings (*spt-12* vs. Col-0); 734 genes were upregulated, and 789 genes were downregulated (FC >1 or <-1, p<0.05). *35S::SPT-VP16-GR* (GSE12913) data were compared with *spt-12* (NASCARRAYS-505), and a Venn diagram was generated using VENNY 2.1. The Venn diagram shows 107 differentially expressed genes in *35S::SPT-VP16-GR* seedlings (DEX+CHY vs. CHY) labelled in the blue intersecting circle, 1517 differentially expressed genes in *spt-12* seedlings (*spt-12* vs. Col-0) labelled in the yellow intersecting circle, and the overlapping region shows 7 genes differentially regulated in both datasets (Fig 4.8A). The *PHB, PHV, REV, CUC1* and *HEC1* genes were not on that list. However, genes *AT1G19310*, *TZF5* and *PYL4* were downregulated in *spt-12* seedlings (*spt-12* vs. Col-0) and uprregulated in *35S::SPT-VP16-GR* seedlings (DEX+CHY vs. CHY). This suggests SPT may directly regulate *AT1G19310*, TANDEM CCCH ZINC FINGER PROTEIN 5 (*TZF5*) and *PYRABACTIN RESISTANCE 1-LIKE 4* (*PYL4*) gene expression. *PYL4* is an ABA receptor, which is known to regulate ABA signalling (Gonzalez-Guzman et al., 2012). SPT promotes seed dormancy by regulating ABA signalling (Vaistij et al., 2013), SPT many regulate this process possibly by directly regulating *PYL4.*

The *PHB, PHV, REV, CUC1* and *HEC1* gene expression fold change (*spt-12* vs. Col-0 and *35S::SPT-VP16-GR* DEX+CHY vs. CHY) is presented Figures 4.8B and C. The expression of *PHB, PHV* and *REV* was significantly decreased in *spt-12* seedlings (*spt-12* vs. Col-0, p<0.05, Fig 4.8B). No change in *CUC1* and *HEC1* gene expression was observed in *spt-12* seedlings (*spt-12* vs. Col-0, Fig 4.8B). No change in *PHB, PHV, REV, CUC1* and *HEC1* gene expression was observed in *35S::SPT-VP16-GR* seedlings (DEX+CHY vs. CHY, Fig 4.8C).
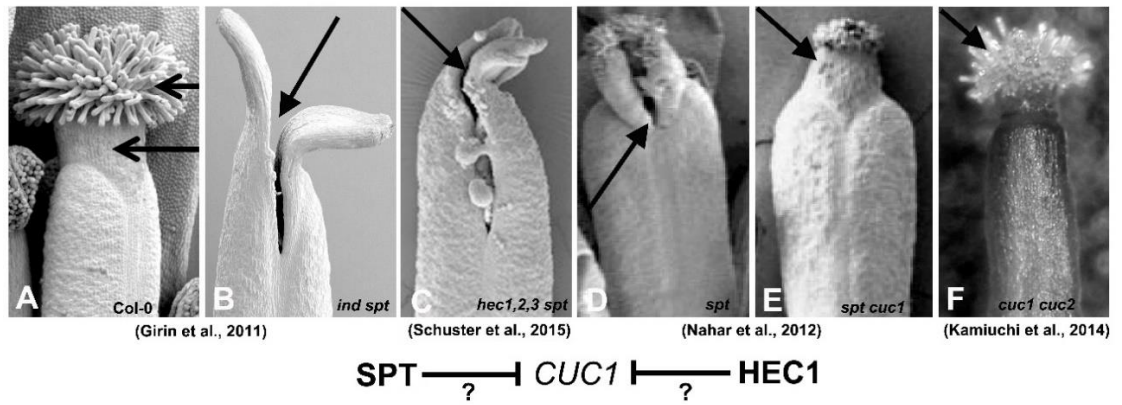
Figure 4.7 The *spt cuc1, ind spt* and *hec1,2,3 spt* fruit phenotype images from (Girin et al., 2011; Kamiuchi et al., 2014; Nahar et al., 2012; Schuster et al., 2015). **(A)** Col-0 fruit image shows stigma (top arrow) and style (bottom arrow). **(B-D)** *spt, ind spt* and *hec1,2,3 spt* fruit image show stigma and style defective unfused carpels (arrow). **(E)** *spt cuc1* fruit image shows style and stigma (arrow) without split phenotype. **(F)** *cuc1 cuc2 spt* fruit image shows normal style and stigma (arrow) without replum. It is not known if SPT and HEC1 can directly downregulate *CUC1* gene expression.
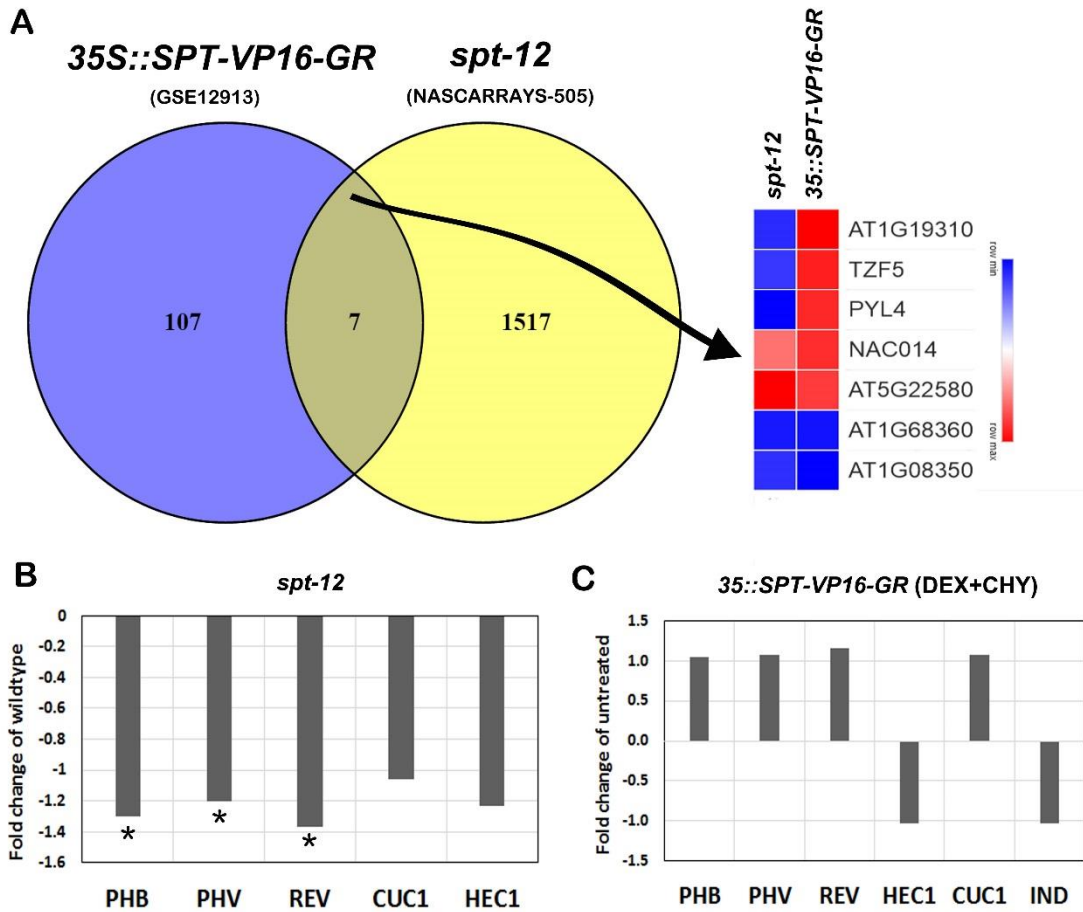
Figure 4.8 *35S::SPT-VP16-GR* and *spt-12* microarray. (A) The overlapping region of the Venn diagram shows 7 genes differentially expressed in both *35S::SPT-VP16-GR* seedlings (p<0.05, DEX+CHY vs. CHY) and *spt-12* seedlings (p<0.05, *spt-12* vs. Col-0). **(B)** The bar chart shows *PHB, PHV, REV, CUC1* and *HEC1* gene expression in *spt-12* seedlings (*spt-12* vs. Col-0). **(C)** The bar chart shows *PHB, PHV, REV, HEC1, CUC1* and *IND* gene expression in *35S::SPT-VP16-GR* seedlings (DEX+CHY vs. CHY). One-Way ANOVA *p<0.05, Gene Fold Change (linear) >1 or <-1, Blue: decreased gene expression, Red: increased gene expression.
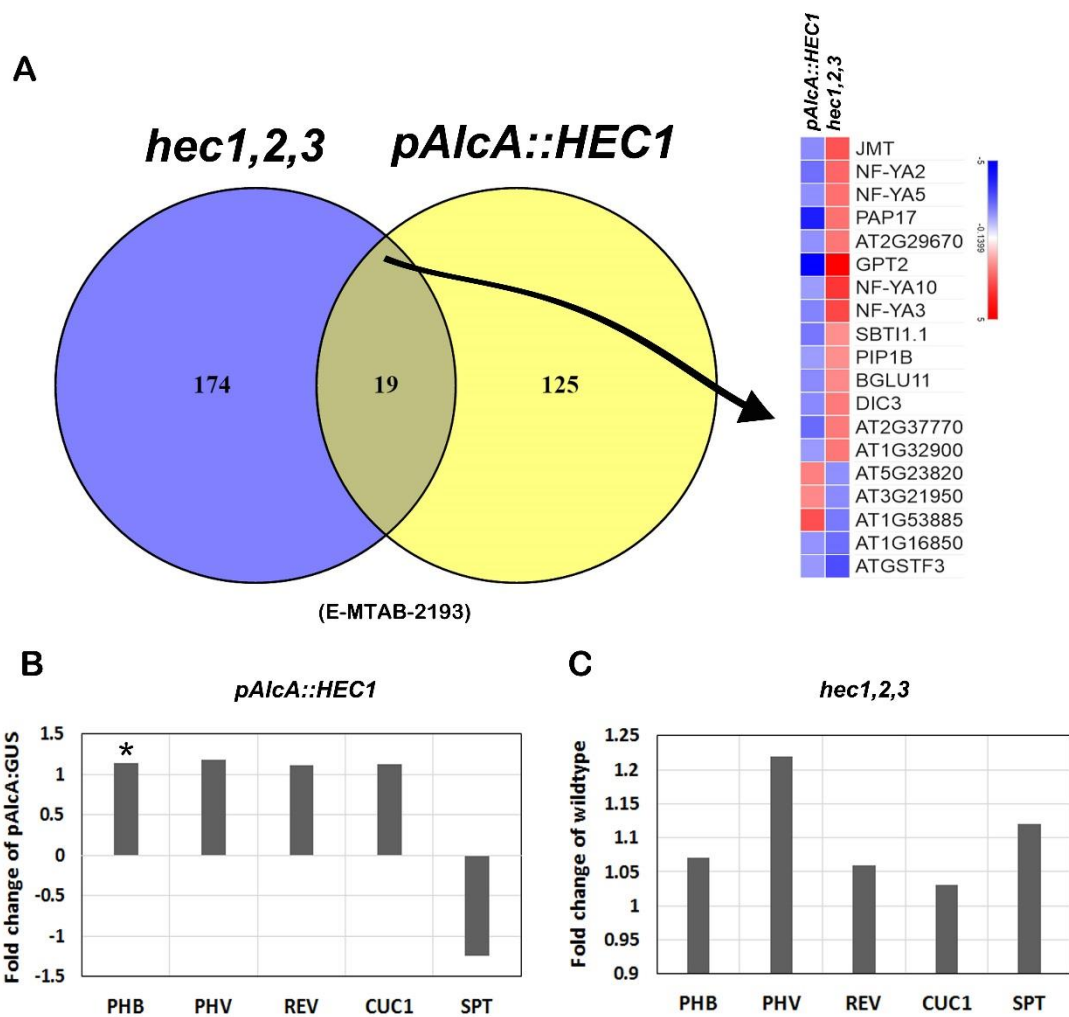
Figure 4.9 *pAlcA::HEC1* **and** *hec1,2,3* **microarray. (A)** The overlapping region of the Venn diagram shows 19 genes differentially expressed in both *hec1,2,3* Inflorescence apices ($p<0.05$, *hec1,2,3* vs. Col-0) and *pAlcA::HEC1* Inflorescence apices ($p<0.05$, *pAlcA::HEC1*+EtH vs. *pAlcA::GUS*+EtH). **(B)** The bar chart shows *PHB, PHV, REV, CUC1* and *SPT* gene expression in *pAlcA::HEC1* inflorescence apices (*pAlcA::HEC1*+EtH vs. *pAlcA::GUS*+EtH). **(C)** The bar chart shows *PHB, PHV, REV, HEC1, CUC1* and *SPT* gene expression *hec1,2,3* Inflorescence apices (*hec1,2,3* vs. Col-0). One-Way ANOVA *$p<0.05$, Gene Fold Change (linear) >1 or <-1, Blue: decreased gene expression, Red: increased gene expression.

4.2.5.2 pAlcA:HEC1 and *hec1,2,3* microarray data analysis

In *Arabidopsis*, HEC1, HEC2 and HEC3 are essential for transmitting tract formation. Schuster *et al.* demonstrated that HEC1 interacts with SPT to control carpel fusion, and stigma-style defects in the *spt* mutant gynoecium were strongly enhanced in the *hec1,2,3 spt* quadruple mutant (Fig 4.7C and D) (Gremski et al., 2007; Schuster et al., 2015). SPT promotes carpel fusion in the apical gynoecium by inhibiting *CUC1* expression (Nahar et al., 2012), but the results from section 4.2.5.1 suggest SPT does not directly regulate *CUC1* gene expression. It is not known if SPT downregulation of *CUC1* is HEC1-dependent or if HEC1 alone can downregulate *CUC1* gene expression. To test this, gene expression was analysed in microarray datasets that characterise the *hec1,2,3* triple mutant (*hec1,2,3,* ATH1 Genome Array, n=2, E-MTAB-2193) and ethanol (EtH)-mediated overexpression of HEC1 (*pAlcA::HEC1*, ATH1 Genome Array, n=2, E-MTAB-2193) (Schuster et al., 2014). The *PHB, PHV* and *REV* were also included in the analysis because Chapter 3 shows that they regulate *HEC1.*

A list of differentially expressed genes was generated from these analyses and these are presented in a table (Table 8.3). A total of 193 genes were differentially expressed in *hec1,2,3* Inflorescence apices (*hec1,2,3* vs. Col-0) (FC >1.5 or <-1.5, p<0.05): 106 genes were upregulated and 87 genes were downregulated. Similarly, a total of 144 genes were differentially expressed in *pAlcA::HEC1* Inflorescence apices (*pAlcA::HEC1*+EtH vs. *pAlcA::GUS*+EtH): 43 genes were upregulated, and 101 genes were downregulated. The *hec1,2,3* data was compared with *pAlcA::HEC1* and a Venn diagram was generated using VENNY 2.1. The Venn diagram shows 174 differentially expressed genes in *hec1,2,3* Inflorescence apices (*hec1,2,3* vs. Col-0) labelled in the blue intersecting circle, 124 differentially expressed genes in *pAlcA::HEC1* Inflorescence apices (*pAlcA::HEC1*+EtH vs. *pAlcA::GUS*+EtH) labelled in the yellow intersecting circle, and the overlapping region shows 19 genes differentially regulated in both datasets (Fig 4.9A). The *PHB, PHV, REV, CUC1* and *SPT* genes were not on that list. However, genes *AT5G23820, AT3G21950* and *AT1G53885* were upregulated in *pAlcA::HEC1* Inflorescence apices (*pAlcA::HEC1*+EtH vs. *pAlcA::GUS*+EtH) and downregulated in *hec1,2,3* Inflorescence apices (*hec1,2,3* vs. Col-0). This suggests HEC1 may positively regulate *AT5G23820, AT3G21950* and *AT1G53885* gene expression. Alternatively, genes *NUCLEAR FACTOR Y, SUBUNIT A10* (*NF-YA10*), *NUCLEAR FACTOR Y, SUBUNIT A3* (*NF-YA3*)*, NUCLEAR FACTOR Y, SUBUNIT A2* (*NF-YA2*)*,

NUCLEAR FACTOR Y, SUBUNIT A5 (*NF-YA5*), *SUBTILISIN-LIKE PROTEASE SBT1.1* (*SBTI1*), *AQUAPORIN PIP1-2* (*PIP1B*), *PURPLE ACID PHOSPHATASE 17* (*PAP17*), *MITOCHONDRIAL UNCOUPLING PROTEIN 6* (*DIC3*), *GLUCOSE-6-PHOSPHATE/PHOSPHATE TRANSLOCATOR 2* (*GPT2*), *JASMONATE O-METHYLTRANSFERASE* (*JMT*), *AT2G37770, AT1G32900* and *AT2G29670* were downregulated in *pAlcA::HEC1* Inflorescence apices (*pAlcA::HEC1*+EtH vs. *pAlcA::GUS*+EtH) and upregulated in *hec1,2,3* Inflorescence apices (*hec1,2,3* vs. Col-0). This suggests HEC1 may negatively regulate *NF-YA10, NF-YA3, NF-YA2, NF-YA5, SBTI1, PIP1B, PAP17, DIC3, GPT2, JMT, AT2G37770, AT1G32900* and *AT2G29670* gene expression. NF-YA Proteins positively regulate flowering via FLOWERING LOCUS T (Siriwardana et al., 2016), this suggests HEC1 may control flowering by regulating *NF-YA10, NF-YA3, NF-YA2* and *NF-YA5* gene expression.

The *PHB, PHV, REV, CUC1* and *SPT* gene expression fold change (*hec1,2,3* vs. Col-0 and *pAlcA::HEC1*+EtH vs. *pAlcA::GUS*+EtH) is presented in Figures 4.9B and C. No change in *PHB, PHV, REV, CUC1* and *SPT* gene expression was observed in *hec1,2,3* Inflorescence apices and *pAlcA::HEC1* seedlings (*hec1,2,3* vs. Col-0 and *pAlcA::HEC1*+EtH vs. *pAlcA::GUS*+EtH, Fig 4.9B and C).

4.2.5.3 Summary

In summary, these results demonstrate that HEC1 does not regulate *SPT* gene expression and SPT does not regulate *IND* and *HEC1* gene expression. SPT and HEC1 do not regulate *CUC1* gene expression. This suggests that SPT and HEC1 were not required for IND downregulation of *CUC1* gene expression. Downregulation of *PHB, PHV* and *REV* in *spt-12* suggests that SPT may positively regulate *PHB, PHV* and *REV*.

4.2.6 35S:CUC1 and *cuc1* microarray data analysis

In *Arabidopsis*, *CUC* genes prevent the fusion of cotyledons and are essential for the formation of carpel margin meristems (CMMs) during fruit development (Kamiuchi et al., 2014). *cuc1 cuc2* double mutant fruits also often lack the repla in their upper parts (Fig 4.7F) (Ishida et al., 2000; Kamiuchi et al., 2014). During embryogenesis, the KNOX I protein STM positively regulates *CUC* gene expression and CUC1 also activates *STM* gene expression (Aida et al., 1999; Spinelli et al., 2011). The *STM* expression in CMMs was strictly dependent on *CUC1* and *CUC2* activity. This regulatory activity increases the

amount of the STM-RPL complex in CMMs and antagonises the valve/valve margin factors (Kamiuchi et al., 2014). The results from section 4.2.4 show that the valve margin factor IND downregulates *CUC1* gene expression. It is not known if CUC1 can downregulate *IND* gene expression. To test this, gene expression was analysed from microarray datasets characterising *cuc1* mutant (*cuc1,* Agilent *Arabidopsis* V3 (4x44k) Microarray, n=3, GSE20705) and overexpression of CUC1 (*35S::CUC1*, Agilent *Arabidopsis* 1 Microarray, n=2, GSE27482) (Koyama et al., 2010; Takeda et al., 2011). The *PHB, PHV* and *REV* were also included in the analysis because section 4.2.3 shows that PHB and REV upregulate *CUC1.* A list of differentially expressed genes is presented in a table (Table 8.4). A total of 4648 genes were differentially expressed in *cuc1* seedlings (*cuc1* vs. Col-0) (FC >1.5 or <-1.5, p<0.05): 2319 genes were upregulated and 2329 genes were downregulated. A total of 326 genes were differentially expressed in *35S::CUC1* seedlings (*35S::CUC1* vs. L*er*) (FC >1 or <-1, p<0.05): 245 genes were upregulated, and 81 genes were downregulated. *cuc1* (GSE20705) data were compared with *35S::CUC1* (GSE27482), and a Venn diagram was generated using VENNY 2.1. The Venn diagram shows 4574 differentially expressed genes in *cuc1* seedlings (*cuc1* vs. Col-0) labelled in the blue intersecting circle, 252 differentially expressed genes in *35S::CUC1* seedlings (*35S::CUC1* vs. L*er*) labelled in the yellow intersecting circle, and the overlapping region shows 74 genes differentially regulated in both datasets (Fig 4.10A). The *PHB, PHV, REV, SPT, IND* and *HEC1* genes were not on that list.

However, *STM* expression was increased in *35S::CUC1* seedlings (*35S::CUC1* vs. L*er,* p<0.05, Fig 4.10A) and this is consistent with previously published work (Kamiuchi et al., 2014). Interestingly, *RPL* expression was also increased in *35S::CUC1* seedlings (*35S::CUC1* vs. L*er*). This suggests that CUC1 upregulates *RPL* gene expression (p<0.05, Fig 4.10A). *GA3ox1* expression was increased in *cuc1* seedlings (*cuc1* vs. Col-0) and decreased in *35S::CUC1* seedlings (*35S::CUC1* vs. L*er*). This suggests that CUC1 downregulates *GA3ox1* gene expression (p<0.05, Fig 4.10A). In addition, genes *BETA-GLUCOSIDASE 1* (*BGLU18*), *PROBABLE CARBOXYLESTERASE 13* (*CXE13*), *FERREDOXIN/THIOREDOXIN REDUCTASE SUBUNIT A2* (*FTRA2*), *LOB DOMAIN-CONTAINING PROTEIN 40* (*LBD40*), *26S PROTEASOME NON-ATPASE REGULATORY SUBUNIT 4 HOMOLOG* (*MBP1*), *PROBABLE INACTIVE PURPLE ACID PHOSPHATASE 1* (*PAP1*), *PROBABLE PEROXYGENASE 3* (*RD20*), and *RAN-BINDING PROTEIN 1 HOMOLOG*

A (*SIRANBP*) were upregulated in *cuc1* seedlings (*cuc1* vs. Col-0) and downregulated in *35S::CUC1* seedlings (*35S::CUC1* vs. L*er*). This suggests CUC1 may negatively regulate *BGLU18, CXE13, FTRA2, LBD40, MBP1, PAP1, RD20*, and *SIRANBP* gene expression. Alternatively, genes *PROBABLE ACYL-ACTIVATING ENZYME 17* (*AAE17*), *CASEIN KINASE II SUBUNIT ALPHA-3* (*CKA3*), *CYSTEINE-RICH RECEPTOR-LIKE PROTEIN KINASE 10* (*CRK10*), *CDPK-RELATED KINASE 3* (*CRK3*), *PROTEIN EARLY RESPONSIVE TO DEHYDRATION 15* (*ERD15*), *ENT-KAURENOIC ACID OXIDASE 2* (*KAO2*), *INOSITOL TRANSPORTER 1* (*INT1*), *TRANSCRIPTION FACTOR PIF3* (*PIF3*) and *SMALL AUXIN UPREGULATED RNA 1* (*SAUR1*) were downregulated in *cuc1* seedlings (*cuc1* vs. Col-0) and upregulated in *35S::CUC1* seedlings (*35S::CUC1* vs. L*er*). This suggests CUC1 may positively regulate *AAE17, CKA3, CRK10, CRK3, ERD15, KAO2, INT1, PIF3* and *SAUR1* gene expression. PIF3 controls hypocotyl and cotyledon development by regulating photoinduced signal transduction (Kim et al., 2003a; Ni et al., 1998), this suggests CUC1 may possibly regulate cotyledon development via controlling *PIF3* gene expression. *SAUR1* an auxin responsive gene which is induced with auxin treatment (Goda et al., 2008; Goda et al., 2004), this suggests CUC1 may possibly regulate auxin responses. The *PHB, PHV, REV, SPT, IND* and *HEC1* gene expression fold change (*cuc1* vs. Col-0 and *35S::CUC1* vs. L*er*) is presented in Figures 4.10B and C. The *PHB* and *PHV* expression was significantly decreased in *cuc-1* seedlings (*cuc1* vs. Col-0, p<0.05, Fig 4.10B). No change in *REV, SPT, IND* and *HEC1* gene expression was observed in *cuc-1* seedlings (*cuc1* vs. Col-0, Fig 4.10B). *REV* expression was two-fold increased but this was not significant, and no change in *PHB* or *PHV* gene expression was observed in *35S::CUC1* seedlings (*35S::CUC1* vs. L*er*, Fig 4.10C).

In summary, these results demonstrate that CUC1 does not directly regulate *IND* gene expression. Downregulation of *PHB* and *PHV* in *cuc1* suggests that CUC1 may positively regulate *PHB* and *PHV* in seedlings. *STM* and *RPL* expression was increased in *35S::CUC1* seedlings, which suggests that CUC1 may positively regulate replum by directly promoting STM-RPL in CMMs. *GA3ox1* positively regulates gibberellin biosynthesis (Arnaud et al., 2010; Talon et al., 1990). *GA3ox1* gene expression was increased in *cuc1* seedlings and decreased in *35S::CUC1* seedlings. This demonstrates CUC1 may inhibit gibberellin biosynthesis by downregulating *GA3ox1.*
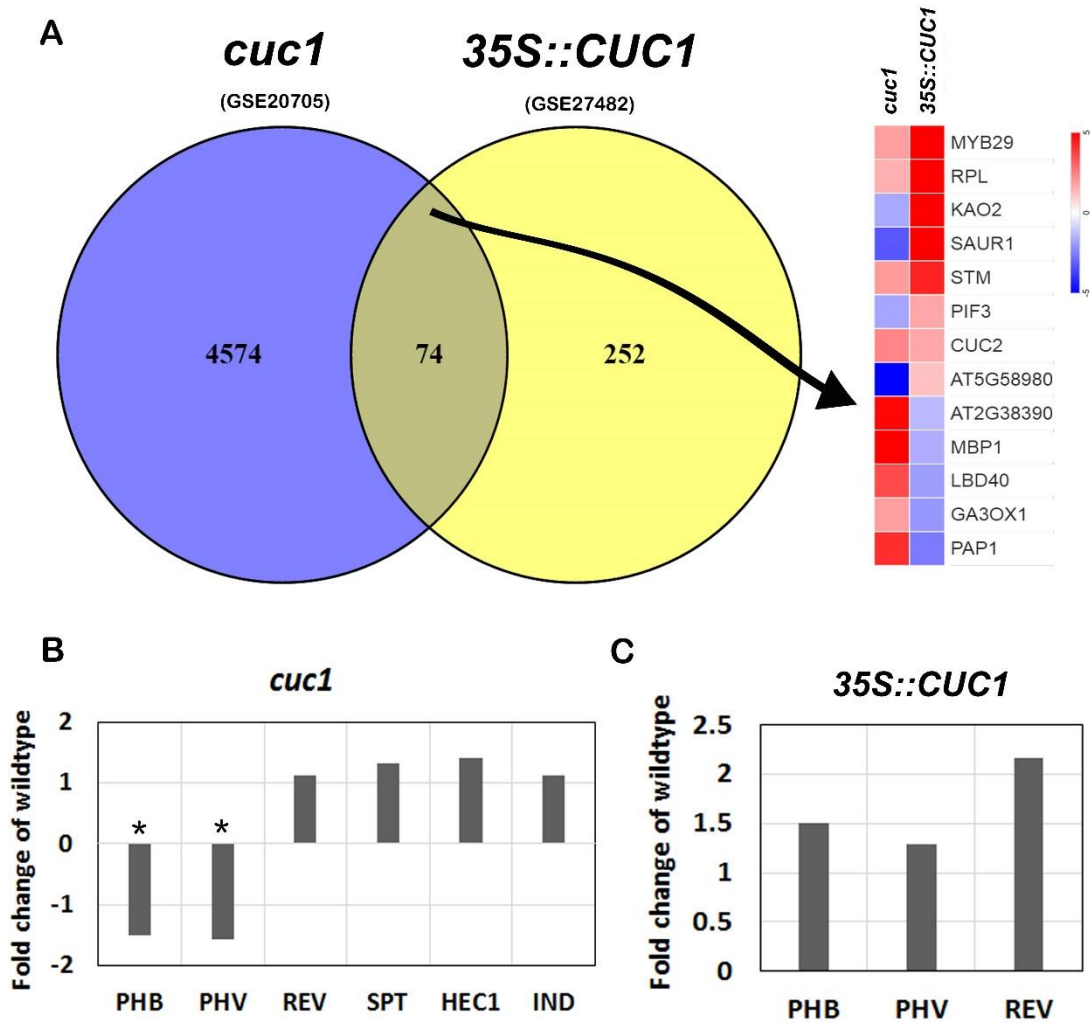
Figure 4.10 *35S::CUC1* and *cuc1* microarray. (A) The overlapping region of Venn diagram shows 74 genes differentially expressed in both *cuc1* seedlings (p<0.05, *cuc1* vs. Col-0) and *35S:CUC1* seedlings (p<0.05, *35S::CUC1* vs. L*er*). **(B)** The bar chart shows *PHB, PHV, REV, SPT, HEC1* and *IND* gene expression in *cuc1* seedlings (*cuc1* vs. Col-0), * denotes significance. **(C)** The bar chart shows *PHB, PHV* and *REV* gene expression in *35S::CUC1* seedlings (*35S::CUC1* vs. L*er*). Unpaired t-test *p<0.05, Gene Fold Change (linear) >1 or <-1, Blue: decreased gene expression, Red: increased gene expression.
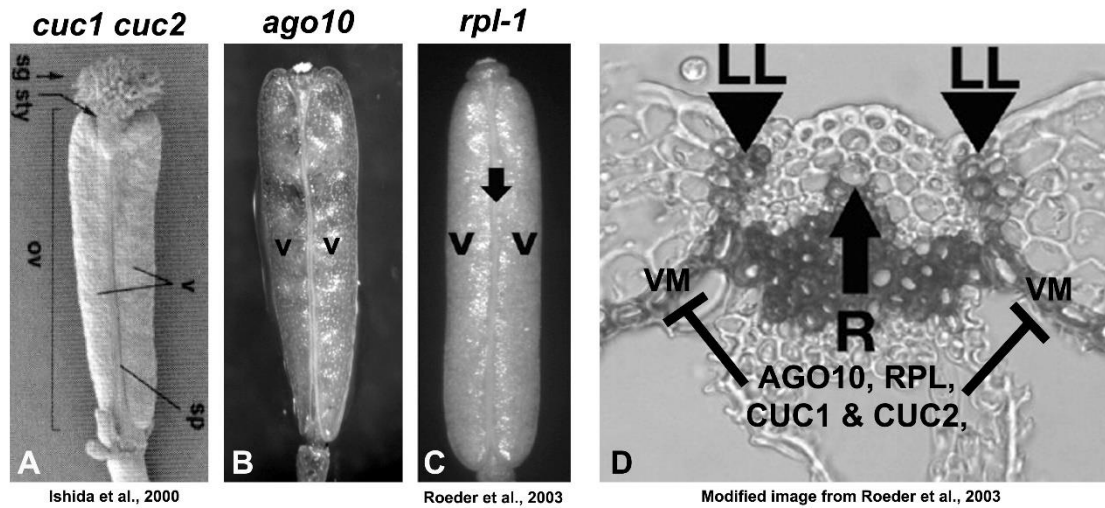
Figure 4.11 The *cuc1 cuc2, ago10 (zwl-3)* and *rpl-1* fruit phenotype images from this study and (Ishida et al., 2000; Roeder et al., 2003). (A) *cuc1 cuc2* fruit image show small replum (sp). **(B)** *ago10^{zwl-3}* fruit image show small replum. **(C)** *rpl-1* fruit image show small replum (Black arrow). **(D)** Cross-section of the wild type replum region showing replum (R), lignified layer (LL) at the valve margins (VM). AGO10, RPL, CUC1 and CUC2 inhibit valve margin factors and promote replum development. V= valves

4.3 Discussion

4.3.1 AGO10 regulates auxin responses

In *Arabidopsis*, PIN1 and PID proteins regulate auxin transport and they are important for proper meristem and leaf development (Heisler et al., 2005; Huang et al., 2010; Larsson et al., 2014). Auxin transport rapidly and dynamically relocalises auxin in plant tissues to form auxin maxima (Larsson et al., 2014; Sorefan et al., 2009a). Auxin maxima in the SAM promote the formation of leaf primordia and auxin minima establish the boundary between the SAM and leaf primordia, which is also known as organ separation (Aida et al., 2002; Christensen et al., 2000; Furutani et al., 2004; Heisler et al., 2005). Multiple studies have demonstrated that *pin1, pid* and *cuc* mutants produce cup and pin shaped phenotypes (Aida et al., 1997; Aida et al., 1999; Aida et al., 2002; Furutani et al., 2004; Hibara et al., 2006). The CUP and PIN phenotypes were also observed in *phb rev* and *ago10*^{zwl-3} mutants, suggesting that the AGO10-HD-ZIPIII pathway regulates auxin responses (Moussian et al., 2003; Moussian et al., 1998; Prigge et al., 2005). Several lines of evidence support this hypothesis. A study by Heisler *et al.* showed that the expression pattern of the *REV* gene (*pREV::REV-VENUS*) coincides with the pattern of auxin distribution and auxin transport (*DR5::GFP*, *pPIN1::PIN1-GFP*) (Heisler et al., 2005). Interestingly, a study by Reinhart *et al.* reported that REV (GR-REV) overexpression upregulated the auxin biosynthesis genes *YUC5* and *TAA1,* suggesting that REV promotes auxin biosynthesis (Reinhart et al., 2013). Therefore, loss of *rev* function may cause CUP and PIN shaped phenotypes by disrupting auxin biosynthesis and auxin distribution. The data presented in this chapter show that *YUC1, PIN,* and *PID* expression are reduced in *zwl-3* (CUP and PIN) and *ind-6 zwl-3* (CUP and PIN) mutants (Fig 4.2 and 4.3B). Since *REV* expression is reduced in *ago10* and *ind6 zwl-3* (CUP and PIN) mutants it is plausible that the CUP and PIN phenotypes are the results of a loss in *rev* dependent auxin responses.

4.3.2 AGO10 regulates cytokinin responses

Cytokinin is an important regulator of meristem development. *ARR7* is the main response gene of cytokinin signalling and is often used as a marker of cytokinin responses. For example, overexpression of *ARR7* suppresses shoot regeneration (Buechel et al., 2010) and constitutive expression of ARR7 (*35S::ARR7*) also results in the PIN phenotype, which is reminiscent of the *zwl-3* PIN and *ind-6 zwl-3* PIN (Leibfried et

al., 2005; Zhao et al., 2010). Cytokinin and auxin signalling are also integrated via ARR7. Auxin downregulates expression of *ARR7*. Zhao *et al.* also observed an increase in *ARR7* expression in the SAM of the *yuc*, *pin1*, *pid* mutants as well as plants treated with auxin transport inhibitor N-1-naphthylphthalamic acid (NPA) (Zhao et al., 2010). This demonstrates that *ARR7* activation can be directly induced by the loss of local auxin accumulation. Results from this chapter also report an increase in *ARR7* gene expression in *zwl-3* (CUP and PIN) and *ind-6 zwl-3* (CUP and PIN) phenotypes (Fig 4.2). Since ARR7 is thought to be a negative regulator of cytokinin signalling, the cup and pin phenotypes of *ago10*$^{zwl-3}$ mutants may be caused by reduced cytokinin signalling.

4.3.3 Understanding the role of miR164a-c in *ago10* mutants

In *Arabidopsis*, *CUC1, CUC2,* and *CUC3* genes regulate organ separation and SAM development. The loss of *CUC* promotes organ fusion and produces fused CUP shaped cotyledons (Aida et al., 1997; Aida et al., 1999; Aida et al., 2002; Furutani et al., 2004; Hibara et al., 2006; Takada et al., 2001). The fused CUP shaped leaves of *zwl-3* and *ind-6 zwl-3* mutants look similar to *cuc* mutant CUP shaped cotyledons. The analysis in this chapter also found decreased expression of *CUC1, CUC2,* and *CUC3* in *zwl-3* and decreased expression of *CUC2* and *CUC3* in *ind-6 zwl-3* (Fig 4.3A). The fused CUP shaped leaf of *zwl-3* may be a result of the decreased *CUC1/2/3* expression. Multiple studies have shown that miR164 targets *CUC1* and *CUC2* transcripts (Hasson et al., 2011; Laufs et al., 2004; Sieber et al., 2007; Spinelli et al., 2011), and overexpression of miR164 in the tomato and *Arabidopsis* plants affects leaf and floral organ development by promoting organ fusion (Rosas Cárdenas et al., 2017). However, results from this chapter suggest that a decrease in *CUC* expression in *zwl-3* and *ind-6 zwl-3* seedlings is probably not caused through misregulation of miR164a-c. We found miR164a-c expression was significantly decreased in *ind-6 zwl-3* seedlings, which would be expected to cause an increase in *CUC* expression (Fig 4.4A and B). It is not known how the loss of *IND* in *ind-6 zwl-3* seedlings can result in significant reduction of miR164a-c, but this is probably not due to changes in AGO10 levels because miR164 does not bind AGO10. Possibly, the decrease in miR164a-c levels in *ind-6 zwl-3* mutants represents a negative feedback response to maintain *CUC* expression.

4.3.4 Understanding the role of IND-CUC1 in *ago10* mutants

Similar to *cuc pin1* mutants (Furutani et al., 2004), overexpression of IND produces PIN and CUP shaped leaves (Chapter 3). To this effect, results from ChIP experiments presented in Section 4.2.4 show that IND can bind to the *CUC1* promoter and downregulate *CUC1* gene expression (Fig 4.6). In addition, a study by Sorefan *et al.* demonstrated that IND promotes auxin minima by downregulation of PIN1 and *PID* (Sorefan et al., 2009a). This suggests that IND repress *CUC1* and *PIN1* expression and may impair SAM and leaf development. The analysis in this chapter and Chapter 3 also found increased expression of *IND* and decreased expression of *CUC1* in *zwl-3.* The increased *IND* expression and decreased *CUC1* gene expression pattern coincides with an increase in the *zwl-3* PIN phenotype (Fig 4.1E and 4.3A). The loss of *IND* and normal *CUC1* gene expression patterns coincide with decreased *ind-6 zwl-3* PIN phenotype (Fig 4.1E and 4.3A). From this, we can draw that IND may negatively regulate *PIN1, PID,* and *CUC1* in *zwl-3* and may promote CUP and PIN phenotypes. However, IND does not regulate *CUC2* and *CUC3* gene expression. The decreased expression of *CUC2* and *CUC3* in *zwl-3* and *ind-6 zwl-3* may be the result of a loss in *rev* dependent auxin responses. Results from Section 4.2.3 show that AGO10 may positively regulate *CUC1* via PHB and REV (Fig 4.5). AGO10 may also regulate STM via *CUC1* because CUC1 promotes *STM* expression (Aida et al., 1999; Spinelli et al., 2011). However, STM also promotes *AGO10* to maintain central meristem cells (Endrizzi et al., 1996). These data, in agreement with our results, suggest that AGO10 represses *IND* gene expression via HD-ZIP III to regulate *CUC1* expression and to promote SAM development (Fig 4.12).

4.3.5 Understanding the role of IND-CUC1 in gynoecium development

During fruit development, *CUC1* and *CUC2* are expressed in the septum of gynoecium (expressed from stage 7) (Ishida et al., 2000). *CUC1* and *CUC2* are required for the septum and replum formation and overexpression of *CUC* prevents apical carpel fusion (Ishida et al., 2000; Kamiuchi et al., 2014; Nahar et al., 2012) (Fig 4.7D and E, 4.11A). A different study showed that SPT could negatively regulate *CUC1* and *CUC2* expression to promote carpel fusion in the apical gynoecium (Nahar et al., 2012). The results from this chapter suggest that SPT does not directly regulate *CUC1* gene expression (Fig 4.8).

However, SPT and IND interaction is crucial for carpel fusion in the apical gynoecium (Girin et al., 2011). Therefore, IND may be repressing *CUC1* expression.

However in the medial tissue, CUC1 promotes STM expression and acts upstream of STM in replum formation (Kamiuchi et al., 2014). Interestingly, STM also physically interacts with the replum factor RPL (Byrne et al., 2003). The results from this chapter demonstrate that CUC1 significantly upregulates *STM* and *RPL* gene expression (Fig 4.10A). From this, we can draw that CUC1 may promote replum formation by upregulating *STM* and *RPL* and possibly by promoting their interaction in carpel margin meristems. RPL promotes replum development by inhibiting valve margin factors (Roeder et al., 2003). Since CUC1 does not regulate *IND* and *SPT* gene expression (Fig 4.10), CUC1 may inhibit the valve margin factors SPT and IND via *STM* and *RPL.* In *Arabidopsis*, gibberellins promote differentiation of fruit valve margins (Arnaud et al., 2010). The results from this chapter demonstrate that CUC1 may negatively regulate gibberellin biosynthesis by downregulating *GA3ox1* gene expression (Fig 4.10A). Interestingly, *GA3ox1* is a direct target of IND because IND directly upregulates *GA3ox1* gene expression (Arnaud et al., 2010). Taken together, these studies indicate that CUC1 may inhibit valve margin development (Fig 4.11D), SPT and IND may inhibit *CUC1* to promote valve margin development. Similar to *CUC1*, *CUC2* and *RPL*, *AGO10* is also essential for replum and septum development (Fig 4.11) (Lynn et al., 1999). In addition, results from Chapter 3 and other published work demonstrate that AGO10 and RPL inhibit the valve margin factor IND (Roeder et al., 2003). These studies suggest that AGO10 may inhibit *IND* and promote replum development by upregulating *CUC1* expression (Fig 4.12).

4.3.6 Conclusion

This chapter demonstrates that *zwl-3* (CUP and PIN) and *ind-6 zwl-3* (CUP and PIN) phenotypes are defective in auxin and cytokinin signalling. In particular, a decrease in *PIN1, PID,* and *CUC1/2/3* gene expression may promote CUP and PIN phenotypes. Similar to *PIN1* and *PID*, we found that IND can directly downregulate *CUC1* gene expression and may promote CUP and PIN phenotypes in *zwl-3.* Since AGO10 upregulates *CUC1* and downregulates *IND* via PHB and REV, AGO10 may inhibit *IND* to promote *CUC1* gene expression and thus coordinate SAM and leaf development (Fig

4.12). In addition, CUC1 may promote replum development by upregulating *RPL-STM* and may negatively regulate valve margin genes via RPL-STM. Together these studies suggest that AGO10-IND-CUC1 may regulate both SAM and replum development.
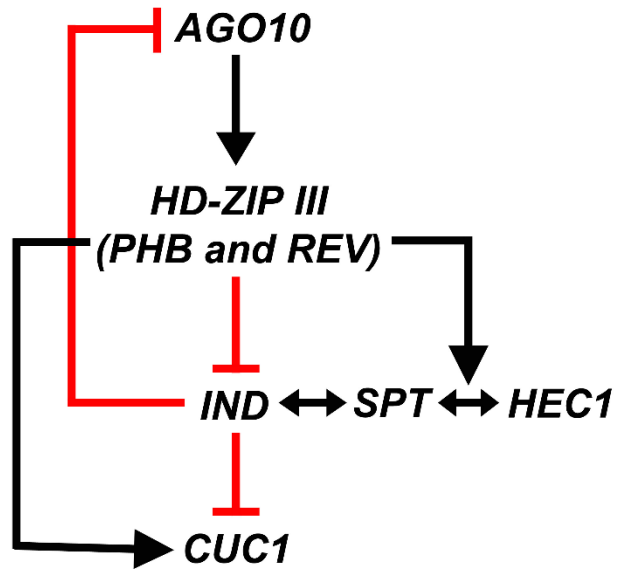
Figure 4.12 Schematic representation of the AGO10-PHB-REV-IND-CUC1 signalling cascade.

Chapter 5

Auxin and cytokinin control IND regulated gene expression

CHAPTER 5. Auxin and cytokinin control IND regulated gene expression

5.1 Introduction

The yin and yang of auxin and cytokinin hormones can control gynoecium and SAM patterning. Polar auxin transport is essential for the radialisation process and medial versus lateral tissue specification in *Arabidopsis* gynoecia (Larsson et al., 2014; Moubayidin and Ostergaard, 2014; Nole-Wilson et al., 2010). Cytokinin signalling is essential for carpel margin meristem (CMM) growth and carpel fusion in *Arabidopsis* gynoecia (Reyes-Olalde et al., 2017; Schuster et al., 2015). Interestingly, a recent study showed that SPT can regulate cytokinin signalling as well as auxin biosynthesis in *Arabidopsis* gynoecia. SPT enables cytokinin signalling by regulating *ARR1*, and both activate auxin biosynthesis via *TAA1* and auxin transport via PIN3 at the medial domain of the gynoecium (Reyes-Olalde et al., 2017). PIN1 proteins regulate auxin flux from the base to the top of the developing gynoecium. Apical PIN localisation at the plasma membrane is regulated by PID, and lateral PIN localisation at the plasma membrane is regulated by SERINE/THREONINE-PROTEIN KINASE 2 (WAG2) (Moubayidin and Ostergaard, 2014; Sorefan et al., 2009a). SPT also interacts with IND and HEC1 to control polar auxin transport (Girin et al., 2011; Schuster et al., 2015). SPT-HEC1 promotes auxin transport by directly inducing *PIN1* expression in the lateral part of gynoecia (Schuster et al., 2015) and SPT-IND regulates auxin transport by repressing *PID* expression and inducing *WAG2* expression in the valve margins as well as in the gynoecium apex (Girin et al., 2011; Sorefan et al., 2009a).

Interestingly, auxin also limits HEC and SPT activity through ETT function (Gremski et al., 2007; Heisler et al., 2001; Nemhauser et al., 2000; Schuster et al., 2015). *ETT* expression is specific to the adaxial domain at an early stage of gynoecium development. Loss of *ETT* results is abnormal patterning of gynoecium (Sessions et al., 1997; Sessions and Zambryski, 1995). Similar to SPT-IND, ETT and IND also regulate carpel development by repressing *PID* expression (Girin et al., 2011; Simonini et al., 2016). Interestingly, ETT and IND most likely heterodimerise to repress *PID* expression. Simonini *et al.* demonstrated that ETT and IND proteins interact in an IAA-sensitive manner. This suggests that auxin can influence IND targeted gene expression. A recent study also showed that cytokinin

can rescue valve margin formation in an *ind* mutant (Marsch-Martinez et al., 2012). These studies demonstrate that auxin-cytokinin and IND-SPT-HEC1 activities are coupled together in controlling gynoecium development.

As in gynoecium development, cytokinin and SPT-HEC1 functions are coupled together in controlling SAM development. Cytokinin regulates the size of the SAM by controlling stem cell proliferation, and cytokinin signalling can also control phyllotaxis via AHP6 (Besnard et al., 2014). *HEC1* and *SPT* are also expressed in the centre of the SAM. Schuster *et al.* demonstrated that HEC1-SPT can regulate the size of SAM (Schuster et al., 2014). HEC1 also promotes stem cell proliferation in the SAM by regulating cytokinin signalling (Schuster et al., 2014). Cytokinin promotes valve margin formation, but we do not know if cytokinin can regulate IND in the SAM.

Polar auxin transport between leaf primordia and the SAM contributes to establishing leaf polarity. Loss of auxin transport can lead to leaf polarity defects (Qi et al., 2014). A recent study demonstrated that PIN1-dependent auxin efflux can play a role in the formation of the auxin minimum at the leaf axil. This is important for axillary meristem initiation (Wang et al., 2014). Interestingly, IND also regulates auxin minimum formation in the fruit valve margin via *PID* and *WAG2* expression (Sorefan et al., 2009a). Since AGO10 negatively regulates *IND* in the SAM (Chapter 3 and 4), IND may possibly interact with ETT to regulate auxin minima in the leaf (abaxial). Similar to gynoecia, auxin may influence IND-ETT activity in the leaf (abaxial). Since *HEC1* is not expressed in leaf primordia, this suggests that ETT may be repressing *HEC1* expression in leaf primordia.

Since auxin and cytokinin are key regulators of SAM and leaf development, it is important to understand the bigger role of IND in SAM and leaf development. This can be investigated by studying IND-regulated gene regulatory networks on their own as well as in the presence of auxin and cytokinin. In this chapter, how auxin and cytokinin can influence IND in regulating target gene networks will be examined.

5.2 Results

Descriptors used for microarray sample comparison: DMSO was used as a vehicle control, DEX was used to induce IND (IND), IAA is an auxin (AUX), and BAP is a cytokinin (CYT). DEX was compared with DMSO (DEX vs. DMSO), DEX plus IAA was compared with IAA (DEX+AUX vs. AUX), and DEX plus BAP was compared with BAP (DEX+BAP vs. BAP).

5.2.1 Microarray analysis of IND-regulated genes

5.2.1.1 Differential gene expression analysis

We have shown that IND regulates several genes associated with SAM development, however it is not known whether IND can affect other gene networks (Arnaud et al., 2010; Girin et al., 2011; Liljegren et al., 2004a; Moubayidin and Ostergaard, 2014; Simonini et al., 2016; Sorefan et al., 2009a). Therefore we investigated the effect of upregulating IND on global gene expression changes using microarray analysis. For the microarray, total RNA was isolated from *35S::IND:GR* seedlings (7DAG), which were treated with either 10 µM DEX or DMSO for 6 hours in liquid media (n=3). Quality control and microarray hybridisation (*Arabidopsis* Gene 1.0 ST Array, Thermofisher, 901915; previously known as an Affymetrix array) was performed at the University of Sheffield core facility for microarray and next-generation sequencing. *Arabidopsis* Gene 1.0 ST Array CEL files were processed and normalised using Affymetrix® Expression Console™ software. Affymetrix® Transcriptome Analysis Console (TAC) software was used to perform differential gene expression analysis.

Genes were considered to be differentially expressed if the per-gene variance with p-value was below 0.05 and the linear fold change was greater than 1.5 or below -1.5 compared to control seedlings. A total of 921 genes were significantly differentially expressed in *35S::IND:GR* seedlings (DEX vs. DMSO, FC >1.5 or <-1.5, p<0.05): 339 genes were upregulated, and 582 genes were downregulated (Fig 5.1). The heat map shows the top 30 differentially expressed genes (Fig 5.1). For example the SENESCENCE-ASSOCIATED GENE 29 (*SAG29, AT5G13170*) was thirteen fold highly upregulated in *35S::IND:GR* seedlings (Fig 5.1). IND *Arabidopsis* Gene 1.0 ST microarray data was also validated using qRT-PCR, and a list of differentially expressed genes was summarised in

a table (Table 8.5 and 8.6). Out of 36, 24 genes broadly showed similar expression in microarray analysis and qRT-PCR experiments (Table 8.5, Pearson correlation coefficient (r): 0.85).

We compared our microarray results with a published IND overexpression and induction dataset to validate our analysis and identify genes that are regulated over time (Table 8.7). The Voinnet *et al.* (2011) microarray used *35S::IND:GR* seedlings but induced IND for 24 hours. This study was published in array express (10 µM DEX-induced vs. non-induced, *Arabidopsis thaliana* 34.6K CATMA_v5 microarray, E-GEOD-28898). To identify co-regulated genes, *35S::IND:GR* (induced for 6 hours) data were compared with *35S::IND:GR* (induced for 24 hours). A Venn diagram of genes from the two datasets was generated using VENNY 2.1 (Fig 5.2A). The Venn diagram shows 2869 (50%) differentially expressed genes in *35S::IND:GR* seedlings (induced for 6 hours, DEX vs. DMSO, FC >1 or <-1, p<0.05) labelled in the blue intersecting circle, 2121 (37%) differentially expressed genes in *35S::IND:GR* seedlings (induced for 24 hours, DEX vs. DMSO, FC >1 or <-1, p<0.05) labelled in the yellow intersecting circle, and the overlapping region shows 746 (13%) genes co-regulated or differentially regulated in both datasets (Fig 5.2A). In the overlapping gene list, 671 genes were co-regulated (Pearson correlation coefficient (r): 0.9) and 75 genes were differentially regulated (Pearson correlation coefficient (r): -0.9). This shows that around 13% of genes were regulated by IND overexpression at 6hrs and 24hrs.

We selected several genes that were shown to be regulated by IND (induced for 6 and 24 hours). An expression profile of these genes were presented in a heat map (Fig 5.2B). At 6 hours and 24 hours the expression of *SAG29*, *GIBBERELLIN 3-BETA-DIOXYGENASE 1 (GA3ox1)* and *SPT* were similar, and this suggests that IND targets *SAG29*, *GA3ox1* and *SPT* (Fig 5.2B). The *GA3ox1* and *SPT* expression patterns were consistent with previously published work (Arnaud et al., 2010; Girin et al., 2011; Groszmann et al., 2010). The HD-ZIP I gene *HOMEOBOX 12* (*HB-12*) regulates leaf growth by promoting cell expansion and endoreduplication (Hur et al., 2015). When compared to 6 hours, *HB-12* was 2-fold downregulated in 24 hours (Fig 5.2B). When compared to 6 hours, leaf polarity genes *PHB, KAN2, ARF4,* and *AS1* were more upregulated. In particular, *WUS related homeobox 1 (WOX1)* was 6.2 fold highly upregulated at 24 hours (Fig 5.2B). *WOX1* promotes margin

formation at the adaxial-abaxial boundary and overexpression of *WOX1* negatively regulate SAM development possibly by polyamine homeostasis or regulating *CLV3* expression (Nakata et al., 2012; Nakata and Okada, 2012; Zhang et al., 2011b). This suggests that IND may negatively regulate leaf growth and SAM development by downregulating *HB-12* and upregulating *WOX1.*

When compared to 6 hours, *TCP5 (TEOSINTE BRANCHED 1, cycloidea and PCF transcription factor 5) was* 2-fold upregulated in 24 hours (Fig 5.2B). A study by Koyama *et al.* showed that TCP3 transcription factors negatively regulate *CUC* by directly activating expression of *AS1* and *miR164* (Koyama et al., 2010). *TCP3, TCP8, TCP11* and *TCP14* were also upregulated in *35S::IND:GR* seedlings in both datasets (DEX vs. DMSO, p<0.05, Fig 5.2C). Data from Chapter 4 suggests that IND directly downregulates *CUC1* gene expression and IND may also downregulate *CUC1* via the TCP pathway (Fig 5.2D). *CUC1/2/3* genes were not differentially expressed in *35S::IND:GR* seedlings at 6 and 24 hours in the microarray datasets (Table 8.5), therefore IND downregulation of *CUC1* may not be an immediate response.
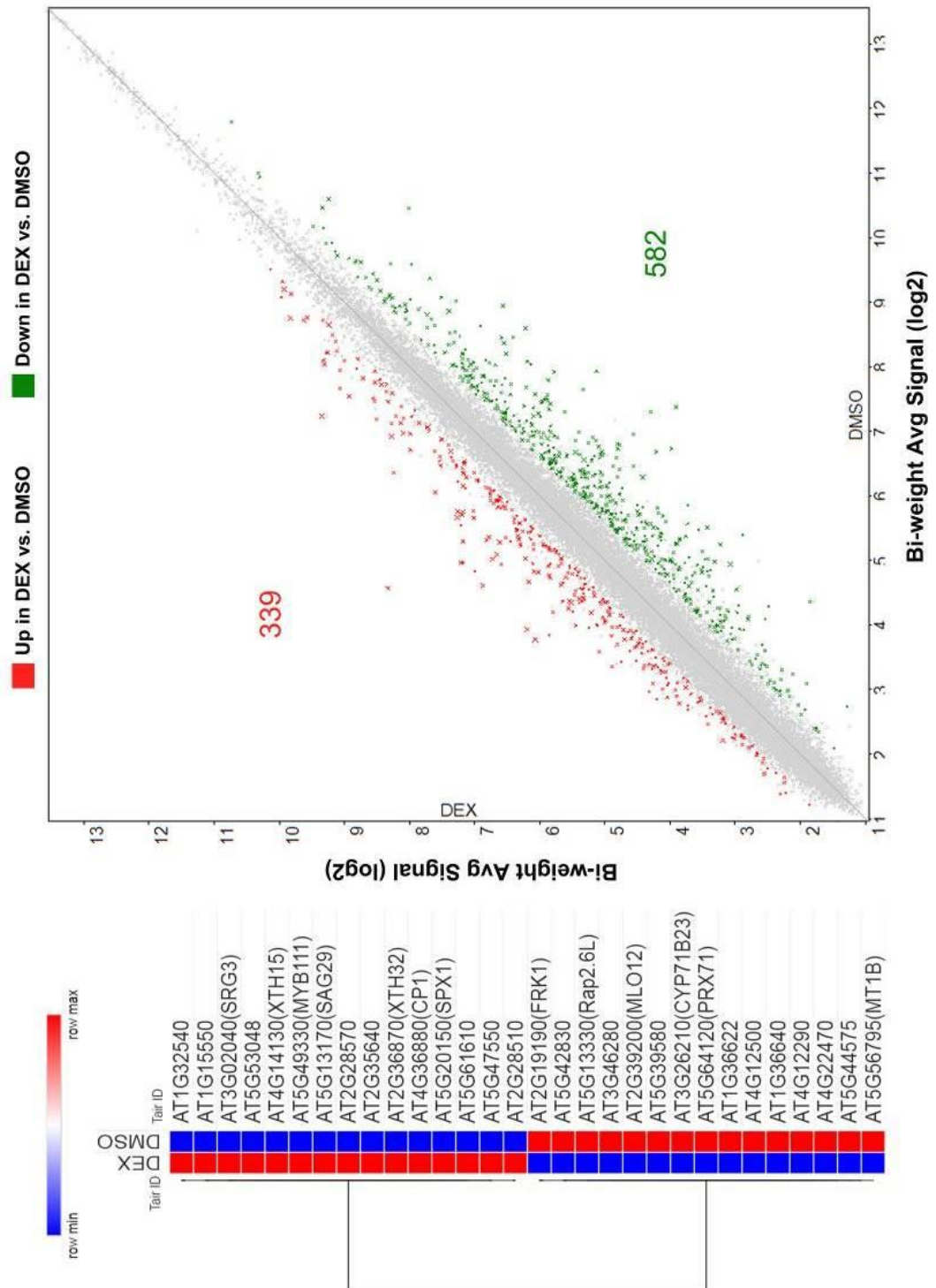
Figure 5.1 *35S::IND:GR* **(DEX vs. DMSO) differential gene expression.** Scatter plot showing Tukey's bi-weight average signal (log2) of 10µM Dexamethasone (DEX) and DMSO treated *35S::IND:GR* samples: 339 genes were upregulated (Red), and 582 genes were downregulated (Green) in DEX vs. DMSO (the smaller p-value, the bigger the X). Heat map of top 30 differentially regulated genes in DEX vs. DMSO (One-Way ANOVA p<0.05, Gene Fold Change (linear) >1.5 or <-1.5). (Blue: low gene expression, Red: high gene expression).
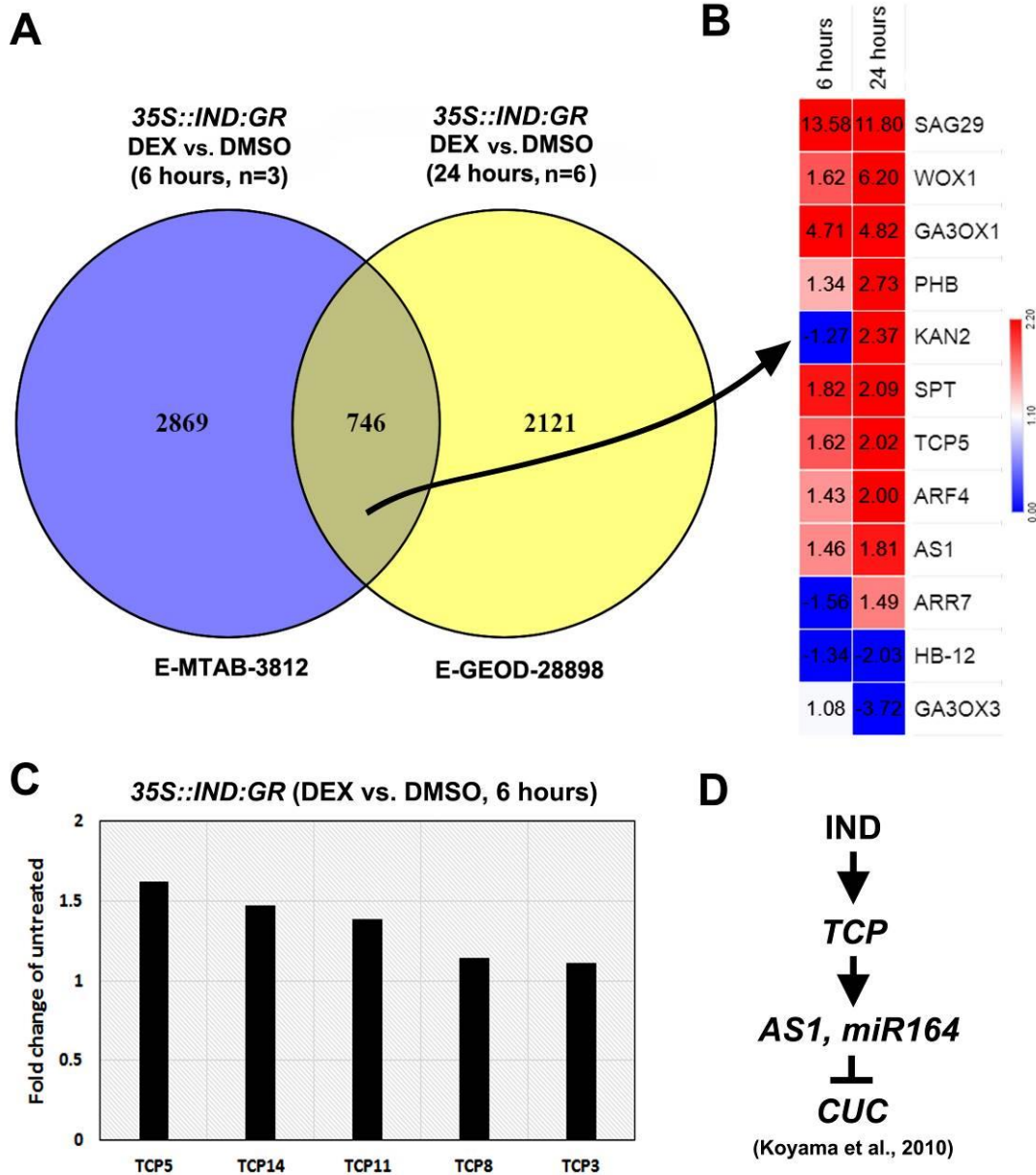
Figure 5.2 Comparative analysis of *35S::IND:GR* microarray data (induced for 6 hours and 24 hours). (A) The overlapping region of the Venn diagram shows 746 genes were expressed in *35S::IND:GR* seedlings (induced for 6 hours, DEX vs. DMSO, FC >1 or <-1, p<0.05) and *35S::IND:GR* seedlings (induced for 24 hours, DEX vs. DMSO, FC >1 or <-1, p<0.05). **(B)** The heatmap shows selected genes from the overlapping gene list, which were differentially expressed following 6 hours of IND induction (DEX vs. DMSO) and 24 hours (DEX vs. DMSO). **(C)** The bar chart shows *TCP3, TCP5, TCP8, TCP11* and *TCP14* gene expression in *35S::IND:GR* seedlings (6 hours induction, DEX vs. DMSO). **(D)** Pathway showing that IND may downregulate *CUC* by upregulating *TCP-AS1.* (Blue: low gene expression, Red: high gene expression)
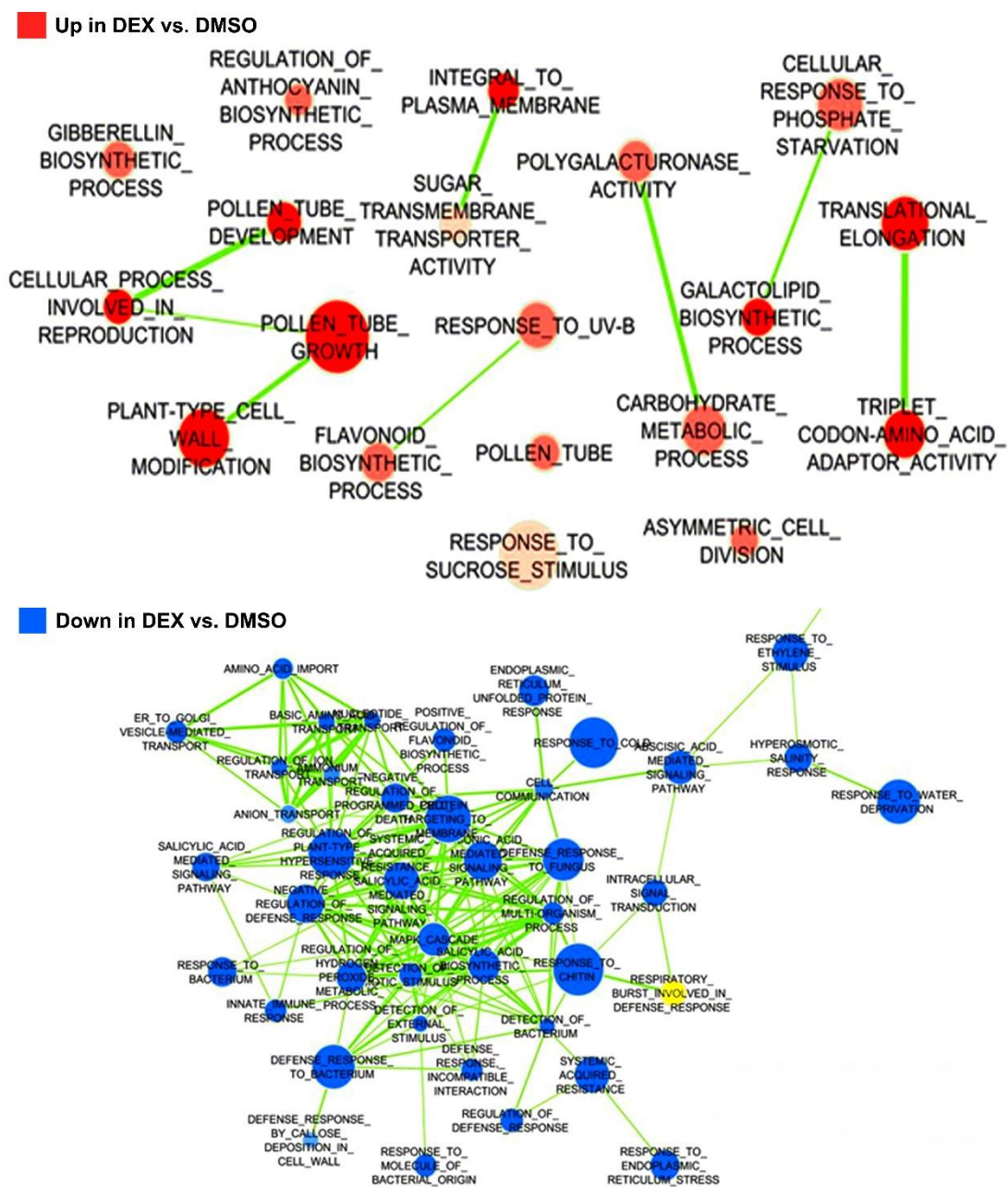
Figure 5.3 *35S::IND:GR* **(DEX vs. DMSO)** *Arabidopsis* **biological process gene-set enrichment analysis (GSEA).** Cytoscape generated GSEA data of *35S::IND:GR* treated with DEX and DMSO showing significantly (p<0.05) enriched gene-sets (Blue - negatively enriched; Red - positively enriched). Closely related gene-sets are connected by a green line. Gene sets for gibberellin biosynthetic process, pollen tube, cell wall modification and asymmetric cell division sets were positively enriched in DEX treated *35S::IND:GR* seedlings. Gene sets for defence response, ethylene, salicylic acid, jasmonic acid, abscisic acid and ion transport signalling sets were negatively enriched in DEX treated *35S::IND:GR* seedlings.

5.2.1.2 Gene-set enrichment analysis (GSEA)

We use GSEA to understand which pathways are regulated by IND overexpression. GSEA is a powerful analytical tool used to study groups of genes or proteins that share common biological function, protein domain, chromosomal location, or regulation in large datasets (Subramanian et al., 2007; Subramanian et al., 2005). For analysis, specific data is required, namely expression datasets, phenotype labels (e.g., control vs. treated), gene sets, and annotations. There are only a few pre-made gene sets in GSEA database, and *Arabidopsis* gene sets are not available in the GSEA database. Yi *et al*. created an *Arabidopsis* GSEA gene set database in 2013, however it is outdated (Yi et al., 2013). We took the initiative to create an *Arabidopsis* gene set GSEA library file based on biological function and protein family in collaboration with Matthew Parker, (UoS, data not shown). We analysed *Arabidopsis* GO annotation files from the Gene Ontology Consortium to create an *Arabidopsis* gene set GSEA library file. *Arabidopsis* Gene 1.0 ST microarray expression data sets (6 hours, DEX vs. DMSO), *Arabidopsis* biological function gene, set GSEA library file, and phenotype label (DEX vs. DMSO) were used for GSEA analysis. Analysed data was exported to Cytoscape for analysis and visualisation (Fig 5.3). When compared to DMSO, 35 gene sets were positively enriched and 147 gene sets were negatively enriched in DEX ($p < 0.05$, Fig 5.3, Table 5.1). Significantly enriched gene sets were summarised in a table (Table 8.10). When compared to DMSO, gene sets for the gibberellin biosynthetic process, pollen tubes, cell wall modification and asymmetric cell division were positively enriched in DEX ($p < 0.05$, Fig 5.3). Consistently, these positively enriched IND biological functions are also reported in different studies (Arnaud et al., 2010; Kay et al., 2013a; Mitsuda and Ohme-Takagi, 2008; Ogawa et al., 2009; Wu et al., 2006). When compared to DMSO, signalling gene sets for defence response, ethylene, salicylic acid, jasmonic acid, abscisic acid and ion transport were negatively enriched in DEX ($p < 0.05$, Fig 5.3). GSEA results suggest that IND may possibly regulate hormone signalling (gibberellin, ethylene, salicylic acid, jasmonic acid and abscisic acid).

5.2.1.3 Induction of IND for 24 hours can affect meristem gene expression

Since overexpression of IND promotes leaf polarity defects (Chapter 3), it is important to understand whether IND regulates any meristem gene sets. GSEA analysis showed that meristem maintenance and meristem initiation gene sets were not significantly

enriched in DEX-treated *35S::IND:GR* seedlings (Fig 5.8A). A total of 29 genes from all meristem gene sets were core enriched in DEX (6 hours) treated *35S::IND:GR* seedlings (p<0.05, Fig 5.8B). *AGO10* was weakly downregulated in DEX (6 hours) treated *35S::IND:GR* seedlings (p<0.05, Fig 5.8C) and this was consistent with qRT-PCR data from Chapter 3. EMBRYONIC FACTOR 1 (FAC1) encodes an AMP deaminase (AMPD) that converts AMP to IMP to maintain the energy potential for the zygote to proceed through development (Xu et al., 2005). FAC1 is essential for further development of the zygote. *FAC1* was weakly downregulated in DEX (6 hours) treated *35S::IND:GR* seedlings (p<0.05, Fig 5.8C). *WALL-ASSOCIATED KINASE 2 (WAK2)* is expressed in shoot apical meristems and in expanding leaves. WAK2 is required for cell expansion (Wagner and Kohorn, 2001), *WAK2* was downregulated in DEX (6 hours) treated *35S::IND:GR* seedlings (p<0.05, Fig 5.8B and C). ARABIDOPSIS THALIANA HOMEOBOX GENE1 (ATH1) interacts with STM and regulates SAM development (Cole et al., 2006; Rutjens et al., 2009). Similar to *CUC* genes, ATH1 is also required for proper development of the basal boundaries of shoot organs (Gomez-Mena and Sablowski, 2008). *ATH1* was downregulated in DEX (6 hours) treated *35S::IND:GR* seedlings (p<0.05, Fig 5.8C). This data suggests that *IND* may negatively regulate SAM development by repressing *FAC1, WAK2, ATH1,* and *AGO10*.

Longer induction of IND may significantly downregulate genes involved in meristem development. To test this, IND-microarray data (induced 6 and 24 hours) was compared with a list of meristem associated genes. Gene expression in the SAM was extensively studied and published by different research groups, and a study from Reddy's lab reported a list of 70 genes that are expressed predominantly in the meristem, characterised by microarray and RNA *in situ* analysis (Yadav et al., 2009). The PID gene was added to the list because *PID* is also expressed in the meristem. These meristem associated genes were compared with DEX (6 hours and 24 hours) (Fig 5.11A and B). The Venn diagram overlapping region shows 6 meristem genes were differentially regulated following 6 hours of IND induction (Fig 5.11A) and 15 meristem genes were differentially regulated by 24 hours of IND induction (Fig 5.11B). When compared to 6 hours of IND induction, 11 meristem genes were differentially regulated by IND following 24 hours of induction.

Here we summarise the expression changes of the 15 genes that were differentially regulated at either 6hrs and/or 24hrs. *ULTRAPETALA1* (*ULT1*) gene controls shoot size and also regulates floral meristem by promoting AGAMOUS (AG) (Engelhorn et al., 2014; Fletcher, 2001). ULT1 also promotes apical polarity by negatively regulating SPT in gynoecium (Pires et al., 2014). *ULT1* and *SPT* were upregulated by IND following both 6 and 24 hours of induction (Fig 5.14E). LATE MERISTEM IDENTITY1/ HOMEOBOX 51 (HB51) is a meristem identity regulator (Saddic et al., 2006), which was upregulated by IND following both 6 and 24 hours of induction (Fig 5.11E). HOMEODOMAIN GLABROUS2 (HDG2) is one of the key regulators of stomatal differentiation (Peterson et al., 2013). *HDG2* was upregulated by IND following 6 hours of induction (Fig 5.11E). *PHB* and *AS1* were both upregulated by IND following 24 hours of induction (Fig 5.2B, Fig 5.11E) (these genes were also discussed in the previous section). CHOLINE KINASES (CK) regulate phospholipid biosynthesis in *Arabidopsis* (Lin et al., 2015; Tasseva et al., 2004): *CK3* was downregulated by IND following both 6 and 24 hours of induction (Fig 5.11E). Lipid transport gene *AT3G53980* was downregulated by IND following 24 hours of induction (Fig 5.11E). Sucrose transporter gene *SWEET10* was also downregulated by IND following 24 hours of induction (Fig 5.11E). TERMINAL FLOWER1 (TFL1) is a key regulator of the development of the inflorescence meristem (Liljegren et al., 1999), *TFL1* was downregulated by IND following 24 hours of induction (Fig 5.11E). GIBBERELLIN 3-OXIDASE 3 (GA3ox3) is one of the key oxidase enzymes in the biosynthesis of gibberellin (Hu et al., 2008). *GA3ox3* was downregulated by IND following 24 hours of induction (Fig 5.11E). PID kinase regulates proper auxin distribution via PIN proteins (Friml et al., 2004). *PID* was downregulated by IND following both 6 and 24 hours (Fig 5.11E) and this result is consistent with previously published work (Sorefan et al., 2009a). AINTEGUMENTA-like 5 (AIL5) and (AIL7) proteins control phyllotaxis, and they are required to maintain PIN1 expression at the periphery of the meristem (Pinon et al., 2013; Prasad et al., 2011), *AIL5* and *AIL7* were downregulated by IND following 24 hours of induction (Fig 5.11E). G-BOX BINDING FACTOR 6 (GBF6) transcription factor recruits the histone acetylation machinery to activate auxin-induced transcription (Weiste and Droge-Laser, 2014), *GBF6* was downregulated by IND following 24 hours of induction (Fig 5.11E). *DWARF IN LIGHT 1* (*DFL1*) belongs to the auxin-inducible gene family. DFL1 regulates hypocotyl elongation (Nakazawa et al., 2001), *DFL1* was downregulated by IND following 24 hours of induction (Fig 5.11E). These results suggest that longer induction of IND may inhibit PAT and auxin

signalling by repressing *PID, AIL5, AIL7,* and *GBF6*. These represent genes that are either regulated by IND over a long time period or are genes that function indirectly after IND induction and have functions later in meristem development.

5.2.1.4 IND regulates genes involved in hormone biosynthesis

Results from GSEA analysis show that IND may regulate hormone signalling (gibberellin, ethylene, salicylic acid, jasmonic acid and abscisic acid). Since IND regulates gibberellin biosynthesis via GA3ox1, IND may also regulate other genes involved in hormone biosynthesis. To test this, gene expression of genes involved in hormone biosynthesis were examined in *35S::IND:GR* seedlings following 6 hours of induction, DEX vs. DMSO, $p < 0.05$, Fig 5.4).

Gibberellin biosynthesis: GA3ox1 is involved in the production of bioactive gibberellin (GA) (Talon et al., 1990). *GA3ox1* was upregulated in *35S::IND:GR* seedlings (DEX vs. DMSO, $p < 0.05$, Fig 5.4).

Auxin biosynthesis: L-TRYPTOPHAN-PYRUVATE AMINOTRANSFERASE 1 (TAA1) is involved in auxin (IAA) biosynthesis. TAA1 can convert L-tryptophan and pyruvate to indole-3-pyruvic acid (IPA) and alanine (Stepanova et al., 2008; Tao et al., 2008). Indole-3-pyruvate monooxygenase YUCCA2 (YUC2) converts the IPA produced by the TAA1 to indole-3-acetic acid (IAA) (Zhao et al., 2001). *TAA1, YUC2, YUC3,* and *YUC5* were upregulated in *35S::IND:GR* seedlings (DEX vs. DMSO, $p < 0.05$, Fig 5.4).

Cytokinin biosynthesis: Adenosine phosphate-isopentenyl transferase (IPT) proteins regulate cytokinin biosynthesis. Loss of *IPT3* abolishes cytokinin production (Galichet et al., 2008). *IPT3* was downregulated in *35S::IND:GR* seedlings (DEX vs. DMSO, $p < 0.05$, Fig 5.4).

Tair ID	DEX Bi-weight Avg Signal (log2)	DMSO Bi-weight Avg Signal (log2)	Fold Change (linear) (DEX vs. DMSO)	ANOVA p-value (DEX vs. DMSO)	Gene Symbol	Hormones
AT3G19820	7	7.3	-1.23	0.03395	DWF1	Brassinolide
AT3G63110	4.67	5.6	-1.9	0.008277	IPT3	Cytokinin
AT1G75450	4.44	3.88	1.47	0.016862	CKX5	
AT5G21482	6.07	5.7	1.3	0.019991	CKX7	
AT2G28305	5.4	5.73	-1.26	0.046469	LOG1	
AT3G14440	3.73	3.21	1.43	0.000877	NCED3	Abscisic acid
AT3G43600	6.92	7.08	-1.12	0.011598	AAO2	
AT2G27150	5.49	6.28	-1.73	0.01418	AAO3	
AT4G16760	8.26	8.43	-1.12	0.002141	ACX1	Jasmonic acid
AT5G20900	7.71	7.27	1.36	0.003656	JAZ12	
AT1G72450	6.59	7.3	-1.64	0.005884	JAZ6	
AT2G06050	5.65	5.39	1.19	0.006091	OPR3	
AT1G20510	6.29	6.51	-1.16	0.006287	OPCL1	
AT3G06860	7.76	8.09	-1.26	0.007614	MFP2	
AT1G76680	3.33	4.43	-2.14	0.043072	OPR1	
AT1G15550	7.21	4.97	4.71	0.000419	GA3OX1	Gibberellin
AT4G02780	2.93	2.42	1.42	0.001571	GA1	
AT1G30040	3.68	4.07	-1.31	0.037584	GA2OX2	
AT4G21690	3.79	3.68	1.08	0.04749	GA3OX3	
AT1G18870	3.76	3.04	1.66	0.000208	ICS2	Salicylic acid
AT4G26200	5.45	6.67	-2.33	0.000067	ACS7	Ethylene
AT2G22810	5	4.03	1.97	0.003354	ACS4	
AT4G11280	4.42	5.3	-1.85	0.01191	ACS6	
AT5G65800	3.13	2.73	1.32	0.025771	ACS5	
AT5G36880	8.81	8.98	-1.13	0.040947	ACS	
AT3G61510	3.28	2.91	1.3	0.043338	ACS1	
AT4G24670	4.13	4.67	-1.45	0.001648	TAR2	Auxin
AT1G70560	5.82	5.32	1.41	0.001914	TAA1	
AT4G13260	4.49	3.71	1.71	0.003359	YUC2	
AT5G43890	5.57	4.81	1.7	0.014994	YUC5	
AT1G04610	4.47	3.99	1.4	0.050694	YUC3	
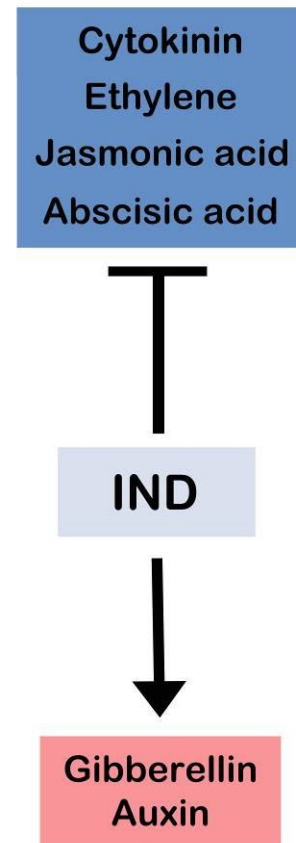
Figure 5.4 IND regulates hormone biosynthesis genes. (A) Table showing a list of differentially expressed genes for hormone biosynthesis in 10 µM Dexamethasone (DEX) and DMSO treated *35S::IND:GR* seedlings. Pathway showing IND may positively regulate gibberellin (*GA3OX1*) and auxin (*TAA1, YUC2, YUC3* and *YUC5*) biosynthesis and may negatively regulate cytokinin (*IPT3* and *CKX5*), ethylene (*ACS6* and *ACS7*), jasmonic acid (*ACX1, JAZ6, OPCL1, MFP2* and *OPR1*) and abscisic acid (*AAO2* and *AAO3*) biosynthesis.

Ethylene biosynthesis: 1-aminocyclopropane-1-carboxylate synthase (ACS) enzymes play a major role in ethylene biosynthesis. ACS catalyse the conversion of S-adenosyl-L-methionine into 1-AMINOCYCLOPROPANE-1-CARBOXYLATE (ACC), a direct precursor of ethylene (Adams and Yang, 1979; Peng et al., 2005; Yang and Hoffman, 1984). *ACS6* and *ACS7* were downregulated in *35S::IND:GR* seedlings (DEX vs. DMSO, $p < 0.05$, Fig 5.4).

Jasmonic acid biosynthesis: PEROXISOMAL ACYL-COENZYME AN OXIDASE 1 (ACX1) is involved in the biosynthesis of jasmonic acid (JA) (Cruz Castillo et al., 2004). 12-OXOPHYTODIENOATE REDUCTASE 1 (OPR1) reduces 12-oxophyodienoic acid (OPDA) to 3-oxo-2-(2'-pentenyl)-cyclopentane-1-octanoic acid (OPC-8:0), the natural precursor of jasmonic acid. OPC-8:0 CoA LIGASE1 (OPCL1) converts OPC-8:0 into OPC-8:0-CoA, respectively (Kienow et al., 2008). OPC-8:0-CoA undergoes three rounds of oxidation to form (+)-7-iso-JA, jasmonic acid (Schaller and Stintzi, 2009). *ACX1, OPCL1,* and *OPR1* were downregulated in *35S::IND:GR* seedlings (DEX vs. DMSO, $p < 0.05$, Fig 5.4).

Abscisic acid biosynthesis: ABSCISIC-ALDEHYDE OXIDASE (AAO) is involved in the last step of the abscisic acid (ABA) biosynthesis. ABA precursor abscisic aldehyde is oxidised to ABA, via AAO (Seo et al., 2000). *AAO2* and *AAO3* were downregulated in *35S::IND:GR* seedlings (DEX vs. DMSO, $p < 0.05$, Fig 5.4).

These results demonstrate that IND may promote auxin and gibberellin biosynthesis and may inhibit cytokinin, ethylene, jasmonic acid and abscisic acid biosynthesis (Fig 5.4).

128
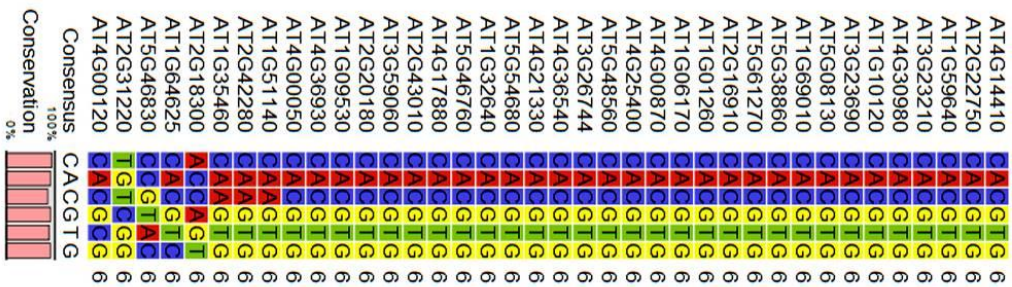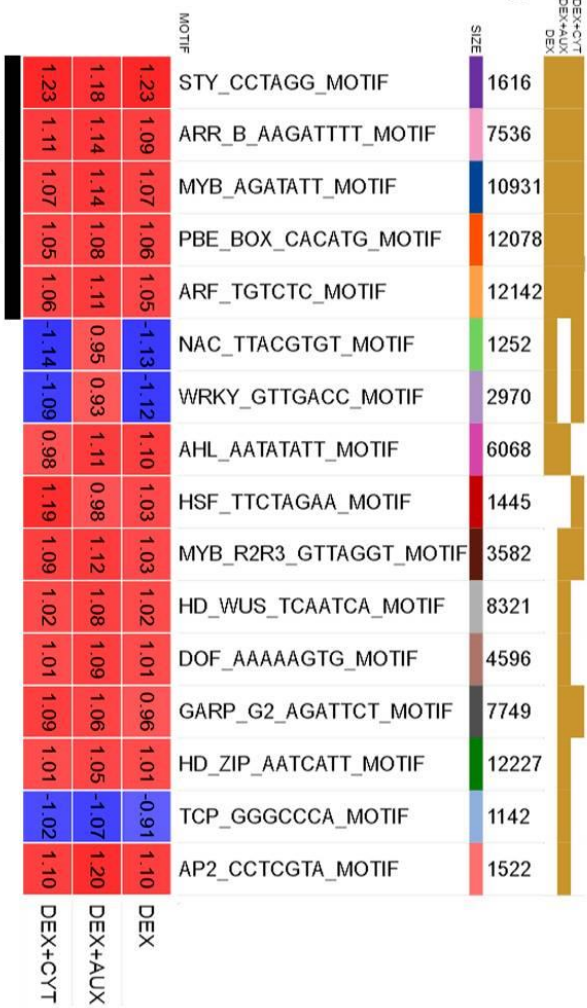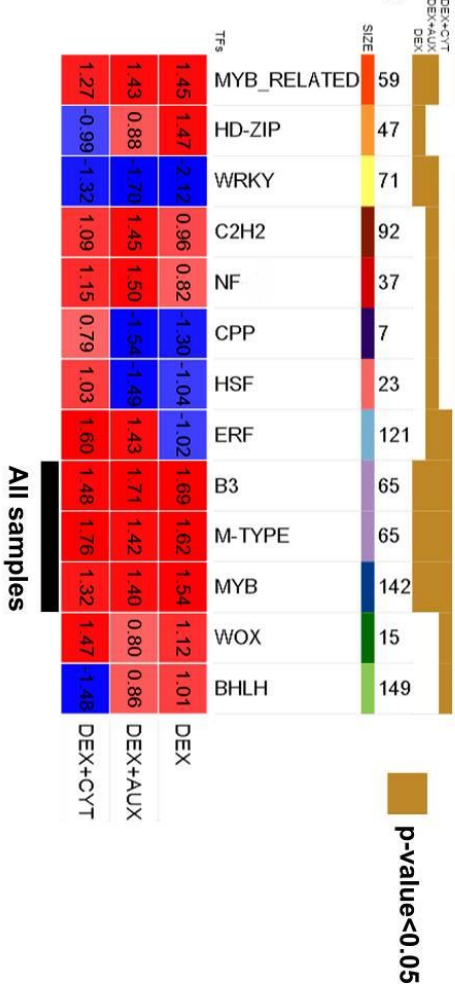
Figure 5.5 *Arabidopsis thaliana* transcription factor (TF) family and DNA motif GSEA. (A) Many of the bHLH family proteins bind to G-box (CACGTG). AT4G00120 (IND) binds to E-box variant (CACGCG). Heat map of GSEA data showing significantly ($p<0.05$) enriched **(B)** Motif and **(C)** TF gene sets that were regulated by IND (DEX vs. DMSO), IND plus IAA (DEX+AUX vs. AUX) and IND plus BAP (DEX+CYT vs. CYT). **(B)** STY, ARR-B, MYB, PBE-BOX and ARF motif gene sets were positively enriched in all conditions ($p<0.05$). AHL Motif gene set was positively enriched in IND (DEX vs. DMSO) and IND plus IAA (DEX+AUX vs. AUX). HD-WUS, DOF, HD-ZIP and AP2 motif gene sets were positively enriched, and the TCP motif gene set was negatively enriched in IND plus IAA (DEX+AUX vs. AUX) ($p<0.05$). NAC and WRKY motif gene sets were negatively enriched in IND (DEX vs. DMSO) and IND plus BAP (DEX+CYT vs. CYT) ($p<0.05$). MYB-R2R3 and GARP-G2 motif gene sets were positively enriched in IND plus IAA (DEX+AUX vs. AUX) and IND plus BAP (DEX+CYT vs. CYT) ($p<0.05$). HSF motif gene set was positively enriched in IND plus BAP (DEX+CYT vs. CYT) ($p<0.05$). **(C)** B3, MYB, and M-TYPE TF gene sets were positively enriched in all conditions ($p<0.05$). HD-ZIP gene set was positively enriched in IND (DEX vs. DMSO) ($p<0.05$). MYB-related TF gene set was positively enriched, and WRKY was negatively enriched in IND (DEX vs. DMSO) and IND plus IAA (DEX+AUX vs. AUX) ($p<0.05$). C2H2 and NFX1 TF gene sets were positively enriched, and CPP and HSF were negatively enriched in IND plus IAA (DEX+AUX vs. AUX) ($p<0.05$). ERF gene set was positively enriched in IND plus IAA (DEX+AUX vs. AUX) and IND plus BAP (DEX+CYT vs. CYT) ($p<0.05$). WOX gene set was positively enriched, and bHLH gene set was negatively enriched in IND plus BAP (DEX+CYT vs. CYT) ($p<0.05$). (Size: Number of genes in each gene set, Blue: negatively enriched, Red: positively enriched and Brown: $p<0.05$).

5.2.1.5 Motif and TF enrichment analysis

It is important to understand if IND regulated genes are enriched in known TF binding motifs and whether IND regulates the corresponding TFs. This was tested using GSEA. Often motifs indicate sequence-specific binding sites for transcription factors. The motifs represent known or likely *cis*-regulatory elements in the 2000bp upstream promoter region (Yu et al., 2016). *Cis*-acting enhancers have key roles in controlling gene transcription (Arnone and Davidson, 1997). Motif enrichment analysis was used to study which DNA-binding transcription factors control the transcription of a set of genes by detecting enrichment of known binding motifs in the gene promoter regions. Motif enrichment analysis was performed using the GSEA tool (Subramanian et al., 2005; Weidner, 2017; Yi et al., 2013). For enrichment analysis, *Arabidopsis* transcriptional regulatory motifs were extracted from a plant cistrome and protein-binding microarray database (Franco-Zorrilla et al., 2014; O'Malley et al., 2016). *Arabidopsis* Motif Scanner and TAIR Patmatch were used to identify the positions of cis-regulatory elements in the *Arabidopsis* genome (Mele, 2016; Yan et al., 2005). Gene sets were created using data curated from *Arabidopsis* Motif Scanner and TAIR Patmatch. Motif gene sets consist of genes grouped by cis-regulatory motifs that they share in their promoter regions. *Arabidopsis* transcription factor family gene sets were created using a plant transcription factor database (Fig 8.4) (Hong, 2016; Jin et al., 2017; Riechmann et al., 2000). Using this we can link changes in putative gene expression to putative *cis*-regulatory elements and transcription factors (Birnbaum et al., 2001). Different data files were used for motif and transcription factor enrichment analysis: *Arabidopsis* Gene 1.0 ST microarray expression data set (DEX vs. DMSO), *Arabidopsis* motif gene set or transcription factor family gene set GSEA library file and phenotype label (DEX vs. DMSO). After analysis, data were presented in a heat map (Fig 5.5B and C).

IND is a bHLH transcription factor so we investigated whether the bHLH *cis*-element was enriched in DEX vs. DMSO. The bHLH family proteins preferably bind to E-box DNA motif CANNTG (N = any nucleotide) and CACGTG (E-box type) G-box motif (Toledo-Ortiz et al., 2003). Toledo *et al*. identified 147 bHLH protein-encoding genes. Several studies have characterised the binding elements for a few of the bHLH family proteins (Franco-Zorrilla et al., 2014; Girin et al., 2011; Heim et al., 2003; Jin et al., 2017; O'Malley et al., 2016). These elements were aligned and presented in Fig 5.5A. *Arabidopsis* bHLH family protein

binding element alignment shows that CACGTG (G-box motif) was a consensus sequence (Fig 5.5A). The E-box variant PBE-BOX (CACATG) motif gene set was positively enriched in DEX vs. DMSO ($p < 0.05$, Fig 5.5B). This suggests that IND may target genes encoding the PBE-BOX. However, only a small enrichment of the PBE element was observed, but this may be because the element was very common (12,078 genes).

Several TF elements were positively enriched in the DEX vs. DMSO. The ARFs are B3 superfamily transcription factors. Auxin-responsive elements (AuxREs) (TGTCNN) and ARF (TGTCTC) motifs are associated with auxin response and mediate auxin responsive upregulation (Boer et al., 2014; Ulmasov et al., 1999; Ulmasov et al., 1995). The ARF (TGTCTC) motif gene set was positively enriched in DEX vs. DMSO ($p < 0.05$, Fig 5.5B). The STYLISH (STY, CCTAGG) motif is associated with IAA biosynthesis rates and IAA levels (Eklund et al., 2010). The STY (CCTAGG) motif gene set was positively enriched in DEX vs. DMSO ($p < 0.05$, Fig 5.5B). AT-hook Motif Nuclear Localized (AHL) proteins recognise A/T-rich motifs (AATATATT) and contribute to downregulation of target genes (Fujimoto et al., 2004). The AHL (AATATATT) motif gene set was positively enriched in DEX vs. DMSO ($p < 0.05$, Fig 5.5B). MYB is one of the largest transcription factor superfamilies in *Arabidopsis*. MYB-related transcription factors bind to the motif sequence AGATATT (Franco-Zorrilla et al., 2014). The MYB (AGATATT) motif gene set was positively enriched in DEX vs. DMSO ($p < 0.05$, Fig 5.5B). MYB GARP type-B ARRs are primary transcription factors involved in cytokinin signalling. Type-B ARRs recognise the motif containing the sequence core element AGAT (Argyros et al., 2008; Hosoda et al., 2002; Sheen, 2002). The ARR-B (AAGATTTT) motif gene set was positively enriched in DEX vs. DMSO ($p < 0.05$, Fig 5.5B).

Several TF elements were negatively enriched in the DEX vs. DMSO. NAC (NAM (no apical meristem), ATAF and CUC (cup-shaped cotyledon)) family transcription factors are involved in regulating several developmental or stress-related responses. NAC transcription factors recognise a motif containing the sequence core element CGT[G/A] (Olsen et al., 2005; Puranik et al., 2012; Tran et al., 2004). The NAC (TTACGTGT) motif gene set was negatively enriched in DEX vs. DMSO ($p < 0.05$, Fig 5.5B). WRKY family transcription factors regulate developmental processes and plant responses to abiotic and biotic stresses. WRKY transcription factors recognise the W-box (TTGAC[C/T])

(Ciolkowski et al., 2008; Eulgem et al., 2000). The WRKY motif gene set was negatively enriched in DEX vs. DMSO (p<0.05, Fig 5.5B).

Since we found several TF elements were enriched in DEX vs. DMSO, we analysed whether the expression of TF gene families were also enriched. M-TYPE (MADS-box) and Homeodomain-leucine zipper (HD-ZIP) transcription factors are the key regulators of developmental processes, such as meristem identity (Alvarez-Buylla et al., 2000; Ariel et al., 2007; Parenicova et al., 2003). R1R2R3-MYB are collectively referred to as MYB-related proteins (Chen et al., 2006). B3, MYB, MYB-related, HD-ZIP and M-TYPE transcription factor family gene sets were positively enriched in DEX vs. DMSO (p<0.05, Fig 5.5C). The WKRY transcription factor family gene set was negatively enriched in DEX vs. DMSO (p<0.05, Fig 5.5C).

Since B3, MYB, and WKRY transcription factor family gene sets and their motif gene sets were enriched in DEX-treated *35S::IND:GR* seedlings, IND may regulate B3, MYB and WKRY transcription factor family genes and their targeted gene expression.

5.2.1.6 Summary

In summary, these results suggest that IND may promote leaf mid and abaxial fate by upregulating *WOX1*. Since *CUC* genes were not differentially regulated after 6 or 24 hours of IND induction, IND may gradually downregulate *CUC* by upregulating *TCP-AS1*. GSEA analysis suggests IND may promote gibberellin and auxin biosynthesis and may inhibit ethylene, jasmonic acid and abscisic acid biosynthesis and signalling. Longer IND expression may negatively regulate SAM development and PAT by repressing *FAC1, WAK2, ATH1, AGO10*, *PID, AIL5, AIL7* and *GBF6*. IND may regulate these functions by upregulating B3, MYB, HD-ZIP, M-TYPE and downregulating WKRY transcription factor family genes.

Table 5.1 Summary of GSEA analysis: Biological process in *Arabidopsis*

DEX and DMSO treated *35S::IND:GR* seedlings (DEX vs. DMSO)	
326 / 835 gene sets were upregulated in phenotype **DEX**, 18 gene sets were significant at FDR < 25%, 18 gene sets were significantly enriched at nominal p-value < 1% and **35** gene sets were significantly enriched at nominal **p-value < 5%**	**509 / 835** gene sets were downregulated in phenotype **DEX**, 154 gene sets were significantly enriched at FDR < 25%, 109 gene sets were significantly enriched at nominal p-value < 1% and **147** gene sets were significantly enriched at nominal **p-value < 5%**
DEX plus IAA and IAA treated *35S::IND:GR* seedlings (DEX+AUX vs. AUX)	
245 / 835 gene sets were upregulated in phenotype **DEX+AUX**, 103 gene sets were significant at FDR < 25%, 54 gene sets were significantly enriched at nominal p-value < 1% and **83** gene sets were significantly enriched at nominal **p-value < 5%**	**590 / 835** gene sets were downregulated in phenotype **DEX+AUX**, 408 gene sets were significantly enriched at FDR < 25%, 225 gene sets were significantly enriched at nominal p-value < 1% and **309** gene sets were significantly enriched at nominal **p-value < 5%**
DEX plus BAP and BAP treated *35S::IND:GR* seedlings (DEX+CYT vs. CYT)	
239 / 835 gene sets were upregulated in phenotype **DEX+CYT**, 78 gene sets were significant at FDR < 25%, 49 gene sets were significantly enriched at nominal p-value < 1% and **72** gene sets were significantly enriched at nominal **p-value < 5%**	**596 / 835** gene sets were downregulated in phenotype **DEX+CYT**, 270 gene sets were significantly enriched at FDR < 25%, 161 gene sets were significantly enriched at nominal p-value < 1% and **227** gene sets were significantly enriched at nominal **p-value < 5%**
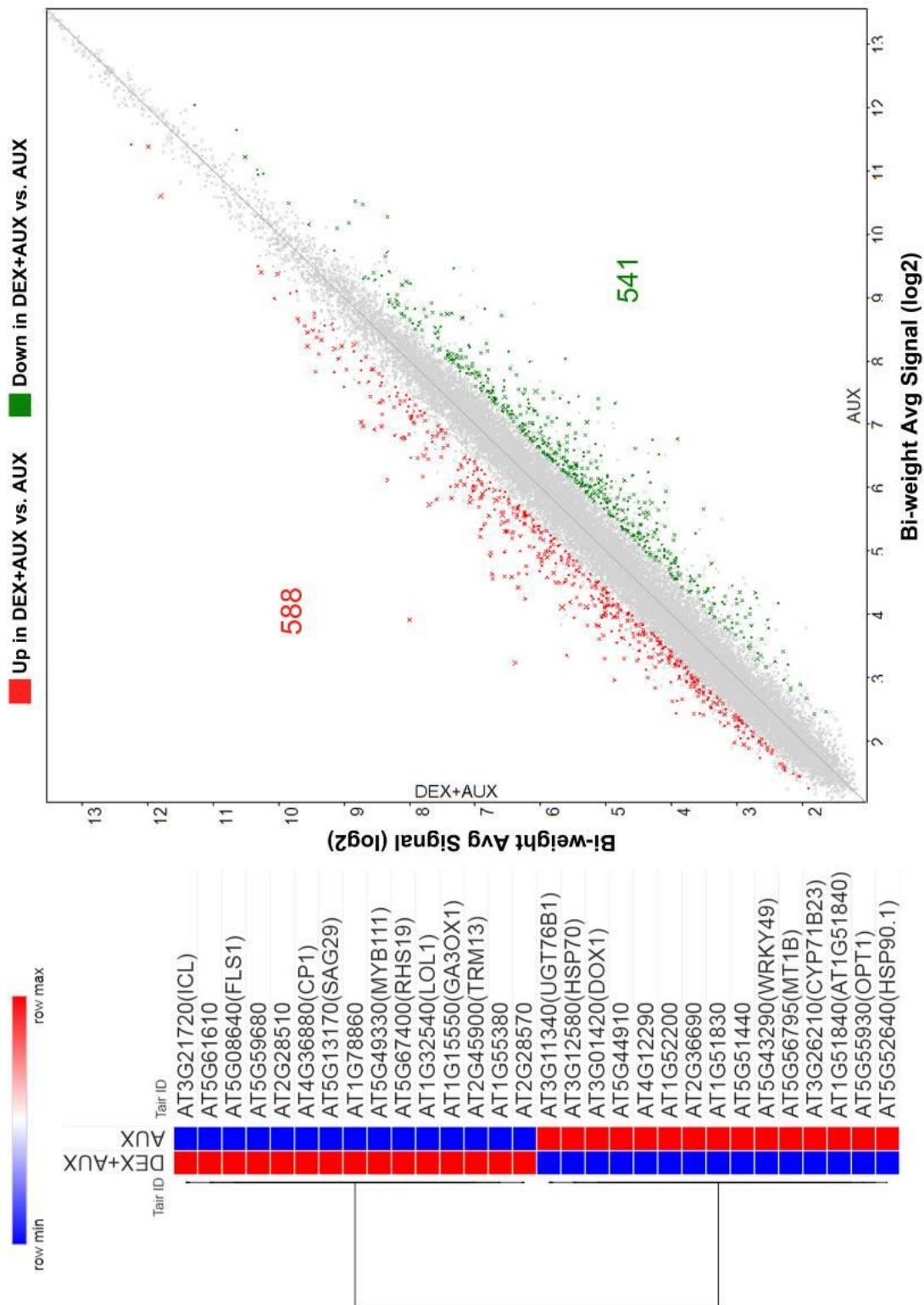
Figure 5.6 _35S::IND:GR_ (DEX+AUX vs. AUX) differential gene expression. Scatter plot showing Tukey's Bi-weight average signal (log2) of 10 µM DEX plus 10 µM IAA (DEX+AUX) and 10 µM IAA (AUX) treated _35S::IND:GR_ samples: 588 genes were upregulated (Red), and 541 genes were downregulated (Green) in DEX+AUX vs. AUX (the smaller p-value, the bigger the X). Heat map of top 30 differentially regulated genes in DEX+AUX vs. AUX (One-Way ANOVA p<0.05, Gene Fold Change (linear) >1.5 and <-1.5). (Blue: low gene expression, Red: high gene expression).

5.2.2 Microarray analysis of IND plus auxin regulated genes

5.2.2.1 Differential gene expression analysis

Since auxin regulates IND and ETT protein interaction (Simonini et al., 2016), it is important to understand whether auxin can influence IND-regulated gene expression. Therefore we investigated the effect of IND plus auxin on global gene expression changes using microarray analysis. For the microarray, total RNA was isolated from *35S::IND:GR* seedlings (7DAG), which were treated with either 10 µM DEX plus 10 µM IAA or 10 µM IAA for 6 hours in liquid media (n=3). The microarray was performed and analysed as described in section 5.2.1.1. A total of 1129 genes were differentially expressed in *35S::IND:GR* seedlings (DEX+AUX vs. AUX, FC >1.5 or <-1.5, p<0.05): 588 genes were upregulated, and 541 genes were downregulated (Fig 5.6). The heat map shows top 30 differentially expressed genes in *35S::IND:GR* seedlings (DEX+AUX vs. AUX) (Fig 5.6). *SAG29* and *GA3ox1* were also upregulated in *35S::IND:GR* seedlings (DEX+AUX vs. AUX, p<0.05, Fig 5.6). When compared to IND (921 genes, Fig 5.1), a large number of genes were upregulated by IND plus IAA alone (1129 genes, Fig 5.6). This shows that IAA treatment enhanced IND-associated gene expression. A list of differentially expressed genes was summarised in a table (Table 8.8).

5.2.2.2 Gene-set enrichment analysis (GSEA)

It is important to understand the biological function of IND + IAA regulated genes, and this was studied using GSEA. *Arabidopsis* Gene 1.0 ST microarray expression datasets (DEX+AUX vs. AUX), *Arabidopsis* biological function gene, set GSEA library file and phenotype label (DEX+AUX vs. AUX) were used for GSEA analysis. Analysed data was exported to Cytoscape for analysis and visualisation (Fig 5.7). When compared to IAA, 83 gene sets were positively enriched (p<0.05) and 309 gene sets were negatively enriched in DEX plus IAA (p<0.05; Fig 5.7, Table 5.1). When compared to IND (Section 5.2.1.2), a large number of gene sets were enriched in IND plus IAA (Table 5.1). Significantly enriched gene sets were summarised in a table (Table 8.11).
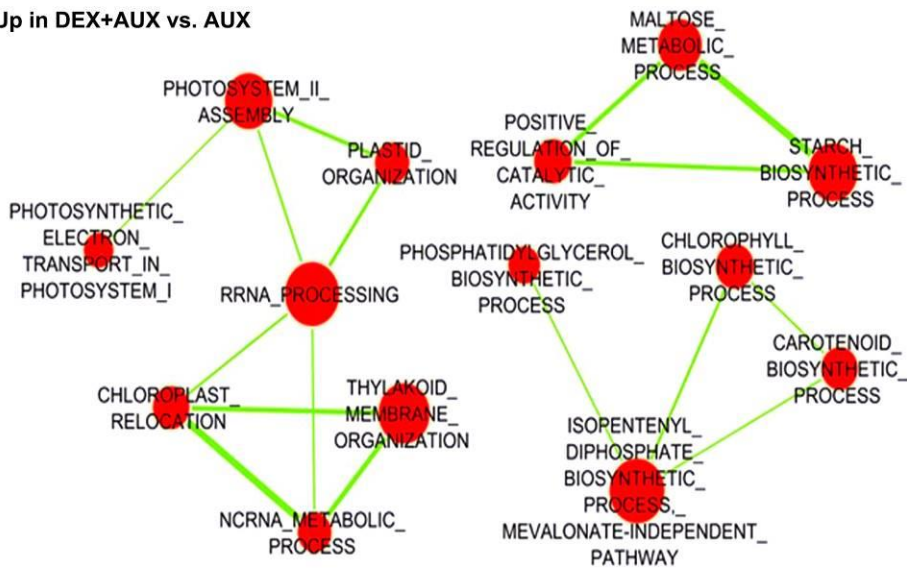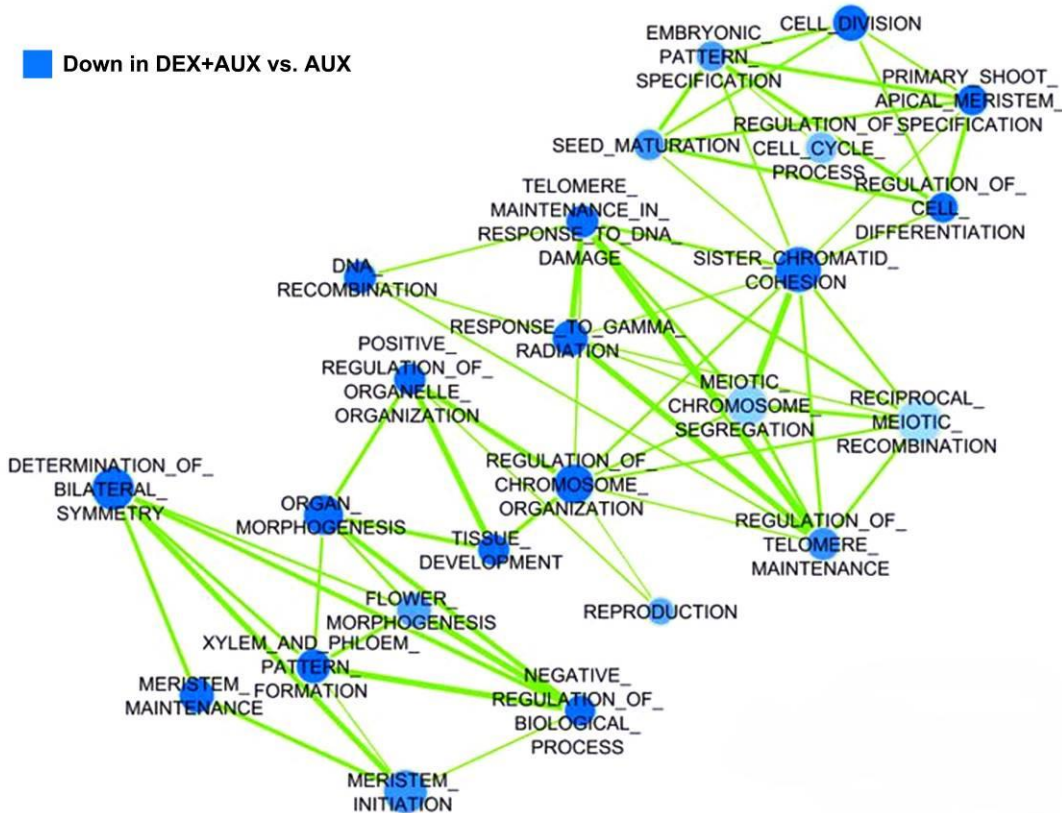
Figure 5.7 *35S::IND:GR* **(DEX+AUX vs. AUX)** *Arabidopsis* **biological process GSEA.** Cytoscape generated image of GSEA data from *35S::IND:GR* seedlings treated with both 10 µM DEX + 10 µM IAA (DEX+AUX) and 10 µM IAA (AUX) alone, showing significantly (p<0.05) enriched gene-sets (Blue: low, Red: high). Closely related gene-sets were connected by a green line. Photosynthetic, rRNA processing, and starch biosynthetic process sets were positively enriched in DEX+AUX treated *35S::IND:GR* seedlings. Meristem, bilateral symmetry, organ morphogenesis, telomere maintenance and cell division sets were negatively enriched in DEX+AUX treated *35S::IND:GR* seedlings.

Several gene sets were positively or negatively enriched in the IND plus IAA (DEX+AUX vs. AUX). Photosynthetic, rRNA processing, and starch biosynthetic process gene sets were positively enriched in DEX plus IAA (p<0.05, Fig 5.7). Meristem, bilateral symmetry, organ morphogenesis, telomere maintenance and cell division gene sets were negatively enriched in DEX plus IAA (p<0.05, Fig 5.7). GSEA results suggest that IND plus auxin may negatively regulate meristem and organ development processes.

5.2.2.3 IND plus auxin negatively regulate meristem associated gene sets

GSEA analysis from section 5.2.2.2 suggests that IND plus auxin negatively regulate meristem gene sets. In particular, meristem maintenance and meristem initiation gene sets were negatively enriched in DEX plus IAA treated *35S::IND:GR* seedlings (p<0.05; Fig 5.8A). A total of 66 genes from all meristem gene sets were core enriched in DEX plus IAA treated *35S::IND:GR* seedlings (p<0.05; Fig 5.8B). APETALA2 (AP2) regulates the stem cell niche in the SAM and is also essential for flower development (Kunst et al., 1989; Wurschum et al., 2006). Interestingly, AP2 prevents replum and valve margin overgrowth by negatively regulating *SHP, IND, BP* and *RPL* (Ripoll et al., 2011). *AP2* was downregulated in DEX plus IAA treated *35S::IND:GR* seedlings (p<0.05; Fig 5.8C). MONOPTEROS (MP) is an auxin response factor that orientates PIN1 localisation and also regulates apical patterning partially through the control of CUC gene expression (Aida et al., 2002; Bhatia et al., 2016). *MP* was downregulated in DEX plus IAA treated *35S::IND:GR* seedlings (p<0.05; Fig 5.8C). TORNADO2 (TRN2) regulate cell proliferation in SAM, control leaf patterning and promote megasporogenesis (Chiu et al., 2007; Cnops et al., 2006; Lieber et al., 2011). *TRN2* was downregulated in DEX plus IAA treated *35S::IND:GR* seedlings (p<0.05; Fig 5.8C). Similar to DEX treated *35S::IND:GR* seedlings, *FAC1* and *ATH1* were also downregulated in DEX plus IAA treated *35S::IND:GR* seedlings (p<0.05; Fig 5.8B and C). When compared to DEX treated *35S::IND:GR* seedlings, a higher number of meristem genes and gene sets were downregulated in DEX plus IAA treated *35S::IND:GR* seedlings (Fig 5.8). These data suggest that IAA may regulate IND activity to control meristem associated gene expression.

A

GO Biological Process Gene Set	Size	DEX Vs DMSO		AUX+DEX Vs AUX		CYT+DEX Vs CYT	
		NES	NOM p-val	NES	NOM p-val	NES	NOM p-val
MERISTEM MAINTENANCE	67	-1.13	0.235	-2.09	0.000	-1.75	0.000
MERISTEM INITIATION	123	-0.64	1.000	-1.40	0.017	-1.49	0.007
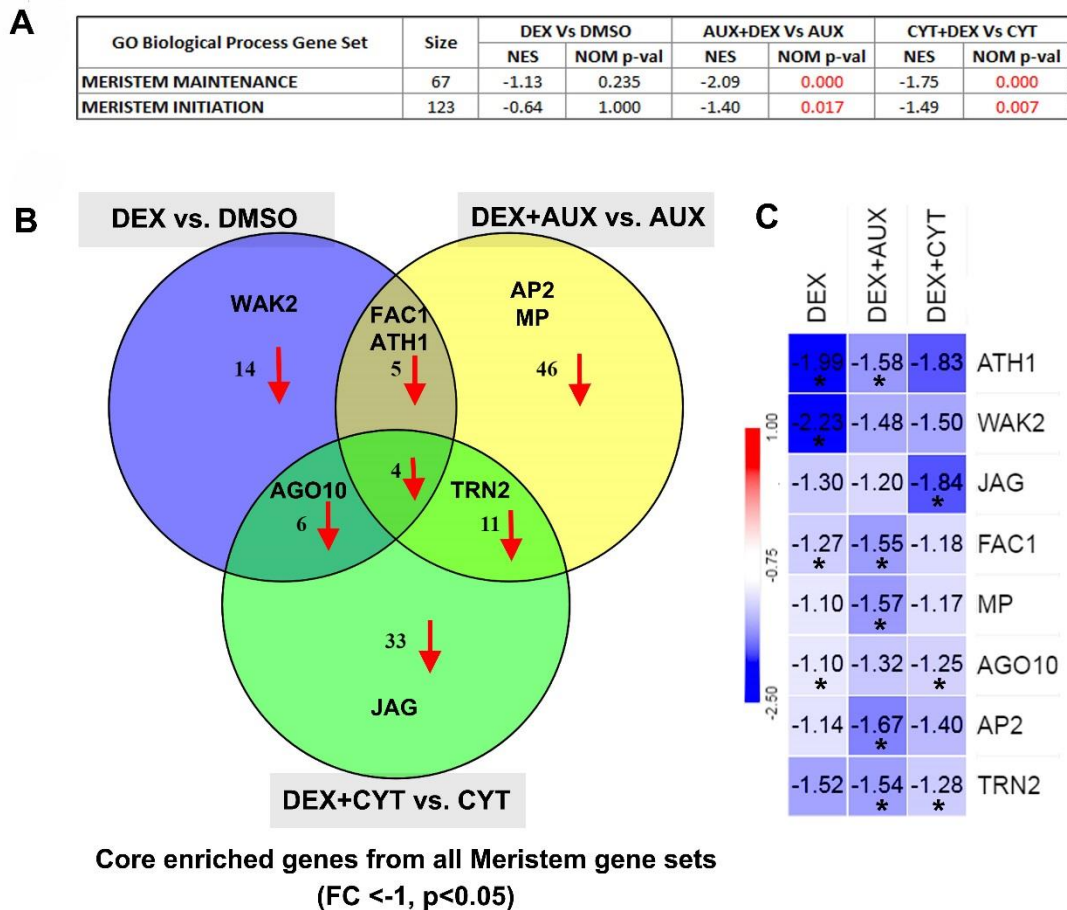
Figure 5.8 IND plus IAA and IND plus BAP downregulate meristem gene expression. (A) The GSEA analysis shows meristem maintenance and meristem initiation gene sets were significantly negatively enriched in 10 µM DEX + 10 µM IAA (DEX+AUX) and 10 µM DEX + 1 µM BAP (DEX+CYT) treated *35S::IND:GR* seedlings. **(B)** Venn diagram showing core enriched genes from all meristem gene sets, which were downregulated in 10 µM DEX, 10 µM DEX + 10 µM IAA (DEX+AUX) and 10 µM DEX + 1 µM BAP (DEX+CYT) treated *35S::IND:GR* seedlings (FC <-1, One-Way ANOVA p<0.05). When compared to DEX (14), more genes were downregulated in DEX+AUX (46) and DEX+CYT (33). **(C)** Heat map showing selected meristem genes were downregulated in DEX (*ATH1*, *WAK2*, *FAC1* and *AGO10*), DEX+AUX (*ATH1*, *FAC1, MP, AP2* and *TRN2*) and DEX+CYT (*JAG, AGO10* and *TRN2*) (*p<0.05).

Similar to section 5.2.1.3, meristem genes were identified within the DEX plus IAA treated *35S::IND:GR* microarray dataset (Fig 5.11C). The Venn diagram overlapping region shows 7 meristem genes that were regulated by IND plus auxin following 6 hours induction (Fig 5.11C). Similar to IND, *ULT1* and *HB51* were also upregulated by IND plus auxin following 6 hours induction (Fig 5.11E). ABNORMAL FLORAL ORGANS (YAB1, AFO) is the member of the YABBY family and regulates abaxial fate specification in leaves (Siegfried et al., 1999), *YAB1* was upregulated by IND plus auxin (Induced for 6 hours, Fig 5.11E). Sucrose transporter gene *SWEET1* was downregulated by 6 hours of IND plus auxin treatment (Fig 5.11E). *MP* was downregulated by 6 hours of IND plus auxin (Fig 5.11E). Similar to DEX-treated, *GBF6* and *PID* were also downregulated by 6 hours of DEX plus IAA treatment (Fig 5.11E). These results suggest that IND plus auxin affect meristem gene expression and also negatively regulate auxin transport and auxin signalling in the meristem.

5.2.2.4 Motif and TF enrichment analysis

It is important to understand if IND plus auxin regulated genes are enriched in known TF binding motifs and whether IND plus auxin regulates the corresponding TF. This was tested using GSEA. Different data files were used for motif and transcription factor enrichment analysis: *Arabidopsis* Gene 1.0 ST microarray expression data set (DEX +AUX vs. AUX), *Arabidopsis* motif gene set or transcription factor family gene set GSEA library file and phenotype label (DEX+AUX vs. AUX). GSEA data was presented in a heat map (Fig 5.5B and C).

Several TF elements were positively or negatively enriched in the IND plus IAA (DEX+AUX vs. AUX). Similar to DEX-treated, STY, ARR-B, MYB, PBE-BOX, ARF and AHL motif gene sets were also positively enriched in DEX plus IAA (p<0.05, Fig 5.5B). WUS homeobox-containing (WOX) proteins may negatively regulate gene expression by recognizing the element TCAATCA (Franco-Zorrilla et al., 2014). The HD-WUS (TCAATCA) motif gene set was positively enriched in IND plus IAA (p<0.05, Fig 5.5B). DOF (DNA-binding with one finger) domain proteins recognise a DNA element AAAG (Franco-Zorrilla et al., 2014). The DOF (AAAAAGTG) motif gene set was positively enriched in IND plus IAA (p<0.05, Fig 5.5B). HD-ZIP binds as dimers to a DNA motif AATNATT (Sessa et al., 1998). The HD-ZIP (AATCATT) motif gene set was positively enriched in IND plus IAA (p<0.05, Fig 5.5B).

AP2 proteins bind to DNA motif CCTCGTAC, and they are involved in repression of flowering (Franco-Zorrilla et al., 2014; Yant et al., 2010). The AP2 (CCTCGTA) motif gene set was positively enriched in IND plus IAA (p<0.05; Fig 5.5B). R2R3 proteins can bind to a different DNA target motif GTTAGNTA and participate in a large variety of biological processes (Prouse and Campbell, 2012). The MYB-R2R3 (GTTAGGT) motif gene set was positively enriched in IND plus IAA (p<0.05; Fig 5.5B). MYB-GARP-G2 transcription factors are required for leaf development, chlorophyll biosynthesis, and light-harvesting functions. MYB-GARP-G2 transcription factors recognise core sequence AGATTCT (Franco-Zorrilla et al., 2014; Waters et al., 2009). The GARP-G2 (AGATTCT) motif gene set was positively enriched in IND plus IAA (p<0.05, Fig 5.5B). TCP transcription factors regulate plant development and defence responses. TCPs bind to GGNCCCAC and G(T/C)GGNCCC sequences (Kosugi and Ohashi, 2002). The TCP (GGGCCCA) motif gene set was negatively enriched in IND plus IAA (p<0.05, Fig 5.5B).

Since we found several TF elements that were enriched in IND plus IAA, we analysed whether the expression of TF gene families was also enriched in IND plus IAA. Similar to DEX-treatment, B3, MYB, MYB-related and M-TYPE TF family gene sets were also positively enriched, and the WRKY TF family gene set was negatively enriched in DEX plus IAA (p<0.05; Fig 5.5C). The ETHYLENE RESPONSE FACTOR (ERF) TFs belong to AP2/ERF family, a large group of plant-specific TFs which are involved in DNA binding. ERF members are involved in responses to biotic stresses and ethylene-responsive gene transcription (Ohmetakagi and Shinshi, 1995). The ERF TF family gene set was positively enriched in IND plus IAA (p<0.05; Fig 5.5C). The C2H2 zinc finger TFs are involved in a wide range of functions such as transcriptional regulation, RNA metabolism and chromatin-remodelling (Englbrecht et al., 2004). The C2H2 TF family gene set was positively enriched in IND plus IAA (p<0.05, Fig 5.5C). The nuclear factor (NF-X1, NF-YA, NF-YB, and NF-YC) TFs are also involved in a wide range of functions such as plant growth, development, and stress responses (Jin et al., 2017). The NF TF family gene set was positively enriched in IND plus IAA (p<0.05; Fig 5.5C). CPP-like (cysteine-rich polycomb-like protein) TFs are involved in the development of reproductive tissue and control of cell division in plants (Yang et al., 2008). The CPP TF family gene set was negatively enriched in IND plus IAA (p<0.05; Fig 5.5C). Heat stress TFs (HSF) are the key

regulators of the plant heat stress response (Kotak et al., 2004). The HSF TF family gene set was negatively enriched in IND plus IAA (p<0.05; Fig 5.5C).

Since B3, MYB, and ERF transcription factor family gene sets and their motif gene sets were enriched in DEX plus IAA, IND plus auxin may regulate B3, MYB, and ERF transcription factor family genes and their targeted gene expression.

5.2.2.5 Summary

In summary, these results suggest that auxin enhances IND-regulated gene expression. GSEA analysis suggests that IND plus auxin may promote starch biosynthesis and may inhibit meristem development and leaf bilateral symmetry. IND plus auxin may regulate these functions by upregulating B3, MYB, C2H2, NF, CPP, HSF, ERF, M-TYPE and downregulating WKRY transcription factor family genes. IND plus auxin may negatively regulate meristem development and leaf bilateral symmetry by repressing *FAC1, MP, PID, GBF6, ATH1* and *TRN2* gene expression. IND plus auxin may also promote style formation by repressing *AP2* gene expression.
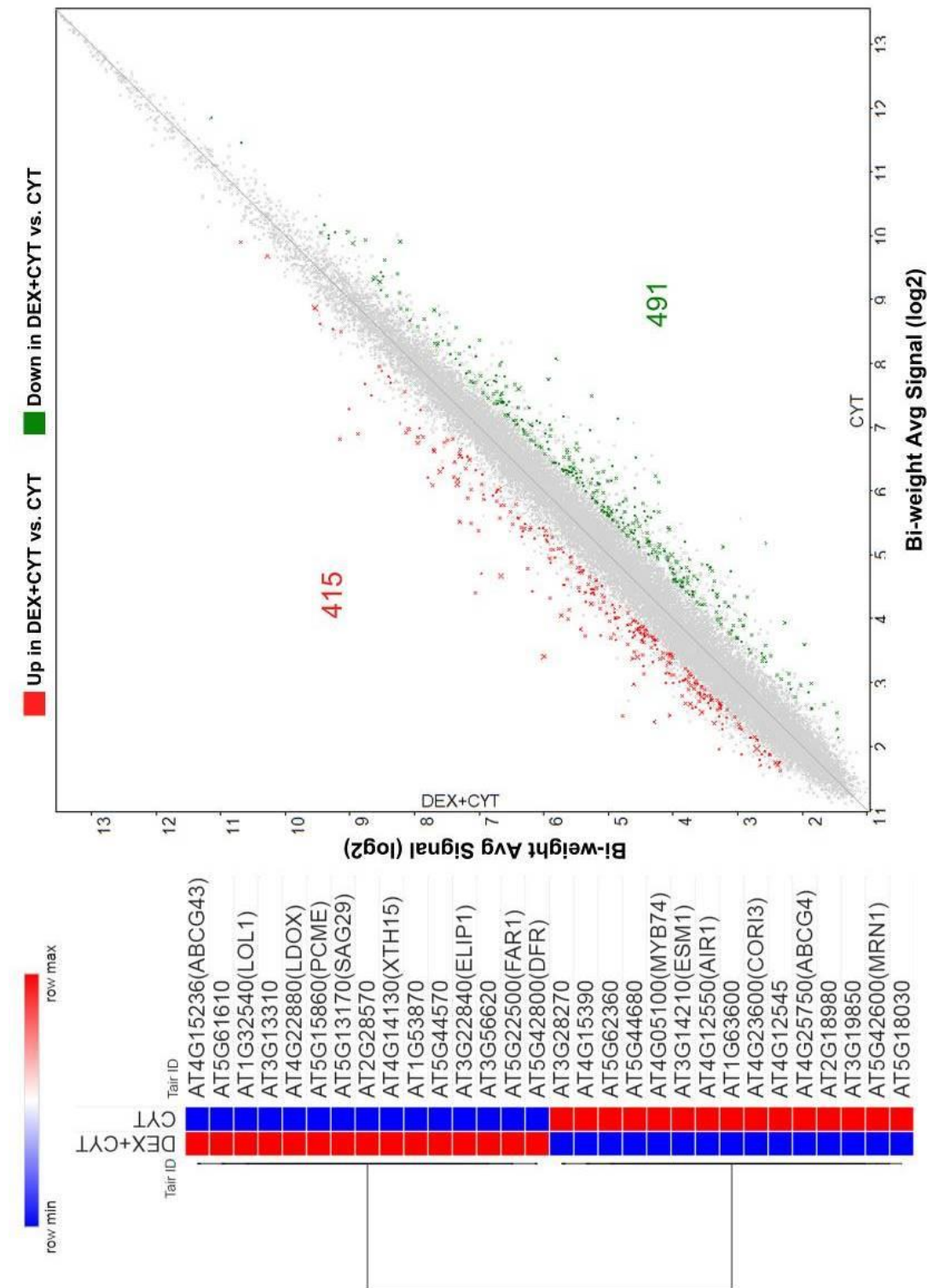
Figure 5.9 *35S::IND:GR* (DEX+CYT vs. CYT) differential gene expression. Scatter plot showing Tukey's Bi-weight average signal (log2) of 10µM DEX plus 1 µM BAP (CYT) and 1 µM BAP treated *35S::IND:GR* samples: 415 genes were upregulated (Red), and 491 genes were downregulated (Green) in DEX+CYT vs. CYT (smaller p-value, the bigger the X). Heat map of the top 30 differentially regulated genes in DEX+CYT vs. CYT (One-Way ANOVA p<0.05, Gene Fold Change (linear) >1.5 and <-1.5). (Blue: low gene expression, Red: high gene expression).

5.2.3 Microarray analysis of IND plus cytokinin regulated genes

5.2.3.1 Differential gene expression analysis

Cytokinin positively regulates valve margin development (Marsch-Martinez et al., 2012). Since IND is a key regulator of fruit valve margins and cytokinin also promote valve margins, it is important to understand if cytokinin can influence IND regulated gene expression. Therefore the effect of IND plus cytokinin on global gene expression changes was investigated using microarray analysis. For the microarray, total RNA was isolated from *35S::IND:GR* seedlings (7DAG), which were treated with either 10 µM DEX plus 1 µM BAP or 1 µM BAP for 6 hours in liquid media (n=3). The microarray was performed and analysed as described in section 5.2.1.1. A total of 906 genes were differentially expressed in *35S::IND:GR* seedlings (DEX+CYT vs. CYT, FC >1.5 or <-1.5, $p<0.05$): 415 genes were upregulated and 491 genes were downregulated (Fig 5.9). The heat map shows the top 30 differentially expressed genes in *35S::IND:GR* seedlings (DEX+CYT vs. CYT, $p<0.05$, Fig 5.7). *SAG29* was also upregulated in *35S::IND:GR* seedlings (DEX+CYT vs. CYT, $p<0.05$, Fig 5.9). A list of differentially expressed genes was summarised in a table (Table 8.9).

5.2.3.2 Gene-set enrichment analysis (GSEA)

We use GSEA to understand which pathways are regulated by IND plus cytokinin. *Arabidopsis* Gene 1.0 ST microarray expression datasets (DEX+CYT vs. CYT), *Arabidopsis* biological function gene, set GSEA library file, and phenotype label (DEX+CYT vs. CYT) were used for GSEA analysis. Analysed data was exported to Cytoscape for analysis and visualisation (Fig 5.10). When compared to BAP-treated, 72 gene sets were positively enriched and 227 gene sets were negatively enriched in DEX + BAP treated *35S::IND:GR* seedlings ($p<0.05$; Fig 5.10, Table 5.1). When compared to IND (Section 5.2.1.2), a large number of gene sets were enriched in IND plus CYT. Significantly enriched gene sets were summarised in a table (Table 8.12).

Several gene sets were positively or negatively enriched in the IND plus cytokinin (DEX+AUX vs. AUX). Photosynthetic, rRNA processing, pollen tube, cell wall modification and defence response gene sets were positively enriched in DEX plus BAP ($p<0.05$; Fig 5.10). Meristem, pattern specification, organ morphogenesis and cell size gene sets

were negatively enriched in DEX plus BAP (p<0.05; Fig 5.10). GSEA results suggest that IND plus cytokinin may negatively regulate meristem and organ development processes.

5.2.3.3 IND plus cytokinin negatively regulate meristem associated gene sets

GSEA analysis from section 5.2.3.2 suggests that IND plus cytokinin negatively regulate meristem gene sets. In particular, meristem maintenance and meristem initiation gene sets were negatively enriched in DEX plus BAP (p<0.05; Fig 5.8A). A total of 54 genes from all meristem gene sets were core enriched in DEX plus BAP (p<0.05, Fig 5.8B). JAGGED (JAG) promote leaf growth, fruit valve and valve margin development (Dinneny et al., 2005; Gonzalez-Reig et al., 2012; Ohno et al., 2004). *JAG* was downregulated in DEX + BAP treated *35S::IND:GR* seedlings (p<0.05, Fig 5.8C). Similar to DEX plus IAA treated *35S::IND:GR* seedlings, *TRN2* was also downregulated in DEX plus BAP treated *35S::IND:GR* seedlings (p<0.05, Fig 5.8C). Similar to DEX treated *35S::IND:GR* seedlings, *AGO10* was also downregulated in DEX plus BAP treated *35S::IND:GR* seedlings (p<0.05, Fig 5.8C). When compared to DEX treated *35S::IND:GR* seedlings, a higher number of meristem genes and gene sets were downregulated in DEX plus BAP treated *35S::IND:GR* seedlings (Fig 5.8). These data suggest that BAP may regulate IND activity to control meristem associated gene expression.

Similar to section 5.2.1.3, meristem genes were identified within the DEX + BAP treated *35S::IND:GR* microarray dataset (Fig 5.11D). The Venn diagram overlapping region shows 3 meristem genes regulated by IND plus cytokinin following 6 hours of induction, Fig 5.11D). Similar to DEX-treatment, *HDG2* and *HB51* were upregulated and *PID* was downregulated by DEX plus BAP following 6 hours of induction (Fig 5.14E).
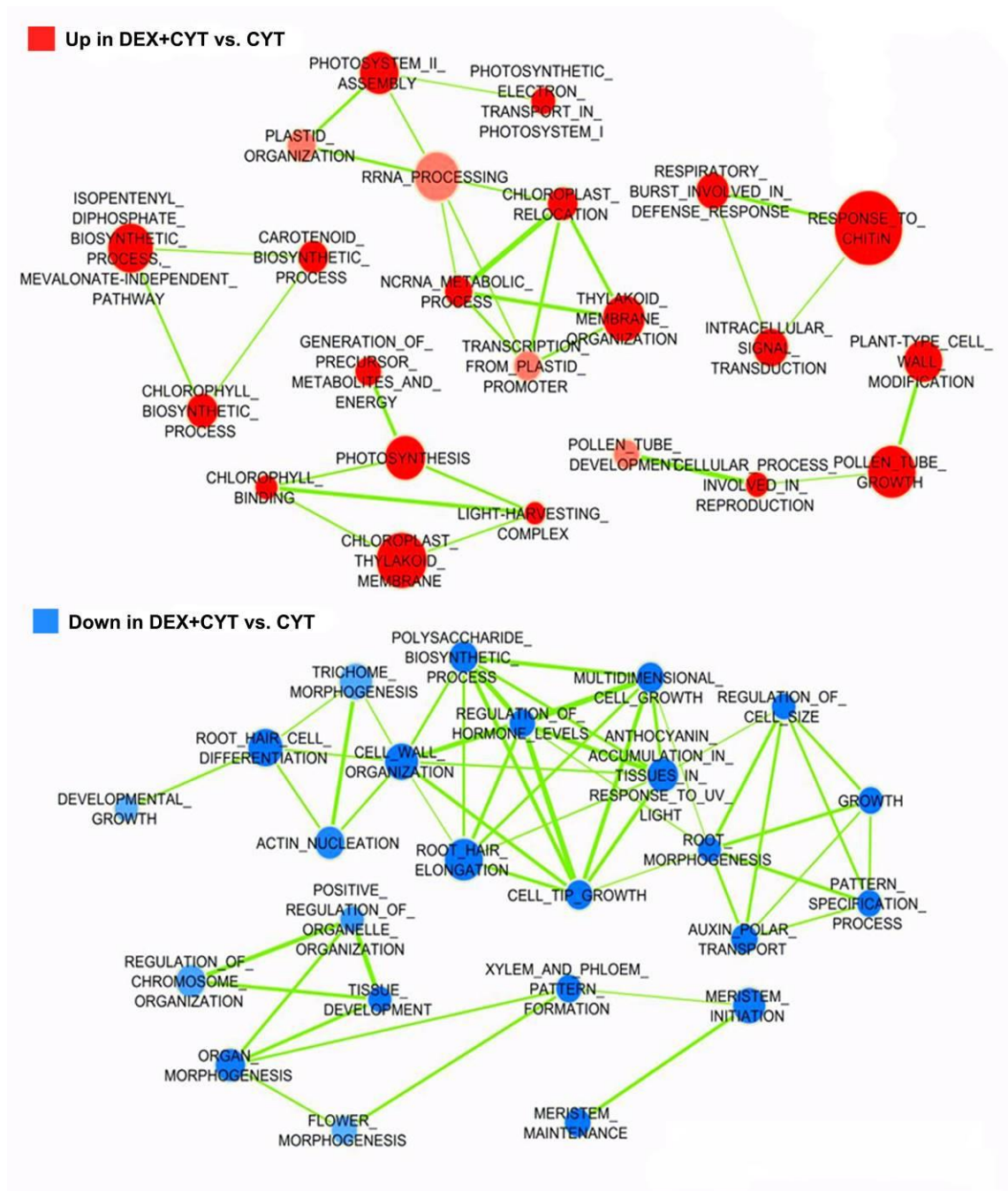
Figure 5.10 *35S::IND:GR* (DEX+CYT vs. CYT) *Arabidopsis* biological process GSEA. Cytoscape generated image of the GSEA data output from microarray analysis following 10 µM DEX + 1 µM BAP (DEX+CYT), and 1 µM BAP (CYT) treated *35S::IND:GR* seedlings showing significantly (p<0.05) enriched gene-sets (Blue: negatively enriched, Red: positively enriched). Closely related gene sets were connected by a green line. Photosynthetic, rRNA processing, pollen tube, cell wall modification and defence response sets were positively enriched. Meristem, pattern specification, organ morphogenesis and cell size sets were negatively enriched.

5.2.3.4 Motif and TF enrichment analysis

It is important to understand if IND plus cytokinin regulated genes are enriched in known TF binding motifs and whether IND plus cytokinin regulates the corresponding TF. This was tested using GSEA. Different data files were used for motif and transcription factor enrichment analysis: *Arabidopsis* Gene 1.0 ST microarray expression data set (DEX+CYT vs. CYT), *Arabidopsis* motif gene set or transcription factor family gene set GSEA library file and phenotype label (DEX+CYT vs. CYT). After analysis, data was presented in a heat map (Fig 5.5B and C).

Several TF elements were positively or negatively enriched by IND in the presence of cytokinin (DEX+CYT vs. CYT). Similar to the DEX-treatment, STY, ARR-B, MYB, PBE-BOX and ARF motif gene sets were positively enriched, and NAC and WRKY motif gene sets were negatively enriched in in DEX plus BAP ($p<0.05$, Fig 5.5B). Similar to DEX plus IAA, MYB-R2R3 and GARP-G2 Motif gene sets were positively enriched in DEX plus BAP treated *35S::IND:GR* seedlings ($p<0.05$, Fig 5.5B). Heat shock transcription factors (HSFs) are a group of proteins highly induced under stress conditions. HSFs can bind to both primary and secondary motifs (GAAGCTTC and TTCTAGAA, respectively). HSF (TTCTAGAA) motif gene set was positively enriched in DEX plus BAP ($p<0.05$, Fig 5.5B).

Since we found several TF elements were enriched we analysed whether the expression of TF gene families were also enriched. Similar to DEX-treatment, B3, MYB and M-TYPE TF family gene sets were also positively enriched in DEX plus BAP ($p<0.05$, Fig 5.5C). Similar to DEX plus IAA, the ERF TF family gene set was positively enriched in DEX plus BAP ($p<0.05$, Fig 5.5C). The WOX TFs are a subclade of the homeobox transcription factor superfamily, they regulate multiple developmental processes in plants by the promotion of cell division activity and also by prevention of premature cell differentiation (van der Graaff et al., 2009). The WOX TF family gene set was positively enriched in DEX plus BAP ($p<0.05$, Fig 5.5C). The bHLH TF family gene set was negatively enriched in DEX plus BAP ($p<0.05$, Fig 5.5C).

Since B3 and MYB family gene sets and their motif gene sets were enriched in DEX plus BAP, IND plus cytokinin may regulate B3 and MYB transcription factor family genes and their targeted gene expression.

5.2.3.5 Summary

In summary, these results suggest that cytokinin enhances IND regulated gene expression. GSEA analysis suggests that IND plus cytokinin may promote pollen tube development and may inhibit meristem and organ development processes. IND plus cytokinin may regulate these functions by upregulating B3, MYB, WOX, ERF, M-TYPE and downregulating bHLH transcription factor family genes. IND plus cytokinin may negatively regulate meristem and organ development process by repressing *PID, GBF6, AGO10* and *TRN2* gene expression. IND plus cytokinin may negatively regulate fruit valve formation by repressing *JAG* gene expression.
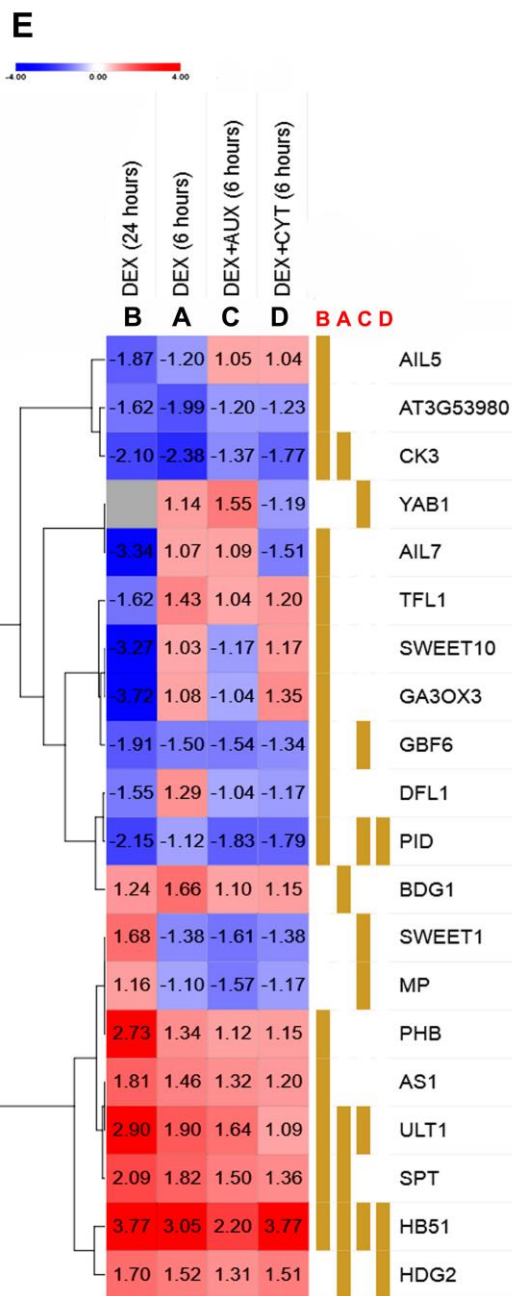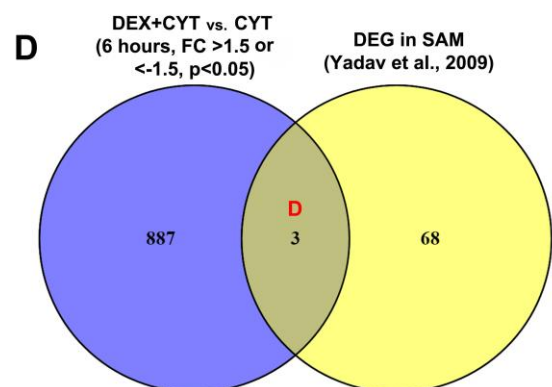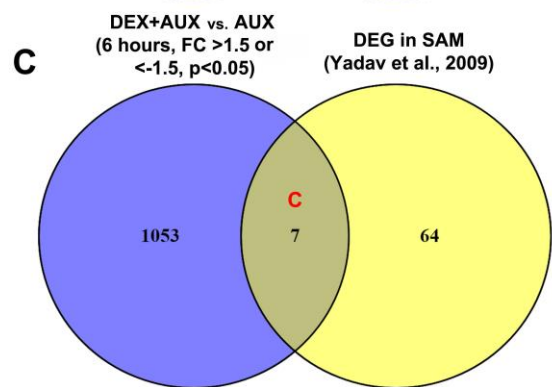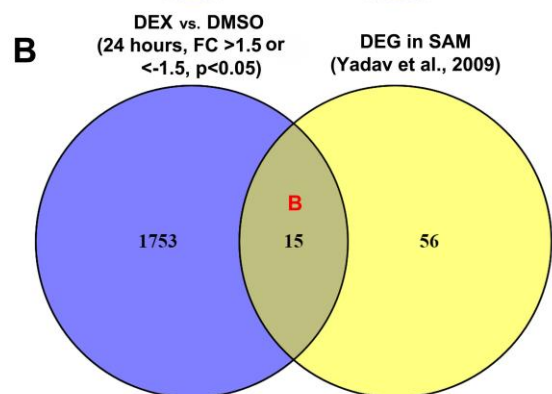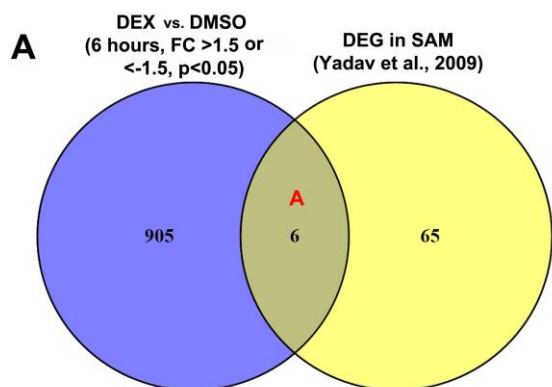
Figure 5.11 IND differentially regulates meristem specific genes; gene list from (Yadav et al., 2009). (A-D) Venn diagrams showing a comparative analysis of DEX (6 and 24 hours induction), DEX+AUX (6 hours induction) and DEX+CYT (6 hours induction) data compared with 71 differentially expressed genes (DEG) in SAM (Yadav et al., 2009)**. (A)** The overlapping region shows 6 meristem genes were regulated by DEX (6 hours induction). **(B)** The overlapping region shows 15 meristem genes were regulated by DEX (24 hours induction). **(C)** The overlapping region shows 7 meristem genes were regulated by DEX+AUX (6 hours induction). **(D)** The overlapping region shows 3 meristem genes were regulated by DEX+CYT (6 hours induction). When compared to other conditions, many meristem genes were regulated by DEX (24 hours induction). **(E)** All differentially regulated meristem genes were presented in a Heatmap. (Blue: low gene expression, Red: high gene expression and Brown denoting p<0.05).
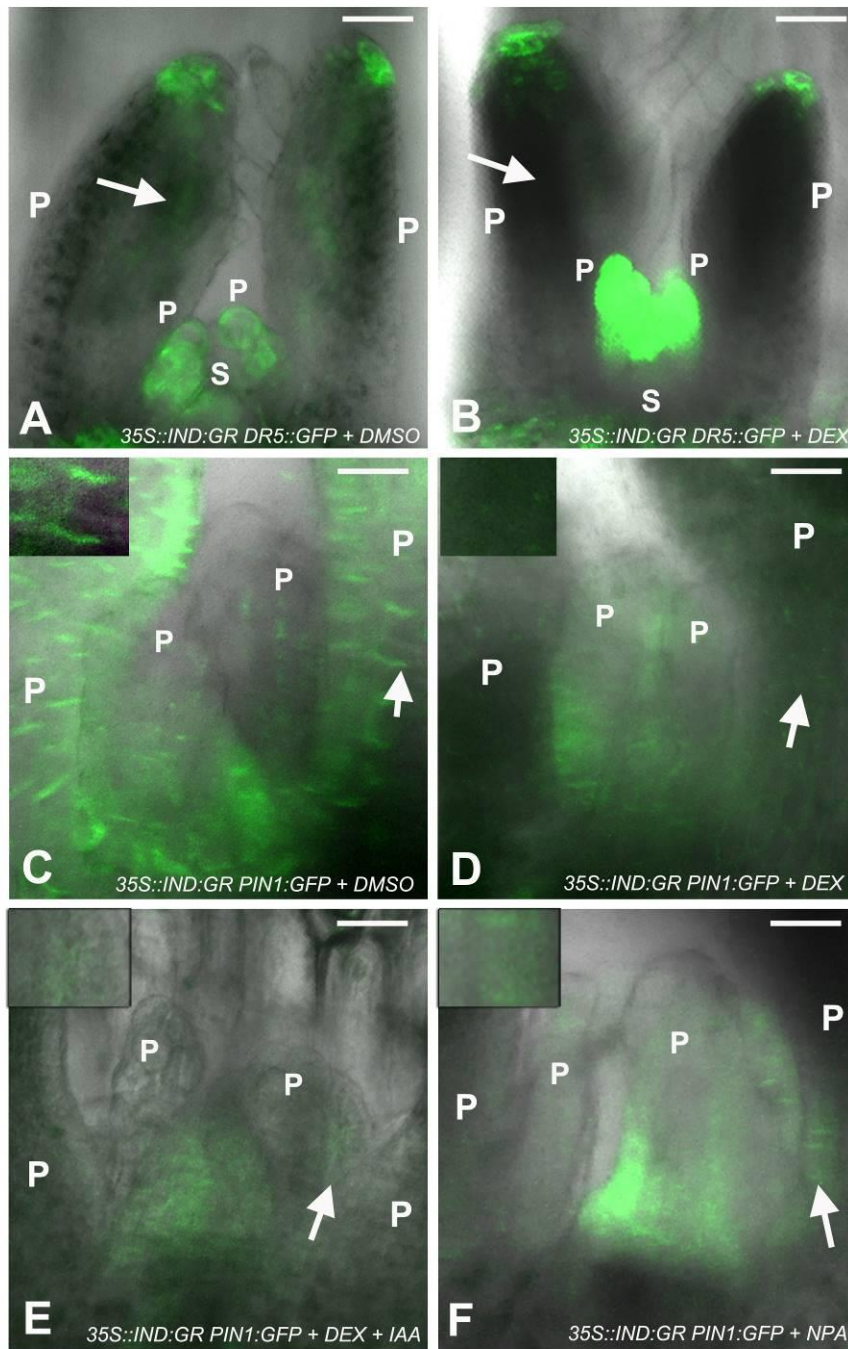
Figure 5.12 IND inhibits auxin transport in leaf primordia. Confocal images of *DR5rev::GFP* in **(A)** *35S::IND:GR*+DMSO and **(B)** *35S::IND:GR*+DEX (24 hours induction) at 4DAG SAM (S) and leaf primordia (P). **(A)** GFP expression was observed in the SAM at the tip of leaf primordia and in mid domain of leaf primordia. **(B)** GFP expression was increased at the tip of leaf primordia, and no GFP expression was observed in mid domain of leaf primordia. Confocal images of *pPIN1::PIN1:GFP* in **(C)** *35S::IND:GR*+DMSO, **(D)** *35S::IND:GR*+DEX, **(E)** *35S::IND:GR*+DEX+IAA and **(E)** *35S::IND:GR*+NPA at leaf primordia (24 hours induction). The *PIN1:GFP* signal in *35S::IND:GR* leaf primordia **(C)** was decreased with 10µM DEX **(D),** 10µM DEX+AUX **(E)** and 10µM NPA **(F)** treatment (indicated with an arrowhead). (Scale bar = 50 µm).

5.2.4 IND overexpression inhibits auxin transport in leaf primordia

Results from the IND microarray study suggest that induction of IND (including IND plus IAA and IND plus BAP) can downregulate *PID* expression in seedlings (Section 5.2). Sorefan *et al.* demonstrated that IND regulates auxin transport in the separation layer by repressing *PID* and inducing *WAG2* expression at the valve margins, which leads to PIN relocation from apico-basal to apolar-lateral (Sorefan et al., 2009a). It is not known if IND can regulate auxin transport in the SAM and leaf primordia by altering *PIN1* expression. This hypothesis was tested using *pPIN1::PIN1:GFP 35S::IND:GR* and *DR5rev*::GFP *35S::IND:GR* double-transgenic lines. The *DR5rev::GFP* reporter was used to visualise auxin responses in the SAM and leaf primordia. The *pPIN1::PIN1:GFP* reporter was used to visualise PIN1 expression in leaf primordia. These double transgenic lines were grown on plant agar plates for 3 days, and seedlings were transferred to plant liquid media supplemented with DMSO, 10 µM DEX, 10 µM DEX plus IAA and 10 µM NPA. DMSO was a vehicle control, DEX was used to induce IND and NPA was a polar auxin transport inhibitor. After 24 hours of treatment, seedlings were dissected and imaged for GFP expression in the SAM and leaf primordia using confocal microscopy.

In the vehicle control, the *pPIN1::PIN1-GFP* signal was detected in the leaf primordia, and PIN1 appears to be polarly localised in cells of leaf primordia (Fig 5.12C). This expression pattern was consistent with another published study (Chen et al., 2013). The *pPIN1::PIN1-GFP* signal was decreased in the leaf primordia of DEX (Fig 5.12D), and DEX plus IAA (Fig 5.12E) treated *35S::IND:GR* seedling. Interestingly, Sorefan *et al.* also reported similar *pPIN1::PIN1-GFP* expression pattern in valve cells of a stage-10 induced *35S::IND:GR* gynoecium (Sorefan et al., 2009a). In the NPA treatment, the *pPIN1::PIN1-GFP* signal was decreased in the leaf primordia, and this expression pattern was consistent with published studies (Heisler et al., 2005; Qi et al., 2014; Wenzel et al., 2007). NPA inhibits PIN1 expression and loss of PIN1 results in inhibition of auxin transport between leaf primordia and the SAM (Guenot et al., 2012; Qi et al., 2014). The PIN1 pattern of expression in response to NPA treatment was similar to that observed with the DEX or DEX plus IAA treatment (Fig 5.12D-F). These data suggest that IND may inhibit auxin transport in leaf primordia by downregulating PIN1 protein levels.

We predicted that IND downregulation of PIN1 in leaf primordia would cause a change in auxin responses in DEX treated *35S::IND:GR* seedlings. In the vehicle control, the *DR5rev::GFP* signal was detected in the SAM at the tip and mid domain of leaf primordia as well as in the areas of presumptive leaf primordia initiation (Fig 5.12A) and this expression pattern was consistent with another published study (Chen et al., 2013; Guenot et al., 2012) (Fig 8.5). After IND induction, increased *DR5rev::GFP* signal was detected in areas of presumptive leaf primordia initiation as well as in the tips of leaf primordia, and no signal was detected in the mid domain of leaf primordia (Fig 5.12B). In the DEX treated *35S::IND:GR* seedlings, auxin may be accumulating at the tip of leaf primordia because the PIN1 expression was decreased in the mid domain of leaf primordia (Fig 8.5). *pPIN1::PIN1-GFP* expression correlates with *DR5rev::GFP* suggesting that IND may inhibit auxin transport between leaf primordia and the SAM (Fig 5.12B, D, and F).

5.2.5 IND signalling network analysis

A network representation of pathway models involving many functional partnerships, and interactions that occur between genes, proteins or metabolites was carefully assembled into a graph. However, since this information was sourced from multiple resources it was important to understand which elements were associated with IND from these multiple resources. Therefore, STRING (Search Tool for the Retrieval of Interacting Genes/Proteins) was used to study known and predicted IND-protein interactions and IND signalling cascades. The network showed that IND was associated with 12 genes/proteins (Fig 5.13A). They were SPT, PAR1, STY1, STY2, ETT, MYB26, JAG, AGL8, RPL, SHP1, SHP2 and AT4G32272 (Fig 5.13A). Other studies also reported that IND interacts with At2g18970, At2g39000, At3g51730, At5g06290, PIF3, PIF4, PIL6 and ALC (Gremski, 2006; Liljegren et al., 2004a). These additional data exhibit notable differences in terms of quality and completeness. Many of these proteins are involved in patterning of the gynoecium. SPT, ETT, HEC, PIF3, PIF4 and PIL6 proteins regulate Style formation (Gremski, 2006; Gremski et al., 2007; Heisler et al., 2001; Schuster et al., 2015). SHP1, SHP2, ALC and SPT proteins regulate valve margin formation (Girin et al., 2011; Liljegren et al., 2000; Liljegren et al., 2004a). Additionally, HEC proteins regulate valve margin

formation (Schuster et al., 2015). JAG promotes valve and valve margin formation (Dinneny et al., 2005). RPL and FUL inhibit valve margin formation (Roeder et al., 2003).

The gene expression analysis shows that IND overexpression can also regulate some of the genes identified in the network in seedlings (Fig 5.13B). An expression profile of these genes was presented in a heatmap (Fig 5.13B). *SPT* was upregulated in both DEX (DEX vs. DMSO) as well as DEX plus IAA (DEX+AUX vs. AUX) ($p<0.05$, Fig 5.13B). MYB DOMAIN PROTEIN 26 (MYB26) regulates endothecium lignification as well as anther dehiscence (Steiner-Lange et al., 2003; Yang et al., 2007). *MYB26* was upregulated in DEX (DEX vs. DMSO) ($p<0.05$, Fig 5.13B). PHYTOCHROME INTERACTING FACTOR 3-LIKE 6 (PIL6) induces leaf senescence and also regulates carpel development via SPT (Reymond et al., 2012). *PIL6* was downregulated in DEX (DEX vs. DMSO) ($p<0.05$, Fig 5.13B). SHP1 positively regulates IND and ALC to promote valve margin formation (Liljegren et al., 2000). *SHP1* was weakly upregulated in DEX plus IAA (DEX+AUX vs. AUX) ($p<0.05$, Fig 5.13B). AT4G32272 is a nucleotide/sugar transporter family protein, *AT4G32272* was weakly downregulated in DEX plus IAA (DEX+AUX vs. AUX) ($p<0.05$, Fig 5.13B). JAG protein promotes valve and valve margin formation (Dinneny et al., 2005), *JAG* was downregulated in DEX plus BAP (DEX+BAP vs. BAP) ($p<0.05$, Fig 5.13B). These data suggest that IND may also regulate anther dehiscence in addition to valve margin development.
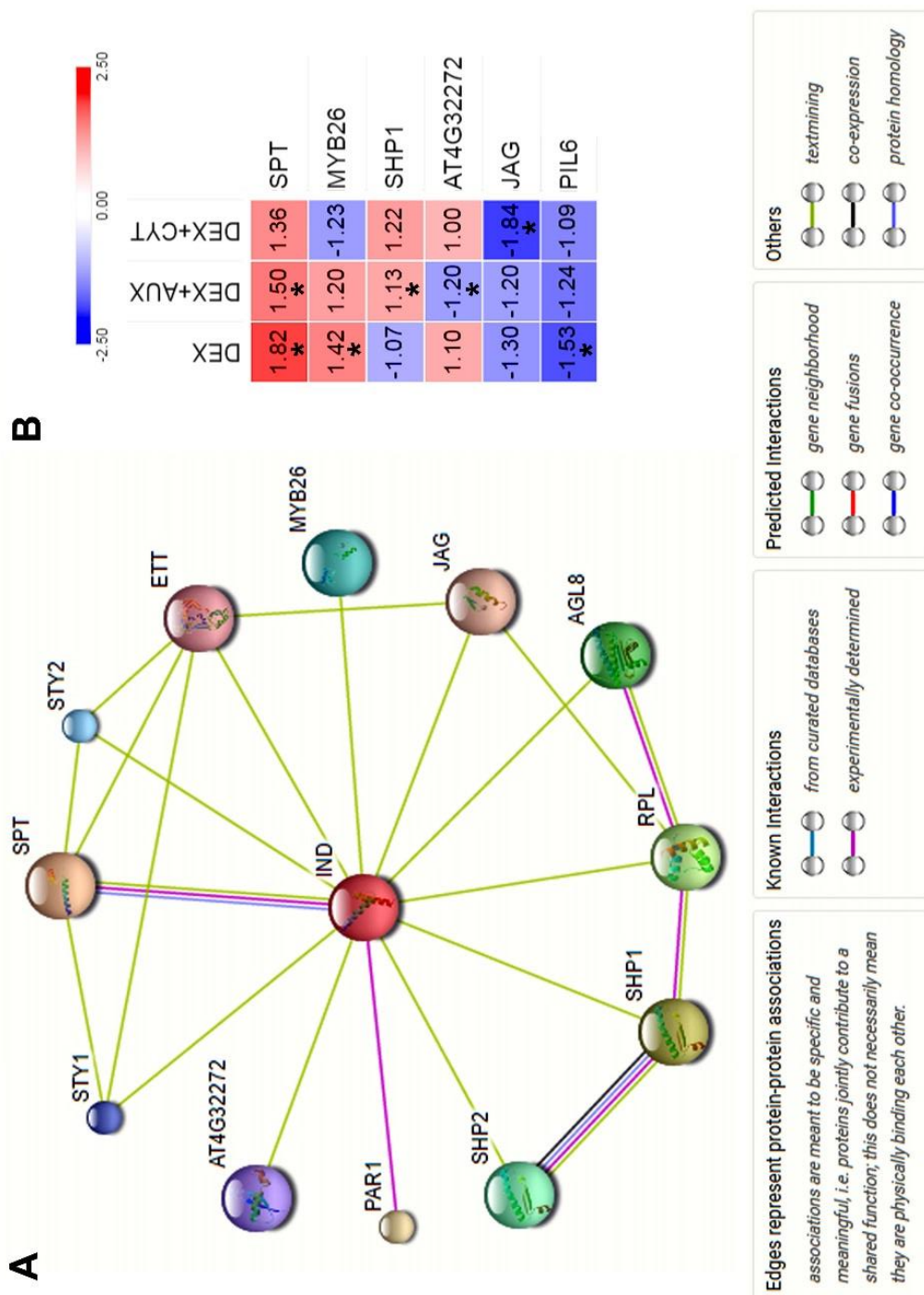
Figure 5.13 IND signalling cascade analysis using STRING. (A) STRING signalling cascade showing known and predicted IND interactions. **(B)** Heat map of the IND pathway associated genes that were differentially expressed following 10 µM DEX**,** 10 µM DEX plus 10 µM IAA (DEX+AUX) and 10 µM DEX plus 1 µM BAP (DEX+CYT) treated *35S::IND:GR* seedlings. *SPT* and *MYB26* were upregulated, and *PIL6* was downregulated by IND (DEX). *SPT* and *SHP1* were upregulated, and *AT4G32272* was downregulated by IND plus IAA (DEX+AUX). *JAG* was downregulated by IND plus BAP (DEX+CYT). ***One-Way ANOVA p<0.05. (Blue: low gene expression, Red: high gene expression).

5.2.6 Methylation and hormones regulate *IND*

5.2.6.1 Cistrome and epicistrome data analysis to study *IND* gene binding TFs

We do not know if any TFs can bind to the *IND* gene. This was studied by analysing *Arabidopsis* cistrome and epicistrome data (O'Malley et al., 2016). The cistrome is the comprehensive set of transcription factor binding *cis*-elements in an organism, and an epicistrome incorporates tissue-specific DNA methylation changes and TF-specific methylation sensitivities to these binding profiles (O'Malley et al., 2016). Using DNA affinity purification sequencing, O'Malley *et al.* defined the *Arabidopsis* cistrome and epicistrome by resolving motifs and peaks for 529 transcription factors (DNA used in DAP-seq retains 5-methylcytosines and methylcytosines were removed by PCR for ampDAP-seq) (O'Malley et al., 2016). The DAP-seq and ampDAP-seq datasets were analysed to examine if any of the 529 transcription factors can bind to the *cis*-elements of the *IND* gene. Analysed DAP-seq and ampDAP-seq data was presented in figure 5.14A and B. DAP-seq data analysis shows 59 TFs that bind to the *IND* gene (Table 5.2) and ampDAP-seq data analysis shows that 59 TFs bind to the *IND* gene (methylcytosines were removed) and 29 TFs were common to both data sets (Fig 5.14B). Since this DNA is from young leaf tissue, this data suggests that methylation in the *IND* gene can affect *IND*-TF interactions in a young leaf. DNA methylation acts to repress gene transcription and this can be tissue specific (Saze et al., 2012; Widman et al., 2014). H3 lysine 27 trimethylation (H3K27me3) is one of the major determinants of tissue-specific expression patterns in plants (Zhang et al., 2007). In *Arabidopsis*, Polycomb-group (Pc-G) proteins can repress target genes by catalysing H3K27me3 (Lafos et al., 2011). The H3K27me3-ChIP (GEO:GSE24474) data suggest that H3K27me3 can target *IND* in a young leaf (Fig 5.14C). H3K27me3-ChIP data in conjugation with ampDAP-seq data suggest that *IND* gene transcription may be controlled by methylation in leaf tissue.

Gene Ontology (GO) biological process analysis was performed to determine the function of the *IND* gene-binding transcription factors (59 TFs from DAP-seq). Gene Ontology (GO) biological process analysis was done using PANTHER (http://pantherdb.org/). Gene Ontology (GO) biological process terms that were enriched by more than 10 fold were listed in Table 5.3. The data suggest that many of the *IND* gene-binding TFs are involved in a hormone-mediated signalling pathway,

particularly ethylene signalling (Table 5.3). A large number of *IND*-TFs belongs to APETALA2-ETHYLENE-RESPONSIVE ELEMENT BINDING PROTEIN (AP2-EREBP) family (23 and 20) (Fig 5.14A). AP2-EREBP family TFs are mediators of stress responses and developmental programs (Licausi et al., 2013).

The gene expression analysis shows that IND can regulate few of the *IND*-TFs (Fig 5.14C). Gene expression profiling of these TFs was presented in a heatmap (Fig 5.14C). *HB51* was upregulated by IND (DEX vs. DMSO), IND plus IAA (DEX+AUX vs. AUX) and IND plus BAP (DEX+CYT vs. CYT) ($p<0.05$, Fig 5.14C). SQUAMOSA PROMOTER BINDING PROTEIN-LIKE 5 (SPL5) is involved in regulation of flowering and vegetative phase change (Jung et al., 2016), *SPL5* was upregulated by IND, IND plus IAA and IND plus BAP ($p<0.05$, Fig 5.14C). DREB and EAR motif protein 2 (DEAR2) is an AP2-EREBP family protein, *DEAR2* was upregulated by IND and IND plus IAA ($p<0.05$, Fig 5.14C). HOMEOBOX-LEUCINE ZIPPER 4 (HAT2) regulates auxin-mediated morphogenesis (Bou-Torrent et al., 2012; Sawa et al., 2002; Sorin et al., 2009), *HAT2* was upregulated by IND and IND plus BAP ($p<0.05$, Fig 5.14C). KUODA1 (KUA1) specifically controls cell expansion during leaf development (Lu et al., 2014), *KUA1* was upregulated by IND plus IAA ($p<0.05$, Fig 5.14C). Ethylene and salt inducible 3 (ESE3) is upregulated in response to ethylene and high salt (Zhang et al., 2011a), *ESE3* was upregulated by IND and IND plus BAP ($p<0.05$, Fig 5.14C). HB51, SPL5, DEAR2, HAT2, KUA1, and ESE3 may promote or repress *IND* gene expression, and this should be investigated.

A

Transcription factors bind to cis-elements of *IND* gene

	IND-TF (DAP-seq)	*IND*-TF (ampDAP-seq)	
	23	20	AP2-EREBP *
	7	2	C2C2-DOF
	5	9	MYB-related
	4	4	HB
	3	3	MYB
	2	0	C2H2
	2	1	Homeobox
	2	2	Trihelix
	1	3	CPP
	1	2	G2-like
	1	0	HSF
	1	0	LOB-AS2
	1	1	MADS
	1	0	mTERF
	1	0	NAC
	1	0	Orphan
	1	1	REM
	1	3	SBP
	1	3	ZF-HD
	0	4	bZIP
	0	1	C2C2-GATA
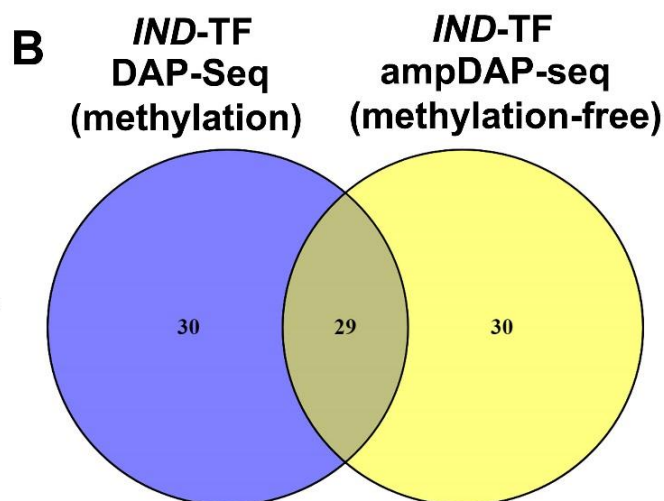
B

IND-TF DAP-Seq (methylation)   *IND*-TF ampDAP-seq (methylation-free)

30   29   30

C

	DEX	DEX+AUX	DEX+CYT		
HB51	3.05	2.20	3.77		ampDAP-seq
SPL5	2.11	2.28	1.59		ampDAP-seq
DEAR2	1.55	1.82	1.27		ampDAP-seq
HAT2	2.55	1.14	2.59		DAP-seq
KUA1	1.19	1.52	1.29		DAP-seq
ESE3	1.66	1.08	2.18		DAP-seq

D

Pc-G   Young leaf

H3K27me3

IND coding gene

157
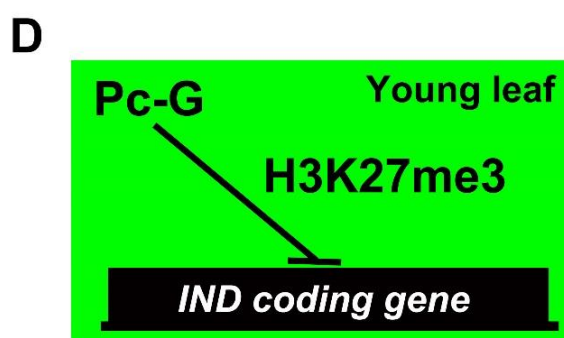
Figure 5.14 Different family TFs bind to the *IND* gene, and *IND* gene methylation can affect *IND*-TF interactions. (A) DAP-Seq and ampDAP-Seq (methylation-free) data (GEO:GSM1925338) analysis presented in the heat map shows different family TFs bind to the *IND* gene and particularly large number of AP2-EREBP TFs bind to the *IND* gene (both methylation and methylation-free). **(B)** The Venn diagram shows that removing methylcytosines from the *IND* gene (ampDAP-seq) can alter the TF binding pattern, in particular 30 TFs prefer to bind methylation-free *IND* gene alone (ampDAP-seq in yellow circle). **(C)** The heat map shows a few of these TF family genes were also regulated by IND (DEX vs. DMSO), IND plus IAA (DEX+AUX vs. AUX) and IND plus BAP (DEX+CYT vs. CYT) (p<0.05). **(D)** In a young leaf, Polycomb-group (Pc-G) proteins can repress *IND* gene expression by catalysing histone H3 lysine 27 trimethylation (H3K27me3) (GEO:GSE24474).

Table 5.2 *IND* gene binding transcription factors from DAP-Seq data (GEO: GSM1925338) analysis.

TF Family	Transcription factors bind to cis-elements of IND gene
AP2-EREBP	RAP2.10, RAP2.6, AT2G33710, ESE3, AT1G71450, AT5G65130, CEJ1, CBF1, ERF7, AT1G19210, ERF38, ERF8, DEAR3, ERF11, AT4G16750, ERF10, ERF4, RRTF1, ERF15, AT1G22810, AT1G12630, CBF4 and CRF10
C2C2-DOF	AT2G28810, AT5G62940, AT3G45610, OBP3, AT5G02460, AT5G66940 and DOF45
MYB-related	KUA1, AT1G49010, LHY1, RVE1, and AT3G09600
HB	ATHB21, ATHB53, ATHB5 and ATHB40
MYB	MYB119, MYB98 and MYB67
Homeobox	HAT2 and HDG1
Trihelix	GT2 and GTL1
C2H2	AT5G22990 and AT2G15740
CPP	AT2G20110
G2-like	AT2G01060
HSF	HSFA6B
LOB-AS2	LBD2
MADS	SVP
mTERF	AT5G23930
NAC	SND3
Orphan	BBX31
REM	REM19
SBP	SPL9
ZF-HD	ATHB23

Table 5.3 GO Term Enrichment analysis of *IND* gene-binding transcription factors p<0.05.

GO biological process	GO ID	Fold Enrichment
Ethylene-activated signaling pathway	GO:0009873	34.2
Cellular response to ethylene stimulus	GO:0071369	30.23
Phosphorelay signal transduction system	GO:0000160	27.09
Response to ethylene	GO:0009723	23.5
Negative regulation of transcription, DNA-templated	GO:0045892	16.1
Negative regulation of RNA biosynthetic process	GO:1902679	14.76
Negative regulation of nucleic acid-templated transcription	GO:1903507	14.76
Hormone-mediated signaling pathway	GO:0009755	10.67
Cellular response to hormone stimulus	GO:0032870	10.06

5.2.6.2 Hormone treatment regulates GUS activity in *pIND::GUS* seedlings

Results from the previous section suggest that ethylene can possibly regulate *IND*. Similar to ethylene, other hormones may also regulate *IND* gene expression. This was examined using *pIND::GUS* seedlings. *pIND::GUS* seedlings were germinated on plant agar media supplemented with 10 µM jasmonic acid (JA), 10 µM abscisic acid (ABA), 10 µM indole-3-acetic acid (IAA, auxin), 10 µM 6-benzylaminopurine (BAP, cytokinin) and 10 µM 1-aminocyclopropane carboxylic acid (ACC, an ethylene precursor). After two weeks, GUS staining was performed in untreated and hormone-treated *pIND::GUS* seedlings. When compared to untreated seedlings, no GUS staining was observed in seedlings grown on abscisic acid (Fig 5.15A and C). However, ABA treatment for 12 hours did not affect *IND* expression in seedlings (Fig 8.6). Loss of GUS expression may be the result of impaired seed germination. When compared to untreated seedlings, reduced GUS staining was observed in seedlings grown on ACC and jasmonic acid (Fig 5.15A, B, and F). Higher GUS staining was observed in seedlings grown on cytokinin (BAP) (Fig 5.15E). No difference in GUS staining was observed in untreated seedlings and seedlings grown on auxin (IAA) (Fig 5.15A and D). These data suggest that ethylene (ACC) and jasmonic acid inhibit *IND* expression whereas cytokinin (BAP) induces *IND* expression.

5.2.6.3 Summary

In summary, these results suggest that *IND* gene transcription may be controlled by methylation (DNA/Histone) in leaf tissue. Different families of TFs can bind to the *IND* gene, and GO analysis suggests that most of them are ethylene responsive. GUS activity in *pIND::GUS* seedlings suggest that ethylene and jasmonic acid may negatively regulate *IND* and cytokinin may positively regulate *IND*.
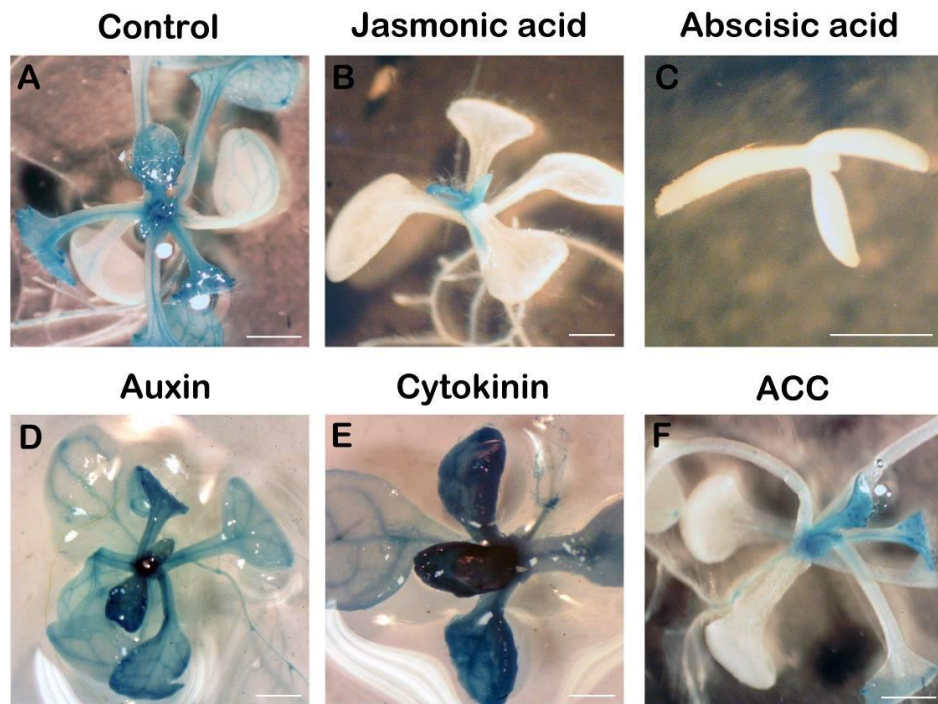
Figure 5.15 Hormonal treatments regulate IND-GUS activity in *pIND::GUS* seedlings. (A-F) GUS activity accumulation driven by the IND promoter in *pIND::GUS* seedlings (16 DAG): images show high expression in cytokinin **(E)** and reduced expression in jasmonic acid **(B),** abscisic acid **(C)**, and ACC **(F)** treated seedlings. When compared to untreated control **(A)**, no change in expression was observed in auxin **(D).** (Scale bar for A, B, D and F = 1.5 mm, E = 1 mm and C = 0.5 mm).
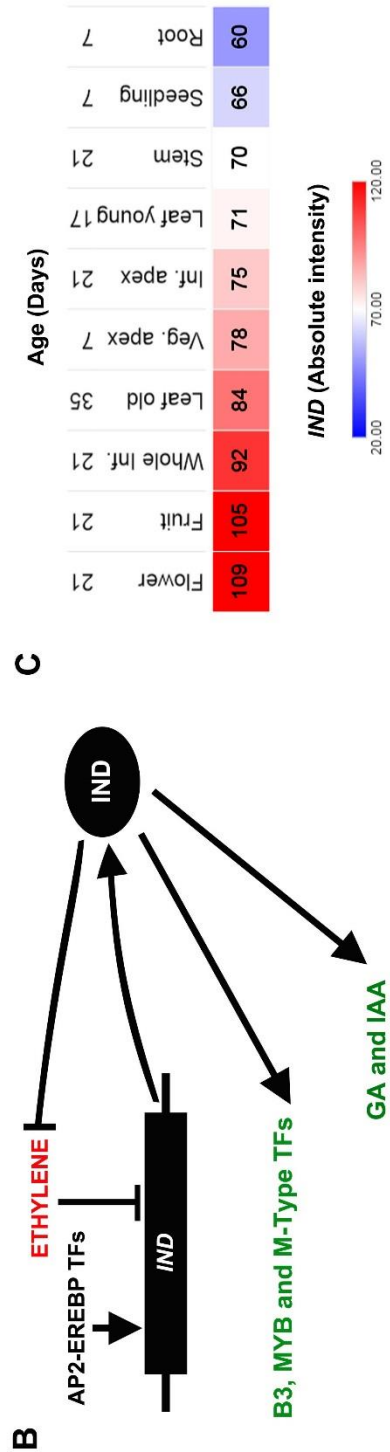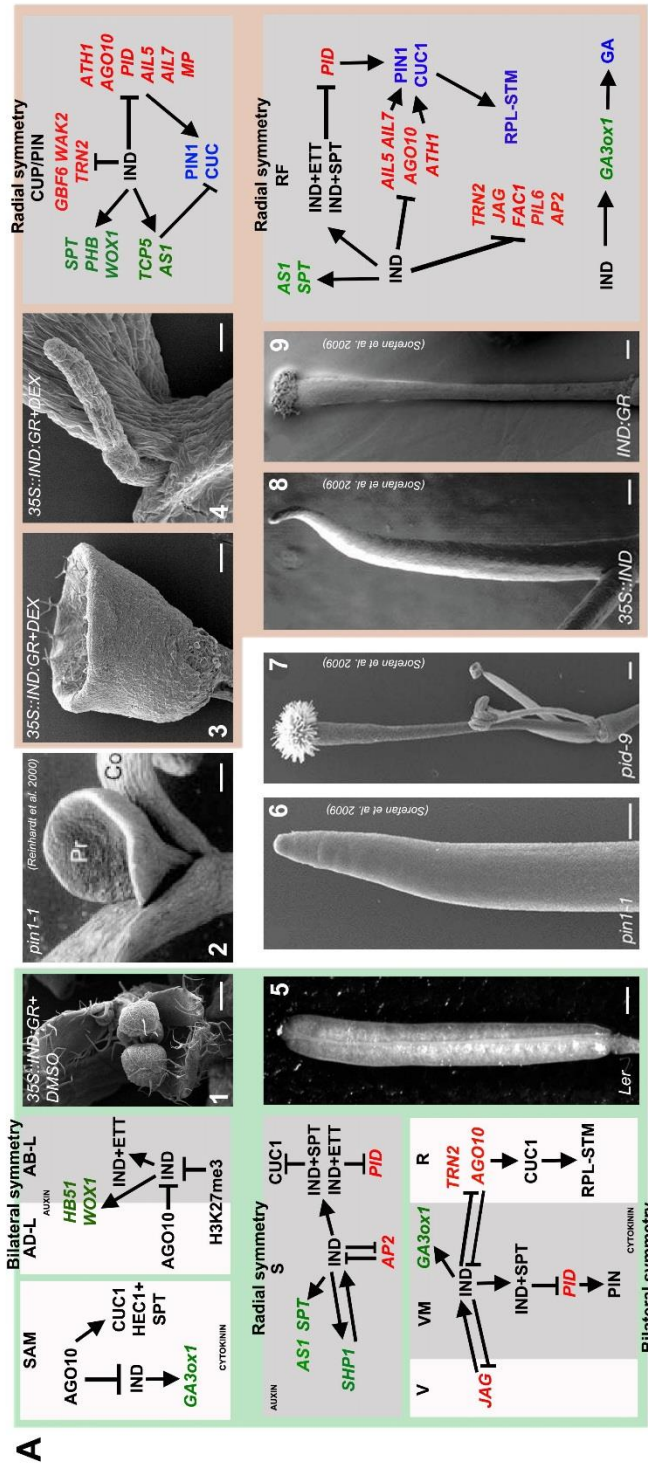
Figure 5.16 Schematic representation of IND regulated gene networks and associated leaf and fruit phenotypes. Overexpression of IND plants produce **(A3 and A4)** cup or pin shaped leaves, **(A8)** pin shaped inflorescence and **(A9)** radially symmetric fruit (similar to monocarpous). These phenotypes look similar to **(A2 and A6)** *pin1-1* and **(A7)** *pid-9* mutants. Schematic IND gene regulatory network involved in **(A1, A3, and A4)** seedling and **(A5, A8, and A9)** fruit development are outlined above as discussed in the text. **(B)** AP2-EREBP TFs and ethylene may regulate *IND,* and in response, IND may inhibit ethylene signalling and promote GA as well as IAA biosynthesis by upregulating *B3, MYB* and *M-Type* TFs. **(C)** The heat map shows absolute intensity values of *IND* (Gene expression data from At-TAX) in different tissues of *Arabidopsis* and high *IND* expression is observed in reproductive tissues and low expression in root and seedlings.

5.3 Discussion

5.3.1 Overexpression of IND impairs bilateral symmetry

Auxin and cytokinin hormones play a key role in development and patterning of SAM and gynoecium tissues (Besnard et al., 2014; Larsson et al., 2014; Moubayidin and Ostergaard, 2014; Qi et al., 2014; Reyes-Olalde et al., 2017). Auxin and cytokinin can regulate IND and orchestrate patterning in gynoecium. Auxin regulates polarity at the gynoecium apex by modulating IND and ETT interaction, and cytokinin promotes valve margin formation by regulating IND and SHP (Marsch-Martinez et al., 2012; Simonini et al., 2016). In addition, the data from this chapter also suggest auxin and cytokinin can modulate IND-regulated gene expression. In particular, functional gene expression analysis suggests that IND significantly downregulates meristem identity and bilateral symmetry genes in the presence of auxin and cytokinin. Bilateral symmetry is a symmetrical arrangement of an organism or part of an organism (e.g. leaf adaxial-abaxial) along a central axis divided into two identically reflected halves (Moubayidin and Ostergaard, 2015). Auxin transport is crucial for tuning bilateral symmetry in leaf (adaxial-abaxial) and gynoecium (medial-lateral) (Larsson et al., 2014; Qi et al., 2014). PID kinase regulates polar auxin transport via PIN proteins (Christensen et al., 2000; Friml et al., 2004). Results from this chapter show that IND can significantly downregulate *PID* expression in the presence of auxin and cytokinin. In addition to *PID*, IND may also repress PIN1 by downregulating *AGO10, AIL5, AIL7* and *MP* gene expression (Aida et al., 2002; Bhatia et al., 2016; Nole-Wilson et al., 2010; Pinon et al., 2013; Prasad et al., 2011; Roodbarkelari et al., 2015; Wenzel et al., 2007) (Fig 5.16). IND minimises auxin flow in the style (gynoecium apex) and valve margins by downregulating PIN1 (Moubayidin and Ostergaard, 2014). Similar to the gynoecium, overexpression of IND may minimise auxin flow between leaf and the SAM by downregulating PIN1 (Fig 5.12). Inhibition of auxin transport between leaf primordia and the SAM enhances leaf polarity defects and promotes abaxialised radially symmetric leaves (Qi et al., 2014). Overexpression of IND also produces radially symmetric leaves (PIN and CUP shaped), inflorescence (PIN shaped) and fruits (apical-basal monocarpous looking), and these phenotypes resemble *pin1, pid* and *cuc* mutants (Aida et al., 1997; Aida et al., 1999; Aida et al., 2002; Furutani et al., 2004; Moubayidin and Ostergaard, 2014; Reinhardt et al., 2000; Sorefan et al., 2009a) (Fig 5.16 A). Similar to the gynoecium apex, overexpression

of IND may be mimicking bilateral-to-radial transition in the leaf primordia (Moubayidin and Ostergaard, 2014). These studies suggest that overexpression of IND minimises auxin flow and impairs bilateral symmetry.

CUC genes also regulate bilateral symmetry (Furutani et al., 2004). PIN1, MP, ATH1, and AGO10-REV promote *CUC* function (Aida et al., 2002; Furutani et al., 2004; Gomez-Mena and Sablowski, 2008). PIN1 and MP regulate apical patterning (shift from radial to bilateral symmetry) in the embryo, partially by controlling *CUC* expression (Aida et al., 2002; Furutani et al., 2004). ATH1 also regulates the boundary between the stem and both vegetative and reproductive organs by partially controlling *CUC* genes (Gomez-Mena and Sablowski, 2008). The data in Chapter 3 and 4 suggest that AGO10-REV regulates bilateral symmetry of the leaf by promoting *CUC1* expression. IND, AS1, and TCPs negatively regulate *CUC1* (Koyama et al., 2010). Chapter 4 data suggest that IND negatively regulates *CUC1* and can directly repress *CUC1* expression. In addition to IND, CIN-like TCPs also negatively regulate *CUC1* via AS1, and overexpression of TCPs also suppresses the formation of shoot meristems by promoting fusion of cotyledons (Koyama et al., 2010). This suggests that overexpression of TCPs may impair the bilateral symmetry of the leaf (Koyama et al., 2010). Results from this chapter demonstrate that overexpression of IND may also negatively regulate *CUC1* expression by downregulating PIN1*, MP,* and *ATH1,* and upregulating *TCP5* and *AS1.* Loss of *cuc* can also affect RPL-STM and disrupt the replum-septum formation (Kamiuchi et al., 2014). These studies suggest that overexpression of IND gradually downregulates *CUC1* and impairs bilateral symmetry.

Overexpression of IND with auxin and cytokinin downregulates *TRN2* and *WAK2* expression. TRN2 and WAK2 proteins regulate leaf and SAM development (Chiu et al., 2007; Cnops et al., 2006; Wagner and Kohorn, 2001). TRN2 is a transmembrane tetraspanin protein, loss of *trn2* leads to asymmetric leaf growth and can affect leaf and SAM development (Chiu et al., 2007; Cnops et al., 2006). WAK2 regulates pectin activation and leaf cell expansion (Wagner and Kohorn, 2001). In addition to auxin minima and CUC1, IND may also impair the bilateral symmetry of the leaf by repressing *TRN2* and *WAK2*.

5.3.2 IND redundantly regulates floral development

The *Arabidopsis* gynoecium is a complex structure, which exhibits radial symmetry at the apex (similar to monocarpous) and bilateral symmetry at the medial-lateral domain (similar to syncarpous) (Smyth et al., 1990). Valve, valve margin and replum factors regulate gynoecium (medial-lateral) bilateral symmetry by competitively regulating each other. IND is one of the key factors for valve margin development (Liljegren et al., 2004a). IND regulates valve margin development by minimising auxin flow and also by promoting *SPT* and *GA3ox1* (Arnaud et al., 2010; Girin et al., 2011; Sorefan et al., 2009a). *IND-GUS, SPT-GUS* and *GA3ox1-GUS* expression in valve margins were previously reported in different studies and *Ind* or *spt* or *ga3ox1* mutants also failed to establish valve margin (Arnaud et al., 2010; Girin et al., 2011; Liljegren et al., 2004a). Which suggests IND and its downstream targets *SPT* and *GA3ox1* are required for valve margin development.

The valve factor JAG regulates valve margin development by promoting *SHP* and *IND* (Dinneny et al., 2005; Gonzalez-Reig et al., 2012). Data from this chapter suggests that overexpression of IND with cytokinin downregulates *JAG* expression. Alternatively, JAG may also negatively regulate *SHP* and *IND* by promoting *FUL* (Alonso-Cantabrana et al., 2007; Dinneny et al., 2005; Liljegren et al., 2004a). This suggests that IND may repress JAG/FUL to preserve the valve margin domain. Data from Chapters 3 and 4 suggest that AGO10-HD-ZIP III negatively regulates *IND* to promote replum development. In addition to AGO10, TRN2 also regulates carpel and replum development (Chiu et al., 2007). Data from this chapter suggests that overexpression of IND with cytokinin downregulates *AGO10* and *TRN2* expression. Together these studies demonstrate that IND may promote valve margin development by repressing valve and replum factors.

At stage 8/9, the apical style becomes radially symmetric. Different studies demonstrate that SHP1, SHP2, IND, SPT, ETT and HEC proteins promote style development (Colombo et al., 2010; Girin et al., 2011; Moubayidin and Ostergaard, 2014; Schuster et al., 2015; Sessions et al., 1997; Sessions and Zambryski, 1995; Simonini et al., 2016). In particular, IND-SPT proteins orchestrate the switch from bilateral to radial symmetry by controlling PIN protein localisation and thus generating the auxin ring at the apex (Girin et al., 2011; Moubayidin and Ostergaard, 2014). In addition, IND-ETT also contributes to the

166

formation of an auxin ring (auxin maxima) at the apex by repressing *PID* (Simonini et al., 2016). However, Chapter 4 results suggest that IND and SPT may repress *CUC1* and promote carpel fusion at the gynoecium apex (Nahar et al., 2012). Interestingly, AS1 and AS2 negatively regulate *CUCs* to promote the development of perianth organs (Xu et al., 2008). In addition, IND may also repress *CUC1* by promoting AS1 in gynoecium apex. But we do not know if ETT represses AS1 in the gynoecium apex because ETT and ARF4 promote leaf abaxial domain by epigenetically repressing AS1-AS2 (Machida et al., 2015). SHP1 and SHP2 promote *IND* and regulate valve margin development (Dinneny et al., 2005; Liljegren et al., 2000). AP2 negatively regulates *SHP* and *IND* to control the overgrowth of valve margin (Ripoll et al., 2011). In addition to valve margins, SHPs also regulate style development (Colombo et al., 2010). Interestingly, overexpression of IND with auxin downregulates *AP2* expression and upregulates *SHP1* expression. Therefore this suggests that IND may promote SHP1 in the gynoecium apex by repressing *AP2.* However, the loss of *ind* mutant fruits do not show any defects in style development, although *ind spt* double mutant fruits do show defects in style development (unfused carpels) (Girin et al., 2011). Together, these studies suggest that IND redundantly regulates symmetry transition and thus style development.

Interestingly, *IND* expression is also observed around stage 8 in anther and pollen of a wild-type *Arabidopsis* (Kay et al., 2013b). IND regulates anther and pollen development by promoting GA biosynthesis via GA3ox1 (Kay et al., 2013a). Similar to IND in the gynoecium, the MYB26 protein regulates anther indehiscence in *Arabidopsis* (Steiner-Lange et al., 2003; Yang et al., 2007). Data from this chapter suggest that overexpression of IND upregulates *MYB26* and *GA3ox1* expression. Together these studies demonstrate that IND may contribute to anther indehiscence by promoting *MYB26* and *GA3ox1*.

5.3.3 IND redundantly regulate leaf development

The *Arabidopsis* leaf is a complex structure that exhibits bilateral symmetry at the medial-lateral domain. Several proteins regulate leaf polarity (adaxial-abaxial) and bilateral symmetry. Loss or overexpression of polarity proteins can impair the leaf bilateral symmetry (Dello Ioio et al., 2012; Eshed et al., 2004; Ikezaki et al., 2010; Iwasaki et al., 2013; Kim et al., 2008; Koyama et al., 2010; Kumaran et al., 2002; Machida et al., 2015; McConnell et al., 2001; Nakata et al., 2012; Siegfried et al., 1999; Xu et al., 2003).

IND is also expressed in wild-type leaves, and overexpression of IND disrupts leaf bilateral symmetry and promotes radial symmetry. However, leaf bilateral symmetry is still intact in *ind* mutant plants, therefore IND may regulate leaf development by promoting *SPT* as well as interacting with SPT and ETT. However, overexpression of SPT decreases the cell size in fully expanded leaves (Ichihashi et al., 2010a). Alternatively, similar to the gynoecium, IND-SPT and IND-ETT may repress *PID* to control auxin transport in the leaf. Auxin transport from leaves to the shoot apex creates a lower auxin zone on the adaxial side of the leaf, and this auxin depletion is essential for leaf adaxial development (Qi et al., 2014). IND-SPT and IND-ETT may control PID-PIN1 and thus limit auxin in the adaxial side of the leaf. However, overexpression of IND may totally repress PID-PIN1 and promote auxin accumulation in leaf primordia (Caggiano et al., 2017; Guenot et al., 2012; Sorefan et al., 2009a) (Fig 5.12).

Auxin accumulation in leaf primordia significantly upregulates *WOX1* expression (Caggiano et al., 2017). Interestingly, overexpression of IND also significantly upregulates *WOX1* expression. Similar to *pWOX1::GUS*, *IND* promoter-driven GUS expression is also observed in leaf margin serrated regions (Nakata et al., 2012). WOX1 regulates blade outgrowth, and leaf adaxial-abaxial patterning and overexpression of WOX1 leads to defects in meristem development (Nakata et al., 2012; Zhang et al., 2011b). These studies suggest that IND-SPT and IND-ETT may promote *WOX1* in leaf primordia by modulating auxin transport. HB51 also regulates leaf margin development and serration (Saddic et al., 2006). In addition to WOX1 and IND, *HB51* promoter-driven GUS expression is also observed in the leaf margin and serrated regions (Saddic et al., 2006). This suggests that IND may regulate leaf serration by promoting *HB51* and *WOX1* expression. The leaf serration phenotype should be analysed in *ind* mutant plants. Together these studies demonstrate that IND redundantly regulates leaf development.

The results from Chapters 3 and 4 demonstrate that AGO10 can repress *IND* expression and suggests that minimising *IND* expression is essential for establishing leaf bilateral symmetry as well as for normal SAM development. Interestingly Pc-G proteins can also repress *IND* in leaf tissue by catalysing H3K27me3 methylation (Lafos et al., 2011). In addition to H3K27me, ampDAP-seq data analysis suggests that DNA methylation can also regulate TF and *IND* gene interactions (O'Malley et al., 2016). Together, these

studies suggest that histone and DNA methylation may also repress *IND* expression in the leaf tissue.

5.3.4 Hormones and IND can regulate each other

Auxin and cytokinin responses during gynoecium development are well studied using reporter lines *TCS::GUS* or *TCS::GFP* (Cytokinin) and *DR5::GUS* or *DR5::GFP* (Auxin) (Sabatini et al., 1999; Zurcher et al., 2013). At stage 8/9, cytokinin responses are previously observed in valve margin and medial tissues (CMMs) and auxin responses are previously observed in style as well as in medial-lateral tissues (replum and valves) (Larsson et al., 2014; Marsch-Martinez et al., 2012; Moubayidin and Ostergaard, 2014). However, cytokinin treatment can also rescue the valve margin in *shp* and *ind* mutants (Marsch-Martinez et al., 2012). Furthermore, results from this chapter show that cytokinin (BAP) can also promote *IND* promoter-driven GUS expression. Exogenous BAP application can also affect apical-basal patterning in gynoecium (Zuniga-Mayo et al., 2014). BAP-induced gynoecium apical-basal phenotypes also look similar to *ett, pin1* and overexpression of IND gynoecium phenotypes (Sessions et al., 1997; Sessions and Zambryski, 1995; Sorefan et al., 2009a; Zuniga-Mayo et al., 2014). These studies suggest that cytokinin may promote IND and redundantly regulate valve margin development. IND may also regulate cytokinin signalling via *SPT* because SPT promotes ARR1 and activates auxin biosynthesis via *TAA1* (Reyes-Olalde et al., 2017). Alternatively, IND may also control cytokinin biosynthesis because results from this data suggest that overexpression of IND can repress *IPT3* expression. IPT3 is one of the key regulators of cytokinin biosynthesis, and loss of *IPT3* can affect cytokinin production (Galichet et al., 2008). These studies suggest that IND may control cytokinin levels to promote apical tissue development because auxin maxima are essential for apical tissue patterning in gynoecia. Similar to SPT, IND may promote auxin biosynthesis because results from this chapter suggest that overexpression of IND can upregulate *TAA1* expression. We do not know if IND is regulating *TAA1* via *SPT*. Together these studies suggest that IND-SPT and auxin-cytokinin work together to establish patterning during gynoecium development.

Ethylene, JA and ABA are stress response hormones (Nguyen et al., 2016) and the results from this chapter show that ethylene and JA can repress *IND* promoter-driven GUS expression. In addition, *Arabidopsis thaliana* Tiling Array Express (At-TAX) abiotic stress

data also suggests that 12 hours of salt, osmotic and cold stress can repress *IND* expression (Fig 8.6) (Zeller et al., 2009). This suggests that stress responses can negatively regulate *IND* gene expression. However, overexpression of IND may also inhibit ethylene, JA and ABA biosynthesis and signalling. Therefore, IND may negatively regulate stress response signalling by repressing ethylene, JA and ABA. Ethylene, JA and ABA hormones crosstalk through ERFs under abiotic stress (Muller and Munne-Bosch, 2015). In addition, DAP-seq data analysis suggests that ERFs (AP2-EREBP TFs) can bind to cis-elements of the *IND* gene (O'Malley et al., 2016). We do not know if these ERFs can repress or induce *IND* expression. Together, these studies suggest that IND and stress response hormones may negatively regulate each other.

5.3.5 Conclusion

Even though gene expression study conducted in seedlings, still similar genes can regulate both seedling and floral development. So, results were discussed from the point of seedling as well as gynoecium development. This chapter demonstrates that auxin and cytokinin can enhance IND regulated gene expression. In particular, IND with auxin and cytokinin may promote radial symmetry by inhibiting bilateral symmetry. IND may regulate radial symmetry by indirectly repressing PIN1 and CUC1 by downregulating *PID* and also by regulating other elements as shown in figure 5.16A. IND also regulates genes involved in floral and leaf development. Gene expression data suggest that IND may redundantly regulate style development and apical carpel fusion by upregulating *AS1, SPT,* and *SHP1* and also by downregulating *AP2, PID* and *CUC1* (Fig 5.16 A5). Gene expression data suggest that IND may redundantly regulate leaf development by upregulating *WOX1* and *HB51* (Fig 5.16 A1). The functional relationship of these genes should be investigated by classical genetic studies. In addition to AGO10, H3K27me may promote bilateral symmetry of the leaf by repressing *IND* (Fig 5.16 A1). A large number of AP2-EREBP family TFs bind to the IND gene. AP2-EREBP TFs and cytokinins may promote *IND* gene expression (Fig 5.16 B). Interestingly, many of the IND binding TFs are involved in ethylene signalling. However, IND and ethylene responses may negatively regulate each other (Fig 5.16 B).

Chapter 6

General Discussion
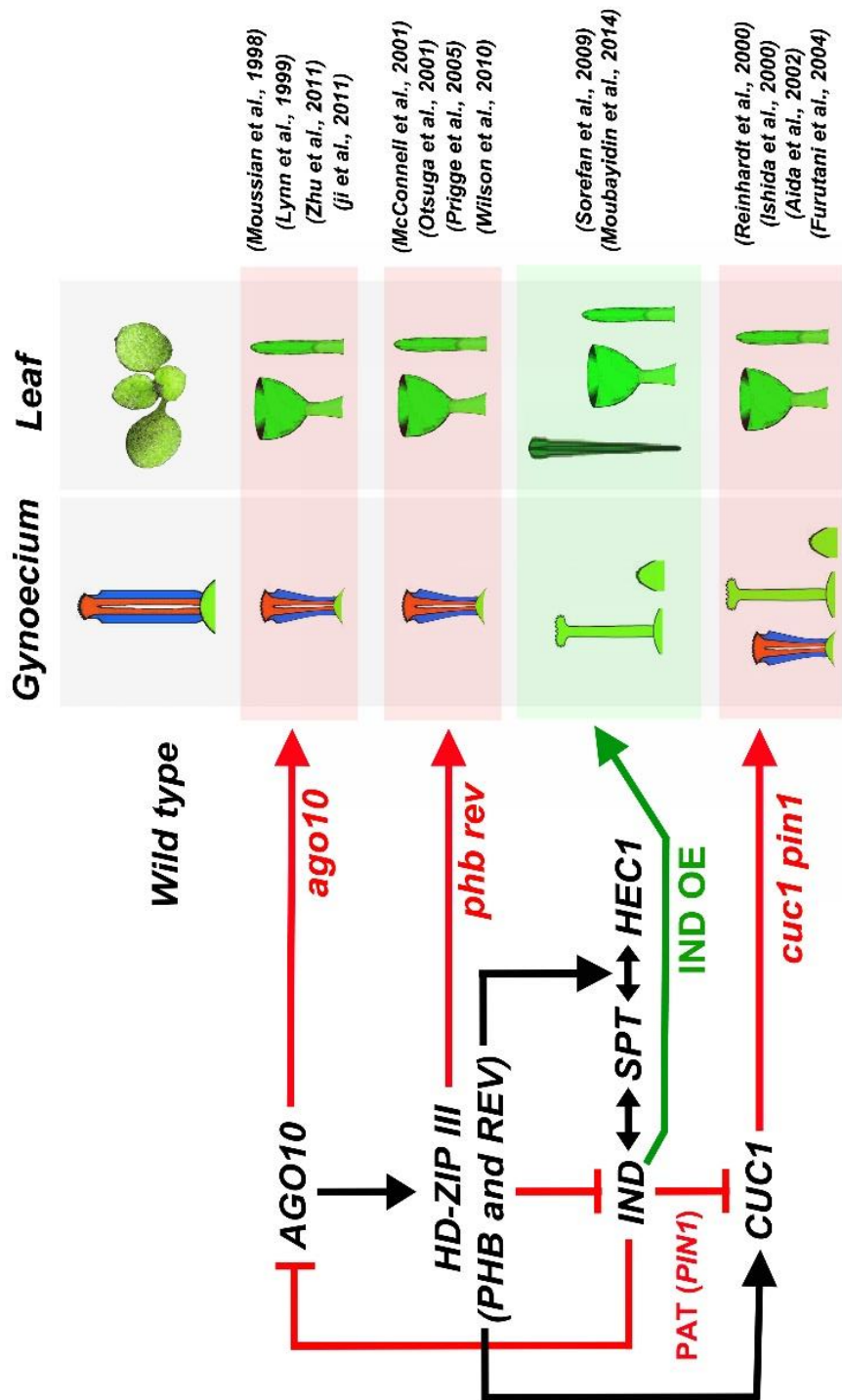
Figure 6.1 Schematic representation of the AGO10-PHB-REV-IND-CUC1 signalling cascade and associated mutant or overexpression phenotypes. The *ago10, phb rev,* and *cuc1 pin1* mutants produce identical leaf (CUP and PIN) and gynoecium (small bulged) phenotypes. Overexpression of IND also produces similar phenotypes possibly by repressing PAT, *CUC1,* and *AGO10*. However, AGO10 promotes *CUC1, SPT-HEC1* and represses *IND* via PHB and REV. This suggests that AGO10 and IND repress each other's expression.

CHAPTER 6. General Discussion

We found that AGO10 and IND antagonise each other's expression as a mechanism to maintain repression of IND in AGO10 expressing tissues. Morphological analysis from Chapter 3 suggests that repression of IND by AGO10 is essential for SAM and replum tissue polarity because overexpression of IND impairs bilateral tissue symmetry. Molecular and cell biology analysis from Chapters 4 and 5 demonstrate that IND overexpression may negatively regulate bilateral tissue symmetry by repressing polar auxin transport (PAT), *CUC1* and *AGO10*. I suggest that the ability of AGO10 to switch off IND activity in SAM and replum tissue may be essential for establishing tissue bilateral symmetry.

6.1 Understanding the role of IND in gynoecium and SAM development

The *Arabidopsis* gynoecium is the most complex structure in plants, and its patterning occurs along three axes: apical-basal, medial-lateral, and abaxial-adaxial. TFs, hormones and transport proteins orchestrate gynoecium patterning. We show that IND dependent gene regulatory networks may be conserved in the seedlings and gynoecium (Chapter 5). Therefore, the genetic networks we identify in our microarray analysis may have important implications for understanding gynoecium development. In particular SHP1, SHP2, IND, SPT, ETT and HEC proteins as well as auxin maxima are important for apical gynoecium patterning (Colombo et al., 2010; Girin et al., 2011; Moubayidin and Ostergaard, 2014; Schuster et al., 2015; Sessions et al., 1997; Sessions and Zambryski, 1995; Simonini et al., 2016).

Interactions between SHP1, SHP2, IND, SPT, ETT and HEC proteins are essential for proper gynoecium development. SHP1 and SHP2 proteins promote *IND* expression in the gynoecium (Liljegren et al., 2004a). AP2 acts upstream of SHP1, SHP2 and IND by repressing their expression in the gynoecium (Ripoll et al., 2011). I show that inducing IND in the presence of auxin (Chapter 5) downregulates *AP2* and upregulate *SPT* and *SHP1* expression. This suggests that in the absence of auxin, AP2 represses SPT and SHP1, however IND integrates auxin signals to promote expression of *SHP1* and *SPT*, thereby promoting apical gynoecium development through a positive feedback mechanism.

IND-SPT, IND-ETT, and SPT-HEC proteins interact to orchestrate the switch from bilateral (medial-lateral) to radial (apical) symmetry (Girin et al., 2011; Gremski et al., 2007; Moubayidin and Ostergaard, 2014; Schuster et al., 2015; Simonini et al., 2016). Functional loss of these proteins can impair apical tissue growth (e.g., unfused carpels) (Girin et al., 2011; Schuster et al., 2015). In particular, *CUC1* and *CUC2* genes inhibit the radiality of apical gynoecia (Nahar et al., 2012), and SPT and AS1 act upstream of CUC1/2 by repressing their expression. (Gonzalez-Reig et al., 2012; Nahar et al., 2012). Inducible SPT gene-expression data from Chapter 4 suggests that SPT does not directly regulate *CUC1* and *CUC2* expression. However, IND can directly repress *CUC1* and *PID* expression and upregulate *AS1* expression (Chapter 4 and 5). PID promotes *CUC* expression in the *Arabidopsis* embryo, and we do not know whether PID can regulate *CUC1* and *CUC2* expression in gynoecium (Furutani et al., 2004). This suggests that IND may directly or indirectly repress *CUC1* expression and may promote apical gynoecium patterning. However, this should be investigated by conducting classical genetic studies.

Valve, valve margin, and replum factors regulate medial-lateral gynoecium patterning by competitively regulating each other. IND is an essential factor for valve margin development (Liljegren et al., 2004a). IND and SPT regulate valve margin development by minimising auxin flow and by promoting cytokinin responses in the valve margin (Arnaud et al., 2010; Girin et al., 2011; Sorefan et al., 2009a). JAG positively regulates the valve margin identity gene *IND* and the valve-promoting gene *FUL* (Dinneny et al., 2005; Gonzalez-Reig et al., 2012). However, FUL negatively regulates IND and restricts IND expression to the valve margin (Liljegren et al., 2004a). We show that inducing IND in the presence of cytokinin (Chapter 5) downregulates *JAG* expression, and this demonstrates that IND may restrict *JAG-FUL* expression to the valve by a negative feedback mechanism. However, this phenomenon should be investigated further.

IND is weakly expressed in seedlings and the vegetative meristem (Laubinger et al., 2008). However, there are no research studies to support a functional role for IND in SAM development. Morphological studies from Chapter 3 demonstrate that IND is required to promote meristem size. However, the reduced *ind^{ind-6}* SAM size did not affect SAM and leaf development. Interestingly, overexpression of IND resulted in a large meristem, and leaf development was arrested (Chapter 3). Both the published

literature and *ind*[ind-6] SAM size data from Chapter 3 suggest that IND may regulate SAM size by controlling polar nuclei fusion during female gametogenesis (Pagnussat et al., 2005) or by controlling cytokinesis (by unequal cell division) (Wu et al., 2006). However, the pattern of cytokinesis in the *ind*[ind-6] SAM should be investigated further. Similar to their role in the gynoecium, IND-SPT and IND-ETT may repress *PID* and control auxin transport in the leaf (Girin et al., 2011; Simonini et al., 2016). However, loss of *ind*[ind-6] did not affect leaf bilateral symmetry (Chapter 3). The *Arabidopsis* leaf exhibits bilateral symmetry at the medial-lateral domain. Interestingly, overexpression of IND disrupted bilateral leaf symmetry and promoted abaxialised radial symmetry (PIN and CUP shaped) (Chapter 3) (Moubayidin and Ostergaard, 2014). Auxin transport from leaves to the shoot apex creates a lower auxin zone on the adaxial side of the leaf, and this auxin depletion is essential for leaf adaxial development (Qi et al., 2014). Overexpression of IND downregulates *PID-PIN1* and thus impairs the bilateral leaf symmetry (Chapter 3 and 5) (Caggiano et al., 2017; Guenot et al., 2012; Sorefan et al., 2009a). This suggests that IND may establish leaf polarity by regulating PAT. However, the role of IND-SPT and IND-ETT in leaf tissue should be investigated by conducting classical genetic studies. Different proteins regulate leaf polarity (adaxial-abaxial) and loss or overexpression of polarity proteins can impair leaf bilateral symmetry (Dello Ioio et al., 2012; Eshed et al., 2004; Ikezaki et al., 2010; Iwasaki et al., 2013; Kim et al., 2008; Koyama et al., 2010; Kumaran et al., 2002; Machida et al., 2015; McConnell et al., 2001; Nakata et al., 2012; Siegfried et al., 1999; Xu et al., 2003). Overexpression of IND can also upregulate or downregulate leaf polarity genes. WOX1 regulates leaf adaxial-abaxial patterning (Nakata et al., 2012; Zhang et al., 2011b) and we have found in Chapter 3 and 5 that overexpression of IND significantly upregulates *WOX1* expression. However, auxin accumulation in leaf primordia also significantly upregulates WOX1 expression (Caggiano et al., 2017). This suggests that IND may indirectly promote *WOX1* by controlling PAT in leaf primordia. AGO10 regulates leaf adaxial fate (Liu et al., 2009) and induction of IND can directly downregulate *AGO10* expression (Chapter 3). Taken together, these studies support the findings in this thesis that overexpression of IND may impair bilateral leaf symmetry by altering leaf polarity gene expression.

6.2 Understanding the role of AGO10-IND in SAM development

In *Arabidopsis*, AGO10 is expressed in seedlings, particularly in the SAM and adaxial domain of the leaf. AGO10 regulates SAM development and leaf polarity by preserving *HD-ZIP III* gene expression (Liu et al., 2009; Tucker et al., 2008; Zhang and Zhang, 2012; Zhu et al., 2011b). Loss of *AGO10* impairs SAM and leaf development (Endrizzi et al., 1996; Moussian et al., 1998). In particular, the *ago10^{zwl-3}* seedlings produced CUP and PIN phenotypes (Chapter 3). However, several studies have demonstrated that *pin1, pid,* and *cuc* mutants can produce CUP- and PIN-shaped phenotypes (Aida et al., 1997; Aida et al., 1999; Aida et al., 2002; Furutani et al., 2004; Hibara et al., 2006) (Fig 6.1). PIN1, PID and CUC genes are important for proper meristem and leaf development because these proteins regulate auxin responses (Aida et al., 2002; Furutani et al., 2004; Heisler et al., 2005; Huang et al., 2010; Larsson et al., 2014). Interestingly, *PIN1, PID,* and *CUC1/2/3* expression are decreased in *ago10^{zwl-3}* (CUP and PIN) seedlings, and this data suggests that *ago10^{zwl-3}* (CUP and PIN) phenotypes are defective in auxin signalling (Chapter 4). However, several studies suggest that auxin responses and *HD-ZIP III* (*PHB* and *REV*) genes can regulate each other (Bou-Torrent et al., 2012; Muller et al., 2016; Nole-Wilson et al., 2010; Reinhart et al., 2013). In addition, PHB and REV can upregulate *CUC1* expression (Chapter 4). Taken together, these studies support the findings of this thesis that the AGO10-HD-ZIP III pathway can control auxin responses as well as *CUC1* expression and thus regulate SAM development.

Overexpression of IND can impair bilateral leaf symmetry by inhibiting PAT as well as by directly downregulating *CUC1* (Chapter 3, 4 and 5)*.* Interestingly, *IND* expression was increased whereas *PIN1* and *CUC1* were decreased in *ago10^{zwl-3}* seedlings (Chapter 3 and 4). We found that loss of *IND* partially rescues *CUC1* expression as well as *ago10* phenotypes, and this suggests that increased IND expression may have promoted CUP and PIN phenotypes in *ago10^{zwl-3}*. IND may also modulate PAT and *CUC1* expression by regulating *AS1, TCP, AIL5, AIL7* and *MP* expression (Chapter 5) (Aida et al., 2002; Bhatia et al., 2016; Koyama et al., 2010; Pinon et al., 2013; Prasad et al., 2011; Wenzel et al., 2007)*.* However, PHB and REV can indirectly downregulate *IND* gene expression (Chapter 3), and this suggests that AGO10 indirectly inhibits *IND* via HD-ZIP III transcription factors in wild-type seedlings. Together these studies suggest that AGO10-PHB-REV may promote SAM development and leaf bilateral symmetry by repressing *IND* (Fig 6.1).

6.3 Understanding the role of AGO10-IND in replum development

AGO10-REV regulate floral meristem differentiation and gynoecium development (Ji et al., 2011; Nole-Wilson et al., 2010). In particular, REV promotes CMM development (Nole-Wilson et al., 2010). In addition, *CUC1* and *CUC2* genes promote CMM development (Ishida et al., 2000; Kamiuchi et al., 2014; Nahar et al., 2012). Interestingly, REV can directly upregulate *CUC1* expression (Chapter 4). However, the *ago10* and *cuc1 cuc2* mutants produce small fruits with reduced replum (width), and these fruits are identical to *rpl* mutants (Chapter 3 and 4) (Ishida et al., 2000; Roeder et al., 2003) (Fig 6.1). STM and RPL proteins regulate replum development (Bhatt et al., 2004; Ragni et al., 2008; Roeder et al., 2003). Overexpression of CUC1 upregulates *STM* and *RPL,* which suggests that CUC1 may regulate replum development by promoting *STM-RPL* (Chapter 4). Together these studies suggest that AGO10-REV may regulate replum development by promoting *CUC1, STM,* and *RPL.* However, the role of AGO10-CUC1 and AGO10-RPL in gynoecium tissue should be investigated by conducting classical genetic studies.

Replum factors and valve margin factors regulate each other in an antagonistic fashion. *IND* promotes valve margin development, and it has been demonstrated that *IND* expression is inhibited in the replum by RPL (Liljegren et al., 2000; Liljegren et al., 2004a; Roeder et al., 2003). In addition, AGO10 may promote replum development by repressing *IND* expression because the loss of *IND* rescues *ago10* replum phenotype in *ind ago10* double mutants (Chapter 3). IND may promote valve margin development by repressing *AGO10* and *CUC1* expression. IND represses *CUC1,* both directly but also possibly indirectly by inhibiting PAT and upregulating *AS1* (Chapter 4 and 5). AS1 negatively regulates replum development by repressing medial factors *BP, RPL, CUC1* and *CUC2* (Gonzalez-Reig et al., 2012; Xu et al., 2008). These studies suggest that AGO10 and IND may antagonistically regulate each other along the mediolateral axis of the *Arabidopsis* fruit (Fig 6.1). However, the role of AGO10-IND-CUC1 in the gynoecium tissue should be investigated further.

6.4 Summary of findings

To summarise, this thesis has found:

- Overexpression of IND inhibits SAM development and tissue bilateral symmetry.
- Overexpression of IND impairs leaf bilateral symmetry by repressing PAT, *AGO10* and *CUC1* expression.
- *AGO10-PHB-REV* promote SAM and replum development by repressing *IND*.

Further research should focus on:

- Investigating the role of IND-ETT and IND-SPT in leaf development.
- Investigating the role of AGO10 and IND in CMM development.

Chapter 7

References

CHAPTER 7. References

- Adams, D.O., and Yang, S.F. (1979). Ethylene Biosynthesis - Identification of 1-Aminocyclopropane-1-Carboxylic Acid as an Intermediate in the Conversion of Methionine to Ethylene. Proceedings of the National Academy of Sciences of the United States of America *76*, 170-174.

- Aida, M., Ishida, T., Fukaki, H., Fujisawa, H., and Tasaka, M. (1997). Genes involved in organ separation in Arabidopsis: an analysis of the cup-shaped cotyledon mutant. The Plant cell *9*, 841-857.

- Aida, M., Ishida, T., and Tasaka, M. (1999). Shoot apical meristem and cotyledon formation during Arabidopsis embryogenesis: interaction among the CUP-SHAPED COTYLEDON and SHOOT MERISTEMLESS genes. Development *126*, 1563-1570.

- Aida, M., Vernoux, T., Furutani, M., Traas, J., and Tasaka, M. (2002). Roles of PIN-FORMED1 and MONOPTEROS in pattern formation of the apical region of the Arabidopsis embryo. Development *129*, 3965-3974.

- Alonso-Cantabrana, H., Ripoll, J.J., Ochando, I., Vera, A., Ferrandiz, C., and Martinez-Laborda, A. (2007). Common regulatory networks in leaf and fruit patterning revealed by mutations in the Arabidopsis ASYMMETRIC LEAVES1 gene. Development *134*, 2663-2671.

- Alvarez-Buylla, E.R., Liljegren, S.J., Pelaz, S., Gold, S.E., Burgeff, C., Ditta, G.S., Vergara-Silva, F., and Yanofsky, M.F. (2000). MADS-box gene evolution beyond flowers: expression in pollen, endosperm, guard cells, roots and trichomes. The Plant journal : for cell and molecular biology *24*, 457-466.

- Argyros, R.D., Mathews, D.E., Chiang, Y.H., Palmer, C.M., Thibault, D.M., Etheridge, N., Argyros, D.A., Mason, M.G., Kieber, J.J., and Schaller, G.E. (2008). Type B response regulators of Arabidopsis play key roles in cytokinin signaling and plant development. Plant Cell *20*, 2102-2116.

- Ariel, F.D., Manavella, P.A., Dezar, C.A., and Chan, R.L. (2007). The true story of the HD-Zip family. Trends in plant science *12*, 419-426.

- Arnaud, N., Girin, T., Sorefan, K., Fuentes, S., Wood, T.A., Lawrenson, T., Sablowski, R., and Ostergaard, L. (2010). Gibberellins control fruit patterning in Arabidopsis thaliana. Genes & development *24*, 2127-2132.

- Arnone, M.I., and Davidson, E.H. (1997). The hardwiring of development: organization and function of genomic regulatory systems. Development *124*, 1851-1864.

- Aulie, R.P. (1961). Caspar Friedrich Wolff and his 'Theoria generationis', 1759. J Hist Med Allied Sci *16*, 124-144.

- Axtell, M.J. (2013). Classification and comparison of small RNAs from plants. Annu Rev Plant Biol *64*, 137-159.

- Barkoulas, M., Galinha, C., Grigg, S.P., and Tsiantis, M. (2007). From genes to shape: regulatory interactions in leaf development. Current opinion in plant biology *10*, 660-666.

- Barton, M.K. (2010). Twenty years on: the inner workings of the shoot apical meristem, a developmental dynamo. Developmental biology *341*, 95-113.

- Besnard, F., Refahi, Y., Morin, V., Marteaux, B., Brunoud, G., Chambrier, P., Rozier, F., Mirabet, V., Legrand, J., Laine, S*., et al.* (2014). Cytokinin signalling inhibitory fields provide robustness to phyllotaxis. Nature *505*, 417-421.

- Bhatia, N., Bozorg, B., Larsson, A., Ohno, C., Jonsson, H., and Heisler, M.G. (2016). Auxin Acts through MONOPTEROS to Regulate Plant Cell Polarity and Pattern Phyllotaxis. Current Biology *26*, 3202-3208.

- Bhatt, A.A., Etchells, J.P., Canales, C., Lagodienko, A., and Dickinson, H. (2004). VAAMANA - a BEL1-like homeodomain protein, interacts with KNOX proteins BP and STM and regulates inflorescence stem growth in Arabidopsis. Gene *328*, 103-111.

- Birnbaum, K., Benfey, P.N., and Shasha, D.E. (2001). cis element/transcription factor analysis (cis/TF): a method for discovering transcription factor/cis element relationships. Genome Res *11*, 1567-1573.

- Boer, D.R., Freire-Rios, A., van den Berg, W.A., Saaki, T., Manfield, I.W., Kepinski, S., Lopez-Vidrieo, I., Franco-Zorrilla, J.M., de Vries, S.C., Solano, R*., et al.* (2014). Structural basis for DNA binding specificity by the auxin-dependent ARF transcription factors. Cell *156*, 577-589.

- Bou-Torrent, J., Salla-Martret, M., Brandt, R., Musielak, T., Palauqui, J.C., Martinez-Garcia, J.F., and Wenkel, S. (2012). ATHB4 and HAT3, two class II HD-

ZIP transcription factors, control leaf development in Arabidopsis. Plant signaling & behavior *7*, 1382-1387.

- Brandt, R., Salla-Martret, M., Bou-Torrent, J., Musielak, T., Stahl, M., Lanz, C., Ott, F., Schmid, M., Greb, T., Schwarz, M.*, et al.* (2012). Genome-wide binding-site analysis of REVOLUTA reveals a link between leaf patterning and light-mediated growth responses. The Plant journal : for cell and molecular biology *72*, 31-42.

- Brodersen, P., and Voinnet, O. (2006). The diversity of RNA silencing pathways in plants. Trends in genetics : TIG *22*, 268-280.

- Buechel, S., Leibfried, A., To, J.P., Zhao, Z., Andersen, S.U., Kieber, J.J., and Lohmann, J.U. (2010). Role of A-type ARABIDOPSIS RESPONSE REGULATORS in meristem maintenance and regeneration. European journal of cell biology *89*, 279-284.

- Byrne, M.E., Groover, A.T., Fontana, J.R., and Martienssen, R.A. (2003). Phyllotactic pattern and stem cell fate are determined by the Arabidopsis homeobox gene BELLRINGER. Development *130*, 3941-3950.

- Caggiano, M.P., Yu, X.L., Bhatia, N., Larsson, A., Ram, H., Ohno, C., Sappl, P., Meyerowitz, E.M., Jonsson, H., and Heisler, M.G. (2017). Cell type boundaries organize plant development. Elife *6*.

- Chen, M.K., Wilson, R.L., Palme, K., Ditengou, F.A., and Shpak, E.D. (2013). ERECTA Family Genes Regulate Auxin Transport in the Shoot Apical Meristem and Forming Leaf Primordia. Plant physiology *162*, 1978-1991.

- Chen, Y.H., Yang, X.Y., He, K., Liu, M.H., Li, J.G., Gao, Z.F., Lin, Z.Q., Zhang, Y.F., Wang, X.X., Qiu, X.M.*, et al.* (2006). The MYB transcription factor superfamily of arabidopsis: Expression analysis and phylogenetic comparison with the rice MYB family. Plant Mol Biol *60*, 107-124.

- Cheng, Y., Dai, X., and Zhao, Y. (2006). Auxin biosynthesis by the YUCCA flavin monooxygenases controls the formation of floral organs and vascular tissues in Arabidopsis. Genes & development *20*, 1790-1799.

- Chiu, W.H., Chandler, J., Cnops, G., Van Lijsebettens, M., and Werr, W. (2007). Mutations in the TORNADO2 gene affect cellular decisions in the peripheral zone of the shoot apical meristem of Arabidopsis thaliana. Plant Mol Biol *63*, 731-744.

- Christensen, S.K., Dagenais, N., Chory, J., and Weigel, D. (2000). Regulation of auxin response by the protein kinase PINOID. Cell *100*, 469-478.

- Chuck, G., Lincoln, C., and Hake, S. (1996). KNAT1 induces lobed leaves with ectopic meristems when overexpressed in Arabidopsis. Plant Cell *8*, 1277-1289.

- Ciolkowski, I., Wanke, D., Birkenbihl, R.P., and Somssich, I.E. (2008). Studies on DNA-binding selectivity of WRKY transcription factors lend structural clues into WRKY-domain function. Plant Mol Biol *68*, 81-92.

- Cnops, G., Neyt, P., Raes, J., Petrarulo, M., Nelissen, H., Malenica, N., Luschnig, C., Tietz, O., Ditengou, F., Palme, K.*, et al.* (2006). The TORNADO1 and TORNADO2 genes function in several patterning processes during early leaf development in Arabidopsis thaliana. Plant Cell *18*, 852-866.

- Cole, M., Nolte, C., and Werr, W. (2006). Nuclear import of the transcription factor SHOOT MERISTEMLESS depends on heterodimerization with BLH proteins expressed in discrete sub-domains of the shoot apical meristem of Arabidopsis thaliana. Nucleic Acids Res *34*, 1281-1292.

- Colombo, M., Brambilla, V., Marcheselli, R., Caporali, E., Kater, M.M., and Colombo, L. (2010). A new role for the SHATTERPROOF genes during Arabidopsis gynoecium development. Developmental biology *337*, 294-302.

- Cruz Castillo, M., Martinez, C., Buchala, A., Metraux, J.P., and Leon, J. (2004). Gene-specific involvement of beta-oxidation in wound-activated responses in Arabidopsis. Plant physiology *135*, 85-94.

- Dello Ioio, R., Galinha, C., Fletcher, A.G., Grigg, S.P., Molnar, A., Willemsen, V., Scheres, B., Sabatini, S., Baulcombe, D., Maini, P.K.*, et al.* (2012). A PHABULOSA/cytokinin feedback loop controls root growth in Arabidopsis. Current biology : CB *22*, 1699-1704.

- Dharmasiri, N., Dharmasiri, S., and Estelle, M. (2005). The F-box protein TIR1 is an auxin receptor. Nature *435*, 441.

- Dinneny, J.R., Weigel, D., and Yanofsky, M.F. (2005). A genetic framework for fruit patterning in Arabidopsis thaliana. Development *132*, 4687-4696.

- Dodsworth, S. (2009). A diverse and intricate signalling network regulates stem cell fate in the shoot apical meristem. Developmental biology *336*, 1-9.

- Eklund, D.M., Staldal, V., Valsecchi, I., Cierlik, I., Eriksson, C., Hiratsu, K., Ohme-Takagi, M., Sundstrom, J.F., Thelander, M., Ezcurra, I*., et al.* (2010). The Arabidopsis thaliana STYLISH1 Protein Acts as a Transcriptional Activator Regulating Auxin Biosynthesis. Plant Cell *22*, 349-363.

- Elhiti, M., and Stasolla, C. (2009). Structure and function of homodomain-leucine zipper (HD-Zip) proteins. Plant signaling & behavior *4*, 86-88.

- Emery, J.F., Floyd, S.K., Alvarez, J., Eshed, Y., Hawker, N.P., Izhaki, A., Baum, S.F., and Bowman, J.L. (2003). Radial patterning of Arabidopsis shoots by class III HD-ZIP and KANADI genes. Current biology : CB *13*, 1768-1774.

- Endo, Y., Iwakawa, H.O., and Tomari, Y. (2013). Arabidopsis ARGONAUTE7 selects miR390 through multiple checkpoints during RISC assembly. EMBO reports *14*, 652-658.

- Endrizzi, K., Moussian, B., Haecker, A., Levin, J.Z., and Laux, T. (1996). The SHOOT MERISTEMLESS gene is required for maintenance of undifferentiated cells in Arabidopsis shoot and floral meristems and acts at a different regulatory level than the meristem genes WUSCHEL and ZWILLE. Plant Journal *10*, 967-979.

- Engelhorn, J., Moreau, F., Fletcher, J.C., and Carles, C.C. (2014). ULTRAPETALA1 and LEAFY pathways function independently in specifying identity and determinacy at the Arabidopsis floral meristem. Ann Bot-London *114*, 1497-1505.

- Englbrecht, C.C., Schoof, H., and Bohm, S. (2004). Conservation, diversification and expansion of C2H2 zinc finger proteins in the Arabidopsis thaliana genome. Bmc Genomics *5*.

- Eshed, Y., Izhaki, A., Baum, S.F., Floyd, S.K., and Bowman, J.L. (2004). Asymmetric leaf development and blade expansion in Arabidopsis are mediated by KANADI and YABBY activities. Development *131*, 2997-3006.

- Eulgem, T., Rushton, P.J., Robatzek, S., and Somssich, I.E. (2000). The WRKY superfamily of plant transcription factors. Trends in plant science *5*, 199-206.

- Fahlgren, N., Montgomery, T.A., Howell, M.D., Allen, E., Dvorak, S.K., Alexander, A.L., and Carrington, J.C. (2006). Regulation of AUXIN RESPONSE FACTOR3 by TAS3 ta-siRNA affects developmental timing and patterning in Arabidopsis. Current biology : CB *16*, 939-944.

- Fambrini, M., and Pugliesi, C. (2013). Usual and unusual development of the dicot leaf: involvement of transcription factors and hormones. Plant cell reports *32*, 899-922.

- Fletcher, J.C. (2001). The ULTRAPETALA gene controls shoot and floral meristem size in Arabidopsis. Development *128*, 1323-1333.

- Fletcher, J.C. (2002). Shoot and floral meristem maintenance in arabidopsis. Annu Rev Plant Biol *53*, 45-66.

- Franco-Zorrilla, J.M., Lopez-Vidriero, I., Carrasco, J.L., Godoy, M., Vera, P., and Solano, R. (2014). DNA-binding specificities of plant transcription factors and their potential to define target genes. Proceedings of the National Academy of Sciences of the United States of America *111*, 2367-2372.

- Friml, J., Vieten, A., Sauer, M., Weijers, D., Schwarz, H., Hamann, T., Offringa, R., and Jurgens, G. (2003). Efflux-dependent auxin gradients establish the apical-basal axis of Arabidopsis. Nature *426*, 147-153.

- Friml, J., Yang, X., Michniewicz, M., Weijers, D., Quint, A., Tietz, O., Benjamins, R., Ouwerkerk, P.B.F., Ljung, K., Sandberg, G.*, et al.* (2004). A PINOID-dependent binary switch in apical-basal PIN polar targeting directs auxin efflux. Science *306*, 862-865.

- Fujimoto, S., Matsunaga, S., Yonemura, M., Uchiyama, S., Azuma, T., and Fukui, K. (2004). Identification of a novel plant MAR DNA binding protein localized on chromosomal surfaces. Plant Mol Biol *56*, 225-239.

- Furutani, M., Vernoux, T., Traas, J., Kato, T., Tasaka, M., and Aida, M. (2004). PIN-FORMED1 and PINOID regulate boundary formation and cotyledon development in Arabidopsis embryogenesis. Development *131*, 5021-5030.

- Galichet, A., Hoyerova, K., Kaminek, M., and Gruissem, W. (2008). Farnesylation directs AtIPT3 subcellular localization and modulates cytokinin biosynthesis in Arabidopsis. Plant physiology *146*, 1155-1164.

- Garcia, D., Collier, S.A., Byrne, M.E., and Martienssen, R.A. (2006). Specification of leaf polarity in Arabidopsis via the trans-acting siRNA pathway. Current biology : CB *16*, 933-938.

- Girin, T., Paicu, T., Stephenson, P., Fuentes, S., Korner, E., O'Brien, M., Sorefan, K., Wood, T.A., Balanza, V., Ferrandiz, C.*, et al.* (2011). INDEHISCENT and

SPATULA interact to specify carpel and valve margin tissue and thus promote seed dispersal in Arabidopsis. Plant Cell *23*, 3641-3653.

- Girin, T., Sorefan, K., and Ostergaard, L. (2009). Meristematic sculpting in fruit development. Journal of experimental botany *60*, 1493-1502.

- Goda, H., Sasaki, E., Akiyama, K., Maruyama-Nakashita, A., Nakabayashi, K., Li, W., Ogawa, M., Yamauchi, Y., Preston, J., Aoki, K.*, et al.* (2008). The AtGenExpress hormone and chemical treatment data set: experimental design, data evaluation, model data analysis and data access. The Plant journal : for cell and molecular biology *55*, 526-542.

- Goda, H., Sawa, S., Asami, T., Fujioka, S., Shimada, Y., and Yoshida, S. (2004). Comprehensive comparison of auxin-regulated and brassinosteroid-regulated genes in Arabidopsis. Plant physiology *134*, 1555-1573.

- Gomez-Mena, C., and Sablowski, R. (2008). ARABIDOPSIS THALIANA HOMEOBOX GENE1 establishes the basal boundaries of shoot organs and controls stem growth. Plant Cell *20*, 2059-2072.

- Gonzalez-Guzman, M., Pizzio, G.A., Antoni, R., Vera-Sirera, F., Merilo, E., Bassel, G.W., Fernandez, M.A., Holdsworth, M.J., Perez-Amador, M.A., Kollist, H.*, et al.* (2012). Arabidopsis PYR/PYL/RCAR receptors play a major role in quantitative regulation of stomatal aperture and transcriptional response to abscisic acid. Plant Cell *24*, 2483-2496.

- Gonzalez-Reig, S., Ripoll, J.J., Vera, A., Yanofsky, M.F., and Martinez-Laborda, A. (2012). Antagonistic gene activities determine the formation of pattern elements along the mediolateral axis of the Arabidopsis fruit. PLoS genetics *8*, e1003020.

- Gray, W.M., Kepinski, S., Rouse, D., Leyser, O., and Estelle, M. (2001). Auxin regulates SCFTIR1-dependent degradation of AUX/IAA proteins. Nature *414*, 271.

- Gregory, B.D., O'Malley, R.C., Lister, R., Urich, M.A., Tonti-Filippini, J., Chen, H., Millar, A.H., and Ecker, J.R. (2008). A link between RNA metabolism and silencing affecting Arabidopsis development. Developmental cell *14*, 854-866.

- Gremski, K. (2006). Gynoecium patterning in Arabidopsis thaliana : control of transmitting tract development by the HECATE genes (UC San Diego Electronic Theses and Dissertations: University of California, San Diego).

- Gremski, K., Ditta, G., and Yanofsky, M.F. (2007). The HECATE genes regulate female reproductive tract development in Arabidopsis thaliana. Development *134*, 3593-3601.

- Groszmann, M., Bylstra, Y., Lampugnani, E.R., and Smyth, D.R. (2010). Regulation of tissue-specific expression of SPATULA, a bHLH gene involved in carpel development, seedling germination, and lateral organ growth in Arabidopsis. Journal of experimental botany *61*, 1495-1508.

- Groszmann, M., Paicu, T., and Smyth, D.R. (2008). Functional domains of SPATULA, a bHLH transcription factor involved in carpel and fruit development in Arabidopsis. The Plant journal : for cell and molecular biology *55*, 40-52.

- Guenot, B., Bayer, E., Kierzkowski, D., Smith, R.S., Mandel, T., Zadnikova, P., Benkova, E., and Kuhlemeier, C. (2012). PIN1-Independent Leaf Initiation in Arabidopsis. Plant physiology *159*, 1501-1510.

- Hasson, A., Plessis, A., Blein, T., Adroher, B., Grigg, S., Tsiantis, M., Boudaoud, A., Damerval, C., and Laufs, P. (2011). Evolution and diverse roles of the CUP-SHAPED COTYLEDON genes in Arabidopsis leaf development. Plant Cell *23*, 54-68.

- Hay, A., Kaur, H., Phillips, A., Hedden, P., Hake, S., and Tsiantis, M. (2002). The gibberellin pathway mediates KNOTTED1-type homeobox function in plants with different body plans. Current biology : CB *12*, 1557-1565.

- Heim, M.A., Jakoby, M., Werber, M., Martin, C., Weisshaar, B., and Bailey, P.C. (2003). The basic helix-loop-helix transcription factor family in plants: a genome-wide study of protein structure and functional diversity. Molecular biology and evolution *20*, 735-747.

- Heisler, M.G., Atkinson, A., Bylstra, Y.H., Walsh, R., and Smyth, D.R. (2001). SPATULA, a gene that controls development of carpel margin tissues in Arabidopsis, encodes a bHLH protein. Development *128*, 1089-1098.

- Heisler, M.G., Ohno, C., Das, P., Sieber, P., Reddy, G.V., Long, J.A., and Meyerowitz, E.M. (2005). Patterns of auxin transport and gene expression during primordium development revealed by live imaging of the Arabidopsis inflorescence meristem. Current biology : CB *15*, 1899-1911.

- Hibara, K., Karim, M.R., Takada, S., Taoka, K.I., Furutani, M., Aida, M., and Tasaka, M. (2006). Arabidopsis CUP-SHAPED COTYLEDON3 regulates postembryonic shoot meristem and organ boundary formation. Plant Cell *18*, 2946-2957.

- Hock, J., and Meister, G. (2008). The Argonaute protein family. Genome biology *9*, 210.

- Hollister, J.D., Smith, L.M., Guo, Y.L., Ott, F., Weigel, D., and Gaut, B.S. (2011). Transposable elements and small RNAs contribute to gene expression divergence between Arabidopsis thaliana and Arabidopsis lyrata. Proceedings of the National Academy of Sciences of the United States of America *108*, 2322-2327.

- Hong, J.C. (2016). Chapter 3 - General Aspects of Plant Transcription Factor Families A2 - Gonzalez, Daniel H. In Plant Transcription Factors (Boston: Academic Press), pp. 35-56.

- Hosoda, K., Imamura, A., Katoh, E., Hatta, T., Tachiki, M., Yamada, H., Mizuno, T., and Yamazaki, T. (2002). Molecular structure of the GARP family of plant Myb-related DNA binding motifs of the Arabidopsis response regulators. Plant Cell *14*, 2015-2029.

- Hu, J.H., Mitchum, M.G., Barnaby, N., Ayele, B.T., Ogawa, M., Nam, E., Lai, W.C., Hanada, A., Alonso, J.M., Ecker, J.R.*, et al.* (2008). Potential sites of bioactive gibberellin production during reproductive growth in Arabidopsis. Plant Cell *20*, 320-336.

- Huang, F., Zago, M.K., Abas, L., van Marion, A., Galvan-Ampudia, C.S., and Offringa, R. (2010). Phosphorylation of conserved PIN motifs directs Arabidopsis PIN1 polarity and auxin transport. Plant Cell *22*, 1129-1142.

- Hunter, C., Willmann, M.R., Wu, G., Yoshikawa, M., de la Luz Gutierrez-Nava, M., and Poethig, S.R. (2006). Trans-acting siRNA-mediated repression of ETTIN and ARF4 regulates heteroblasty in Arabidopsis. Development *133*, 2973-2981.

- Hur, Y.S., Um, J.H., Kim, S., Kim, K., Park, H.J., Lim, J.S., Kim, W.Y., Jun, S.E., Yoon, E.K., Lim, J.*, et al.* (2015). Arabidopsis thaliana homeobox 12 (ATHB12), a homeodomain-leucine zipper protein, regulates leaf growth by promoting cell expansion and endoreduplication. New Phytol *205*, 316-328.

- Hutchison, C.E., Li, J., Argueso, C., Gonzalez, M., Lee, E., Lewis, M.W., Maxwell, B.B., Perdue, T.D., Schaller, G.E., Alonso, J.M.*, et al.* (2006). The Arabidopsis Histidine Phosphotransfer Proteins Are Redundant Positive Regulators of Cytokinin Signaling. The Plant cell *18*, 3073-3087.

- Hwang, I., and Sheen, J. (2001). Two-component circuitry in Arabidopsis cytokinin signal transduction. Nature *413*, 383.

- Ichihashi, Y., Horiguchi, G., Gleissberg, S., and Tsukaya, H. (2010a). The bHLH Transcription Factor SPATULA Controls Final Leaf Size in Arabidopsis thaliana. Plant and Cell Physiology *51*, 252-261.

- Ichihashi, Y., Horiguchi, G., Gleissberg, S., and Tsukaya, H. (2010b). The bHLH transcription factor SPATULA controls final leaf size in Arabidopsis thaliana. Plant & cell physiology *51*, 252-261.

- Ikezaki, M., Kojima, M., Sakakibara, H., Kojima, S., Ueno, Y., Machida, C., and Machida, Y. (2010). Genetic networks regulated by ASYMMETRIC LEAVES1 (AS1) and AS2 in leaf development in Arabidopsis thaliana: KNOX genes control five morphological events. The Plant journal : for cell and molecular biology *61*, 70-82.

- Ishida, T., Aida, M., Takada, S., and Tasaka, M. (2000). Involvement of CUP-SHAPED COTYLEDON genes in gynoecium and ovule development in Arabidopsis thaliana. Plant & cell physiology *41*, 60-67.

- Iwasaki, M., Takahashi, H., Iwakawa, H., Nakagawa, A., Ishikawa, T., Tanaka, H., Matsumura, Y., Pekker, I., Eshed, Y., Vial-Pradel, S.*, et al.* (2013). Dual regulation of ETTIN (ARF3) gene expression by AS1-AS2, which maintains the DNA methylation level, is involved in stabilization of leaf adaxial-abaxial partitioning in Arabidopsis. Development *140*, 1958-1969.

- Jasinski, S., Piazza, P., Craft, J., Hay, A., Woolley, L., Rieu, I., Phillips, A., Hedden, P., and Tsiantis, M. (2005). KNOX action in Arabidopsis is mediated by coordinate regulation of cytokinin and gibberellin activities. Current biology : CB *15*, 1560-1565.

- Jennifer, P., Haberer, G., Ferreira, F.J., Deruère, J., Mason, M.G., Schaller, G.E., Alonso, J.M., Ecker, J.R., and Kieber, J.J. (2004). Type-A Arabidopsis Response

Regulators Are Partially Redundant Negative Regulators of Cytokinin Signaling. The Plant cell *16*, 658-671.

- Ji, L., Liu, X., Yan, J., Wang, W., Yumul, R.E., Kim, Y.J., Dinh, T.T., Liu, J., Cui, X., Zheng, B.*, et al.* (2011). ARGONAUTE10 and ARGONAUTE1 regulate the termination of floral stem cells through two microRNAs in Arabidopsis. PLoS genetics *7*, e1001358.

- Jin, J., Tian, F., Yang, D.C., Meng, Y.Q., Kong, L., Luo, J., and Gao, G. (2017). PlantTFDB 4.0: toward a central hub for transcription factors and regulatory interactions in plants. Nucleic Acids Res *45*, D1040-D1045.

- Johansen, T.K. (1997). Sight. In Aristotle on the Sense-Organs, T.K. Johansen, ed. (Cambridge: Cambridge University Press), pp. 23-115.

- Josse, E.M., Gan, Y., Bou-Torrent, J., Stewart, K.L., Gilday, A.D., Jeffree, C.E., Vaistij, F.E., Martinez-Garcia, J.F., Nagy, F., Graham, I.A.*, et al.* (2011). A DELLA in disguise: SPATULA restrains the growth of the developing Arabidopsis seedling. Plant Cell *23*, 1337-1351.

- Jung, J.H., Lee, H.J., Ryu, J.Y., and Park, C.M. (2016). SPL3/4/5 Integrate Developmental Aging and Photoperiodic Signals into the FT-FD Module in Arabidopsis Flowering. Molecular plant *9*, 1647-1659.

- Kamiuchi, Y., Yamamoto, K., Furutani, M., Tasaka, M., and Aida, M. (2014). The CUC1 and CUC2 genes promote carpel margin meristem formation during Arabidopsis gynoecium development. Front Plant Sci *5*, 165.

- Kay, P., Groszmann, M., Ross, J.J., Parish, R.W., and Swain, S.M. (2013a). Modifications of a conserved regulatory network involving INDEHISCENT controls multiple aspects of reproductive tissue development in Arabidopsis. New Phytol *197*, 73-87.

- Kay, P., Groszmann, M., Ross, J.J., Parish, R.W., and Swain, S.M. (2013b). Modifications of a conserved regulatory network involving INDEHISCENT controls multiple aspects of reproductive tissue development in Arabidopsis. New Phytol *197*, 73-87.

- Kelley, D.R., Arreola, A., Gallagher, T.L., and Gasser, C.S. (2012). ETTIN (ARF3) physically interacts with KANADI proteins to form a functional complex essential

for integument development and polarity determination in Arabidopsis. Development *139*, 1105-1109.

- Kelley, L.A., Mezulis, S., Yates, C.M., Wass, M.N., and Sternberg, M.J. (2015). The Phyre2 web portal for protein modeling, prediction and analysis. Nature protocols *10*, 845-858.

- Kepinski, S., and Leyser, O. (2005). The Arabidopsis F-box protein TIR1 is an auxin receptor. Nature *435*, 446.

- Kieber, J.J., and Schaller, G.E. (2014). Cytokinins. The Arabidopsis book / American Society of Plant Biologists *12*, e0168.

- Kienow, L., Schneider, K., Bartsch, M., Stuible, H.P., Weng, H., Miersch, O., Wasternack, C., and Kombrink, E. (2008). Jasmonates meet fatty acids: functional analysis of a new acyl-coenzyme A synthetase family from Arabidopsis thaliana. Journal of experimental botany *59*, 403-419.

- Kim, J., Yi, H., Choi, G., Shin, B., Song, P.S., and Choi, G. (2003a). Functional characterization of phytochrome interacting factor 3 in phytochrome-mediated light signal transduction. Plant Cell *15*, 2399-2407.

- Kim, K.W., Eames, Andrew L., & Waterhouse, Peter M (2011). RNA Processing Activities of the Arabidopsis Argonaute Protein Family. In RNA Processing, P. Grabowski, ed. (University of Pittsburgh, USA: INTECH Open Access Publisher), pp. 136-156.

- Kim, M., Canio, W., Kessler, S., and Sinha, N. (2001). Developmental changes due to long-distance movement of a homeobox fusion transcript in tomato. Science *293*, 287-289.

- Kim, M., McCormick, S., Timmermans, M., and Sinha, N. (2003b). The expression domain of PHANTASTICA determines leaflet placement in compound leaves. Nature *424*, 438-443.

- Kim, Y.S., Kim, S.G., Lee, M., Lee, I., Park, H.Y., Seo, P.J., Jung, J.H., Kwon, E.J., Suh, S.W., Paek, K.H.*, et al.* (2008). HD-ZIP III activity is modulated by competitive inhibitors via a feedback loop in Arabidopsis shoot apical meristem development. Plant Cell *20*, 920-933.

- Kosugi, S., and Ohashi, Y. (2002). DNA binding and dimerization specificity and potential targets for the TCP protein family. The Plant journal : for cell and molecular biology *30*, 337-348.

- Kotak, S., Port, M., Ganguli, A., Bicker, F., and von Koskull-Doring, P. (2004). Characterization of C-terminal domains of Arabidopsis heat stress transcription factors (Hsfs) and identification of a new signature combination of plant class A Hsfs with AHA and NES motifs essential for activator function and intracellular localization. Plant Journal *39*, 98-112.

- Koyama, T., Mitsuda, N., Seki, M., Shinozaki, K., and Ohme-Takagi, M. (2010). TCP transcription factors regulate the activities of ASYMMETRIC LEAVES1 and miR164, as well as the auxin response, during differentiation of leaves in Arabidopsis. Plant Cell *22*, 3574-3588.

- Kumaran, M.K., Bowman, J.L., and Sundaresan, V. (2002). YABBY polarity genes mediate the repression of KNOX homeobox genes in Arabidopsis. Plant Cell *14*, 2761-2770.

- Kunst, L., Klenz, J.E., Martinez-Zapater, J., and Haughn, G.W. (1989). AP2 Gene Determines the Identity of Perianth Organs in Flowers of Arabidopsis thaliana. The Plant cell *1*, 1195-1208.

- Lafos, M., Kroll, P., Hohenstatt, M.L., Thorpe, F.L., Clarenz, O., and Schubert, D. (2011). Dynamic Regulation of H3K27 Trimethylation during Arabidopsis Differentiation. PLoS genetics *7*.

- Landau, U., Asis, L., and Eshed Williams, L. (2015). The ERECTA, CLAVATA and class III HD-ZIP Pathways Display Synergistic Interactions in Regulating Floral Meristem Activities. Plos One *10*, e0125408.

- Larsson, E., Roberts, C.J., Claes, A.R., Franks, R.G., and Sundberg, E. (2014). Polar Auxin Transport Is Essential for Medial versus Lateral Tissue Specification and Vascular-Mediated Valve Outgrowth in Arabidopsis Gynoecia[W]. Plant physiology *166*, 1998-U1237.

- Laubinger, S., Zeller, G., Henz, S.R., Sachsenberg, T., Widmer, C.K., Naouar, N., Vuylsteke, M., Scholkopf, B., Ratsch, G., and Weigel, D. (2008). At-TAX: a whole genome tiling array resource for developmental expression analysis and transcript identification in Arabidopsis thaliana. Genome biology *9*, R112.

- Laufs, P., Peaucelle, A., Morin, H., and Traas, J. (2004). MicroRNA regulation of the CUC genes is required for boundary size control in Arabidopsis meristems. Development *131*, 4311-4322.

- Lee, C., and Clark, S.E. (2015). A WUSCHEL-Independent Stem Cell Specification Pathway Is Repressed by PHB, PHV and CNA in Arabidopsis. Plos One *10*.

- Leibfried, A., To, J.P., Busch, W., Stehling, S., Kehle, A., Demar, M., Kieber, J.J., and Lohmann, J.U. (2005). WUSCHEL controls meristem function by direct regulation of cytokinin-inducible response regulators. Nature *438*, 1172-1175.

- Li, X., Duan, X., Jiang, H., Sun, Y., Tang, Y., Yuan, Z., Guo, J., Liang, W., Chen, L., Yin, J., *et al.* (2006). Genome-wide analysis of basic/helix-loop-helix transcription factor family in rice and Arabidopsis. Plant physiology *141*, 1167-1184.

- Licausi, F., Ohme-Takagi, M., and Perata, P. (2013). APETALA2/Ethylene Responsive Factor (AP2/ERF) transcription factors: mediators of stress responses and developmental programs. New Phytol *199*, 639-649.

- Lieber, D., Lora, J., Schrempp, S., Lenhard, M., and Laux, T. (2011). Arabidopsis WIH1 and WIH2 Genes Act in the Transition from Somatic to Reproductive Cell Fate. Current Biology *21*, 1009-1017.

- Liljegren, S.J., Ditta, G.S., Eshed, Y., Savidge, B., Bowman, J.L., and Yanofsky, M.F. (2000). SHATTERPROOF MADS-box genes control seed dispersal in Arabidopsis. Nature *404*, 766-770.

- Liljegren, S.J., Gustafson-Brown, C., Pinyopich, A., Ditta, G.S., and Yanofsky, M.F. (1999). Interactions among APETALA1, LEAFY, and TERMINAL FLOWER1 specify meristem fate. Plant Cell *11*, 1007-1018.

- Liljegren, S.J., Roeder, A.H., Kempin, S.A., Gremski, K., Ostergaard, L., Guimil, S., Reyes, D.K., and Yanofsky, M.F. (2004a). Control of fruit patterning in Arabidopsis by INDEHISCENT. Cell *116*, 843-853.

- Liljegren, S.J., Roeder, A.H.K., Kempin, S.A., Gremski, K., Ostergaard, L., Guimil, S., Reyes, D.K., and Yanofsky, M.F. (2004b). Control of fruit patterning in Arabidopsis by INDEHISCENT. Cell *116*, 843-853.

- Lin, Y.C., Liu, Y.C., and Nakamura, Y. (2015). The Choline/Ethanolamine Kinase Family in Arabidopsis: Essential Role of CEK4 in Phospholipid Biosynthesis and Embryo Development. Plant Cell *27*, 1497-1511.

- Lincoln, C., Britton, J.H., and Estelle, M. (1990). Growth and development of the axr1 mutants of Arabidopsis. Plant Cell *2*, 1071-1080.

- Liu, C., Xu, Z., and Chua, N.H. (1993). Auxin Polar Transport Is Essential for the Establishment of Bilateral Symmetry during Early Plant Embryogenesis. The Plant cell *5*, 621-630.

- Liu, Q., Yao, X., Pi, L., Wang, H., Cui, X., and Huang, H. (2009). The ARGONAUTE10 gene modulates shoot apical meristem maintenance and establishment of leaf polarity by repressing miR165/166 in Arabidopsis. The Plant journal : for cell and molecular biology *58*, 27-40.

- Lu, D., Wang, T., Persson, S., Mueller-Roeber, B., and Schippers, J.H.M. (2014). Transcriptional control of ROS homeostasis by KUODA1 regulates cell expansion during leaf development. Nat Commun *5*.

- Lynn, K., Fernandez, A., Aida, M., Sedbrook, J., Tasaka, M., Masson, P., and Barton, M.K. (1999). The PINHEAD/ZWILLE gene acts pleiotropically in Arabidopsis development and has overlapping functions with the ARGONAUTE1 gene. Development *126*, 469-481.

- Machida, C., Nakagawa, A., Kojima, S., Takahashi, H., and Machida, Y. (2015). The complex of ASYMMETRIC LEAVES (AS) proteins plays a central role in antagonistic interactions of genes for leaf polarity specification in Arabidopsis. Wires Dev Biol *4*, 655-671.

- Mallory, A.C., Hinze, A., Tucker, M.R., Bouche, N., Gasciolli, V., Elmayan, T., Lauressergues, D., Jauvion, V., Vaucheret, H., and Laux, T. (2009). Redundant and specific roles of the ARGONAUTE proteins AGO1 and ZLL in development and small RNA-directed gene silencing. PLoS genetics *5*, e1000646.

- Mallory, A.C., Reinhart, B.J., Jones-Rhoades, M.W., Tang, G., Zamore, P.D., Barton, M.K., and Bartel, D.P. (2004). MicroRNA control of PHABULOSA in leaf development: importance of pairing to the microRNA 5' region. The EMBO journal *23*, 3356-3364.

- Marsch-Martinez, N., Ramos-Cruz, D., Reyes-Olalde, J.I., Lozano-Sotomayor, P., Zuniga-Mayo, V.M., and de Folter, S. (2012). The role of cytokinin during Arabidopsis gynoecia and fruit morphogenesis and patterning. Plant Journal *72*, 222-234.

- Mason, M.G., Mathews, D.E., Argyros, D.A., Maxwell, B.B., Kieber, J.J., Alonso, J.M., Ecker, J.R., and Schaller, G.E. (2005). Multiple Type-B Response Regulators Mediate Cytokinin Signal Transduction in Arabidopsis. The Plant cell *17*, 3007-3018.

- Mcconnell, J.R., and Barton, M.K. (1995). Effect of Mutations in the Pinhead Gene of Arabidopsis on the Formation of Shoot Apical Meristems. Dev Genet *16*, 358-366.

- McConnell, J.R., Emery, J., Eshed, Y., Bao, N., Bowman, J., and Barton, M.K. (2001). Role of PHABULOSA and PHAVOLUTA in determining radial patterning in shoots. Nature *411*, 709-713.

- Meister, G. (2013). Argonaute proteins: functional insights and emerging roles. Nature reviews Genetics *14*, 447-459.

- Mele, G. (2016). Arabidopsis Motif Scanner. BMC Bioinformatics *17*, 50.

- Mitchum, M.G., Yamaguchi, S., Hanada, A., Kuwahara, A., Yoshioka, Y., Kato, T., Tabata, S., Kamiya, Y., and Sun, T.P. (2006). Distinct and overlapping roles of two gibberellin 3-oxidases in Arabidopsis development. The Plant journal : for cell and molecular biology *45*, 804-818.

- Mitsuda, N., and Ohme-Takagi, M. (2008). NAC transcription factors NST1 and NST3 regulate pod shattering in a partially redundant manner by promoting secondary wall formation after the establishment of tissue identity. The Plant journal : for cell and molecular biology *56*, 768-778.

- Miwa, H., Kinoshita, A., Fukuda, H., and Sawa, S. (2009). Plant meristems: CLAVATA3/ESR-related signaling in the shoot apical meristem and the root apical meristem. Journal of plant research *122*, 31-39.

- Miyashima, S., Honda, M., Hashimoto, K., Tatematsu, K., Hashimoto, T., Sato-Nara, K., Okada, K., and Nakajima, K. (2013). A comprehensive expression analysis of the Arabidopsis MICRORNA165/6 gene family during embryogenesis reveals a conserved role in meristem specification and a non-cell-autonomous function. Plant & cell physiology *54*, 375-384.

- Montgomery, T.A., Howell, M.D., Cuperus, J.T., Li, D., Hansen, J.E., Alexander, A.L., Chapman, E.J., Fahlgren, N., Allen, E., and Carrington, J.C. (2008). Specificity

of ARGONAUTE7-miR390 interaction and dual functionality in TAS3 trans-acting siRNA formation. Cell *133*, 128-141.

- Moubayidin, L., and Ostergaard, L. (2014). Dynamic control of auxin distribution imposes a bilateral-to-radial symmetry switch during gynoecium development. Current biology : CB *24*, 2743-2748.

- Moubayidin, L., and Ostergaard, L. (2015). Symmetry matters. New Phytol *207*, 985-990.

- Moussian, B., Haecker, A., and Laux, T. (2003). ZWILLE buffers meristem stability in Arabidopsis thaliana. Development genes and evolution *213*, 534-540.

- Moussian, B., Schoof, H., Haecker, A., Jurgens, G., and Laux, T. (1998). Role of the ZWILLE gene in the regulation of central shoot meristem cell fate during Arabidopsis embryogenesis. The EMBO journal *17*, 1799-1809.

- Muller, B., and Sheen, J. (2008). Cytokinin and auxin interaction in root stem-cell specification during early embryogenesis. Nature *453*, 1094-1097.

- Muller, C.J., Valdes, A.E., Wang, G.D., Ramachandran, P., Beste, L., Uddenberg, D., and Carlsbecker, A. (2016). PHABULOSA Mediates an Auxin Signaling Loop to Regulate Vascular Patterning in Arabidopsis. Plant physiology *170*, 956-970.

- Muller, M., and Munne-Bosch, S. (2015). Ethylene Response Factors: A Key Regulatory Hub in Hormone and Stress Signaling. Plant physiology *169*, 32-41.

- Murashige, T., and Skoog, F. (1962). A Revised Medium for Rapid Growth and Bio Assays with Tobacco Tissue Cultures. Physiol Plantarum *15*, 473-497.

- Nahar, M.A., Ishida, T., Smyth, D.R., Tasaka, M., and Aida, M. (2012). Interactions of CUP-SHAPED COTYLEDON and SPATULA genes control carpel margin development in Arabidopsis thaliana. Plant & cell physiology *53*, 1134-1143.

- Nakata, M., Matsumoto, N., Tsugeki, R., Rikirsch, E., Laux, T., and Okada, K. (2012). Roles of the middle domain-specific WUSCHEL-RELATED HOMEOBOX genes in early development of leaves in Arabidopsis. Plant Cell *24*, 519-535.

- Nakata, M., and Okada, K. (2012). The three-domain model: a new model for the early development of leaves in Arabidopsis thaliana. Plant signaling & behavior *7*, 1423-1427.

- Nakazawa, M., Yabe, N., Ichikawa, T., Yamamoto, Y.Y., Yoshizumi, T., Hasunuma, K., and Matsui, M. (2001). DFL1, an auxin-responsive GH3 gene homologue,

negatively regulates shoot cell elongation and lateral root formation, and positively regulates the light response of hypocotyl length. Plant Journal *25*, 213-221.

- Nemhauser, J.L., Feldman, L.J., and Zambryski, P.C. (2000). Auxin and ETTIN in Arabidopsis gynoecium morphogenesis. Development *127*, 3877-3888.

- Nguyen, D., Rieu, I., Mariani, C., and van Dam, N.M. (2016). How plants handle multiple stresses: hormonal interactions underlying responses to abiotic stress and insect herbivory. Plant Mol Biol *91*, 727-740.

- Ni, M., Tepperman, J.M., and Quail, P.H. (1998). PIF3, a phytochrome-interacting factor necessary for normal photoinduced signal transduction, is a novel basic helix-loop-helix protein. Cell *95*, 657-667.

- Nole-Wilson, S., Azhakanandam, S., and Franks, R.G. (2010). Polar auxin transport together with aintegumenta and revoluta coordinate early Arabidopsis gynoecium development. Developmental biology *346*, 181-195.

- O'Malley, R.C., Huang, S.S., Song, L., Lewsey, M.G., Bartlett, A., Nery, J.R., Galli, M., Gallavotti, A., and Ecker, J.R. (2016). Cistrome and Epicistrome Features Shape the Regulatory DNA Landscape. Cell *165*, 1280-1292.

- Ogawa, M., Kay, P., Wilson, S., and Swain, S.M. (2009). ARABIDOPSIS DEHISCENCE ZONE POLYGALACTURONASE1 (ADPG1), ADPG2, and QUARTET2 are Polygalacturonases required for cell separation during reproductive development in Arabidopsis. Plant Cell *21*, 216-233.

- Ohmetakagi, M., and Shinshi, H. (1995). Ethylene-Inducible DNA-Binding Proteins That Interact with an Ethylene-Responsive Element. Plant Cell *7*, 173-182.

- Ohno, C.K., Reddy, G.V., Heisler, M.G.B., and Meyerowitz, E.M. (2004). The Arabidopsis JAGGED gene encodes a zinc finger protein that promotes leaf tissue development. Development *131*, 1111-1122.

- Olsen, A.N., Ernst, H.A., Leggio, L.L., and Skriver, K. (2005). NAC transcription factors: structurally distinct, functionally diverse. Trends in plant science *10*, 79-87.

- Ostergaard, L. (2009). Don't 'leaf' now. The making of a fruit. Current opinion in plant biology *12*, 36-41.

- Otsuga, D., DeGuzman, B., Prigge, M.J., Drews, G.N., and Clark, S.E. (2001). REVOLUTA regulates meristem initiation at lateral positions. Plant Journal *25*, 223-236.

- Pagnussat, G.C., Yu, H.J., Ngo, Q.A., Rajani, S., Mayalagu, S., Johnson, C.S., Capron, A., Xie, L.F., Ye, D., and Sundaresan, V. (2005). Genetic and molecular identification of genes required for female gametophyte development and function in Arabidopsis. Development *132*, 603-614.

- Parenicova, L., de Folter, S., Kieffer, M., Horner, D.S., Favalli, C., Busscher, J., Cook, H.E., Ingram, R.M., Kater, M.M., Davies, B.*, et al.* (2003). Molecular and phylogenetic analyses of the complete MADS-box transcription factor family in Arabidopsis: new openings to the MADS world. Plant Cell *15*, 1538-1551.

- Peng, H.P., Lin, T.Y., Wang, N.N., and Shih, M.C. (2005). Differential expression of genes encoding 1-aminocyclopropane-1-carboxylate synthase in Arabidopsis during hypoxia. Plant Mol Biol *58*, 15-25.

- Perales, M., and Reddy, G.V. (2012). Stem cell maintenance in shoot apical meristems. Current opinion in plant biology *15*, 10-16.

- Peterson, K.M., Shyu, C., Burr, C.A., Horst, R.J., Kanaoka, M.M., Omae, M., Sato, Y., and Torii, K.U. (2013). Arabidopsis homeodomain-leucine zipper IV proteins promote stomatal development and ectopically induce stomata beyond the epidermis. Development *140*, 1924-1935.

- Pinon, V., Prasad, K., Grigg, S.P., Sanchez-Perez, G.F., and Scheres, B. (2013). Local auxin biosynthesis regulation by PLETHORA transcription factors controls phyllotaxis in Arabidopsis. Proceedings of the National Academy of Sciences of the United States of America *110*, 1107-1112.

- Pires, H.R., Monfared, M.M., Shemyakina, E.A., and Fletcher, J.C. (2014). ULTRAPETALA trxG Genes Interact with KANADI Transcription Factor Genes to Regulate Arabidopsis Gynoecium Patterning. Plant Cell *26*, 4345-4361.

- Poulsen, C., Vaucheret, H., and Brodersen, P. (2013). Lessons on RNA silencing mechanisms in plants from eukaryotic argonaute structures. Plant Cell *25*, 22-37.

- Prasad, K., Grigg, S.P., Barkoulas, M., Yadav, R.K., Sanchez-Perez, G.F., Pinon, V., Blilou, I., Hofhuis, H., Dhonukshe, P., Galinha, C.*, et al.* (2011). Arabidopsis

PLETHORA transcription factors control phyllotaxis. Current biology : CB *21*, 1123-1128.

- Prigge, M.J., Otsuga, D., Alonso, J.M., Ecker, J.R., Drews, G.N., and Clark, S.E. (2005). Class III homeodomain-leucine zipper gene family members have overlapping, antagonistic, and distinct roles in Arabidopsis development. Plant Cell *17*, 61-76.

- Prouse, M.B., and Campbell, M.M. (2012). The interaction between MYB proteins and their target DNA binding sites. Bba-Gene Regul Mech *1819*, 67-77.

- Puranik, S., Sahu, P.P., Srivastava, P.S., and Prasad, M. (2012). NAC proteins: regulation and role in stress tolerance. Trends in plant science *17*, 369-381.

- Qi, J., Wang, Y., Yu, T., Cunha, A., Wu, B., Vernoux, T., Meyerowitz, E., and Jiao, Y. (2014). Auxin depletion from leaf primordia contributes to organ patterning. Proceedings of the National Academy of Sciences of the United States of America *111*, 18769-18774.

- Ragni, L., Belles-Boix, E., Gunl, M., and Pautot, V. (2008). Interaction of KNAT6 and KNAT2 with BREVIPEDICELLUS and PENNYWISE in Arabidopsis inflorescences. Plant Cell *20*, 888-900.

- Reinhardt, D., Mandel, T., and Kuhlemeier, C. (2000). Auxin regulates the initiation and radial position of plant lateral organs. Plant Cell *12*, 507-518.

- Reinhardt, D., Pesce, E.R., Stieger, P., Mandel, T., Baltensperger, K., Bennett, M., Traas, J., Friml, J., and Kuhlemeier, C. (2003). Regulation of phyllotaxis by polar auxin transport. Nature *426*, 255-260.

- Reinhart, B.J., Liu, T., Newell, N.R., Magnani, E., Huang, T., Kerstetter, R., Michaels, S., and Barton, M.K. (2013). Establishing a framework for the Ad/abaxial regulatory network of Arabidopsis: ascertaining targets of class III homeodomain leucine zipper and KANADI regulation. Plant Cell *25*, 3228-3249.

- Reyes-Olalde, J.I., Zuniga-Mayo, V.M., Serwatowska, J., Chavez Montes, R.A., Lozano-Sotomayor, P., Herrera-Ubaldo, H., Gonzalez-Aguilera, K.L., Ballester, P., Ripoll, J.J., Ezquer, I.*, et al.* (2017). The bHLH transcription factor SPATULA enables cytokinin signaling, and both activate auxin biosynthesis and transport genes at the medial domain of the gynoecium. PLoS genetics *13*, e1006726.

- Reymond, M.C., Brunoud, G., Chauvet, A., Martinez-Garcia, J.F., Martin-Magniette, M.L., Moneger, F., and Scutt, C.P. (2012). A Light-Regulated Genetic Module Was Recruited to Carpel Development in Arabidopsis following a Structural Change to SPATULA. Plant Cell *24*, 2812-2825.

- Riechmann, J.L., Heard, J., Martin, G., Reuber, L., Jiang, C.Z., Keddie, J., Adam, L., Pineda, O., Ratcliffe, O.J., Samaha, R.R.*, et al.* (2000). Arabidopsis transcription factors: Genome-wide comparative analysis among eukaryotes. Science *290*, 2105-2110.

- Riefler, M., Novak, O., Strnad, M., and Schmülling, T. (2006). Cytokinin Receptor Mutants Reveal Functions in Shoot Growth, Leaf Senescence, Seed Size, Germination, Root Development, and Cytokinin Metabolism. The Plant cell *18*, 40-54.

- Ripoll, J.J., Roeder, A.H.K., Ditta, G.S., and Yanofsky, M.F. (2011). A novel role for the floral homeotic gene APETALA2 during Arabidopsis fruit development. Development *138*, 5167-5176.

- Roeder, A.H., Ferrandiz, C., and Yanofsky, M.F. (2003). The role of the REPLUMLESS homeodomain protein in patterning the Arabidopsis fruit. Current biology : CB *13*, 1630-1635.

- Roeder, A.H., and Yanofsky, M.F. (2006). Fruit development in Arabidopsis. The Arabidopsis book / American Society of Plant Biologists *4*, e0075.

- Roodbarkelari, F., Du, F., Truernit, E., and Laux, T. (2015). ZLL/AGO10 maintains shoot meristem stem cells during Arabidopsis embryogenesis by down-regulating ARF2-mediated auxin response. BMC Biol *13*, 74.

- Rosas Cárdenas, F., Ruiz Suárez, Y., Cano Rangel, R., Luna Garcia, V., González Aguilera, K., Marsch Martínez, N., and de Folter, S. (2017). Effect of Constitutive miR164 Expression on Plant Morphology and Fruit Development in Arabidopsis and Tomato. Agronomy *7*, 48.

- Rouse, D., Mackay, P., Stirnberg, P., Estelle, M., and Leyser, O. (1998). Changes in auxin response from mutations in an AUX/IAA gene. Science *279*, 1371-1373.

- Rubio-Somoza, I., and Weigel, D. (2011). MicroRNA networks and developmental plasticity in plants. Trends in plant science *16*, 258-264.

- Rutjens, B., Bao, D.P., van Eck-Stouten, E., Brand, M., Smeekens, S., and Proveniers, M. (2009). Shoot apical meristem function in Arabidopsis requires the combined activities of three BEL1-like homeodomain proteins. Plant Journal *58*, 641-654.

- Sabatini, S., Beis, D., Wolkenfelt, H., Murfett, J., Guilfoyle, T., Malamy, J., Benfey, P., Leyser, O., Bechtold, N., Weisbeek, P.*, et al.* (1999). An auxin-dependent distal organizer of pattern and polarity in the Arabidopsis root. Cell *99*, 463-472.

- Saddic, L.A., Huvermann, B.R., Bezhani, S., Su, Y.H., Winter, C.M., Kwon, C.S., Collum, R.P., and Wagner, D. (2006). The LEAFY target LMI1 is a meristem identity regulator and acts together with LEAFY to regulate expression of CAULIFLOWER. Development *133*, 1673-1682.

- Santner, A., Calderon-Villalobos, L.I., and Estelle, M. (2009). Plant hormones are versatile chemical regulators of plant growth. Nature chemical biology *5*, 301-307.

- Sarojam, R., Sappl, P.G., Goldshmidt, A., Efroni, I., Floyd, S.K., Eshed, Y., and Bowman, J.L. (2010). Differentiating Arabidopsis shoots from leaves by combined YABBY activities. Plant Cell *22*, 2113-2130.

- Savidge, B., Rounsley, S.D., and Yanofsky, M.F. (1995). Temporal relationship between the transcription of two Arabidopsis MADS box genes and the floral organ identity genes. The Plant cell *7*, 721-733.

- Sawa, S., Ohgishi, M., Goda, H., Higuchi, K., Shimada, Y., Yoshida, S., and Koshiba, T. (2002). The HAT2 gene, a member of the HD-Zip gene family, isolated as an auxin inducible gene by DNA microarray screening, affects auxin response in Arabidopsis. Plant Journal *32*, 1011-1022.

- Saze, H., Tsugane, K., Kanno, T., and Nishimura, T. (2012). DNA Methylation in Plants: Relationship to Small RNAs and Histone Modifications, and Functions in Transposon Inactivation. Plant and Cell Physiology *53*, 766-784.

- Schaller, A., and Stintzi, A. (2009). Enzymes in jasmonate biosynthesis - structure, function, regulation. Phytochemistry *70*, 1532-1538.

- Schmittgen, T.D., and Livak, K.J. (2008). Analyzing real-time PCR data by the comparative C(T) method. Nature protocols *3*, 1101-1108.

- Schuster, C., Gaillochet, C., and Lohmann, J.U. (2015). Arabidopsis HECATE genes function in phytohormone control during gynoecium development. Development *142*, 3343-3350.

- Schuster, C., Gaillochet, C., Medzihradszky, A., Busch, W., Daum, G., Krebs, M., Kehle, A., and Lohmann, J.U. (2014). A regulatory framework for shoot stem cell control integrating metabolic, transcriptional, and phytohormone signals. Developmental cell *28*, 438-449.

- Scutt, C.P., Vinauger-Douard, M., Fourquin, C., Finet, C., and Dumas, C. (2006). An evolutionary perspective on the regulation of carpel development. Journal of experimental botany *57*, 2143-2152.

- Seo, M., Peeters, A.J., Koiwai, H., Oritani, T., Marion-Poll, A., Zeevaart, J.A., Koornneef, M., Kamiya, Y., and Koshiba, T. (2000). The Arabidopsis aldehyde oxidase 3 (AAO3) gene product catalyzes the final step in abscisic acid biosynthesis in leaves. Proceedings of the National Academy of Sciences of the United States of America *97*, 12908-12913.

- Serrano-Mislata, A., Schiess, K., and Sablowski, R. (2015). Active Control of Cell Size Generates Spatial Detail during Plant Organogenesis. Current Biology *25*, 2991-2996.

- Sessa, G., Steindler, C., Morelli, G., and Ruberti, I. (1998). The Arabidopsis Athb-8, -9 and -14 genes are members of a small gene family coding for highly related HD-ZIP proteins. Plant Mol Biol *38*, 609-622.

- Sessions, A., Nemhauser, J.L., McColl, A., Roe, J.L., Feldmann, K.A., and Zambryski, P.C. (1997). ETTIN patterns the Arabidopsis floral meristem and reproductive organs. Development *124*, 4481-4491.

- Sessions, R.A., and Zambryski, P.C. (1995). Arabidopsis gynoecium structure in the wild and in ettin mutants. Development *121*, 1519-1532.

- Seymour, G.B., Ostergaard, L., Chapman, N.H., Knapp, S., and Martin, C. (2013). Fruit development and ripening. Annu Rev Plant Biol *64*, 219-241.

- Shamir, R., Maron-Katz, A., Tanay, A., Linhart, C., Steinfeld, I., Sharan, R., Shiloh, Y., and Elkon, R. (2005). EXPANDER--an integrative program suite for microarray data analysis. BMC Bioinformatics *6*, 232.

- Sheen, J. (2002). Phosphorelay and transcription control in cytokinin signal transduction. Science *296*, 1650-1652.

- Sieber, P., Wellmer, F., Gheyselinck, J., Riechmann, J.L., and Meyerowitz, E.M. (2007). Redundancy and specialization among plant microRNAs: role of the MIR164 family in developmental robustness. Development *134*, 1051-1060.

- Siegfried, K.R., Eshed, Y., Baum, S.F., Otsuga, D., Drews, G.N., and Bowman, J.L. (1999). Members of the YABBY gene family specify abaxial cell fate in Arabidopsis. Development *126*, 4117-4128.

- Simonini, S., Deb, J., Moubayidin, L., Stephenson, P., Valluru, M., Freire-Rios, A., Sorefan, K., Weijers, D., Friml, J., and Østergaard, L. (2016). A noncanonical auxin-sensing mechanism is required for organ morphogenesis in Arabidopsis. Genes & development *30*, 2286-2296.

- Siriwardana, C.L., Gnesutta, N., Kumimoto, R.W., Jones, D.S., Myers, Z.A., Mantovani, R., and Holt, B.F., 3rd (2016). NUCLEAR FACTOR Y, Subunit A (NF-YA) Proteins Positively Regulate Flowering and Act Through FLOWERING LOCUS T. PLoS genetics *12*, e1006496.

- Smyth, D.R., Bowman, J.L., and Meyerowitz, E.M. (1990). Early flower development in Arabidopsis. Plant Cell *2*, 755-767.

- Sorefan, K., Girin, T., Liljegren, S.J., Ljung, K., Robles, P., Galvan-Ampudia, C.S., Offringa, R., Friml, J., Yanofsky, M.F., and Ostergaard, L. (2009a). A regulated auxin minimum is required for seed dispersal in Arabidopsis. Nature *459*, 583-U114.

- Sorefan, K., Girin, T., Liljegren, S.J., Ljung, K., Robles, P., Galvan-Ampudia, C.S., Offringa, R., Friml, J., Yanofsky, M.F., and Ostergaard, L. (2009b). A regulated auxin minimum is required for seed dispersal in Arabidopsis. Nature *459*, 583-586.

- Sorefan, K., Pais, H., Hall, A.E., Kozomara, A., Griffiths-Jones, S., Moulton, V., and Dalmay, T. (2012). Reducing ligation bias of small RNAs in libraries for next generation sequencing. Silence *3*, 4.

- Sorin, C., Salla-Martret, M., Bou-Torrent, J., Roig-Villanova, I., and Martinez-Garcia, J.F. (2009). ATHB4, a regulator of shade avoidance, modulates hormone response in Arabidopsis seedlings. Plant Journal *59*, 266-277.

- Sparks, E., Wachsman, G., and Benfey, P.N. (2013). Spatiotemporal signalling in plant development. Nature reviews Genetics *14*, 631-644.

- Sparks, E.E., and Benfey, P.N. (2014). HEC of a job regulating stem cells. Developmental cell *28*, 349-350.

- Spinelli, S.V., Martin, A.P., Viola, I.L., Gonzalez, D.H., and Palatnik, J.F. (2011). A mechanistic link between STM and CUC1 during Arabidopsis development. Plant physiology *156*, 1894-1904.

- Steiner-Lange, S., Unte, U.S., Eckstein, L., Yang, C.Y., Wilson, Z.A., Schmelzer, E., Dekker, K., and Saedler, H. (2003). Disruption of Arabidopsis thaliana MYB26 results in male sterility due to non-dehiscent anthers. Plant Journal *34*, 519-528.

- Stepanova, A.N., and Alonso, J.M. (2016). Auxin catabolism unplugged: Role of IAA oxidation in auxin homeostasis. Proceedings of the National Academy of Sciences of the United States of America *113*, 10742-10744.

- Stepanova, A.N., Robertson-Hoyt, J., Yun, J., Benavente, L.M., Xie, D.Y., DoleZal, K., Schlereth, A., Jurgens, G., and Alonso, J.M. (2008). TAA1-mediated auxin biosynthesis is essential for hormone crosstalk and plant development. Cell *133*, 177-191.

- Stepanova, A.N., Yun, J., Robles, L.M., Novak, O., He, W., Guo, H., Ljung, K., and Alonso, J.M. (2011). The Arabidopsis YUCCA1 flavin monooxygenase functions in the indole-3-pyruvic acid branch of auxin biosynthesis. Plant Cell *23*, 3961-3973.

- Su, Y.H., Liu, Y.B., and Zhang, X.S. (2011). Auxin-cytokinin interaction regulates meristem development. Molecular plant *4*, 616-625.

- Subramanian, A., Kuehn, H., Gould, J., Tamayo, P., and Mesirov, J.P. (2007). GSEA-P: a desktop application for Gene Set Enrichment Analysis. Bioinformatics *23*, 3251-3253.

- Subramanian, A., Tamayo, P., Mootha, V.K., Mukherjee, S., Ebert, B.L., Gillette, M.A., Paulovich, A., Pomeroy, S.L., Golub, T.R., Lander, E.S*., et al.* (2005). Gene set enrichment analysis: a knowledge-based approach for interpreting genome-wide expression profiles. Proceedings of the National Academy of Sciences of the United States of America *102*, 15545-15550.

- Sun, T.-p. (2008). Gibberellin Metabolism, Perception and Signaling Pathways in Arabidopsis. The Arabidopsis book / American Society of Plant Biologists *6*, e0103.

- Szakonyi, D., Moschopoulos, A., and Byrne, M.E. (2010). Perspectives on leaf dorsoventral polarity. Journal of plant research *123*, 281-290.

- Takada, S., Hibara, K., Ishida, T., and Tasaka, M. (2001). The CUP-SHAPED COTYLEDON1 gene of Arabidopsis regulates shoot apical meristem formation. Development *128*, 1127-1135.

- Takahashi, H., Iwakawa, H., Ishibashi, N., Kojima, S., Matsumura, Y., Prananingrum, P., Iwasaki, M., Takahashi, A., Ikezaki, M., Luo, L.*, et al.* (2013). Meta-analyses of microarrays of Arabidopsis asymmetric leaves1 (as1), as2 and their modifying mutants reveal a critical role for the ETT pathway in stabilization of adaxial-abaxial patterning and cell division during leaf development. Plant & cell physiology *54*, 418-431.

- Takeda, S., Hanano, K., Kariya, A., Shimizu, S., Zhao, L., Matsui, M., Tasaka, M., and Aida, M. (2011). CUP-SHAPED COTYLEDON1 transcription factor activates the expression of LSH4 and LSH3, two members of the ALOG gene family, in shoot organ boundary cells. The Plant journal : for cell and molecular biology *66*, 1066-1077.

- Talon, M., Koornneef, M., and Zeevaart, J.A. (1990). Endogenous gibberellins in Arabidopsis thaliana and possible steps blocked in the biosynthetic pathways of the semidwarf ga4 and ga5 mutants. Proceedings of the National Academy of Sciences of the United States of America *87*, 7983-7987.

- Tao, Y., Ferrer, J.L., Ljung, K., Pojer, F., Hong, F.X., Long, J.A., Li, L., Moreno, J.E., Bowman, M.E., Ivans, L.J.*, et al.* (2008). Rapid synthesis of auxin via a new tryptophan-dependent pathway is required for shade avoidance in plants. Cell *133*, 164-176.

- Taoka, K., Yanagimoto, Y., Daimon, Y., Hibara, K., Aida, M., and Tasaka, M. (2004). The NAC domain mediates functional specificity of CUP-SHAPED COTYLEDON proteins. The Plant journal : for cell and molecular biology *40*, 462-473.

- Tasseva, G., Richard, L., and Zachowski, A. (2004). Regulation of phosphatidylcholine biosynthesis under salt stress involves choline kinases in Arabidopsis thaliana. FEBS Lett *566*, 115-120.

- Teale, W.D., Paponov, I.A., and Palme, K. (2006). Auxin in action: signalling, transport and the control of plant growth and development. Nature reviews Molecular cell biology *7*, 847-859.

- Telfer, A., Bollman, K.M., and Poethig, R.S. (1997). Phase change and the regulation of trichome distribution in Arabidopsis thaliana. Development *124*, 645-654.

- Toledo-Ortiz, G., Huq, E., and Quail, P.H. (2003). The Arabidopsis basic/helix-loop-helix transcription factor family. Plant Cell *15*, 1749-1770.

- Tran, L.S.P., Nakashima, K., Sakuma, Y., Simpson, S.D., Fujita, Y., Maruyama, K., Fujita, M., Seki, M., Shinozaki, K., and Yamaguchi-Shinozaki, K. (2004). Isolation and functional analysis of Arabidopsis stress-inducible NAC transcription factors that bind to a drought-responsive cis-element in the early responsive to dehydration stress 1 promoter. Plant Cell *16*, 2481-2498.

- Tsukaya, H. (2013). Leaf development. The Arabidopsis book / American Society of Plant Biologists *11*, e0163.

- Tucker, M.R., Hinze, A., Tucker, E.J., Takada, S., Jurgens, G., and Laux, T. (2008). Vascular signalling mediated by ZWILLE potentiates WUSCHEL function during shoot meristem stem cell development in the Arabidopsis embryo. Development *135*, 2839-2843.

- Tucker, M.R., Roodbarkelari, F., Truernit, E., Adamski, N.M., Hinze, A., Lohmuller, B., Wurschum, T., and Laux, T. (2013). Accession-specific modifiers act with ZWILLE/ARGONAUTE10 to maintain shoot meristem stem cells during embryogenesis in Arabidopsis. BMC Genomics *14*, 809.

- Ulmasov, T., Hagen, G., and Guilfoyle, T.J. (1999). Activation and repression of transcription by auxin-response factors. Proceedings of the National Academy of Sciences of the United States of America *96*, 5844-5849.

- Ulmasov, T., Liu, Z.B., Hagen, G., and Guilfoyle, T.J. (1995). Composite structure of auxin response elements. Plant Cell *7*, 1611-1623.

- Vaistij, F.E., Gan, Y., Penfield, S., Gilday, A.D., Dave, A., He, Z., Josse, E.M., Choi, G., Halliday, K.J., and Graham, I.A. (2013). Differential control of seed primary dormancy in Arabidopsis ecotypes by the transcription factor SPATULA. Proceedings of the National Academy of Sciences of the United States of America *110*, 10866-10871.

- van der Graaff, E., Laux, T., and Rensing, S.A. (2009). The WUS homeobox-containing (WOX) protein family. Genome biology *10*, 248.

- Vanneste, S., and Friml, J. (2009). Auxin: a trigger for change in plant development. Cell *136*, 1005-1016.

- Vernoux, T., Besnard, F., and Traas, J. (2010). Auxin at the Shoot Apical Meristem. Csh Perspect Biol *2*.

- Vieten, A., Vanneste, S., Wiśniewska, J., Benková, E., Benjamins, R., Beeckman, T., Luschnig, C., and Friml, J. (2005). Functional redundancy of PIN proteins is accompanied by auxin-dependent cross-regulation of PIN expression. Development *132*, 4521-4531.

- Vijayraghavan, U., Prasad, K., and Meyerowitz, E. (2005). Specification and maintenance of the floral meristem: interactions between positively-acting promoters of flowering and negative regulators. Curr Sci India *89*, 1835-1843.

- Voinnet, O. (2009). Origin, biogenesis, and activity of plant microRNAs. Cell *136*, 669-687.

- Wagner, T.A., and Kohorn, B.D. (2001). Wall-associated kinases are expressed throughout plant development and are required for cell expansion. Plant Cell *13*, 303-318.

- Wang, Q., Hasson, A., Rossmann, S., and Theres, K. (2016). Divide et impera: boundaries shape the plant body and initiate new meristems. New Phytol *209*, 485-498.

- Wang, Y., Wang, J., Shi, B.H., Yu, T., Qi, J.Y., Meyerowitz, E.M., and Jiao, Y.L. (2014). The Stem Cell Niche in Leaf Axils Is Established by Auxin and Cytokinin in Arabidopsis. Plant Cell *26*, 2055-2067.

- Waters, M.T., Wang, P., Korkaric, M., Capper, R.G., Saunders, N.J., and Langdale, J.A. (2009). GLK Transcription Factors Coordinate Expression of the Photosynthetic Apparatus in Arabidopsis. Plant Cell *21*, 1109-1128.

- Weidner, C., Steinfath, M., Wistorf, E., Oelgeschläger, M., Schneider, M. R., Schönfelder, G. (2017). A Protocol for Using Gene Set Enrichment Analysis to Identify the Appropriate Animal Model for Translational Research. J Vis Exp *126*.

- Weiste, C., and Droge-Laser, W. (2014). The Arabidopsis transcription factor bZIP11 activates auxin-mediated transcription by recruiting the histone acetylation machinery. Nat Commun *5*.

- Wenkel, S., Emery, J., Hou, B.H., Evans, M.M., and Barton, M.K. (2007). A feedback regulatory module formed by LITTLE ZIPPER and HD-ZIPIII genes. Plant Cell *19*, 3379-3390.

- Wenzel, C.L., Schuetz, M., Yu, Q., and Mattsson, J. (2007). Dynamics of MONOPTEROS and PIN-FORMED1 expression during leaf vein pattern formation in Arabidopsis thaliana. Plant Journal *49*, 387-398.

- White, J.L., and Kaper, J.M. (1989). A Simple Method for Detection of Viral Satellite Rnas in Small Plant-Tissue Samples. Journal of virological methods *23*, 83-93.

- Widman, N., Feng, S., Jacobsen, S.E., and Pellegrini, M. (2014). Epigenetic differences between shoots and roots in Arabidopsis reveals tissue-specific regulation. Epigenetics-Us *9*, 236-242.

- Williams, L., and Fletcher, J.C. (2005). Stem cell regulation in the Arabidopsis shoot apical meristem. Current opinion in plant biology *8*, 582-586.

- Wolters, H., and Jurgens, G. (2009). Survival of the flexible: hormonal growth control and adaptation in plant development. Nature reviews Genetics *10*, 305-317.

- Wu, H., Mori, A., Jiang, X., Wang, Y., and Yang, M. (2006). The INDEHISCENT protein regulates unequal cell divisions in Arabidopsis fruit. Planta *224*, 971-979.

- Wu, X., Weigel, D., and Wigge, P.A. (2002). Signaling in plants by intercellular RNA and protein movement. Genes & development *16*, 151-158.

- Wurschum, T., Gross-Hardt, R., and Laux, T. (2006). APETALA2 regulates the stem cell niche in the Arabidopsis shoot meristem. Plant Cell *18*, 295-307.

- Wyrzykowska, J., and Fleming, A. (2003). Cell division pattern influences gene expression in the shoot apical meristem. Proceedings of the National Academy of Sciences of the United States of America *100*, 5561-5566.

- Xu, B., Li, Z., Zhu, Y., Wang, H., Ma, H., Dong, A., and Huang, H. (2008). Arabidopsis genes AS1, AS2, and JAG negatively regulate boundary-specifying genes to promote sepal and petal development. Plant physiology *146*, 566-575.

- Xu, J., Zhang, H.Y., Xie, C.H., Xue, H.W., Dijkhuis, P., and Liu, C.M. (2005). EMBRYONIC FACTOR 1 encodes an AMP deaminase and is essential for the zygote to embryo transition in Arabidopsis. Plant Journal *42*, 743-756.

- Xu, L., Xu, Y., Dong, A., Sun, Y., Pi, L., Xu, Y., and Huang, H. (2003). Novel as1 and as2 defects in leaf adaxial-abaxial polarity reveal the requirement for ASYMMETRIC LEAVES1 and 2 and ERECTA functions in specifying leaf adaxial identity. Development *130*, 4097-4107.

- Yadav, R.K., Girke, T., Pasala, S., Xie, M., and Reddy, G.V. (2009). Gene expression map of the Arabidopsis shoot apical meristem stem cell niche. Proceedings of the National Academy of Sciences of the United States of America *106*, 4941-4946.

- Yadav, R.K., Tavakkoli, M., Xie, M., Girke, T., and Reddy, G.V. (2014). A high-resolution gene expression map of the Arabidopsis shoot meristem stem cell niche. Development *141*, 2735-2744.

- Yan, T., Yoo, D., Berardini, T.Z., Mueller, L.A., Weems, D.C., Weng, S., Cherry, J.M., and Rhee, S.Y. (2005). PatMatch: a program for finding patterns in peptide and nucleotide sequences. Nucleic Acids Res *33*, W262-266.

- Yanai, O., Shani, E., Dolezal, K., Tarkowski, P., Sablowski, R., Sandberg, G., Samach, A., and Ori, N. (2005). Arabidopsis KNOXI proteins activate cytokinin biosynthesis. Current biology : CB *15*, 1566-1571.

- Yang, C.Y., Xu, Z.Y., Song, J., Conner, K., Barrena, G.V., and Wilson, Z.A. (2007). Arabidopsis MYB26/MALE STERILE35 regulates secondary thickening in the endothecium and is essential for anther dehiscence. Plant Cell *19*, 534-548.

- Yang, S.F., and Hoffman, N.E. (1984). Ethylene Biosynthesis and Its Regulation in Higher-Plants. Annu Rev Plant Phys *35*, 155-189.

- Yang, Z.F., Gu, S.L., Wang, X.F., Li, W.J., Tang, Z.X., and Xu, C.W. (2008). Molecular evolution of the CPP-like gene family in plants: Insights from comparative genomics of Arabidopsis and rice. J Mol Evol *67*, 266-277.

- Yant, L., Mathieu, J., Dinh, T.T., Ott, F., Lanz, C., Wollmann, H., Chen, X.M., and Schmid, M. (2010). Orchestration of the Floral Transition and Floral Development in Arabidopsis by the Bifunctional Transcription Factor APETALA2. Plant Cell *22*, 2156-2170.

- Yi, X., Du, Z., and Su, Z. (2013). PlantGSEA: a gene set enrichment analysis toolkit for plant community. Nucleic Acids Res *41*, W98-103.

- Yu, C.P., Lin, J.J., and Li, W.H. (2016). Positional distribution of transcription factor binding sites in Arabidopsis thaliana. Sci Rep *6*, 25164.

- Yu, Y., Ji, L.J., Le, B.H., Zhai, J.X., Chen, J.Y., Luscher, E., Gao, L., Liu, C.Y., Cao, X.F., Mo, B.X.*, et al.* (2017). ARGONAUTE10 promotes the degradation of miR165/6 through the SDN1 and SDN2 exonucleases in Arabidopsis. Plos Biol *15*.

- Zeller, G., Henz, S.R., Widmer, C.K., Sachsenberg, T., Ratsch, G., Weigel, D., and Laubinger, S. (2009). Stress-induced changes in the Arabidopsis thaliana transcriptome analyzed using whole-genome tiling arrays. Plant Journal *58*, 1068-1082.

- Zhang, J., and Peer, W.A. (2017). Auxin homeostasis: the DAO of catabolism. Journal of experimental botany *68*, 3145-3154.

- Zhang, L.X., Li, Z.F., Quan, R.D., Li, G.J., Wang, R.G., and Huang, R.F. (2011a). An AP2 Domain-Containing Gene, ESE1, Targeted by the Ethylene Signaling Component EIN3 Is Important for the Salt Response in Arabidopsis. Plant physiology *157*, 854-865.

- Zhang, X.Y., Clarenz, O., Cokus, S., Bernatavichute, Y.V., Pellegrini, M., Goodrich, J., and Jacobsen, S.E. (2007). Whole-genome analysis of histone H3 lysine 27 trimethylation in Arabidopsis. Plos Biol *5*, 1026-1035.

- Zhang, Y., Wu, R., Qin, G., Chen, Z., Gu, H., and Qu, L.J. (2011b). Over-expression of WOX1 leads to defects in meristem development and polyamine homeostasis in Arabidopsis. Journal of integrative plant biology *53*, 493-506.

- Zhang, Z., and Zhang, X. (2012). Argonautes compete for miR165/166 to regulate shoot apical meristem development. Current opinion in plant biology *15*, 652-658.

- Zhao, H., Li, X., and Ma, L. (2012). Basic helix-loop-helix transcription factors and epidermal cell fate determination in Arabidopsis. Plant signaling & behavior *7*, 1556-1560.

- Zhao, Y., Christensen, S.K., Fankhauser, C., Cashman, J.R., Cohen, J.D., Weigel, D., and Chory, J. (2001). A role for flavin monooxygenase-like enzymes in auxin biosynthesis. Science *291*, 306-309.

- Zhao, Z., Andersen, S.U., Ljung, K., Dolezal, K., Miotk, A., Schultheiss, S.J., and Lohmann, J.U. (2010). Hormonal control of the shoot stem-cell niche. Nature *465*, 1089-1092.

- Zhou, G.K., Kubo, M., Zhong, R., Demura, T., and Ye, Z.H. (2007). Overexpression of miR165 affects apical meristem formation, organ polarity establishment and vascular development in Arabidopsis. Plant & cell physiology *48*, 391-404.

- Zhou, Y., Honda, M., Zhu, H., Zhang, Z., Guo, X., Li, T., Li, Z., Peng, X., Nakajima, K., Duan, L.*, et al.* (2015). Spatiotemporal sequestration of miR165/166 by Arabidopsis Argonaute10 promotes shoot apical meristem maintenance. Cell Rep *10*, 1819-1827.

- Zhu, H., Hu, F., Wang, R., Zhou, X., Sze, S.-H., Liou, L.W., Barefoot, A., Dickman, M., and Zhang, X. (2011a). Arabidopsis ARGONAUTE10 specifically sequesters miR166/165 to regulate ahoot apical meristem development. Cell *145*, 242-256.

- Zhu, H., Hu, F., Wang, R., Zhou, X., Sze, S.H., Liou, L.W., Barefoot, A., Dickman, M., and Zhang, X. (2011b). Arabidopsis Argonaute10 specifically sequesters miR166/165 to regulate shoot apical meristem development. Cell *145*, 242-256.

- Zoulias, N., Koenig, D., Hamidi, A., McCormick, S., and Kim, M. (2012). A role for PHANTASTICA in medio-lateral regulation of adaxial domain development in tomato and tobacco leaves. Ann Bot *109*, 407-418.

- Zuniga-Mayo, V.M., Reyes-Olalde, J.I., Marsch-Martinez, N., and de Folter, S. (2014). Cytokinin treatments affect the apical-basal patterning of the Arabidopsis gynoecium and resemble the effects of polar auxin transport inhibition. Frontiers in Plant Science *5*.

- Zurcher, E., Tavor-Deslex, D., Lituiev, D., Enkerli, K., Tarr, P.T., and Muller, B. (2013). A Robust and Sensitive Synthetic Sensor to Monitor the Transcriptional

Output of the Cytokinin Signaling Network in Planta. Plant physiology *161*, 1066-1075.

Chapter 8

Appendix

CHAPTER 8. Appendix
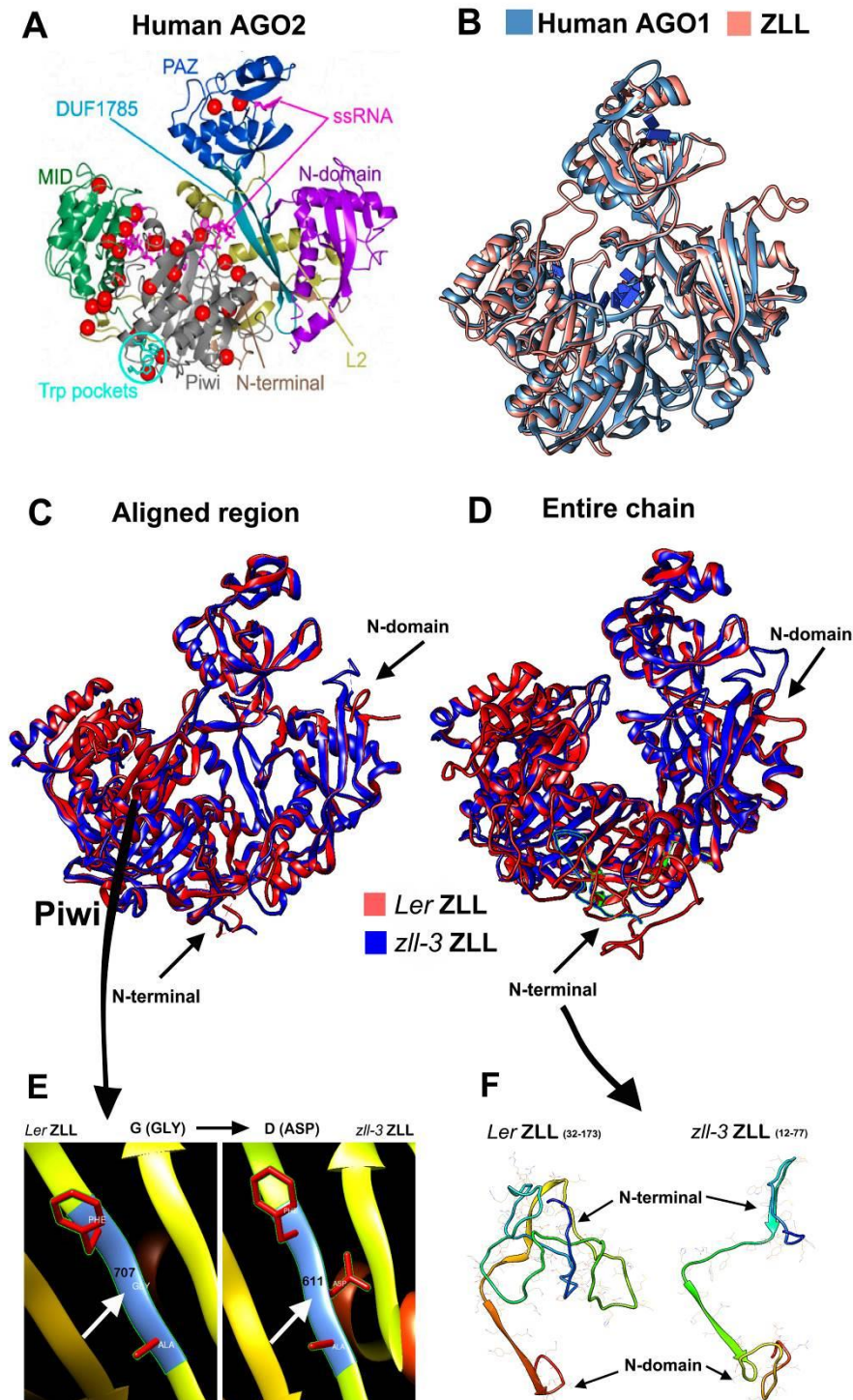
Figure 8.1 Structural mapping of mutations in *ZLL^zll-3*. (A) Topology diagram of the human Ago2 structure adapted from (Poulsen et al., 2013). **(B)** Human AGO1 and *Arabidopsis* ZLL structure comparison using TM-align. **(C and D)** N-terminal and partial N-domain of ZLL ^Ler^ are not aligned with ZLL^zll-3^. **(E)** Close-up view of the Piwi domain containing the modelled G707D *ZLL^zll-3^* mutation. **(F)** Close-up view of the modelled ZLL ^Ler^ and ZLL^zll-3^ N-terminal and partial N-domain.
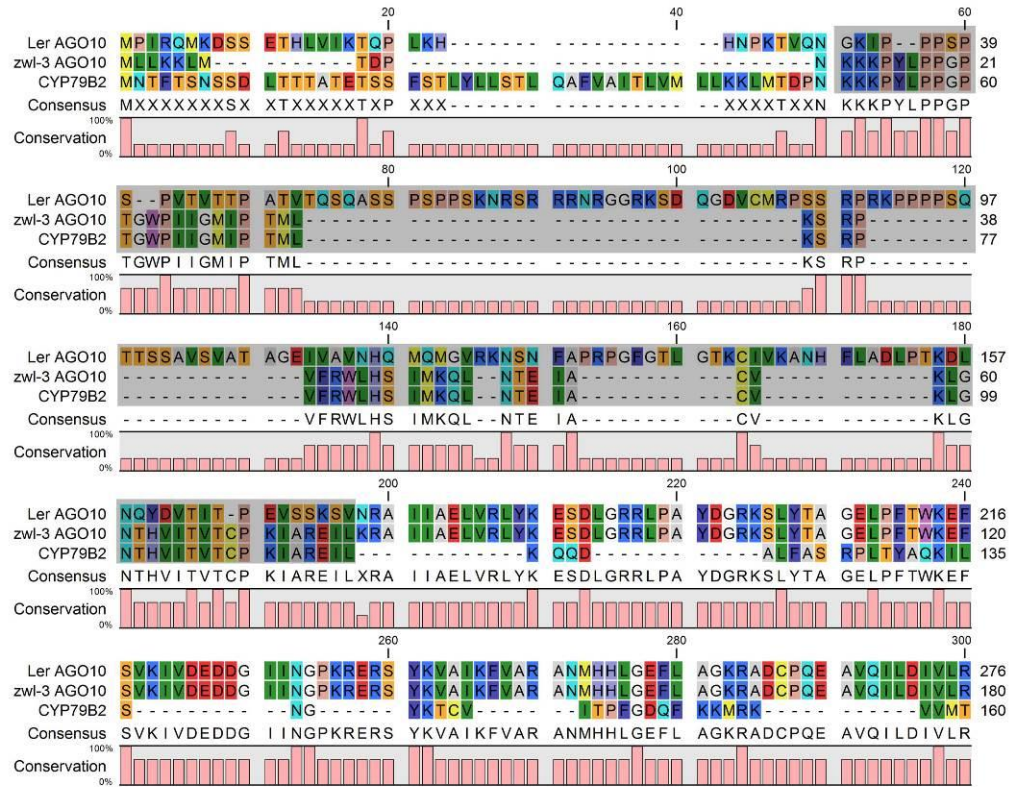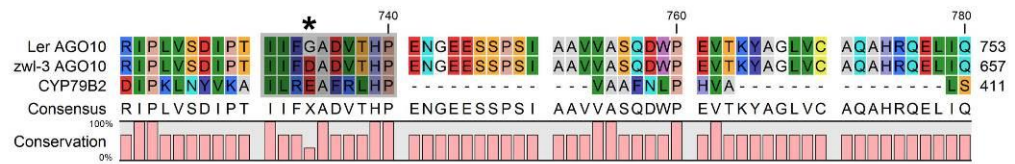
Figure 8.2 Mutations in *zwl-3* change the amino acid sequence in N-terminal, partial N-domain and Piwi-domain of ZLL/AGO10. When compared to wild-type AGO10 **(A),** *zwl-3* possesses a missense mutation (G to D) in the Piwi-domain and also harbours an insertion (cytochrome P450: CYP79B2) in the N-terminal and N-domain.
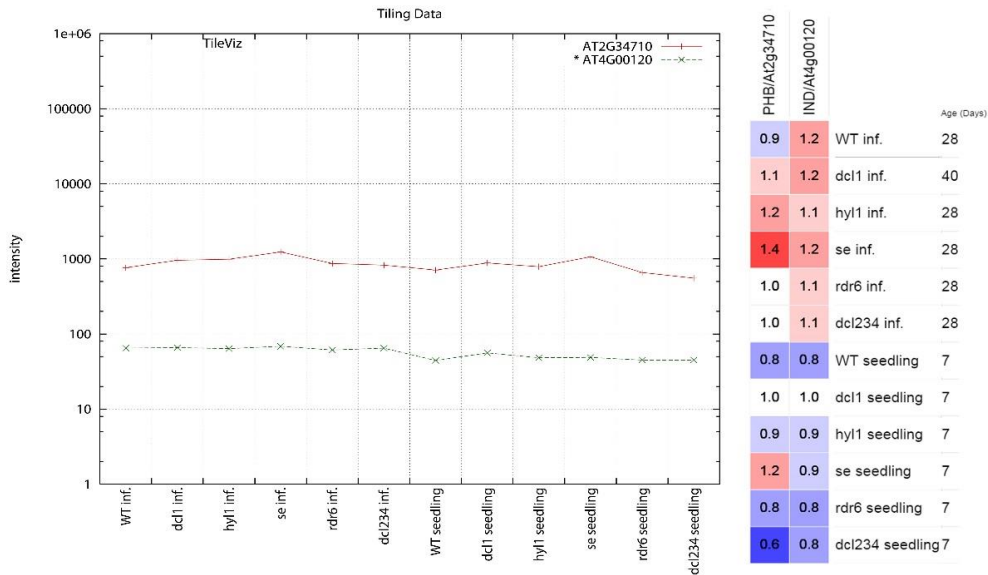
Figure 8.3 *PHB* and *IND* **gene expression in dcl and other mutants impaired in small RNA biogenesis (Laubinger et al., 2010).** On the left line graph display Intensity values of *PHB* or *IND* vs. tissue samples and on the right heat map display mean-normalised values of *PHB* or *IND* vs. tissue samples. When compared to WT, *PHB* expression increased in *se* mutants. Stable *IND* expression observed in the inflorescence or seedling samples.

Table 8.1 Gene expression values ($2^{-\Delta CT}$) used for the heat map in Chapter 4 (Fig 4.2).

Sample	Ler	Ind-6	zwl-3 WT	zwl-3 CUP	zwl-3 PIN	zwl-3 NM	ind-6 zwl-3 WT	ind-6 zwl-3 CUP	ind-6 zwl-3 PIN
CUC1	0.002	0.002	0.001	0.000	0.000	0.000	0.003	0.002	0.002
YUC1	0.003	0.003	0.003	0.001	0.001	0.001	0.003	0.001	0.002
STM	0.008	0.007	0.006	0.007	0.005	0.005	0.009	0.006	0.006
CUC3	0.009	0.006	0.006	0.005	0.004	0.003	0.005	0.004	0.002
CUC2	0.009	0.008	0.006	0.005	0.003	0.003	0.007	0.004	0.002
PHV	0.015	0.012	0.009	0.008	0.006	0.006	0.011	0.007	0.006
ARF4	0.019	0.016	0.023	0.022	0.023	0.016	0.019	0.017	0.015
REV	0.029	0.020	0.017	0.015	0.009	0.011	0.018	0.016	0.014
PHB	0.035	0.033	0.015	0.018	0.013	0.010	0.029	0.018	0.012
AS2	0.049	0.050	0.040	0.019	0.030	0.016	0.033	0.031	0.019
BP	0.071	0.070	0.084	0.080	0.090	0.050	0.099	0.094	0.065
KAN	0.076	0.051	0.063	0.057	0.066	0.035	0.063	0.039	0.041
ARF3	0.095	0.045	0.072	0.082	0.068	0.045	0.052	0.049	0.036
PID	0.101	0.057	0.123	0.077	0.082	0.058	0.077	0.056	0.037
ARR7	0.169	0.102	0.266	0.355	0.462	0.299	0.191	0.381	0.294
PIN1	0.227	0.230	0.179	0.205	0.143	0.210	0.195	0.171	0.124
RPL	0.428	0.354	0.294	0.346	0.332	0.325	0.230	0.227	0.153
YAB3	0.608	0.670	0.505	0.303	0.310	0.149	0.384	0.291	0.168
AS1	1.173	1.334	1.619	1.481	1.561	1.126	1.243	0.986	0.834

Table 8.2 Differentially regulated genes in both *35S::SPT-VP16-GR* seedlings (p<0.05, DEX+CHY vs. CHY) and *spt-12* seedlings (p<0.05, *spt-12* vs. Col-0).

GS	35S::SPT-VP16-GR	spt-12
AT1G19310	1.356579	-1.4625
TZF5	1.203	-1.36616
PYL4	1.158247	-1.79431
NAC014	1.132099	1.31552
AT5G22580	1.06268	2.196684
AT1G68360	-1.08489	-1.61543
AT1G08350	-1.17451	-1.4226

Table 8.3 Differentially regulated genes in both *hec1,2,3* Inflorescence apices (p<0.05, *hec1,2,3* vs. Col-0) and *pAlcA::HEC1* Inflorescence apices (p<0.05, *pAlcA::HEC1*+EtH vs. *pAlcA::GUS*+EtH).

GS	hec1,2,3	pAlcA::HEC1
GPT2	9.09	-5.35
NF-YA10	3.2	-1.51
NF-YA3	2.82	-1.87
JMT	2.58	-1.74
NF-YA2	2.2	-2.22
NF-YA5	2.03	-1.68
PAP17	2.01	-3.85
AT2G29670	1.91	-1.66
AT1G32900	1.89	-1.53
AT2G37770	1.86	-2.29
DIC3	1.86	-1.79
BGLU11	1.61	-1.78
PIP1B	1.52	-1.52
SBTI1.1	1.51	-2.11
AT5G23820	-1.68	1.78
AT3G21950	-1.75	1.6
AT1G53885	-2.05	2.66
AT1G16850	-2.23	-1.63
ATGSTF3	-2.8	-1.56

Table 8.4 Differentially regulated genes in both *cuc1* seedlings (p<0.05, *cuc1* vs. Col-0) and *35S::CUC1* seedlings (p<0.05, *35S::CUC1* vs. L*er*).

GS	cuc1	35S::CUC1
AT5G58980	-6.42531	1.200286
AT2G17975	-3.42775	1.25874
AT4G34770	-3.28304	5.004542
UBC17	-2.871	-1.95598
AT5G02610	-2.61046	-1.08348
CAT3	-2.28821	-1.24534
AT3G27200	-2.26497	1.535055
AT4G28240	-2.05639	1.615215
IAA6	-2.00651	-1.81687
AT2G04570	-1.89925	-1.30852
AT1G01770	-1.83727	-1.2631
AT3G60510	-1.80683	1.363822
PIF3	-1.75915	1.702813
AT1G67300	-1.75844	1.190356
AAE17	-1.72599	1.609895
AT1G73980	-1.71718	1.317883
ERD15	-1.71345	1.68441
AT1G76630	-1.70675	1.961813
CER26-LIKE	-1.70511	-1.88722
KAO2	-1.69564	5.046723
AT5G40540	-1.68935	1.318511
CRK3	-1.64251	2.080767
MSRB1	-1.63843	-1.11209
AT2G47250	-1.63491	1.378063
AT1G18270	-1.62829	1.81654
CRK10	-1.58383	1.354056
CKA3	-1.5786	2.352427
ATCTH	-1.54279	1.385844
INT1	-1.53668	1.242063

AT1G32580	1.521208	1.54025		*FTRA2*	1.919676	-1.20814
AT4G37250	1.523126	2.416576		*KNATM*	1.934229	1.161482
AT1G06010	1.541731	1.215343		*AT1G62190*	1.937868	1.181389
RPL	1.555367	11.30851		*AT5G67150*	1.953362	1.949194
AT5G07820	1.571736	1.495227		*STM*	1.958376	4.307137
TOPII	1.572114	1.537849		*IAR3*	2.006088	-1.39985
PMEPCRF	1.583181	3.640814		*RD20*	2.015566	-1.80066
IPMI2	1.596806	2.655957		*AT1G12960*	2.023285	1.130521
ENODL13	1.597188	2.662754		*SRG1*	2.149221	3.331493
CYCA3;4	1.650558	1.045567		*JAL22*	2.263742	3.475705
AT3G07270	1.651075	1.681018		*AT2G34810*	2.273639	-1.98812
TINY2	1.68977	1.249884		*AT3G15720*	2.368176	2.529814
AT3G17940	1.723295	2.078132		*CUC2*	2.380805	1.698123
UGT71B1	1.736684	1.585383		*AT5G17160*	2.707963	2.520414
SIRANBP	1.768175	-1.20958		*AT3G60270*	2.83153	1.812063
GTR1	1.81729	1.301557		*AT3G51930*	3.325268	1.573045
BAG4	1.828396	1.328216		*LBD40*	3.523152	-1.9024
CXE13	1.867473	-1.49537		*BGLU18*	3.528023	-4.67844
RLK902	1.869506	2.007074		*PAP1*	4.0895	-2.58709
MYB29	1.891197	11.58867		*AT4G17920*	4.263427	2.729153
GA3OX1	1.898537	-2.04158		*AT2G38390*	4.853381	-1.35231
AT3G53190	1.909437	3.386096		*MBP1*	5.540413	-1.58017
SCPL45	1.910643	1.755524				

Table 8.5 24 genes broadly showed similar expression in microarray analysis and qRT-PCR experiments (*35S::IND:GR* seedlings, DEX vs. DMSO, 6 hours). *CUC1/2/3* genes were not differentially regulated in *35S::IND:GR* seedlings at 6 and 12 hours in the microarray datasets (DEX vs. DMSO).

GS	qRT-PCR	Microarray
IPT3	-2.4	-1.9
ARR7	-3.2	-1.6
CKX4	-8.4	-1.1
PID	-4.8	-1.1
AGO10	-1.6	-1.1
IPT7	-3.2	-1.1
IPT8	-1.2	-1.0
HEC1	3.2	1.0
YAB2	1.4	1.1
PHV	1.1	1.1
PID2	1.5	1.1
YAB1	2.5	1.1
ARF3	1.3	1.2
CLV3	1.8	1.2
STM	1.5	1.3
ZPR1	2.5	1.3
PHB	1.7	1.3
KNAT1	2.2	1.4
ARF4	1.4	1.4
AS1	1.8	1.5
CKX5	2.2	1.5
WOX1	4.9	1.6
AGO7	3.6	1.7
SPT	1.3	1.8

GS	qRT-PCR	Microarray 6hrs	Microarray 12hrs
CUC1	-1.6	1.3	1.1
CUC2	1.3	-1.1	1.1
CUC3	-1.1	1.0	-1.3

Table 8.6 Differentially regulated genes in *35S::IND:GR* seedlings (DEX vs. DMSO 6 hours, One-Way ANOVA p<0.05, Gene Fold Change (linear) >3 or <-3)

GS	Fold Change (linear) (DEX vs. DMSO) 6 hrs	GS	FC	GS	FC
SAG29	13.58	AT5G43450	-3.03	AT2G36690	-3.7
AT2G28570	4.92	AT1G51890	-3.05	AT1G51820	-3.74
AT2G35640	4.85	UMAMIT29	-3.05	CORI3	-3.74
LOL1	4.82	AT1G65845	-3.07	AT4G12490	-3.76
GA3OX1	4.71	AT1G52200	-3.08	AT3G16530	-3.77
SRG3	4.67	AT1G51790	-3.09	GSTF7	-3.81
AT5G53048	4.51	AT4G16260	-3.11	KCS12	-3.99
XTH15	4.29	PER4	-3.12	AT4G01870	-4.01
MYB111	4.03	PDF1.4	-3.18	AT4G15700	-4.06
AT2G28510	3.7	AT3G19850	-3.19	SQE6	-4.11
AT5G47550	3.67	PTR3	-3.19	FRK1	-4.23
AT5G61610	3.26	NRT1.7	-3.21	AT5G42830	-4.36
SPX1	3.17	UGT74F2	-3.21	Rap2.6L	-4.41
CP1	3.13	HLECRK	-3.23	AT3G46280	-4.96
XTH32	3.06	AT2G43620	-3.28	MLO12	-5.17
HB51	3.05	AT5G44585	-3.28	AT5G39580	-5.17
TI1	-3.02	RLP21	-3.29	CYP71B23	-5.25
AT2G41230	-3.02	PR4	-3.31	PRX71	-5.46
OPT1	-3.02	cPT4	-3.4	AT1G36622	-5.56
		AT2G17740	-3.47	AT4G12500	-5.68
		IOS1	-3.54	AT1G36640	-5.69
		HSP90.1	-3.59	AT4G12290	-6.73
		CYP72A8	-3.62	AT4G22470	-6.93
		AT3G28270	-3.66	AT5G44575	-8.01
		NAC6	-3.67	MT1B	-11.07

Table 8.7 Differentially regulated genes in *35S::IND:GR* seedlings (DEX vs. DMSO 12 hours, One-Way ANOVA p<0.05, Gene Fold Change (linear) >3 or <-3)

GS	Fold Change (linear) (DEX vs. DMSO) 12hrs	GS	FC	GS	FC
DFR	14.2	GSTF12	7.3	FLS1	4.9
SAG29	11.8	AT2G34020	7.3	GA3OX1	4.8
AT5G61610	11.3	UF3GT	6.9	PAP1	4.8
LDOX	8.5	AT2G28510	6.7	AT1G08590	4.7
TOM20-2	8.2	ETC1	6.5	PUB22	4.6
		AT5G45650	6.4	BOR1	4.6
		AT2G11880	6.2	AT5G45276	4.5
		WOX1	6.2	CIPK18	4.4
		MYB111	6.1	PAP14	4.4
		AT1G74010	6.0	AT5G66500	4.3
		PMEPCRF	5.4	SCPL13	4.3
		SLAH2	5.2	AT3G14820	4.2

Gene	Value	Gene	Value	Gene	Value
CER1	4.2	AT1G43770	3.2	AT4G00780	-3.2
AT5G50060	4.2	AT1G52470	3.2	UGT85A3	-3.2
TBL34	4.2	AT5G56400	3.1	AT3G12260	-3.2
TIL1	4.2	AT3G14560	3.1	AT3G48640	-3.2
LRX2	4.1	AT3G51660	3.1	AT1G29140	-3.2
SPL5	4.1	AT4G37530	3.1	AT4G16000	-3.2
AT1G13750	4.0	AT5G38900	3.1	AT1G35380	-3.2
DCF	4.0	ZFP8	3.1	AGP4	-3.2
AT1G33440	4.0	AT5G19110	3.1	FDH	-3.2
XTH32	3.9	AT3G44970	3.1	GAMMA-TIP	-3.2
SWEET8	3.8	AT3G62270	3.1	MYBL2	-3.2
AT3G61490	3.8	AT1G06000	3.1	AT5G64090	-3.2
AT5G34880	3.8	PAL1	3.0	UBC17	-3.2
HB51	3.8	SIP2	3.0	AT1G27670	-3.3
AT4G05220	3.8	UGT78D1	3.0	AT4G16670	-3.3
CM1	3.7	AT3G16330	3.0	AT1G51720	-3.3
AT2G40250	3.7	AT4G15590	3.0	SWEET10	-3.3
AT3G21660	3.7	AT3G45400	-3.0	AT2G21680	-3.3
PAP15	3.7	CIPK16	-3.0	RECQSIM	-3.3
TT4	3.7	AT5G49170	-3.0	AT5G65120	-3.3
AT5G50620	3.7	HAT1	-3.0	AT1G09460	-3.3
AT1G31510	3.7	EXPA17	-3.0	AIF1	-3.3
OFP5	3.6	AT1G19100	-3.0	AT4G27300	-3.3
SULTR1;1	3.6	AT4G22470	-3.0	AIL7	-3.3
AT1G54120	3.6	AT1G69526	-3.0	PIP2A	-3.4
VDD	3.6	CYP710A2	-3.0	ABCG5	-3.4
AT5G13200	3.5	AT5G01015	-3.0	PIN5	-3.4
F3H	3.5	APG8A	-3.0	AT5G27220	-3.4
AT1G42980	3.4	AT3G62550	-3.0	At5g57880	-3.4
CHIL	3.4	AT2G44380	-3.0	AT4G01410	-3.4
AT1G21320	3.4	AT3G04250	-3.1	GSTF2	-3.4
MLO2	3.4	AT4G12410	-3.1	AT3G25190	-3.4
AT1G72140	3.4	PPDK	-3.1	AT5G62730	-3.4
AT4G33170	3.4	ERF9	-3.1	PDF1.4	-3.4
AT4G10500	3.3	AT1G52200	-3.1	AT2G19970	-3.4
AT2G40460	3.3	CYP81H1	-3.1	AT2G11640	-3.5
AT4G19720	3.3	AT1G67390	-3.1	AT3G12710	-3.5
BGLU47	3.3	4CL3	-3.1	HB2	-3.5
AT5G22540	3.3	AT3G22060	-3.1	AT2G41570	-3.5
GDPD6	3.2	E12A11	-3.1	AT1G27100	-3.6
TAT3	3.2	AT1G12845	-3.1	AT5G12940	-3.6
AT5G19100	3.2	AT5G48900	-3.1	DIT2.1	-3.6
MAP65-9	3.2	AT3G26960	-3.1	AT5G62280	-3.6
AT1G56710	3.2	AT4G36660	-3.2	NAC3	-3.6
AT5G44950	3.2	CASP2	-3.2	PR-1-LIKE	-3.6
AT3G56620	3.2	AT4G00870	-3.2	AT1G65280	-3.7
GDU2	3.2	AT2G06980	-3.2	AT1G09320	-3.7
PME3	3.2	WOX5	-3.2		

Gene	Fold Change	Gene	Fold Change	Gene	Fold Change
CYP71B24	-3.7	SECA2	-4.2	THA1	-5.1
AT1G09390	-3.7	AT2G29500	-4.3	AT3G12910	-5.1
MEE3	-3.7	RCI3	-4.3	AT3G62930	-5.2
GA3OX3	-3.7	BG1	-4.4	AT2G10260	-5.3
AT1G11070	-3.7	AT4G34419	-4.4	CYP71B23	-5.6
AT3G02670	-3.7	AT5G66420	-4.6	AT3G14210	-5.8
AT2G17740	-3.8	UMAMIT14	-4.6	AT5G44585	-6.4
NAC010	-3.8	AT4G08300	-4.6	AT5G19890	-6.6
EXPA11	-3.9	AT4G35720	-4.6	ARCK1	-6.8
HSP17.4	-3.9	GLYI4	-4.6	AT1G16950	-6.9
IAA32	-4.0	UMAMIT29	-4.6	CHAT	-7.1
SQE6	-4.1	RALFL18	-4.6	AT5G01740	-7.8
PLA2-ALPHA	-4.1	DIR1	-4.7	AT5G39520	-8.2
ABCI7	-4.1	BEE1	-4.7	OPT1	-8.4
AT4G26485	-4.1	GLYI7	-4.8	AT1G26761	-8.6
		AT4G30450	-5.0		

Table 8.8 Differentially regulated genes in *35S::IND:GR* seedlings (DEX+AUX vs. AUX 6 hours, One-Way ANOVA $p<0.05$, Gene Fold Change (linear) >3 or <-3)

M Symbol	Fold Change (linear) (DEX+AUX vs. AUX)	M Symbol	Fold Change	M Symbol	Fold Change
SAG29	17	RHS19	3.43	AT2G18193	-3.49
AT1G78860	8.92	AT3G13310	3.35	SQE6	-3.55
MYB111	4.77	GPAT1	3.3	AtCDC48B	-3.61
ICL	4.62	PMEPCRF	3.28	UGT76B1	-3.67
AT5G61610	4.52	CEL5	3.24	HSP70	-3.85
FLS1	4.3	AT5G55970	3.23	DOX1	-3.91
AT5G59680	3.97	AT5G47050	3.09	AT5G44910	-4.04
AT2G28510	3.94	KMD1	3.06	AT4G12290	-4.16
CP1	3.9	TT4	3.06	AT1G52200	-4.29
AT2G28570	3.79	GolS1	-3.02	AT2G36690	-4.38
AT1G55380	3.76	SAUR19	-3.08	AT1G51830	-4.41
TRM13	3.63	CRK14	-3.12	AT5G51440	-4.43
GA3OX1	3.61	AT2G29500	-3.16	WRKY49	-4.86
LOL1	3.44	NRT1.7	-3.18	MT1B	-5.03
		GSTU24	-3.22	CYP71B23	-5.34
		KCS12	-3.27	AT1G51840	-5.49
		CORI3	-3.36	OPT1	-5.54
		PRX71	-3.37	HSP90.1	-7.23
		ABCB15	-3.4		
		ROF2	-3.41		

Table 8.9 Differentially regulated genes in *35S::IND:GR* seedlings (DEX+CYT vs. CYT 6 hours, One-Way ANOVA p<0.05, Gene Fold Change (linear) >3 or <-3)

M Symbol	Fold Change (linear) (DEX+CYT vs. CYT)
SAG29	6.34
AT2G28570	6.1
XTH15	5.04
ABCG43	4.98
AT5G61610	4.83
LOL1	3.97
AT3G13310	3.95
LDOX	3.77

PCME	3.48
DFR	3.37
FAR1	3.33
AT3G56620	3.2
ELIP1	3.14
AT1G53870	3.11
PUB22	3.11
AT5G44570	3.11
AT4G03140	3.1
AT5G66650	3.1
HB51	3.03
AT4G15390	-3.08
AT5G62360	-3.08

AT5G44680	-3.14
MYB74	-3.15
AIR1	-3.54
AT1G63600	-3.7
CORI3	-3.78
AT4G12545	-3.84
ABCG4	-3.9
AT2G18980	-4.7
AT3G19850	-4.77
MRN1	-4.83
AT5G18030	-6.17

Table 8.10 *35S::IND:GR* (DEX vs. DMSO 6hours) significantly enriched gene-sets (FDR q-val <0.05).

NAME	SIZE	NES
Cellular process involved in reproduction	35	1.96
Galactolipid biosynthetic process	51	1.88
Plant-type cell wall modification	167	1.81
Pollen tube development	59	1.8
Defense response	359	-1.64
Response to symbiotic fungus	36	-1.64
Karyogamy	32	-1.65
Oxygen binding	231	-1.65
Response to jasmonic acid stimulus	262	-1.65
Defense response by callose deposition in cell wall	16	-1.65
S-adenosylmethionine-dependent methyltransferase activity	26	-1.67
Regulation of cell proliferation	41	-1.67
Positive regulation of flavonoid biosynthetic process	103	-1.69
Peroxidase activity	80	-1.69
Metal ion transport	29	-1.69
UDP-glycosyltransferase activity	99	-1.7
Response to absence of light	32	-1.7
Regulation of gene expression	26	-1.71
Protein import into nucleus	95	-1.72

Regulation of ion transport	26	-1.73
Ammonium transport	28	-1.74
Response to mechanical stimulus	54	-1.75
Cellular response to hypoxia	23	-1.76
ER to Golgi vesicle-mediated transport	89	-1.77
Nucleotide transport	25	-1.78
Salicylic acid mediated signaling pathway	156	-1.79
Response to ethylene stimulus	253	-1.79
Electron carrier activity	53	-1.79
Cell death	58	-1.8
Anion transport	37	-1.81
Response to fungus	103	-1.81
Glutathione transferase activity	46	-1.82
Pyrimidine ribonucleotide biosynthetic process	130	-1.84
Protein folding	285	-1.86
Embryo sac egg cell differentiation	137	-1.86
Basic amino acid transport	26	-1.86
Tryptophan biosynthetic process	19	-1.87
Response to virus	30	-1.87
Cellular amino acid metabolic process	24	-1.88
Heat acclimation	79	-1.9
Cellular response to heat	15	-1.9
Cellular response to nitric oxide	20	-1.91
Hyperosmotic salinity response	159	-1.91
Detection of bacterium	15	-1.92
Response to zinc ion	58	-1.94
Endoplasmic reticulum unfolded protein response	183	-1.95
Response to oxidative stress	181	-1.98
Protein targeting to mitochondrion	102	-1.98
Response to insect	43	-1.99
Innate immune response	89	-2
Defense response, incompatible interaction	85	-2
Leaf senescence	66	-2.01
Response to other organism	81	-2.03
Response to wounding	321	-2.04
Nucleotide biosynthetic process	84	-2.06
Jasmonic acid mediated signaling pathway	274	-2.07
Defense response to fungus, incompatible interaction	41	-2.07
Plant-type hypersensitive response	37	-2.07
Response to bacterium	167	-2.09
Response to salicylic acid stimulus	140	-2.1
Response to heat	228	-2.13
Transition metal ion transport	112	-2.13
Detection of external stimulus	17	-2.13
Response to high light intensity	205	-2.14

224

Amino acid import	72	-2.15
Nitrate transport	204	-2.19
Regulation of hydrogen peroxide metabolic process	181	-2.2
RNA methylation	168	-2.21
Defense response to bacterium, incompatible interaction	35	-2.23
Regulation of multi-organism process	89	-2.25
Defense response to bacterium	327	-2.25
Organ senescence	28	-2.26
Response to nitrate	193	-2.29
Protein targeting to membrane	362	-2.3
Regulation of plant-type hypersensitive response	365	-2.31
Systemic acquired resistance, salicylic acid mediated signaling pathway	249	-2.32
Response to hydrogen peroxide	186	-2.33
Response to molecule of bacterial origin	94	-2.34
Oligopeptide transport	104	-2.34
Negative regulation of defense response	263	-2.39
Regulation of defense response	102	-2.4
Para-aminobenzoic acid metabolic process	36	-2.41
Response to cyclopentenone	146	-2.41
Response to chitin	415	-2.45
Detection of biotic stimulus	100	-2.46
Negative regulation of programmed cell death	164	-2.47
Toxin catabolic process	208	-2.47
Proline transport	73	-2.47
MAPK cascade	203	-2.48
Defense response to fungus	309	-2.54
Salicylic acid biosynthetic process	205	-2.56
Respiratory burst involved in defense response	120	-2.63
Response to endoplasmic reticulum stress	175	-2.69
Systemic acquired resistance	239	-2.73
Amino acid transport	143	-2.75

Table 8.11 *35S::IND:GR* (DEX+AUX vs. AUX 6 hours) significantly enriched gene-sets (FDR q-val <0.05).

NAME	SIZE	NES
Triplet codon-amino acid adaptor activity	109	2.84
Photosystem ii assembly	172	2.79
Photosynthetic electron transport in photosystem i	48	2.69
Pentose-phosphate shunt	173	2.68
Translational elongation	141	2.61
Carotenoid biosynthetic process	95	2.57
Plastid organization	81	2.54

Positive regulation of catalytic activity	103	2.54
Chloroplast thylakoid membrane	270	2.5
mRNA modification	97	2.47
Maltose metabolic process	148	2.47
Starch biosynthetic process	183	2.44
Anthocyanin biosynthetic process	48	2.4
Photosynthesis	183	2.3
Photosynthesis, light reaction	144	2.3
Isopentenyl diphosphate biosynthetic process	224	2.28
ncRNA metabolic process	77	2.28
Thylakoid membrane organization	198	2.26
Chloroplast relocation	96	2.26
Chloroplast thylakoid lumen	68	2.23
Chlorophyll biosynthetic process	108	2.2
Response to far red light	94	2.2
Phosphatidylglycerol biosynthetic process	63	2.19
Response to red light	95	2.18
rRNA processing	219	2.17
Chloroplast photosystem ii	18	2.16
Response to UV-B	96	2.16
Flavonoid biosynthetic process	60	2.14
Chlorophyll binding	31	2.13
PSII associated light-harvesting complex ii catabolic process	28	2.04
Myo-inositol hexakisphosphate biosynthetic process	63	2.03
Trichoblast differentiation	45	2.01
Response to UV	34	2.01
Thylakoid	19	1.98
Regulation of protein dephosphorylation	135	1.87
Response to gibberellin stimulus	94	1.86
Plant-type cell wall modification	167	1.83
Transcription from plastid promoter	72	1.83
Hydrolase activity, acting on glycosyl bonds	40	1.82
Serine-type carboxypeptidase activity	55	1.82
Response to sucrose stimulus	201	1.79
Pectate lyase activity	25	1.78
Stomatal complex morphogenesis	135	1.76
Poly(u) RNA binding	17	1.76
Response to hypoxia	77	1.74
Integral to plasma membrane	39	1.73
Response to karrikin	126	1.7
Peptidyl-cysteine s-nitrosylation	16	1.7
Pollen sperm cell differentiation	27	1.68
Light-harvesting complex	19	1.68
Pectinesterase inhibitor activity	63	1.67
Chloroplast thylakoid	19	1.66

Actin cytoskeleton	15	1.65
Extracellular region	60	1.62
Starch catabolic process	17	1.61
Lateral root development	76	-1.52
Response to iron ion	26	-1.52
Pollen tube guidance	19	-1.53
Defense response	359	-1.53
Cell wall modification involved in abscission	15	-1.53
Brassinosteroid mediated signaling pathway	37	-1.54
Cytokinesis	37	-1.54
Cobalt ion binding	44	-1.54
Signal transduction	337	-1.54
Regulation of organelle organization	15	-1.54
Vegetative phase change	64	-1.54
Lignin biosynthetic process	49	-1.54
Protein auto phosphorylation	145	-1.54
Cell plate	26	-1.55
Cytosolic large ribosomal subunit	120	-1.55
Megagametogenesis	23	-1.55
Seed maturation	42	-1.55
Regulation of chromosome organization	98	-1.55
Cellulose biosynthetic process	76	-1.55
Calcium ion transport	117	-1.56
Transition metal ion transport	112	-1.56
Sister chromatid cohesion	137	-1.56
Nucleolus organization	23	-1.56
Motor activity	17	-1.56
Protein phosphorylation	267	-1.56
Metal ion transport	29	-1.56
Cytoskeleton organization	110	-1.56
Embryonic pattern specification	37	-1.57
Mitochondrial inner membrane	81	-1.57
Ribonuclease activity	20	-1.58
Microtubule binding	37	-1.58
Cellular response to nitrogen starvation	23	-1.58
Nucleoplasm	20	-1.58
Determination of bilateral symmetry	116	-1.59
Positive regulation of abscisic acid mediated signaling pathway	18	-1.59
Protein import into peroxisome matrix	92	-1.59
Iron ion transport	114	-1.6
Long-chain fatty acid metabolic process	25	-1.6
Response to arsenic-containing substance	36	-1.6
Hyperosmotic response	95	-1.6
Cellular amino acid metabolic process	24	-1.61
Regulation of stomatal movement	38	-1.61

Pollen germination	48	-1.62
Defense response to fungus, incompatible interaction	41	-1.62
Brassinosteroid biosynthetic process	115	-1.63
Cell growth	111	-1.63
Clathrin binding	16	-1.63
Response to oxidative stress	181	-1.63
Defense response to virus	56	-1.63
Phosphorylation	20	-1.64
Reproduction	17	-1.64
ATP binding	391	-1.65
Actin nucleation	98	-1.66
Acropetal auxin transport	15	-1.66
Copper ion binding	164	-1.66
Gene silencing	57	-1.66
Cell proliferation	160	-1.66
Protein homodimerization activity	81	-1.66
D-xylose metabolic process	34	-1.67
Regulation of dna replication	110	-1.67
Methyltransferase activity	26	-1.67
Response to wounding	321	-1.67
Response to cadmium ion	290	-1.68
Response to gamma radiation	74	-1.68
Response to ozone	32	-1.68
Response to ethylene stimulus	253	-1.69
Cellular modified amino acid biosynthetic process	34	-1.69
Ubiquitin-dependent protein catabolic process	268	-1.69
Response to cytokinin stimulus	61	-1.69
Cell wall modification	57	-1.69
Golgi organization	177	-1.7
Regulation of telomere maintenance	52	-1.7
Covalent chromatin modification	19	-1.71
Response to superoxide	31	-1.71
Response to other organism	81	-1.71
Vacuole	63	-1.71
Peroxisome organization	28	-1.71
Proteasomal protein catabolic process	93	-1.71
Regulation of multi-organism process	89	-1.72
Nuclear pore	17	-1.72
Telomere maintenance in response to dna damage	52	-1.72
Protein deubiquitination	52	-1.72
Polyamine catabolic process	36	-1.72
Response to chitin	415	-1.73
GTPase activity	42	-1.73
Response to zinc ion	58	-1.73
Response to water deprivation	332	-1.73

Defense response by callose deposition	46	-1.73
Tricarboxylic acid cycle	15	-1.73
Abscisic acid mediated signaling pathway	212	-1.73
Systemic acquired resistance, salicylic acid mediated signaling pathway	249	-1.74
Photomorphogenesis	206	-1.75
Response to glucose stimulus	77	-1.75
Positive regulation of organelle organization	48	-1.75
Glucosinolate biosynthetic process	162	-1.76
Golgi apparatus	295	-1.76
Mitochondrial outer membrane	15	-1.76
Chromatin modification	28	-1.77
Primary shoot apical meristem specification	43	-1.77
Regulation of mitotic cell cycle	28	-1.78
Leaf vascular tissue pattern formation	24	-1.79
Response to abscisic acid stimulus	443	-1.79
Jasmonic acid mediated signaling pathway	274	-1.79
MAPK cascade	203	-1.81
Negative regulation of flower development	43	-1.81
Cell division	76	-1.81
Intracellular membrane-bounded organelle	28	-1.81
ATP-dependent helicase activity	74	-1.82
Nucleotide binding	166	-1.82
Protein serine threonine kinase activity	248	-1.82
Dna methylation	167	-1.82
Endoplasmic reticulum membrane	45	-1.83
Cellular membrane fusion	270	-1.83
Male meiosis	17	-1.83
Somatic cell dna recombination	31	-1.83
Production of ta-siRNAs involved in RNA interference	111	-1.85
Purine nucleotide biosynthetic process	31	-1.85
Nucleolus	85	-1.85
Basipetal auxin transport	20	-1.86
Calcium-mediated signaling	53	-1.86
Negative regulation of biological process	42	-1.86
Protein transporter activity	59	-1.87
Heat acclimation	79	-1.87
RNA splicing	46	-1.88
Leaf development	125	-1.88
Response to bacterium	167	-1.89
Golgi vesicle transport	158	-1.89
Detection of biotic stimulus	100	-1.89
Histone h3-k9 methylation	178	-1.89
Response to insect	43	-1.9
Oligopeptide transporter activity	17	-1.9

Gene silencing by RNA	96	-1.91
Peptidase activity	55	-1.91
Calcium-transporting ATPase activity	16	-1.91
Nitrogen compound metabolic process	15	-1.91
Organ morphogenesis	99	-1.92
Endosome	229	-1.93
Cellular response to iron ion	30	-1.94
Tissue development	46	-1.94
Virus induced gene silencing	99	-1.94
Developmental growth	46	-1.94
Dna recombination	51	-1.95
Protein desumoylation	79	-1.95
Glycolysis	195	-1.95
ATPase activity, coupled to transmembrane movement of substances	100	-1.95
Nuclear-transcribed mRNA catabolic process	96	-1.95
Nuclear envelope	48	-1.95
Detection of bacterium	15	-1.96
Microtubule motor activity	66	-1.96
Response to auxin stimulus	364	-1.96
Cell death	58	-1.96
Root development	127	-1.96
Respiratory burst involved in defense response	120	-1.96
Hydrogen peroxide biosynthetic process	76	-1.96
Detection of external stimulus	17	-1.97
Salicylic acid mediated signaling pathway	156	-1.97
Regulation of cell proliferation	41	-1.98
Leaf senescence	66	-1.98
Regulation of cell differentiation	38	-1.98
Proteasome assembly	84	-1.98
Histone lysine methylation	94	-1.99
Positive regulation of flavonoid biosynthetic process	103	-2
Histone modification	60	-2
Xylem and phloem pattern formation	63	-2.01
Methylation-dependent chromatin silencing	115	-2.02
Endoplasmic reticulum	495	-2.02
Chromatin silencing by small RNA	114	-2.03
Hyperosmotic salinity response	159	-2.03
Proteasome core complex assembly	125	-2.04
RNA interference	72	-2.04
Fatty acid beta-oxidation	168	-2.05
Floral organ formation	73	-2.06
Response to virus	30	-2.06
Pyrimidine ribonucleotide biosynthetic process	130	-2.07
Trans-Golgi network	218	-2.07

Calmodulin binding	183	-2.07
Response to symbiotic fungus	36	-2.08
Negative regulation of defense response	263	-2.08
Ammonium transport	28	-2.08
Cytokinesis by cell plate formation	181	-2.09
Response to misfolded protein	181	-2.09
Meristem maintenance	67	-2.09
Production of siRNA involved in RNA interference	40	-2.09
Cell communication	53	-2.1
Gluconeogenesis	163	-2.1
mRNA export from nucleus	56	-2.11
Regulation of ion transport	26	-2.13
Anion transport	37	-2.13
Glutathione transferase activity	46	-2.13
Histone phosphorylation	61	-2.14
Protein targeting to mitochondrion	102	-2.14
Post-translational protein modification	94	-2.15
Response to carbohydrate stimulus	22	-2.16
RNA processing	135	-2.18
Defense response to bacterium	327	-2.18
Production of miRNAs involved in gene silencing by miRNA	128	-2.18
Proteasome core complex	23	-2.18
Response to molecule of bacterial origin	94	-2.18
Nucleotide transport	25	-2.19
Protein targeting to membrane	362	-2.21
Regulation of plant-type hypersensitive response	365	-2.22
Helicase activity	41	-2.23
Defense response to bacterium, incompatible interaction	35	-2.23
Salicylic acid biosynthetic process	205	-2.23
Defense response by callose deposition in cell wall	16	-2.24
Proteasomal ubiquitin-dependent protein catabolic process	112	-2.26
Cullin deneddylation	101	-2.27
Basic amino acid transport	26	-2.27
Protein maturation	53	-2.3
Defense response to fungus	309	-2.3
Tryptophan biosynthetic process	19	-2.31
Karyogamy	32	-2.32
Mitotic cell cycle	160	-2.32
Indole acetic acid biosynthetic process	108	-2.33
Embryo sac egg cell differentiation	137	-2.33
Oligopeptide transport	104	-2.34
Plant-type hypersensitive response	37	-2.35
Proline transport	73	-2.36
Gravitropism	122	-2.36
Microtubule cytoskeleton organization	139	-2.36

Nitrate transport	204	-2.37
N-terminal protein myristoylation	149	-2.37
Tryptophan catabolic process	79	-2.38
Organ senescence	28	-2.38
Innate immune response	89	-2.4
Endoplasmic reticulum unfolded protein response	183	-2.4
Response to nitrate	193	-2.4
Chromatin silencing	121	-2.4
Protein glycosylation	104	-2.42
RNA methylation	168	-2.44
Proteasome complex	52	-2.44
Regulation of defense response	102	-2.45
Coumarin biosynthetic process	53	-2.45
Protein n-linked glycosylation	93	-2.47
Negative regulation of programmed cell death	164	-2.49
Toxin catabolic process	208	-2.5
Protein folding	285	-2.51
Response to cyclopentenone	146	-2.51
Protein import into nucleus	95	-2.52
Response to high light intensity	205	-2.56
Amino acid import	72	-2.56
Para-aminobenzoic acid metabolic process	36	-2.59
Nucleotide biosynthetic process	84	-2.61
ER to Golgi vesicle-mediated transport	89	-2.64
Response to heat	228	-2.69
Systemic acquired resistance	239	-2.82
Amino acid transport	143	-2.86
Response to hydrogen peroxide	186	-2.96
Response to endoplasmic reticulum stress	175	-3.18

Table 8.12 *35S::IND:GR* (DEX+CYT vs. CYT 6 hours) significantly enriched gene-sets (FDR q-val <0.05).

NAME	SIZE	NES
Response to absence of light	32	2.78
Response to UV-B	96	2.46
Chlorophyll binding	31	2.34
Anthocyanin biosynthetic process	48	2.33
Response to mechanical stimulus	54	2.27
Photosynthetic electron transport in photosystem I	48	2.25
Intracellular signal transduction	136	2.15
ncRNA metabolic process	77	2.13
Pentose-phosphate shunt	173	2.12
Chloroplast thylakoid membrane	270	2.06

PSII associated light-harvesting complex II catabolic process	28	2.05
Photosynthesis	183	2.04
Plant-type cell wall modification	167	2.03
Photosystem ii assembly	172	1.99
Generation of precursor metabolites and energy	62	1.95
Cellular process involved in reproduction	35	1.95
rRNA modification	20	1.95
Flavonoid biosynthetic process	60	1.93
Carotenoid biosynthetic process	95	1.91
Hydrolase activity, acting on glycosyl bonds	40	1.89
Ethylene mediated signaling pathway	106	1.87
Myo-inositol hexakisphosphate biosynthetic process	63	1.87
Response to red light	95	1.85
Chloroplast relocation	96	1.84
Response to sucrose stimulus	201	1.81
Isopentenyl diphosphate biosynthetic process	224	1.81
Light-harvesting complex	19	1.81
Mitochondrial respiratory chain complex i	66	1.79
Triplet codon-amino acid adaptor activity	109	1.78
Purine base transport	119	1.76
Thylakoid	19	1.75
Anther dehiscence	16	1.74
Cellular response to hypoxia	23	1.72
Purine base transmembrane transporter activity	22	1.7
Response to chitin	415	1.69
Regulation of pollen tube growth	17	1.68
Pollen tube growth	247	1.66
Photosynthesis, light reaction	144	1.65
Fatty acid catabolic process	61	1.65
Chloroplast thylakoid lumen	68	1.65
Translational elongation	141	1.65
Petal morphogenesis	15	1.65
Thylakoid membrane organization	198	1.64
Defense response by callose deposition	46	1.64
Pollen exine formation	59	1.64
Nucleobase-containing compound transport	28	1.63
Toxin catabolic process	208	-1.58
Cell growth	111	-1.58
Positive regulation of cell proliferation	70	-1.58
Positive regulation of organelle organization	48	-1.58
Helicase activity	41	-1.58
Anion transport	37	-1.59
Response to molecule of bacterial origin	94	-1.6
Organ morphogenesis	99	-1.6
ER to Golgi vesicle-mediated transport	89	-1.6

Metal ion transmembrane transporter activity	27	-1.6
ATPase activity, coupled to transmembrane movement of substances	100	-1.61
Tissue development	46	-1.61
Flower morphogenesis	64	-1.62
Plant-type cell wall organization	102	-1.63
Trehalose biosynthetic process	22	-1.63
Heat acclimation	79	-1.63
Nuclear pore	17	-1.63
Ammonium transport	28	-1.63
Lignan biosynthetic process	15	-1.63
RNA interference	72	-1.63
Cellulose metabolic process	31	-1.64
Anchored to membrane	228	-1.64
Response to cyclopentenone	146	-1.64
Translation initiation factor activity	77	-1.64
Gravitropism	122	-1.64
mRNA processing	26	-1.64
Polar nucleus fusion	21	-1.65
Response to heat	228	-1.65
Endoplasmic reticulum	495	-1.65
Plant-type cell wall biogenesis	103	-1.66
Mediator complex	27	-1.66
Protein phosphorylation	267	-1.66
Cell differentiation	136	-1.66
Regulation of plant-type hypersensitive response	365	-1.67
Polysaccharide catabolic process	27	-1.67
Protein targeting to membrane	362	-1.67
Glucuronoxylan metabolic process	173	-1.67
Photomorphogenesis	206	-1.67
Response to desiccation	38	-1.67
Protein homodimerization activity	81	-1.68
Anthocyanin accumulation in tissues in response to uv light	110	-1.68
Response to bacterium	167	-1.68
Xylan biosynthetic process	174	-1.68
Metal ion transport	29	-1.68
Oxidoreductase activity	47	-1.68
Calmodulin binding	183	-1.68
Root development	127	-1.69
Response to zinc ion	58	-1.69
Methyltransferase activity	26	-1.69
Protein glycosylation	104	-1.69
Basic amino acid transport	26	-1.69
ATP binding	391	-1.71
Maintenance of meristem identity	26	-1.73
Nuclear-transcribed mRNA catabolic process	96	-1.74

Developmental growth	46	-1.74
Histone modification	60	-1.75
Nuclear mRNA splicing, via spliceosome	95	-1.75
Pseudouridine synthase activity	17	-1.75
Meristem maintenance	67	-1.75
Tryptophan biosynthetic process	19	-1.75
Cell death	58	-1.75
Regulation of ion transport	26	-1.75
Protein n-linked glycosylation	93	-1.76
Response to xenobiotic stimulus	77	-1.76
Auxin homeostasis	21	-1.76
Positive regulation of cellular process	30	-1.76
Coumarin biosynthetic process	53	-1.77
Nucleotide transport	25	-1.77
Positive regulation of flavonoid biosynthetic process	103	-1.77
Hydrogen peroxide biosynthetic process	76	-1.77
Protein desumoylation	79	-1.77
Protein folding	285	-1.78
Xylem and phloem pattern formation	63	-1.78
Nucleoplasm	20	-1.78
ATP-dependent helicase activity	74	-1.78
Leaf senescence	66	-1.78
Histone methylation	66	-1.78
Regulation of meristem growth	147	-1.79
Cellular amino acid metabolic process	24	-1.79
Tryptophan catabolic process	79	-1.79
Positive gravitropism	25	-1.8
Response to cytokinin stimulus	61	-1.8
Cytokinin metabolic process	18	-1.8
Cell tip growth	75	-1.81
Growth	56	-1.81
Megagametogenesis	23	-1.81
Protein deubiquitination	52	-1.82
Protein serine threonine kinase activity	248	-1.83
Floral organ formation	73	-1.83
Leaf development	125	-1.83
Post-translational protein modification	94	-1.84
Protein maturation	53	-1.85
Sterol biosynthetic process	160	-1.86
Amino acid import	72	-1.87
Polysaccharide biosynthetic process	89	-1.87
Para-aminobenzoic acid metabolic process	36	-1.88
Leaf vascular tissue pattern formation	24	-1.89
Nuclear envelope	48	-1.89
Regulation of anion channel activity	30	-1.89

|		
Indole acetic acid biosynthetic process	108	-1.9
Cullin deneddylation	101	-1.9
RNA processing	135	-1.9
Proline transport	73	-1.91
Glucosinolate biosynthetic process	162	-1.91
Regulation of hormone levels	64	-1.92
Auxin polar transport	73	-1.93
Response to hydrogen peroxide	186	-1.93
Regulation of cell size	49	-1.93
Lateral root formation	33	-1.93
Cell wall organization	130	-1.94
Transcription factor import into nucleus	45	-1.94
Systemic acquired resistance	239	-1.95
Purine nucleotide biosynthetic process	31	-1.95
Multidimensional cell growth	80	-1.97
Response to virus	30	-1.97
Transmembrane receptor protein tyrosine kinase signaling pathway	129	-1.97
Root hair elongation	173	-2
Organ senescence	28	-2.02
Root hair cell differentiation	140	-2.03
Peroxidase activity	80	-2.06
Cell wall pectin metabolic process	27	-2.06
Plant-type cell wall cellulose metabolic process	24	-2.09
Root morphogenesis	43	-2.1
Protein targeting to mitochondrion	102	-2.16
RNA methylation	168	-2.16
Pattern specification process	55	-2.2
Karyogamy	32	-2.22
Brassinosteroid biosynthetic process	115	-2.24
Response to endoplasmic reticulum stress	175	-2.27
Nucleotide biosynthetic process	84	-2.3
Oligopeptide transport	104	-2.34
Embryo sac egg cell differentiation	137	-2.37
Amino acid transport	143	-2.37
mRNA export from nucleus	56	-2.42
Pyrimidine ribonucleotide biosynthetic process	130	-2.47
Protein import into nucleus	95	-2.65
Cellular response to iron ion starvation	115	-2.67
Iron ion transport	114	-2.77
Transition metal ion transport	112	-2.82
Nitrate transport	204	-2.96
Response to nitrate	193	-3.05
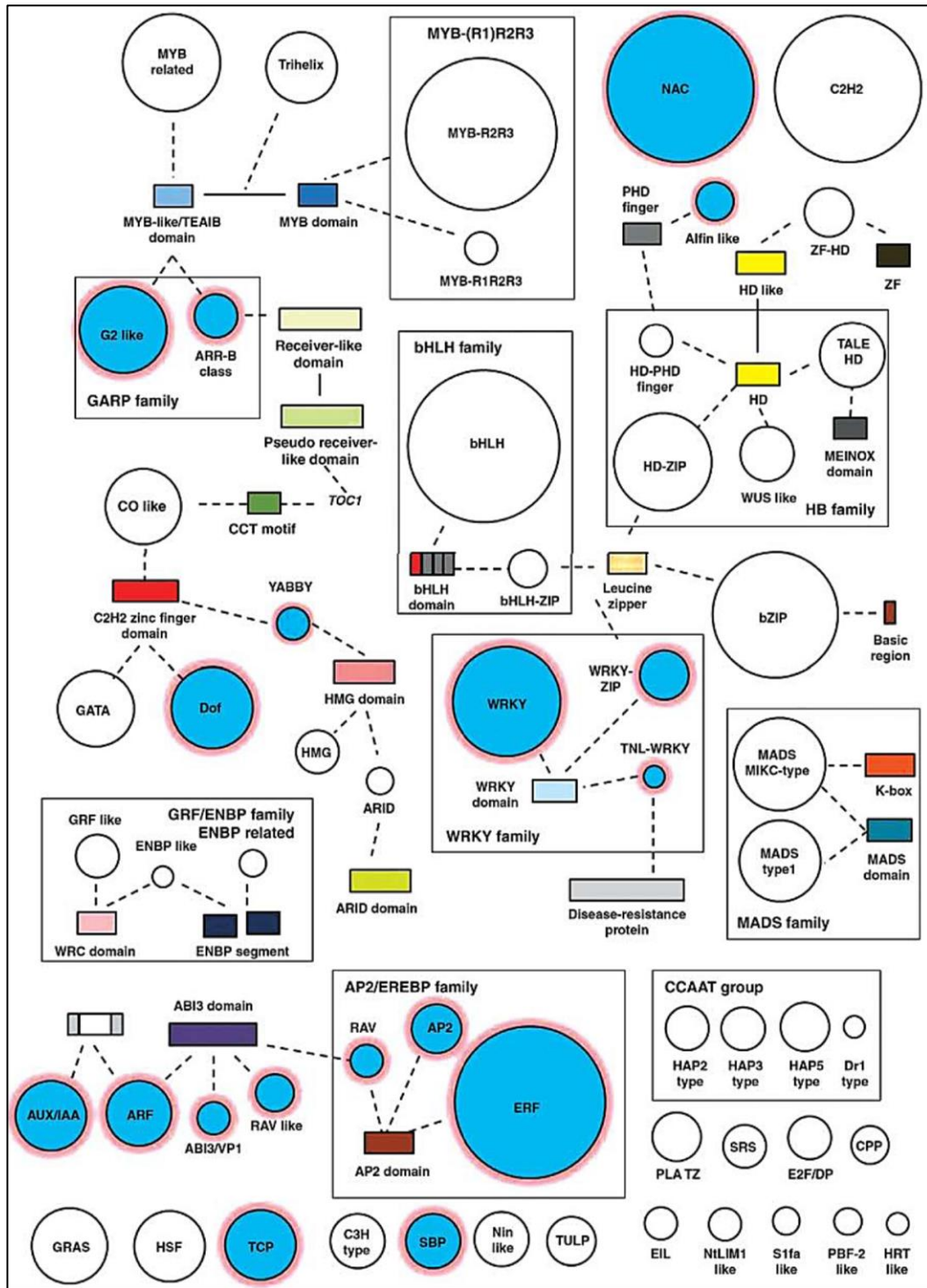
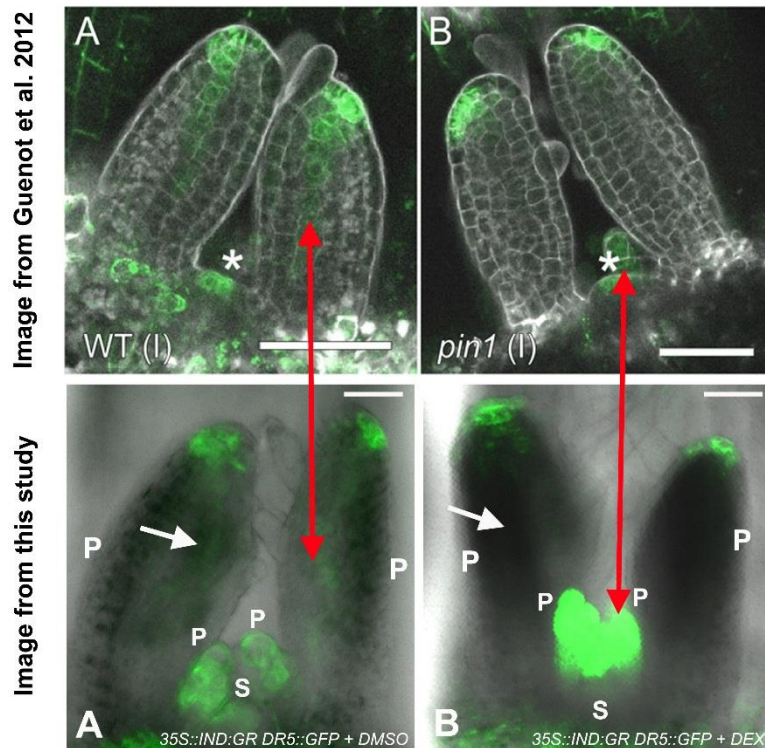**Figure 8.4** *Arabidopsis* TF families image adapted from (Hong, 2016; Riechmann et al., 2000).

Figure 8.5 *DR5rev::GFP* in SAM and leaf primordia. *DR5rev::GFP* in **(A)** *35S::IND:GR*+DMSO is similar to **(A)** WT (Guenot et al., 2012). *DR5rev::GFP* in **(B)** *35S::IND:GR*+DEX (24 hours induction) is similar to **(A)** *pin1* (Guenot et al., 2012).

Figure 8.6 Stress responses regulate IND gene expression (Zeller et al., 2009). Heatmap display intensity values of IND vs. treatments. When compared to mock treatment, *IND* expression decreased in 12 hours of salt, osmotic and cold stress conditions.